ROOT BRANCHING: FROM LATERAL ROOT PRIMORDIUM INITIATION AND MORPHOGENESIS TO FUNCTION

EDITED BY: Joseph G. Dubrovsky, Laurent Laplaze, Hidehiro Fukaki and Marta Joan Laskowski

PUBLISHED IN: Frontiers in Plant Science

frontiers Research Topics

ISSN 1664-8714
ISBN 978-2-88963-291-6
DOI 10.3389/978-2-88963-291-6

About Frontiers

Frontiers is more than just an open-access publisher of scholarly articles: it is a pioneering approach to the world of academia, radically improving the way scholarly research is managed. The grand vision of Frontiers is a world where all people have an equal opportunity to seek, share and generate knowledge. Frontiers provides immediate and permanent online open access to all its publications, but this alone is not enough to realize our grand goals.

Frontiers Journal Series

The Frontiers Journal Series is a multi-tier and interdisciplinary set of open-access, online journals, promising a paradigm shift from the current review, selection and dissemination processes in academic publishing. All Frontiers journals are driven by researchers for researchers; therefore, they constitute a service to the scholarly community. At the same time, the Frontiers Journal Series operates on a revolutionary invention, the tiered publishing system, initially addressing specific communities of scholars, and gradually climbing up to broader public understanding, thus serving the interests of the lay society, too.

Dedication to Quality

Each Frontiers article is a landmark of the highest quality, thanks to genuinely collaborative interactions between authors and review editors, who include some of the world's best academicians. Research must be certified by peers before entering a stream of knowledge that may eventually reach the public - and shape society; therefore, Frontiers only applies the most rigorous and unbiased reviews.
Frontiers revolutionizes research publishing by freely delivering the most outstanding research, evaluated with no bias from both the academic and social point of view. By applying the most advanced information technologies, Frontiers is catapulting scholarly publishing into a new generation.

What are Frontiers Research Topics?

Frontiers Research Topics are very popular trademarks of the Frontiers Journals Series: they are collections of at least ten articles, all centered on a particular subject. With their unique mix of varied contributions from Original Research to Review Articles, Frontiers Research Topics unify the most influential researchers, the latest key findings and historical advances in a hot research area! Find out more on how to host your own Frontiers Research Topic or contribute to one as an author by contacting the Frontiers Editorial Office: researchtopics@frontiersin.org

ROOT BRANCHING: FROM LATERAL ROOT PRIMORDIUM INITIATION AND MORPHOGENESIS TO FUNCTION

Topic Editors:
Joseph G. Dubrovsky, Universidad Nacional Autónoma de México, Mexico
Laurent Laplaze, Institut de recherche pour le développement (IRD), France
Hidehiro Fukaki, Kobe University, Japan
Marta Joan Laskowski, Oberlin College, United States

Citation: Dubrovsky, J. G., Laplaze, L., Fukaki, H., Laskowski, M. J., eds. (2020). Root Branching: from Lateral Root Primordium Initiation and Morphogenesis to Function. Lausanne: Frontiers Media SA. doi: 10.3389/978-2-88963-291-6

Table of Contents

frontiers in Plant Science

EDITORIAL
published: 18 November 2019
doi: 10.3389/fpls.2019.01462

Editorial: Root Branching: From Lateral Root Primordium Initiation and Morphogenesis to Function

Joseph G. Dubrovsky[1], Hidehiro Fukaki[2], Laurent Laplaze[3] and Marta Laskowski[4]*

[1] Departamento de Biología Molecular de Plantas, Instituto de Biotecnología, Universidad Nacional Autónoma de México, Cuernavaca, Mexico, [2] Department of Biology, Graduate School of Science, Kobe University, Kobe, Japan, [3] DIADE, Université de Montpellier, IRD, Montpellier, France, [4] Biology Department, Oberlin College, Oberlin, OH, United States

Keywords: plant development, root system architecture, lateral root, pericycle, branching, morphogenesis

Editorial on the Research Topic

Root Branching: From Lateral Root Primordium Initiation and Morphogenesis to Function

WHY STUDY ROOT BRANCHING?

OPEN ACCESS

Edited by:
José Manuel Pérez-Pérez, Universidad Miguel Hernández de Elche, Spain

Reviewed by:
Julio Salguero, University of Extremadura, Spain

****Correspondence:***
Joseph G. Dubrovsky
jdubrov@ibt.unam.mx

Specialty section:
This article was submitted to Plant Development and EvoDevo, a section of the journal Frontiers in Plant Science

Received: *02 October 2019*
Accepted: *21 October 2019*
Published: *18 November 2019*

Citation:
Dubrovsky JG, Fukaki H, Laplaze L and Laskowski M (2019) Editorial: Root Branching: From Lateral Root Primordium Initiation and Morphogenesis to Function. Front. Plant Sci. 10:1462. doi: 10.3389/fpls.2019.01462

Out of the total biomass of all life kingdoms on our planet (550 Gigatons of C; 1Gt C = 10^{15} g of carbon), belowground biomass, most of which is composed by plant roots, is estimated to be 130 Gt of C (Bar-On et al., 2018). Roots are important not only for soil formation, maintenance, and C input but also for the whole of plant life as they provide and transport water and minerals to the above-ground organs that permit successful photosynthetic nutrition. To forage for nutrients and water, roots grow and spread widely throughout the soil. Their spread is promoted by extensive branching; one plant may have millions of lateral roots (LRs). Despite the importance of LRs, many questions regarding their initiation and development are still not understood. Increasing our understanding of the mechanisms shaping root system architecture (RSA) has become an essential component in devising new strategies to cultivate and breed plants that are more resilient to abiotic stresses, a factor whose importance is rising as the growing human population demands sustainable intensification of agricultural practice and as the impact of global changes increases.

LATERAL ROOT INITIATION AND COMPETENT STATE OF THE PERICYCLE

The first steps in LR formation are related to priming and commitment of the pericycle cells in which the first divisions leading to LR primordium (LRP) formation occur. To elucidate the molecular events that take place during LR initiation and primordium development at cellular/tissue levels, cell type-specific transcriptomics of LR formation based on fluorescent activated cell sorting or laser capture microdissection has been performed using *Arabidopsis thaliana* and cereal model systems, thereby providing us the useful gene catalogues of genes involved in LR initiation. Kortz et al. review the recent advances obtained using this approach and focus on cell type-specific responses to nitrate-linked LR formation in maize, in which auxin transport through ZmPINs and cell cycle inhibition by Kip-related proteins are involved in LR branching from shoot-born brace roots in maize.

Participation of different hormones, chiefly auxin, in LR initiation has been extensively studied in *A. thaliana* and is reviewed by Torres-Martínez et al. In *A. thaliana*, auxin can both promote and inhibit LR

formation, depending on its concentration (Ivanchenko et al., 2010). Importantly, Alarcón et al. found a similar tendency in a monocot species, *Zea mays*. They show that relatively high concentrations of exogenous auxin inhibit LR formation in just that part of the root formed after hormone treatment, and this reduction is accompanied with a reduced pericycle cell length. Their data suggest that pericycle cells undergo a period of competence after which LR initiation does not take place and that root growth, pericycle cell length and LR formation are linked and can be regulated by auxin.

In squash, *Cucurbita pepo*, LR founder cells divide within the root apical meristem rather than the young differentiation zone as occurs in *Arabidopsis*. Kiryushkin et al. used phylogenetic analysis together with auxin-responsive expression in the root to search for putative functional orthologs of two *Arabidopsis* genes associated with the early stages of LR development: *GATA23* and *MAKR4*. They showed that expression of both genes starts in the protoxylem and then spreads to the pericycle founder cells. The authors find it unlikely that there is enough space for auxin oscillations to lead to formation of pre-branch sites prior to *CpMAKR4* expression. In addition, it appears that LR initiation in squash is not induced by an inward-moving auxin signal such as might arise from dying root cap cells.

In the lycophyte, *Selaginella moellendorffii,* roots arise from stem-born structures called rhizophores. Within each root, a single, tetrahedrally-shaped stem cell (apical cell) nucleates the production of new cells that permit growth. These roots branch dichotomously when the root tip bifurcates, with each side having its own apical cell. Fang et al. investigated the extent to which auxin serves as a signal for the formation of new roots in *Selaginella* and concluded that while the plant responds to auxin, root production is indirectly affected, suggesting that the new apical cells formed during root tip dichotomous branching may be generated by an auxin-independent mechanism.

MORPHOGENESIS OF LATERAL ROOT PRIMORDIA

In contemporary studies and reviews, the literature considered is commonly not older than two-three decades. Torres-Martínez et al. made an effort to integrate our knowledge of LR morphogenesis in both old and new literature embracing all angiosperms that include >15,000 genera (Soltis et al., 2018). They overview the participation of pericycle cells and other tissues in LRP morphogenesis and attempt to outline the phylogeny of a temporary cap-like structure of endodermal origin in LRP morphogenesis. Also, they identify categories of mutants affected in LRP morphogenesis and address genetic control and the roles of mechanical forces, cell proliferation, patterning, and cell identity acquisition in LRP morphogenesis.

ROOT BRANCHING PLASTICITY, NUTRIENTS AND MODELING

Compared to the eudicot plants such as *A. thaliana*, monocots such as maize plants form a structurally and functionally complex root system consisting of different root types (primary, seminal, lateral, and crown roots), which shows root branching plasticity. Yu et al. provide an update on the molecular mechanisms in the LR branching response to environmental signals such as nutrients and water in maize. The authors explain the architectural responses of maize LRs to the availability of soil resources such as nitrate, phosphate and water. The LR branching response to the uneven distribution of water and nutrients in soil is also discussed with the aid of molecular genetic data obtained in *A. thaliana* and maize.

Root branching is a plastic trait that responds to signals from other parts of the plant. For instance, root tip excision promotes the developmental progression of previously specified lateral root primordia. Justamante et al. describe the natural variation in RSA after root tip excision among 120 A. *thaliana* accessions. Using a genome-wide association study, they identified 19 genomic loci involved in the regulation of excision-induced changes in RSA. Three candidate loci associated with wound-induced LR formation were further investigated and a potential mechanism involving cytokinin is proposed.

In addition to cereals, root and tuber crops (RTCs) such as cassava, potato, sweet potato, and yams, are also important as a global source of carbohydrates, particularly in regions not suitable for cereal production. However, root branching traits that enhance nutrient acquisition in RTCs has not been well studied. Duque and Villordon provide a comprehensive review of recent literatures on RTCs, including the authors' research on RSA traits under phosphorus deficiency in sweet potato. To manipulate RSA for increased nutrient efficiency in RTCs, new research directions are proposed including strategic translational research using molecular genetic data on RSA and nutrient uptake from *A. thaliana* and cereal model systems.

Root branching is an important component of RSA and has therefore an important role in the adaptation of different plant species to their specific ecosystem. The article by Pages describes an analysis of the inter- and intraspecific variations in inter-branch distance in 36 plant species collected in homogenous soil conditions. It proposes a simple model based on three parameters accounting for two processes: the location of potential branching sites along the root and the emergence of LRs at these sites that simulates the observed variations in the different species. This suggests that these parameters could be useful traits for analysis of plasticity in root branching dependent on genotype and environmental conditions.

FUTURE PERSPECTIVES

To understand the evolution of root system development and branching as well as the biology of crop species, research programs gradually move from a model species, *A. thaliana*, to a wider spectrum of other angiosperms and vascular plants in general. Clearly, this tendency will be maintained. Development of new methodological approaches such as single cell transcriptomics, 4-D imaging microscopy, new phenomics systems, including computer tomography, modeling at different organization levels, and other innovations are already starting and will help further

our understanding of root branching mechanisms. It is a challenge for our community to integrate all this information and comprehend root branching, from LRP initiation and morphogenesis to evolution and function.

AUTHOR CONTRIBUTIONS

JD prepared the outline of the manuscript. All authors wrote parts of the manuscript, improved the draft and revised the final version.

FUNDING

The work in the JD laboratory is partially supported by DGAPA-PAPIIT-UNAM grant IN200818 and CONACyT grant A1-S-9236. The work in the HF laboratory is supported by Grant-in-Aid for Scientific Research (B)(18H02463) from the MEXT, Japan. Work in the ML laboratory is supported by NSF IOS – 1656621, USA. LL acknowledges support from the French National Research Agency (ANR) through the NewRoot project (ANR-17-CE13-0004-01).

REFERENCES

Bar-On, Y. M., Phillips, R., and Milo, R. (2018). The biomass distribution on Earth. *Proc. Natl. Acad. Sci.* 115, 6506–6511. doi: 10.1073/pnas.1711842115

Ivanchenko, M. G., Napsucialy-Mendivil, S., and Dubrovsky, J. G. (2010). Auxin-induced inhibition of lateral root initiation contributes to root system shaping in *Arabidopsis thaliana*. *Plant J.* 64, 740–752. doi: 10.1111/j.1365-313X.2010.04365.x

Soltis, D., Soltis, P., Endress, P., Chase, M. W., Manchester, S., Judd, W., et al. (2018). *Phylogeny and evolution of the angiosperms: revised and updated edition*. Chicago, IL: University of Chicago.

Conflict of Interest: The authors declare that the research was conducted in the absence of any commercial or financial relationships that could be construed as a potential conflict of interest.

frontiers in Plant Science

ORIGINAL RESEARCH
published: 24 January 2019
doi: 10.3389/fpls.2019.00011

Auxin Modulated Initiation of Lateral Roots Is Linked to Pericycle Cell Length in Maize

*M. Victoria Alarcón[1,2†‡], Julio Salguero[3†§] and Pedro G. Lloret[2]**

[1] Departamento de Hortofruticultura, Instituto de Investigaciones Agrarias "La Orden-Valdesequera", CICYTEX, Junta de Extremadura, Badajoz, Spain, [2] Departamento de Anatomía, Biología Celular y Zoología, Facultad de Ciencias, Universidad de Extremadura, Badajoz, Spain, [3] Departamento de Biología Vegetal, Ecología y Ciencias de la Tierra, Universidad de Extremadura, Badajoz, Spain

Auxin is essential for the regulation of root system architecture by controlling primary root elongation and lateral root (LR) formation. Exogenous auxin has been reported to inhibit primary root elongation and promote the formation of LRs. In this study, LR formation in the *Zea mays* primary root was quantitatively evaluated after exogenous auxin treatment by comparing the effects of auxin on two selected zones elongated either before or after auxin application. We determined two main variables in both zones: the LR density per unit of root length (LRD), and the mean phloem pericycle cell length. The total number of phloem pericycle cells (PPCs) per unit of root length was then calculated. Considering that each LR primordium is initiated from four founder cells (FCs), the percentage of PPCs (%PPC) that behave as FCs in a specific root zone was estimated by dividing the number of pericycle cells by four times the LRD. This index was utilized to describe LR initiation. Root zones elongated in the presence of a synthetic auxin (1-naphthalene acetic acid, NAA) at low concentrations (0.01 μM) showed reduced cell length and increased LRD. However, a high concentration of NAA (0.1 μM) strongly reduced both cell length and LRD. In contrast, both low and high levels of NAA stimulated LRD in zones elongated before auxin application. Analysis of the percentage of FCs in the phloem pericycle in zones elongated in the presence or absence of NAA showed that low concentrations of NAA increased the %PFC, indicating that LR initiation is promoted at new sites; however, high concentrations of NAA elicited a considerable reduction in this variable in zones developed in the presence of auxin. As these zones are composed of short pericycle cells, we propose that short pericycle cells are incapable to participate in LR primordium initiation and that auxin modulated initiation of LRs is linked to pericycle cell length.

Keywords: lateral root development, auxin action, root elongation, pericycle, maize, *Zea mays*, cell growth

OPEN ACCESS

Edited by:
Joseph G. Dubrovsky, National Autonomous University of Mexico, Mexico

Reviewed by:
Peng Yu, Universität Bonn, Germany
Aleš Soukup, Charles University, Czechia

****Correspondence:***
Pedro G. Lloret
plloret@unex.es
orcid.org/0000-0001-5051-8463

†These authors have contributed equally to this work

‡M. Victoria Alarcón
orcid.org/0000-0003-3874-0226

§Julio Salguero
orcid.org/0000-0002-6348-3965

Specialty section:
This article was submitted to Plant Development and EvoDevo, a section of the journal Frontiers in Plant Science

Received: *11 July 2018*
Accepted: *07 January 2019*
Published: *24 January 2019*

Citation:
Alarcón MV, Salguero J and Lloret PG (2019) Auxin Modulated Initiation of Lateral Roots Is Linked to Pericycle Cell Length in Maize. Front. Plant Sci. 10:11. doi: 10.3389/fpls.2019.00011

INTRODUCTION

Auxin is considered a key regulator of root growth, gravitropism, and lateral root (LR) formation (Muday and Haworth, 1994). Exogenous auxin treatment has typically resulted in inhibited root growth rate (Zeadan and Macleod, 1984; Hurren et al., 1988; Lloret and Pulgarín, 1992; Gaspar et al., 2003). Nevertheless, in *Arabidopsis* roots, it has been demonstrated that low concentrations

of auxin can substantially stimulate primary root elongation (Evans et al., 1994). Auxin action on root development is not only a question of concentration but also of its polar translocation (Muday and DeLong, 2001). The auxin indole-3-acetic acid (IAA) is predominantly synthesized in shoots and transported basipetally from the apex to the base of the shoot (Lomax et al., 1995; Muday and DeLong, 2001; Casson and Lindsey, 2003). Once in the root, IAA moves acropetally toward the root apex through the central cylinder (Mitchell and Davies, 1975; Muday and DeLong, 2001) and basipetally from the root apex toward the elongation zone through the outer root tissues (Ohwaki and Tsurumi, 1976; Tsurumi and Ohwaki, 1978; Rashotte et al., 2000; Muday and DeLong, 2001; Ruzicka et al., 2007). Acropetal transport of IAA in the root is involved in the regulation of LR formation in *Arabidopsis* (Reed et al., 1998). Because basipetal IAA transport controls elongation of epidermal cells, it has been implicated in the regulation of gravitropism (Rashotte et al., 2001). As application of the auxin transport inhibitor naphthylphthalamic acid (NPA) to the tip of *Arabidopsis* roots inhibits both basipetal auxin transport and root elongation (Rashotte et al., 2000), it is likely that primary root elongation would also be controlled by the basipetal auxin transport mechanism. In some *Arabidopsis* mutants, it has been demonstrated that a reduced growth rate in primary roots is related, at least in part, to reduced elongation of individual cells (Hauser et al., 1995).

Auxin also regulates root system architecture by promoting the acquisition of founder cell (FC) identity in pericycle cells (Dubrovsky et al., 2008), and by stimulating LR development (Laskowski et al., 1995; Casimiro et al., 2003). Nevertheless, it has been reported that auxin loses its LR-promoting effect in newly formed regions of the *Arabidopsis* primary root growing at lower rate (Ivanchenko et al., 2010), suggesting that LR formation may be linked to cell length. Interestingly, regulation of initiation and subsequent development of LRs could be differentially controlled by basipetal (Casimiro et al., 2001) and acropetal auxin polar transport, respectively (Reed et al., 1998).

Lateral root initiation in maize begins with transversal divisions of pericycle cells associated with phloem poles, when two adjacent cells opposite the phloem undergo two almost simultaneous oblique asymmetrical divisions and later more transversal and periclinal divisions (Casero et al., 1995). In maize, periclinal divisions related to LR initiation occur 21–24 mm behind the tip (Casero et al., 1995). In most species, initiating LR primordia are located in the maturation zone (Lloret and Casero, 2002); consequently, the pericycle cells involved in this process are usually considered to be differenciated at the moment of LR initiation (Alarcón et al., 2016).

Several methods have been used to analyze LR development. The absolute number of LRs is not a good parameter of LR formation because it is strongly dependent on parent root length (Lloret and Pulgarín, 1992). Consequently, it evaluates not only LR formation but also main root elongation. The lateral root density (LRD) method determines the number of LRs per unit length of parent root. Currently, there is a trend to consider both emerged LRs and LR primordia, and to analyze exclusively the parent root zone that bears LRs and/or LR primordia (Lloret et al., 1988; Pulgarín et al., 1988; Dubrovsky et al., 2009). This is a better index of LR formation because it avoids distortions caused by the mother root zones where no LR initiation occurs. Another advantage of the LRD index is that it allows the comparison of LR formation in primary roots with different elongation rates. The recent implementation of the method to analyze LR formation through the determination of the "lateral root initiation index" (I_{LRI}) represents a new and significant advance (Dubrovsky et al., 2009). This index describes the number of LR initiation anlages occurring along a root portion corresponding to 100 cortical cells in a file. The main advantage of using this index to describe LR initiation is that it offers a more integrative and cellular perspective, since it considers both the growth and rate of cell formation.

In this work, we show that exogenous auxin treatment of maize primary roots has a dual effect on LR formation, i.e., low doses promote the initiation of new primordia, whereas high doses inhibit this process. Therefore, the concept of auxin as a phytohormone which stimulates LR initiation should be re-evaluated, as was the role of ethylene as a general root growth inhibitor (Pierik et al., 2006). To explain the contrasting effects of auxin treatment on LR initiation, we propose that auxin modulated initiation of LRs is linked to pericycle FC length.

MATERIALS AND METHODS

Plant Material and Growth Conditions

Seeds of the *Zea mays* L. hybrid, DK 626, were sterilized by immersion in ethanol for 5 min. They were then washed three times and soaked in distilled water with aeration at 30°C. After 24 h, the seedlings, with radicles approximately 1 mm long, were placed vertically in holders made of Styrofoam disks, transferred into boxes, and placed in a humid environment, in the dark, at 30°C. They were kept in these boxes for 24 h until the roots reached a length of 20 ± 5 mm. Disks with 10 selected seedlings of equal root length were placed in bottles containing 1.5 L aerated growth solution and grown at 30°C in the dark. As Ca^{2+} and K^{+} are required for proper development of roots growing in hydroponic medium (Lee et al., 1983; Hasenstein and Evans, 1986; Walker et al., 1998), the growth medium consisted of a buffered solution of 1 mM HEPES (4-(2-hydroxyethyl)-1-piperazineethanesulfonic acid) supplemented with 1 mM Ca_2Cl and 10 mM KCl at pH 6.0. HEPES was used as a buffering agent because it is highly soluble and chemically and enzymatically stable, in addition to having other advantages. The experimental conditions used in this study have been shown to be optimal for the growth of maize roots (Alarcón et al., 2009). After acclimation for 24 h, when the roots were 80 mm long, the synthetic auxin 1-naphthalene acetic acid (NAA) was added to the solution and the treatment was maintained for 48 h. Root length was measured with a ruler (accuracy ± 1 mm) before NAA application, and after 24 and 48 h of treatment. After NAA application, two 2-cm long consecutive root zones could be distinguished, that we called zones A and B (**Figure 1**). The proximal A zone elongated before auxin application, indicating that cell elongation occurred in the absence of the exogenous hormone. In contrast, the distal

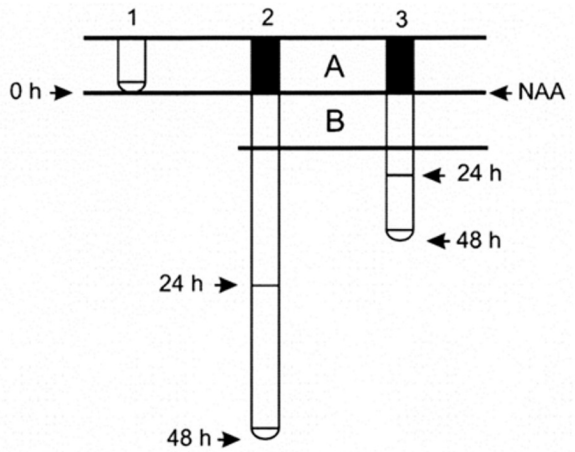

FIGURE 1 | Formation of two 2-cm long consecutive zones in the maize primary root after NAA application. At time 0, treatment was performed by applying NAA to the growth medium (1). Zone A (filled) is elongated before auxin application, hence cell elongation occurred without auxin influence. In contrast, zone B (unfilled) elongated in the presence of auxin. Subsequently, the root grows and lateral roots develop in both zones under the influence of exogenous auxin. Note that after 48 h, root elongation was greater in control (2) than in auxin-treated roots (3).

B zone grew in the presence of exogenous auxin. However, LR development occurred under exogenous auxin influence in both zones.

Chemicals

Concentrated solutions of NAA were prepared in 1 mM HEPES buffer. The volumes added to the growth medium were less than 0.1% of the total volume. All the chemicals were purchased from Sigma, except $CaCl_2$ and KCl (Merck).

Determination of Lateral Root Density in Selected Root Zones

To allow the development of the LR primordia until they were clearly identifiable under a dissecting microscope to facilitate quantification, roots were cultivated in growth medium for 48 h. The primary root length was then measured and zones A and B were selected. The root zones were fixed in FAA fixative for 48 h. FAA is a mixture of 50% ethanol, 36% formaldehyde, and 100% acetic acid (91:6:3, v/v). The roots were subsequently transferred to 70% ethanol. LRs were quantified by observation under a dissecting microscope. The positions of the LRs were also recorded. The number of LRs that were formed during the experimental period was calculated as well as LRD in zones A and B. Both variables were determined as the number of LRs plus LR primordia per cm.

Determination of Cell Length and Parameters of LR Formation

To measure cell length, 5-mm long central segments of zones A and B were selected. These segments were embedded in paraffin and cut into 8-μm serial longitudinal sections. Cell length was determined for at least five root segments for each treatment, measuring 12 cells per segment.

The calculation of the percentage of phloem pericycle cells (PPCs) that behave as FCs requires the previous determination of two variables in zones A and B, namely, LRD and PPC length. To estimate this percentage, each LR primordium is assumed to originate from four phloem pericycle FCs, since LR primordium initiation in maize has been described as involving asymmetrical transverse divisions of a pair of adjacent pericycle FCs in each file (Casero et al., 1995), and that each phloem pole in maize is surrounded by two phloem pericycle cell files. The new index for LR formation that we propose is based on the percentage of PPCs (%PPC) that behave as FCs. The percentage of PPC that become FCs was estimated by dividing the total number of FCs that gave rise to the LRs in a specific zone (equal to the number of LRs multiplied by four cells) by the total number of PPCs present within the same zone and by multiplying this ratio by 100. The results of %PPC are presented as the mean ± SD of at least five root segments per treatment.

Another index of LR formation (I_{LRI}) was calculated as established by Dubrovsky et al. (2009) for *Arabidopsis* roots. This index was defined to analyze the number of LRs and/or LRPs that developed in a primary root segment containing 100 cortical cells. This index was also calculated in at least five root segments per zone, and per treatment.

The relative rate of PPC cell production could be linked to LR formation. This rate of cell production (RCP) (Ivanov and Dubrovsky, 1997) can be calculated for a specific time by dividing the elongation velocity of the primary root by the average cell length of the cell type of interest. We calculated the RCP as the number of PPCs produced per meristem file per unit of time. At least five root segments were used per experimental group.

Measurements and Statistical Analysis

The values obtained for root elongation and LRD are represented as the mean ± SD of 10 roots. The other variables had a sample size of at least five root segments per experimental group. Each experiment was repeated at least twice. Comparison of multiple means was performed using one-way ANOVA and Tukey's test (SPSS 13.0). Differences of means were considered significant at $P < 0.05$.

RESULTS

Exogenous 1-Naphthalene Acid (NAA) Application Increases LRD

The LR distribution pattern along the primary root of maize is shown in **Figure 2**. The number of LRs plus LR primordia per cm was determined in 2-cm long control and 0.01 μM NAA-treated root segments. The distribution of the LRs in control roots showed a characteristic pattern with several different zones. In the basal-most parent root segment, the density was relatively low (15–17 LRs/cm). In the segment between 2 and 4 cm from the base, the LRD then increased until the zone

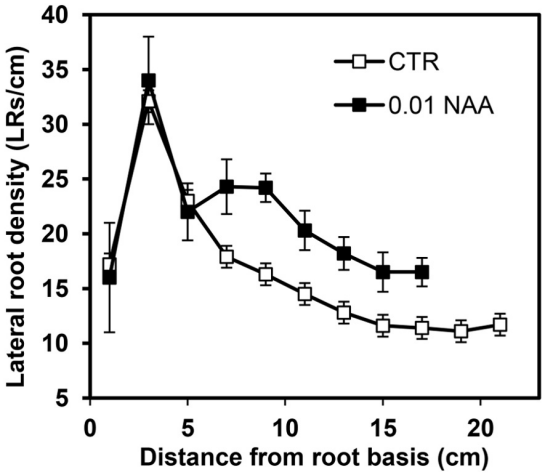

FIGURE 2 | Effect of 0.01 μM NAA treatment on lateral root density (LRD) in the maize primary root. LRD was measured in 2-cm-long root segments from the base to the root tip. Auxin was applied when the roots were 8 cm long and LR formation was followed during a subsequent 48 h period. Note the inhibitory effect of NAA on root elongation and the stimulating effect on LRD in the youngest root zones analyzed. Values represent mean ± SD (n = 10).

of highest density (30–35 LRs/cm), and then decreased sharply to 15 LRs/cm in the segment located 6–8 cm from the root base. From this point toward the apex, the LRD declined slowly and then stabilized at a value close to 12 LRs/cm. LR primordia were not detected in the zone adjacent to the root apex.

The application of 0.01 μM NAA stimulated the formation of LRs in the primary root of maize. This stimulation was observed as a wide extension of the parent root, mainly affecting the more distal root segments (**Figure 2**); in the youngest root segments grown after NAA treatment, significant LRD stimulation (treated: 24.3 ± 3.0 LRs/cm vs. control: 15.9 ± 2.5 LRs/cm) was observed. Promotion of LR formation also occurred in new segments formed after beginning of treatment. In contrast, more proximal root zones were apparently insensitive to auxin treatment (**Figure 2**).

In addition, application of 0.01 μM NAA inhibited primary root elongation by 30% and reduced the number of segments along the root where LRs normally form. Consequently, a relationship between the parent root growth and LR formation was analyzed in more details.

Relationship Between Primary Root Elongation and Lateral Root Formation

Maize primary root elongation was inhibited by NAA treatment in a concentration-dependent manner, with a consequent reduction of the area where LRs can develop (**Table 1**). A low NAA concentration (0.01 μM) marginally inhibited primary root elongation, but increased the total number of LRs after 48 h of treatment (**Figures 3A,B**). However, higher NAA concentrations elicited a large reduction in the absolute number of LRs (**Figure 3A**), as well as a strong concomitant reduction in primary root elongation. Therefore, the inhibition of LR formation could be due, at least in part, to the reduction in primary root elongation. Concentrations of NAA in the 0.05–0.1 μM range resulted in stronger inhibition of root elongation (up to 75%), and 0.5 μM NAA completely inhibited primary root elongation (data not shown). When primary root elongation is inhibited, LR primordia have limited physical space to develop, and LRD (number of LRs and/or LR primordia per unit length) may therefore be a better index to evaluate LR formation than the absolute number of LRs. **Figure 3C** shows that 0.01 and 0.05 μM NAA significantly increased the average LRD. However, the stimulatory effect was lost with application of higher doses of NAA. This suggests that high concentrations of auxin, which resulted in strongly reduced primary root elongation, inhibit LR formation.

Moreover, strong inhibition of primary root elongation could result in segments located in the same position in both control and treated roots not forming at the same time (**Figure 1**). As segments at the same position would not be homologous, comparison of LRD between control and treated roots becomes difficult, and even meaningless in extreme cases. Therefore, it is appropriate, as far as possible, to compare root segments of the same age and similar relative location along the primary root (homologous segments).

TABLE 1 | Concentration-dependent effects of NAA on cell length and root elongation.

Zone	Groups	Root elongation (mm/48 h)	ECL (μm)	CCL (μm)
A	0.00 NAA	129.3 ± 9.1 (100)a	152.8 ± 6.3 (100)a	191.9 ± 14.1 (100)a,b
A	0.01 NAA	–	144.4 ± 17.5 (95)a	182.7 ± 9.5 (95)a,b
A	0.05 NAA	–	150.6 ± 18.9 (99)a	168.6 ± 11.0 (88)b
A	0.10 NAA	–	151.6 ± 21.3 (99)a	204.4 ± 15.5 (107)a
B	0.00 NAA	128.4 ± 17.3 (100)a	154.8 ± 20.5 (100)a	195.6 ± 13.1 (100)a
B	0.01 NAA	97.4 ± 17.0 (76)b	121.2 ± 10.5 (78)b	167.0 ± 16.0 (85)b
B	0.05 NAA	50.7 ± 9.3 (39)c	60.6 ± 11.4 (39)c	91.8 ± 10.5 (47)c
B	0.10 NAA	31.8 ± 3.5 (25)d	48.5 ± 2.5 (31)c	65.2 ± 11.3 (33)d

The mean cell length of the epidermis (ECL) and cortex (CCL) in zones A and B under different experimental conditions are indicated. Different letters indicate significant differences compared to control roots (ANOVA, $P < 0.05$). Cell length values are the mean ± SD of at least five roots (measuring 12 cells per root). The sample size for the root elongation rate was 18 roots. Values in parentheses indicate the percentage compared to untreated roots in the same zone. Zone A developed before NAA treatment, and zone B after NAA treatment.

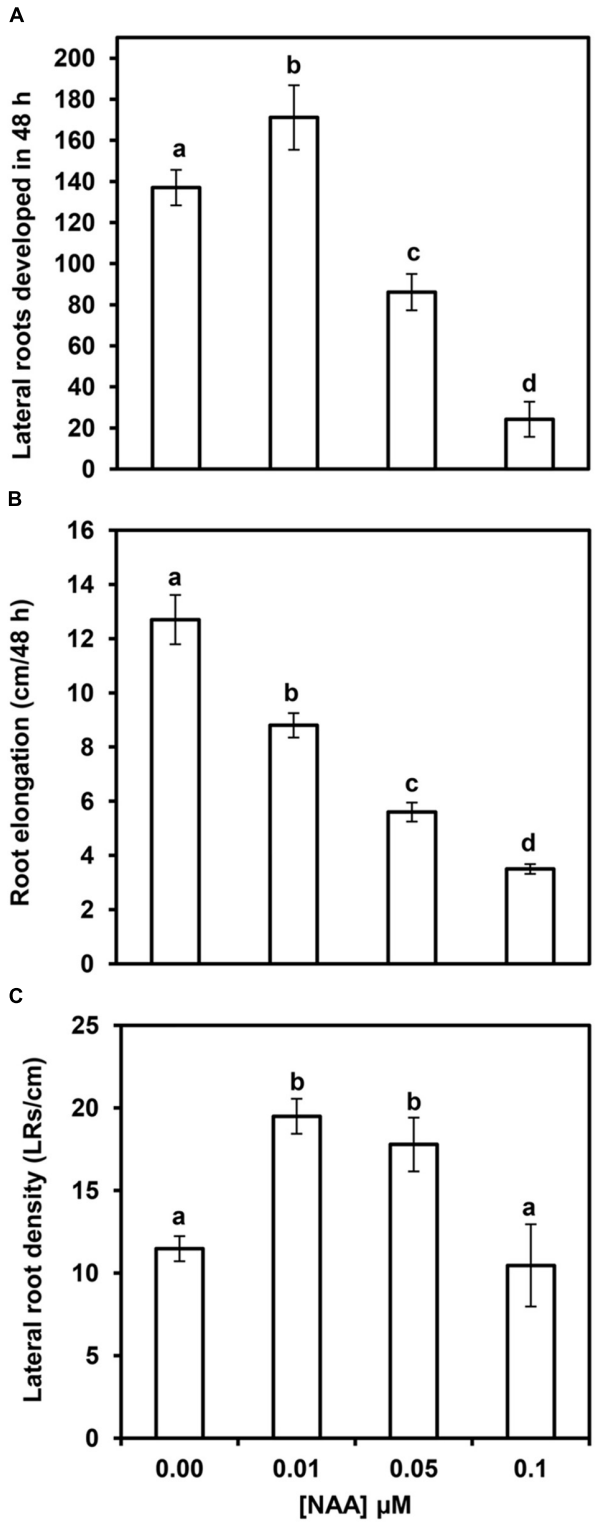

FIGURE 3 | Effects of several NAA concentrations on lateral root (LR) formation and primary root elongation within 48 h after NAA application. Number of LRs plus LR primordia **(A)**, primary root elongation **(B)**, and average LRD **(C)** in the formed segments of primary maize roots. Values are mean ± SD (n = 10). Different letters indicate significant differences at $P < 0.05$ (ANOVA and Tukey's test).

Root Zones Formed Before and After NAA Treatment

At the beginning of NAA treatment, there were two homologous zones in control and treated roots which were formed. We called these zone A and zone B (**Figure 1**), and they exhibit several clear differentiating features. The main difference between the two zones was that the A zone elongated in the absence of exogenous auxin, but LR development occurred in the presence of NAA; as meanwhile, the B zone elongated and initiated LR primordia in the presence of auxin. Corresponding zone in untreated roots was defined as a root portion formed during the same time. Additionally, these two zones showed different thickness, LRD, and stages of LR primordium development (**Figure 4**).

Auxin application elicits a progressive increase in the thickness of zone A (**Figure 4**), without apparently affecting LR primordium initiation or development (**Figure 4**). In contrast, LR development appeared to be altered in the B zone (**Figure 4**). The existence of these two segments that developed in a short period, but under different physiological conditions, allows the separation of the effects of auxin on root elongation and LR formation.

NAA Application Elicits Different Effects on LRD in Zones A and B

The obtained LRD values for untreated primary roots for zones A and B were 18.8 ± 2.9 and 17.6 ± 1.8, respectively (**Table 2**). These results did not differ significantly ($P > 0.05$, ANOVA and Tukey's test for unplanned comparisons). The application of NAA at 0.01, 0.05, and 0.1 µM concentrations significantly increased LRD in zone A. This variable increased from 18.8 ± 2.9 in untreated roots to an average of approximately 25 LRs per cm in NAA-treated roots. No significant differences in LRD were found between different NAA concentrations, showing that the stimulatory effect seen in zone A was independent of NAA concentration (**Table 2**). In contrast, the effect of NAA on LR development in zone B was concentration-dependent. As in zone A, application of 0.01 µM NAA resulted in a significant increase in LRD. However, with 0.05 µM NAA, LRD stimulation was lost, and was reduced to values lower than observed for control roots with the highest NAA doses (**Table 2**).

Reduction of Epidermal and Cortical Cell Length by NAA Treatments

We measured epidermal and cortical cell length in zones A and B of both control and NAA-treated roots. The majority of cells in zone A had finished elongating at the onset of auxin treatment. Therefore, we expected that NAA application would not affect cell length in zone A. Indeed, our results showed that the length of epidermal cells was not reduced in this zone with any NAA dose used (**Table 1**); moreover, cortical cell length in zone A also showed a tendency to maintain cell length. In relation to cortical cell length, the tendency was also to maintain similar values in both treated and control roots. The minimum length was recorded in roots treated with 0.05 µm NAA (12% reduced vs. control roots). However, this reduction in cell length was not statistically significant (**Table 1**).

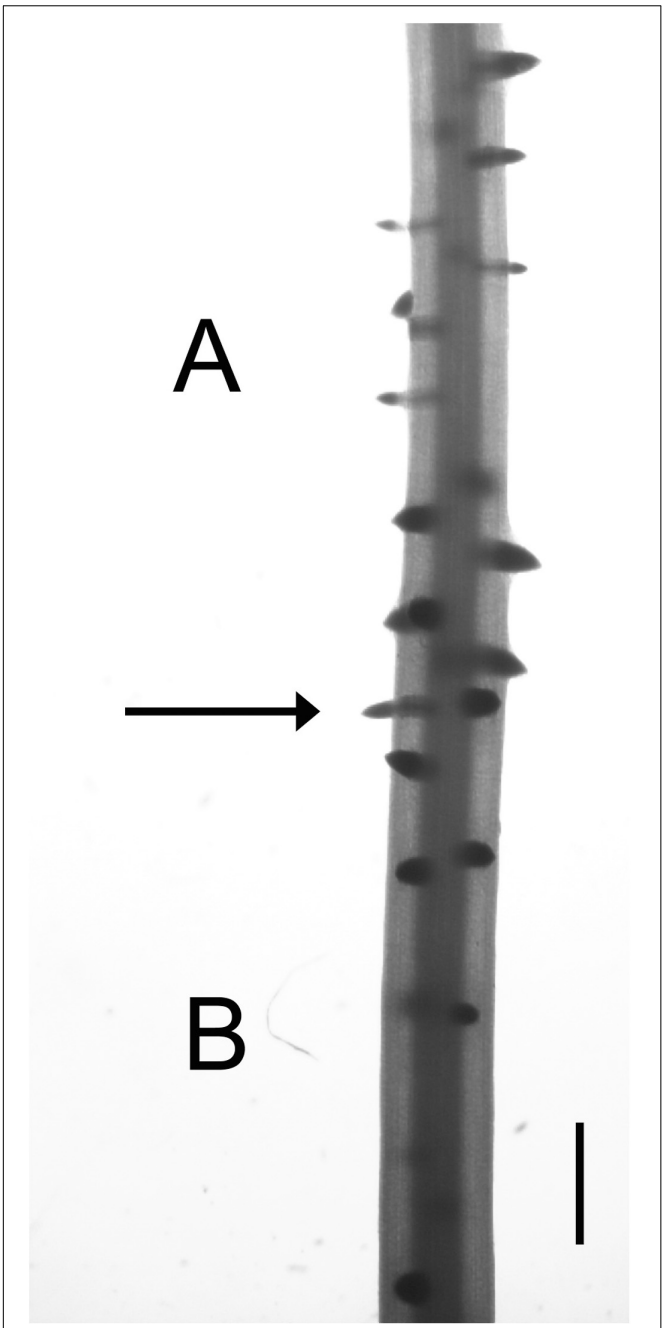

FIGURE 4 | The junction between zones **A** and **B** in 0.1 μM NAA-treated maize roots. Micrograph of a maize root fragment at the junction between zones **A** and **B** (arrow). Note that zone **A** zone is thinner and shows a high LRD with numerous emerged lateral roots (LRs). In contrast, zone **B** is thicker, with relatively few un-emerged LRs. Scale bar = 1 mm.

In zone B, inhibition of root elongation by NAA was always accompanied by a reduction in the length of epidermal and cortical cells (**Table 1**). This reduction was progressive and always statistically significant, except for the epidermal cells of the group treated with 0.1 μM NAA, where cell length was 48.1 μm, likely near the lower limit for non-elongated cells (**Table 1**).

Reduction of Pericycle Cell Length by NAA Results in Decreased LRD

To study a possible relationship between pericycle cell length and LR formation, both parameters were analyzed comparatively in roots treated with several concentrations of NAA (**Table 2**). The mean PPC length in zone A of control roots was 264.3 ± 22.8 μm. In a given root segment, the number of PPCs in a cell file can be calculated by dividing the total length of the segment by the mean length of PPCs. In our sample, the mean number of phloem poles was 15 and the number of PPC cell files at each phloem pole was calculated as two. Consequently, the total number of PPCs in a specific root segment can be estimated by multiplying by 30 (2 PPC cell files per pole and 15 phloem poles) the average number of cells in a pericycle cell file along the entire length of the segment.

As we consider that each LR primordium originated from four FCs per phloem pole, and LRD was 18.8 ± 2.9 in zone A of control roots, the percentage of FCs out of total number of PPC is equal to 6.5 ± 0.5 (**Table 2**). Application of 0.01, 0.05, or 0.1 μM NAA did not significantly affect the length of pericycle cells in zone A, but the LRD was significantly increased (**Figure 3C**). Hence, the percentage of FCs increased from 6.5 to 10.4, 9.6, and 9.1, respectively, after NAA treatment (**Table 2**). A similar increase in LR formation was observed when the lateral root initiation index (I_{LRI}) was calculated according to Dubrovsky et al. (2009).

In zone B of untreated roots, the values for PPC length, LRD, percentage of FCs, and I_{LRI} (265.8 μm, 17.6 LRs/cm, 6.1%, and 33.8, respectively) were similar to those found in zone A (**Table 2**). Application of 0.01 μM NAA promoted a significant increase in LRD (24.9 LRs/cm) in zone B, which was accompanied by a parallel increase in the percentage of FCs (8.2%) and I_{LRI} (41.6%) compared with control roots (**Table 2**). However, treatments with higher concentrations of NAA significantly reduced the mean PPC length, LRD, percentage of FCs, and I_{LRI} (**Table 2**). Taken together, these data clearly show that the inhibition of PPC elongation by high NAA concentrations resulted in a reduced rate of LR formation.

We also determined the RCP values to establish whether there was a reduction in pericycle cell production in roots subjected to treatments with high concentrations of auxin. It was possible that this reduction could be linked to a decrease in the rate of LR primordium production. In control roots, this variable showed values of 7.8 ± 1.3 and 9.6 ± 0.4 cells per row per hour for zones A and B, respectively, when they formed (**Table 2**). This variable decreased in treated roots until reaching a minimum value of 6.1 ± 09 PPCs per cell file per hour in zone B. Consequently, there was a reduction of approximately 35% in the RCP. However, the apical meristem of the root never ceased producing new cells.

DISCUSSION

Competence Period for LR Initiation

Studies in different species have tended to confirm that pericycle cells respond only to factors that trigger LR

TABLE 2 | Lateral root formation in maize roots under different exogenous auxin treatments.

Zone	Groups	PPCL	LRD	%FC	I_{LRI}	RCP
A	0.00 NAA	264.3 ± 22.8a	18.8 ± 2.9a	6.5 ± 0.5a	36.0 ± 5.0a	7.8 ± 1.3a
A	0.01 NAA	279.0 ± 18.1a	25.5 ± 2.8b	10.4 ± 1.2b	50.9 ± 5.2b	6.9 ± 1.6a
A	0.05 NAA	268.8 ± 12.5a	25.9 ± 2.5b	9.6 ± 1.0b	45.2 ± 4.4b	7.7 ± 0.5a
A	0.10 NAA	277.2 ± 32.4a	24.8 ± 2.6b	9.1 ± 1.6b	50.2 ± 7.3b	7.8 ± 1.4a
B	0.00 NAA	265.8 ± 12.8a	17.6 ± 1.8a	6.1 ± 0.9a	33.9 ± 4.7a	9.6 ± 0.4a
B	0.01 NAA	248.1 ± 40.7a	24.9 ± 1.4b	8.2 ± 1.2b	41.6 ± 4.8b	7.2 ± 1.7b
B	0.05 NAA	139.4 ± 23.2b	21.5 ± 3.3c	4.3 ± 0.6c	21.4 ± 1.8c	6.2 ± 0.7b
B	0.10 NAA	110.1 ± 17.4b	10.6 ± 2.6d	1.7 ± 0.3d	7.5 ± 1.4d	6.1 ± 0.9b

The data correspond to zones A and B of the primary root formed, respectively, before or after different NAA treatments (groups). Phloem pericycle cell length in μm (PPCL), mean number of lateral roots per cm of parent root (LRD), percentage of founder cells (%FC), index of lateral root initiation (I_{LRI}) as defined by Dubrovsky et al. (2009), and root production rate per cell file per hour for phloem pericycle cells (RCP) are presented. The figures correspond to mean values ± SD. Different letters indicate statistically significant mean differences within each column and zone (one-way ANOVA, Tukey's test, $P < 0.05$). Values for pericycle cell length correspond to five roots, measuring at least 15 cells per root. The LRD was calculated from 10 roots. The percentage of FCs was calculated based on known values of LRD and PPCL, and assuming that the maize root has 15 poles of phloem, each of them with two columns of pericycle cells, and that each LR is initiated from four PPCLs.

initiation during a short period of time, called the competence period or developmental window (Abadía-Fenoll et al., 1986; Dubrovsky et al., 2006). The existence of a competence period results in LR initiation following an essentially acropetal sequence, with new LR primordia initiating distally to those formed previously (Lloret and Casero, 2002). According to Dubrovsky and Rost (2012), at least two events must occur in *Arabidopsis thaliana* roots before the first cell divisions of LR primordium organogenesis occur, namely, priming and specification of pericycle FCs. Priming can be considered as cell commitment to LR formation. In most higher plant species, this phenomenon occurs in the transition zone between the root apical meristem and the elongation zone (Dubrovsky and Rost, 2012). Specification consists of pericycle FCs acquiring a developmental fate different from other pericycle cells, and participating in LR primordium initiation (Dubrovsky and Rost, 2012). Local accumulation of free auxin has been shown to be a prerequisite for FC specification (Dubrovsky et al., 2008). Priming and specification can occur within a time interval shorter than a cell cycle (Dubrovsky and Rost, 2012). Consequently, these two processes should be concluded when pericycle cells eventually reach the end of the elongation zone, explaining the narrow developmental window for LR initiation.

Our results presented in **Figure 2** support the hypothesis of the existence of a short competence period for LR initiation. Indeed, only the youngest root fragments increase their LRD in response to treatment with 0.01 μm NAA. Stimulation of LR formation by auxin in newly formed root zones is expected as this hormone is considered the main regulator of LR formation (Lloret and Pulgarín, 1992; Hobbie, 1998; Lloret and Casero, 2002), and numerous young pericycle cells capable of becoming FCs exist in this region (Dubrovsky et al., 2006). In the preformed regions close to the root apical meristem, we also found that NAA treatment stimulated LR formation. This suggests that pericycle cells that are primed, but not specified, will eventually develop LRs as a result of the treatment. In this case and under normal conditions, the possible regions for LR formation would be more abundant than regions where LR primordia will eventually develop.

Pericycle Cell Length and Auxin Response During LR Formation

It is well-known that exogenous auxin treatment normally promotes LR formation in several plant species (Zeadan and Macleod, 1984; Hurren et al., 1988; Lloret and Pulgarín, 1992; Zhang and Hasenstein, 1999; Nieuwland et al., 2009). Overall, the high auxin concentrations used in these experiments also inhibited primary root elongation, posing the question as to whether both effects of auxin on root system development are related. Recent evidence suggests complex effects of auxin on LR initiation in *A. thaliana* roots showing reduced cell elongation (Ivanchenko et al., 2010). The above mentioned study demonstrated that when the primary root elongation rate is reduced, the promotion of LR formation by auxin diminishes with increasing concentrations of this phytohormone. Our results in *Z. mays* agree entirely with those obtained in *A. thaliana* roots. The suggested connection between inhibition of primary root elongation and reduced LR formation would be mediated by a decrease in the sensitivity of pericycle cells to auxin under conditions of reduced growth (Ivanchenko et al., 2010).

We propose an alternative hypothesis to explain the same phenomenon in maize roots. The loss of the ability of auxin to stimulate LR formation when applied at high concentration may be due to the substantial reduction in cell length occurring in the pericycle of maize under conditions of reduced growth. Notably, in the study by Ivanchenko et al. (2010), a maximum inhibition of approximately 8% in cortical cell length was achieved, whereas in our experiments we observed a reduction in length of nearly 60% (**Table 2**). Our hypothesis does not exclude that other factors apart from cell length may be linked to the mechanism that controls LR formation under conditions of reduced growth of the primary root. However, variations in the length of pericycle FCs fully and reasonably justify the behavior of LR initiation observed in our experiments.

Our analysis of LRD in zones A and B of the maize root is especially important. Zone A corresponded to the apical-most 2 cm of primary root length when NAA treatment began and, consequently, had a pericycle too young to show advanced stages of LR development. Zone B was generated by the apical meristem during NAA treatment and new LRs were formed during the same time and under the same treatment. Nevertheless, the elongation process was different between the two root zones. In our experiment, zone A cells located proximally to the elongation zone grew without the influence of auxin. In contrast, in the B zone, the root elongation process occurred in the presence of auxin. Consequently, this experimental system can discriminate whether an effect on LR formation is independent or dependent of root elongation.

In our experiments, roots treated with 0.01 and 0.05 μM NAA showed increased LRD, in both the A and B zones. Nevertheless, strong NAA doses (0.1 μM) increased LRD in zone A, but not in zone B. This indicates that the promoting effect of auxin on LR formation is lost in the latter zone with 0.1 μM auxin treatment. The situation in zone B contrasted with the stimulation of LRD in zone A after the same auxin treatment. The most likely explanation for this phenomenon is that the high auxin concentration used in this experiment interacts with another factor to elicit a differential response in zones A and B.

Maize LRs originate from pericycle FCs located opposite the phloem poles of the parent root (Casero et al., 1995). The initiation of LRs depends on a controlled sequence of cell divisions, some of which are asymmetrical (Casero et al., 1995). Studies in diverse organisms, from bacteria to vertebrates, indicate that cell cycle commitment to the G1 to S phase transition requires that cells grow to a critical size, which is an active mechanism to ensure cell size homeostasis (Dungrawala et al., 2012). Recent evidence in plants also suggests that cell size is one of the variables controlling cell cycle progression (Rioboo et al., 2009; Bush et al., 2015; Löfke et al., 2015; Jones et al., 2017). Cells must have a mechanism for coordinating their rates of cell growth and division. In budding yeast, growth to a "critical cell size" must be achieved before cells pass the check point known as START and transition from the G1 to the S phase (Dungrawala et al., 2012). The START point is equivalent to the restriction point in mammalian cells (Dungrawala et al., 2012). Therefore, it is possible that most pericycle cells in zone B in our study, had lost their ability to proliferate and launch LR primordium initiation as a result of their extremely short length after treatment with auxin 0.1 μM NAA. Conversely, it has been demonstrated that when the *Arabidopsis* root is bent there is a strict correlation between cell size, auxin transport, and stimulation of LR formation in the convex side of the curvature (Laskowski et al., 2008). In this system, a maximal level of auxin is established on the convex side of the curvature where LR primordia are initiated, whereas on the concave side of the curvature, where short pericycle cells are located, LR primordia do not develop.

As with other developmental processes, LR initiation requires that a series of asymmetrical cell divisions take place (Casero et al., 1995). Alterations in cell expansion could affect not only the ability of pericycle cells to divide, but also their ability to divide asymmetrically. During the segmentation of new colonies of the green alga *Volvox*, gonidial cells are produced after asymmetrical cell divisions. It has been demonstrated that the large size of the gonidial cells is the primary reason for differences in cell fate, morphologic characteristics, and cell division behavior compared to somatic cells (Kirk et al., 1993). In plants, the polarized expansion of the wall may be a mechanism that promotes asymmetries in cell division (Menke and Scheres, 2009). In addition, it has been proposed an inhibition of asymmetrical divisions in short pericycle cells during LR initiation (De Smet et al., 2008).

Moreover, it was recently shown that overexpression of the small peptide GLV6 disrupted the first asymmetric divisions required for the formation of a viable LR primordium, resulting in a reduced number of emerged LRs (Fernandez et al., 2015). It is well known that GLV peptides are also implicated in the regulation of cell elongation (Ghorbani et al., 2016). Consequently, pericycle cell elongation and LR initiation are likely to be interrelated processes.

The reduction in the density of LR primordia observed when NAA was applied at high concentrations could be related to a reduction in the rate of production of cells in the root apical meristem, or a consequence of the shortening of pericycle cell length. Indeed, cell became shorter even though NAA did not completely inhibit root elongation. Importantly, the RCP value for the PPC responsible for the initiation of LR primordia was maintained at a level of approximately six cells per cell file per hour (**Table 2**), apparently sufficient to promote a high density of LR primordia. However, the results presented here suggest that the specification process for LR initiation in PPCs is highly compromised when cell elongation is strongly reduced.

Therefore, pericycle cell length could play an important role in regulating the formation of LRs. For maize roots at least, LR initiation can no longer be interpreted only from an organismal perspective. In pericycle cells, in addition to regulatory effects that operate at the level of the whole plant, cell length appears to be a possible modulator in the control of LR initiation.

Quantification of LR Formation

The quantification of LR formation is an important but somewhat complex topic (Dubrovsky et al., 2009). One difficulty to consider is that both already emerged LRs and endogenous LR primordia are not visible unless you clear the root or obtain histological sections. Another difficulty is that comparisons must frequently be established between roots of different ages and lengths that have been growing at very different growth rates. Hence, our results should be normalized to enable meaningful comparisons between root zones with homologous development (**Figure 1**).

To compensate for the influence of the primary root length on LR formation, two useful strategies have been developed to date. The first is to divide the number of LRs (independently of whether they are LR initiation events or already emerged roots) by the length of the region of the primary root containing both LRs and LR primordia (Lloret et al., 1988; Lloret and Pulgarín, 1992). A regularly used alternative option for this type of calculation has been to divide the length of the primary root into segments of fixed length and recount the number of LRs present in each segment (Hummon, 1962; Lloret et al., 1988;

MacLeod, 1990; Varney et al., 1991; Lloret and Pulgarín, 1992). The second strategy consists of relating LR formation indices to the intervening cells between successive initiation events (Lloret et al., 1985; Dubrovsky et al., 2009). This protocol is useful because it adjusts the results for the differences in primary root growth rate. Both methods have advantages and disadvantages, but indices based on the latter type are the most appropriate from the point of view of developmental biology because they reveal whether the FCs were produced by the root apex at a regular rhythm.

However, not all FCs formation result in LR development, and then the longitudinal spacing pattern of LRs becomes more difficult to evaluate (Charlton, 1983; Barlow and Adam, 1988; Lloret and Casero, 2002). Recently, this issue was revisited in the model plant *A. thaliana* (Dubrovsky et al., 2006). In the same species, an index based on cortical cell length, called the lateral root initiation index (I_{LRI}), has been applied to study LR distribution patterns (Dubrovsky et al., 2009). Here, we present a new method to evaluate LR formation that is relatively simple but highly effective in estimating LR formation, namely, the percentage of FCs.

The I_{LRI} proposed by Dubrovsky et al. (2009) defines root segments as a function of the length of fully elongated cortical cells. Nevertheless, LR initiation starts in pericycle FCs, and it may be more appropriate to relate the index to pericycle cells instead of cortical cells. Therefore, we directly calculated the percentage of FCs. Despite the differences, these indices produced similar estimations of LR formation under different experimental conditions (see **Table 2**). For example, the increase in the percentage of pericycle FCs compared to the control was 48% in roots treated with 0.05 μM NAA. This change is consistent with the reduced length of epidermal or cortical cells occurring under the same treatment (39 and 47%, see **Table 1**). In contrast, an increase of approximately 30% is observed if the index is calculated using cortical cell length (I_{LRI}).

In summary, a new index based on the percentage of pericycle cells that produce LR primordia is presented in this report. This index provides a more accurate tool for the estimation of LR formation, as the measurements are made on pericycle FCs which initiate LR formation, and are the most directly implicated in this process. In addition, we compared this new index with a previous index based on cortical cell length and obtained similar results. The results of our study also showed that auxin modulated initiation of LRs is closely linked to pericycle cell length.

AUTHOR CONTRIBUTIONS

MA, JS, and PL conceived the study, contributed to methodology, wrote the original draft, and acquired the funding.

FUNDING

This work was supported by grants to research groups GR15158, GR18114 from Junta de Extremadura, and by FEDER funds, and CCESAGROS project.

ACKNOWLEDGMENTS

We thank Alberto Lloret-Salamanca for reviewing our text in English.

REFERENCES

Abadía-Fenoll, F., Casero, P. J., Lloret, P. G., and Vidal, M. R. (1986). Development of lateral primordia in decapitated adventitious roots of *Allium cepa*. *Ann. Bot.* 58, 103–107. doi: 10.1093/oxfordjournals.aob.a087178

Alarcón, M. V., Lloret, P. G., Iglesias, D. J., Talón, M., and Salguero, J. (2009). Response of maize seedling roots to changing ethylene concentrations. *Russ. J. Plant Physiol.* 56, 488–494. doi: 10.1134/S1021443709040074

Alarcón, M. V., Lloret, P. G., Martín-Partido, G., and Salguero, J. (2016). The initiation of lateral roots in the primary roots of maize (*Zea mays* L.) implies a reactivation of cell proliferation in a group of founder pericycle cells. *J. Plant Physiol.* 192, 105–110. doi: 10.1016/j.jplph.2016.02.005

Barlow, P. W., and Adam, J. S. (1988). The position and growth of lateral roots on cultured root axes of tomato, *Lycopersicon esculentum* (Solanaceae). *Plant Syst. Evol.* 158, 141–154. doi: 10.1007/BF00936340

Bush, M. S., Crowe, N., Zheng, T., and Doonan, J. H. (2015). The RNA helicase, eIF4A-1, is required for ovule development and cell size homeostasis in Arabidopsis. *Plant J.* 84, 989–1004. doi: 10.1111/tpj.13062

Casero, P. J., Casimiro, I., and Lloret, P. G. (1995). Lateral root initiation by asymmetrical transverse divisions of pericycle cells in four plant species: *Raphanus sativus*, *Helianthus annuus*, *Zea mays*, and *Daucus carota*. *Protoplasma* 188, 49–58. doi: 10.1007/BF01276795

Casimiro, I., Beeckman, T., Graham, N., Bhalerao, R., Zhang, H. M., Casero, P., et al. (2003). Dissecting Arabidopsis lateral root development. *Trends Plant Sci.* 8, 165–171. doi: 10.1016/S1360-1385(03)00051-7

Casimiro, I., Marchant, A., Bhalerao, R. P., Beeckmann, T., Dhooge, S., Swarup, R., et al. (2001). Auxin transport promotes Arabidopsis lateral root initiation. *Plant Cell* 13, 843–852. doi: 10.1105/tpc.13.4.843

Casson, S. A., and Lindsey, K. (2003). Genes and signalling in root development. *New Phytol.* 158, 11–38. doi: 10.1046/j.1469-8137.2003.t01-1-00705.x

Charlton, W. A. (1983). "Patterns and control of lateral root initiation," in *Growth Regulators in Root Development*, eds M. B. Jackson and A. D. Stead (London: Monograph 10, British Plant Regulator Group), 1–14.

De Smet, I., Vassileva, V., De Rybel, B., Levesque, M. P., Grunewald, W., Van Damme, D., et al. (2008). Receptor-like kinase ACR4 restricts formative cell divisions in the Arabidopsis root. *Science* 322, 594–597. doi: 10.1126/science.1160158

Dubrovsky, J. G., Gambetta, G. A., Hernández-Barrera, A., Shishkova, S., and González, I. (2006). Lateral root initiation in Arabidopsis: developmental window, spatial patterning, density and predictability. *Ann. Bot.* 97, 903–915. doi: 10.1093/aob/mcj604

Dubrovsky, J. G., and Rost, T. L. (2012). "Pericycle," in *eLS*, 2nd Edn, (Chichester: John Whiley and Sons), 1–10. doi: 10.1002/9780470015902.a0002085.pub2

Dubrovsky, J. G., Sauer, M., Napsucialy-Mendivil, S., Ivanchenko, M. G., Friml, J., Shishkova, S., et al. (2008). Auxin acts as a local morphogenetic trigger to specify lateral root founder cells. *Proc. Natl. Acad. Sci. U.S.A.* 105, 8790–8794. doi: 10.1073/pnas.0712307105

Dubrovsky, J. G., Soukup, A., Napsucialy-Mendivil, S., Jeknic, Z., and Ivanchenko, M. G. (2009). The lateral root initiation index: an integrative measure of primordium formation. *Ann. Bot.* 103, 807–817. doi: 10.1093/aob/mcn267

Dungrawala, H., Hua, H., Wright, J., Abraham, L., Kasemsri, T., Mcdowell, A., et al. (2012). Identification of new cell size control genes in *S. cerevisiae*. *Cell Div.* 7:24. doi: 10.1186/1747-1028-7-24

Evans, M. L., Ishikawa, H., and Estelle, M. A. (1994). Responses of Arabidopsis roots to auxin studied with high temporal resolution: comparison of wild

type and auxin-response mutants. *Planta* 194, 215–222. doi: 10.1007/BF01101680

Fernandez, A., Drozdzecki, A., Hoogewijs, K., Vassileva, V., Madder, A., Beeckman, T., et al. (2015). The GLV6/RGF8/CLEL2 peptide regulates early pericycle divisions during lateral root initiation. *J. Exp. Bot.* 66, 5245–5256. doi: 10.1093/jxb/erv329

Gaspar, T. H., Kevers, C., Faivre-Rampant, O., Crèvecour, M., Penel, C. L., Greppin, H., et al. (2003). Changing concepts in plant hormone action. *Vitro Cell. Dev. Biol. Plant* 39, 85–106. doi: 10.1079/IVP2002393

Ghorbani, S., Hoogewijs, K., Pecenkova, T., Fernandez, A., Inze, A., Eeckhout, D., et al. (2016). The SBT6.1 subtilase processes the GOLVEN1 peptide controlling cell elongation. *J. Exp. Bot.* 67, 4877–4887. doi: 10.1093/jxb/erw241

Hasenstein, K. H., and Evans, M. L. (1986). Calcium dependence of rapid auxin action in maize roots. *Plant Physiol.* 81, 439–443. doi: 10.1104/pp.81.2.439

Hauser, M. T., Morikami, A., and Benfey, P. N. (1995). Conditional root expansion mutants of Arabidopsis. *Development* 121, 1237–1252.

Hobbie, L. J. (1998). Auxin: molecular genetic approaches in Arabidopsis. *Plant Physiol. Biochem.* 36, 91–102. doi: 10.1016/S0981-9428(98)80094-6

Hummon, M. R. (1962). The effects of tritiated thymidine incorporation on secondary root production by *Pisum sativum*. *Am. J. Bot.* 49, 1038–1046. doi: 10.1002/j.1537-2197.1962.tb15044.x

Hurren, N. G., Zeadan, S. M., and Macleod, R. D. (1988). Lateral root development in attached and excised roots of *Zea mays* L. cultivated in the presence or absence of indol-3-yl acetic acid. *Ann. Bot.* 61, 573–579. doi: 10.1093/oxfordjournals.aob.a087591

Ivanchenko, M. G., Napsucialy-Mendivil, S., and Dubrovsky, J. G. (2010). Auxin-induced inhibition of lateral root initiation contributes to root system shaping in *Arabidopsis thaliana*. *Plant J.* 64, 740–752. doi: 10.1111/j.1365-313X.2010.04365.x

Ivanov, V. B., and Dubrovsky, J. G. (1997). Estimation of the cell-cycle duration in the root apical meristem: a model of linkage between cell-cycle duration, rate of cell production, and rate of root growth. *Int. J. Plant Sci.* 158, 757–763. doi: 10.1086/297487

Jones, A. R., Forero-Vargas, M., Withers, S. P., Smith, R. S., Traas, J., Dewitte, W., et al. (2017). Cell-size dependent progression of the cell cycle creates homeostasis and flexibility of plant cell size. *Nat. Commun.* 8:15060. doi: 10.1038/ncomms15060

Kirk, M. M., Ransik, A., Mcrae, S. E., and Kirk, D. L. (1993). The relationship between cell size and cell fate in *Volvox carteri*. *J. Cell Biol.* 123, 191–208. doi: 10.1083/jcb.123.1.191

Laskowski, M., Grieneisen, V. A., Hofhuis, H., Ten Hove, C. A., Hogeweg, P., Marée, A. F. M., et al. (2008). Root system architecture from coupling cell shape to auxin transport. *PLoS Biol.* 6:e307. doi: 10.1371/journal.pbio.0060307

Laskowski, M. J., Williams, M. E., Nusbaum, H. C., and Sussex, I. M. (1995). Formation of lateral root meristems is a two-stage process. *Development* 121, 3303–3310.

Lee, J. S., Mulkey, T. L., and Evans, M. L. (1983). Gravity-induced polar transport of calcium across root tips of maize. *Plant Physiol.* 73, 874–876. doi: 10.1104/pp.73.4.874

Lloret, P. G., and Casero, P. J. (2002). "Lateral root initiation," in *Plant Roots: The Hidden Half*, 3rd Edn, eds Y. Waisel, A. Eshel, and U. Kafkafi (New York, NY: Marcel Dekker, Inc.), 127–155. doi: 10.1201/9780203909423.ch8

Lloret, P. G., Casero, P. J., Navascués, J., and Pulgarín, A. (1988). The effects of removal of the root tip on lateral root distribution in adventitious roots of onion. *New Phytol.* 110, 143–149. doi: 10.1111/j.1469-8137.1988.tb00247.x

Lloret, P. G., and Pulgarín, A. (1992). Effect of naphthaleneacetic acid on the formation of lateral roots in the adventitious root of *Allium cepa*: number and arrangement of laterals along the parent root. *Can. J. Bot.* 70, 1891–1896. doi: 10.1139/b92-234

Lloret, P. G., Vidal, M. R., Casero, P. J., and Navascués, J. (1985). The relationship between lateral-root distribution and endodermis and pericycle cell length in *Allium cepa* L. adventitious roots. *Ann. Bot.* 56, 189–195. doi: 10.1093/oxfordjournals.aob.a087002

Löfke, C., Dünser, K., Scheuring, D., and Kleine-Vehn, J. (2015). Auxin regulates SNARE-dependent vacuolar morphology restricting cell size. *eLife* 4:5868. doi: 10.7554/eLife.05868

Lomax, T. L., Muday, G. K., and Rubery, P. H. (1995). "Auxin transport," in *Plant Hormones: Physiology, Biochemistry and Molecular Biology*, ed. P. J. Davies (Dordrecht: Kluwer), 509–530. doi: 10.1007/978-94-011-0473-9_24

MacLeod, R. D. (1990). Lateral root primordium inception in *Zea mays* L. *Environ. Exp. Bot.* 30, 225–234. doi: 10.1016/0098-8472(90)90068-F

Menke, F. L. H., and Scheres, B. (2009). Plant asymmetric cell division, Vive la difference! *Cell* 137, 1189–1192. doi: 10.1016/j.cell.2009.06.007

Mitchell, E. K., and Davies, P. J. (1975). Evidence for three different systems of movement of indoleacetic acid in intact roots of *Phaseolus coccineus*. *Physiol. Plant.* 33, 290–294. doi: 10.1111/j.1399-3054.1975.tb03171.x

Muday, G. K., and DeLong, A. (2001). Polar auxin transport: controlling where and how much. *Trends Plant Sci.* 6, 535–542. doi: 10.1016/S1360-1385(01)02101-X

Muday, G. K., and Haworth, P. (1994). Tomato root growth, gravitropism, and lateral development: correlation with auxin transport. *Plant Physiol. Biochem.* 32, 193–203.

Nieuwland, J., Maughan, S., Dewitte, W., Scofield, S., Sanz, L., and Murray, J. A. H. (2009). The D-type cyclin CYCD4;1 modulates lateral root density in Arabidopsis by affecting the basal meristem region. *Proc. Natl. Acad. Sci. U.S.A.* 106, 22528–22533. doi: 10.1073/pnas.0906354106

Ohwaki, Y., and Tsurumi, S. (1976). Auxin transport and growth in intact roots of *Vicia faba*. *Plant Cell Physiol.* 17, 1329–1342.

Pierik, R., Tholen, D., Poorter, H., Visser, E. J. W., and Voesenek, L. A. C. J. (2006). The janus face of ethylene: growth inhibition and stimulation. *Trends Plant Sci.* 11, 176–183. doi: 10.1016/j.tplants.2006.02.006

Pulgarín, A., Navascués, J., Casero, P. J., and Lloret, P. G. (1988). Branching pattern in onion adventitious roots. *Am. J. Bot.* 75, 425–432. doi: 10.1111/j.1469-8137.1989.tb00347.x

Rashotte, A. M., Brady, S. R., Reed, R. C., Ante, S. J., and Muday, G. K. (2000). Basipetal auxin transport is required for gravitropism in roots of arabidopsis. *Plant Physiol.* 122, 481–490. doi: 10.1104/pp.122.2.481

Rashotte, A. M., Delong, A., and Muday, G. K. (2001). Genetic and chemical reductions in protein phosphatase activity alter auxin transport, gravity response, and lateral root growth. *Plant Cell* 13, 1683–1697. doi: 10.1105/tpc.13.7.1683

Reed, R. C., Brady, S. R., and Muday, G. K. (1998). Inhibition of auxin movement from the shoot into the root inhibits lateral root development in Arabidopsis. *Plant Physiol.* 118, 1369–1378. doi: 10.1104/pp.118.4.1369

Rioboo, C., O'connor, J. E., Prado, R., Herrero, C., and Cid, A. (2009). Cell proliferation alterations in chlorella cells under stress conditions. *Aquat. Toxicol.* 94, 229–237. doi: 10.1016/j.aquatox.2009.07.009

Ruzicka, K., Ljung, K., Vanneste, S., Podhorská, R., Beeckman, T., Firml, J., et al. (2007). Ethylene regulates root growth through effects on auxin biosynthesis and transport-dependent auxin distribution. *Plant Cell* 19, 2197–2212. doi: 10.1105/tpc.107.052126

Tsurumi, S., and Ohwaki, Y. (1978). Transport of 14C-labeled indoleacetic acid in *Vicia faba* root segments. *Plant Cell Physiol.* 19, 1195–1206.

Varney, G. T., Canny, M. J., Wang, X. L., and Mccully, M. E. (1991). The branch roots of Zea. I. First order branches, their number, sizes and division into classes. *Ann. Bot.* 67, 357–364. doi: 10.1093/oxfordjournals.aob.a088203

Walker, D. J., Black, C. R., and Miller, A. J. (1998). The role of cytosolic potassium and pH in the growth of barley roots. *Plant Physiol.* 118, 957–964. doi: 10.1104/pp.118.3.957

Zeadan, S. M., and Macleod, R. D. (1984). Some effects of indol-3-yl-acetic acid on lateral root development in attached and excised roots of *Pisum sativum* L. *Ann. Bot.* 54, 759–766. doi: 10.1093/oxfordjournals.aob.a086848

Zhang, N. G., and Hasenstein, K. H. (1999). Initiation and elongation of lateral roots in *Lactuca sativa*. *Int. J. Plant Sci.* 160, 511–519. doi: 10.1086/314147

Conflict of Interest Statement: The authors declare that the research was conducted in the absence of any commercial or financial relationships that could be construed as a potential conflict of interest.

frontiers in Plant Science

MINI REVIEW
published: 12 February 2019
doi: 10.3389/fpls.2019.00021

Cell Type-Specific Transcriptomics of Lateral Root Formation and Plasticity

Annika Kortz, Frank Hochholdinger and Peng Yu**

INRES, Institute of Crop Science and Resource Conservation, Crop Functional Genomics, University of Bonn, Bonn, Germany

Lateral roots are a major determinant of root architecture and are instrumental for the efficient uptake of water and nutrients. Lateral roots consist of multiple cell types each expressing a unique transcriptome at a given developmental stage. Therefore, transcriptome analyses of complete lateral roots provide only average gene expression levels integrated over all cell types. Such analyses have the risk to mask genes, pathways and networks specifically expressed in a particular cell type during lateral root formation. Cell type-specific transcriptomics paves the way for a holistic understanding of the programming and re-programming of cells such as pericycle cells, involved in lateral root initiation. Recent discoveries have advanced the molecular understanding of the intrinsic genetic control of lateral root initiation and elongation. Moreover, the impact of nitrate availability on the transcriptional regulation of lateral root formation in Arabidopsis and cereals has been studied. In this review, we will focus on the systemic dissection of lateral root formation and its interaction with environmental nitrate through cell type-specific transcriptome analyses. These novel discoveries provide a better mechanistic understanding of postembryonic lateral root development in plants.

Keywords: fluorescence activated cell sorting (FACS), laser capture microdissection (LCM), lateral root, pericycle, transcriptome

OPEN ACCESS

Edited by:
Joseph G. Dubrovsky, National Autonomous University of Mexico, Mexico

Reviewed by:
Alexis Maizel, Universität Heidelberg, Germany
Tom Beeckman, Ghent University, Belgium

****Correspondence:***
Frank Hochholdinger
hochholdinger@uni-bonn.de
Peng Yu
yupeng@uni-bonn.de

Specialty section:
This article was submitted to Plant Development and EvoDevo, a section of the journal Frontiers in Plant Science

Received: *29 October 2018*
Accepted: *08 January 2019*
Published: *12 February 2019*

Citation:
Kortz A, Hochholdinger F and Yu P (2019) Cell Type-Specific Transcriptomics of Lateral Root Formation and Plasticity. Front. Plant Sci. 10:21. doi: 10.3389/fpls.2019.00021

INTRODUCTION

A key strategy of plants to adapt to changing moisture and nutrient availability in soil is the formation of a postembryonic root system. Among postembryonic root types, lateral roots are all roots that emerge from other roots. Highly branched lateral roots absorb most of the soil resources via their large root surface (Yu et al., 2016b). The genetic control of lateral root development in the dicot model plant Arabidopsis (Lavenus et al., 2013) and in monocot cereals (Yu et al., 2016b) has recently been reviewed. RNA sequencing (RNA-seq) has been widely adopted to study the transcriptomic landscape of organ and tissue development in plants (Stelpflug et al., 2016). Transcriptome analysis of lateral roots has been shown to be distinct from that of parent roots in both maize and rice, supporting the notion that fine lateral roots and thicker roots are functionally different (Gutjahr et al., 2015; Yu et al., 2018). Comparative transcriptome analyses of wild-type and mutant root systems in maize and rice have revealed molecular functions involved in auxin signaling and cell cycle regulation during lateral root formation (Zhang et al., 2014; Zhao et al., 2015). However, organs or tissues are composite structures consisting of multiple cell types with different biological functions and thus disparate transcriptome profiles (Schnable et al., 2004).

Transcriptomic analyses of single tissues, single cell types and in its extreme, single cells, have been successfully introduced in medical research and have subsequently been adopted in plant science (reviewed in: Gautam and Sarkar, 2015). There are two main systems that have been utilized in sampling single cell types and single cells. First, fluorescence activated cell sorting (FACS) was initially introduced as a tool to analyze mammalian blood cells (Hulett et al., 1969). This technique requires that cells flow in a fluid stream through the focus of a light source, where detectors can distinguish between different properties of these cells (Galbraith, 2010). Subsequently cells are separated either based on their endogenous or artificially added fluorochromes, or by metric properties estimated from their absorption and scattering behavior (Galbraith, 2010). By using multiple cell type-specific reporters such as green or yellow fluorescent proteins, distinct cell types of a single tissue can be sampled separately (Iyer-Pascuzzi and Benfey, 2010). A drawback of FACS is the requirement of cell type-specific marker lines, which are only available for selected model organisms. Moreover, these marker lines must be protoplasted by enzymatic digestion of the surrounding cell walls, to allow subsequent separation of different types of cells by the FACS system (Galbraith, 2010).

The second technique used for cell type-specific and single cell isolation is laser capture microdissection (LCM). This approach was initially developed to isolate specific tumor cells from infested tissue without compromising their DNA, RNA, and protein integrity (Emmert-Buck et al., 1996). During LCM, the cells of interest are visualized and selected through a light microscope and subsequently excised with a pulsed infrared laser (Nelson et al., 2006). This allows the isolation of specific cells from complex tissue samples comprising distinct cell types (Gautam and Sarkar, 2015). In contrast to FACS, LCM is not confined to cell suspension. Nevertheless, an elaborate sample preparation is still needed to ensure the high quality and integrity of the cells under analysis (Ludwig and Hochholdinger, 2014). The application of these two cell sorting techniques, in combination with downstream transcriptome analyses in lateral root research, will be summarized in the following chapters of this review.

CELL TYPE-SPECIFIC TRANSCRIPTOMICS TARGETING LATERAL ROOT FORMATION IN ARABIDOPSIS

In Arabidopsis, only cells of the pericycle cell layer divide and contribute to lateral root formation (van Norman et al., 2013). Therefore, the pericycle is the most promising target of cell-specific transcriptomics to study lateral root development in this species. The first cell type-specific transcriptome atlas of the Arabidopsis primary root was created by a combination of FACS and microarray experiments (Birnbaum et al., 2003). In this study, stele, endodermis, endodermis plus cortex, epidermis, and lateral root cap cells from the meristematic zone, elongation zone, and differentiation zone were separated and the transcriptomes of these cell and tissue types were analyzed (Birnbaum et al., 2003). This approach did not directly aim at deciphering lateral root development because the pericycle, as the origin of lateral roots, was not separately collected but included in the stele tissue sample. However, it paved the way for cell type-specific transcriptomic analyses and served as a valuable data source for further analyses. To further refine the resolution of cell type-specific expression in roots, the transcriptomes of 14 root cell types, including lateral root primordia, whole pericycle, phloem pole pericycle cells, and xylem pole pericycle cells, were analyzed separately for thirteen regions along the longitudinal root axis in a follow up study. This allowed detecting expression variation between different developmental stages by the combination of manual dissection, FACS and transcriptome profiling via microarray (Brady et al., 2007).

In Arabidopsis, lateral roots initiate from pericycle cells located at the xylem poles (Dolan et al., 1993; Parizot et al., 2008). The usage of two distinct marker lines for xylem and phloem pole cells in FACS experiments enabled the search for variations of the transcriptomic landscape within these distinct pericycle cell types. With this setup, the auxin biosynthetic genes *CYP79B2, CYP79B3, SUPERROOT1*, and *SUPERROOT2* were found to be enriched in lateral root primordia and phloem pole pericycle cells, while tryptophan-dependent auxin biosynthetic genes were enriched in the lateral root primordia and in pericycle cells (Brady et al., 2007). Moreover, FACS sorting of xylem pole pericycle cells of Arabidopsis and subsequent transcriptome analyses, resulted in 1,920 genes differentially expressed at different stages of mitosis (De Smet et al., 2008). Fifteen of these genes were identified as putative key regulators of asymmetric cell division and as being involved in the specification of cell fate during the initiation of lateral roots. Among those, *ARABIDOPSIS CRINKLY4* (*ACR4*, AT3G59420), which encodes a membrane-localized receptor-like kinase, is specifically expressed in the daughter cells, which arose from the first and second asymmetric division of the pericycle cells. This suggests a role of *ACR4* in the regulation of pericycle cell division during the initiation of lateral roots and inhibition of division of neighboring cells (De Smet et al., 2008).

In an effort to utilize transcriptomic data from multiple root cell types generated in different experiments, a spreadsheet application termed VisuaLRTC has been introduced (Parizot et al., 2010). Using this tool, the authors explored the expression of members of the Aux/IAA, AUXIN RESPONSE FACTOR (ARF) and LATERAL ORGAN BOUNDARIES DOMAIN (LBD) families, which are involved in auxin signal transduction. The authors applied multiple criteria including for instance SLR-1 and ARF7-ARF19 dependency of expression, or xylem or phloem pole pericycle expression (Parizot et al., 2010). Through this approach, the authors detected known regulators of auxin signal transduction such as *IAA29, IAA5, IAA11*, *IAA2, LBD17,* and *LBD33* as promising candidates for lateral root development (Parizot et al., 2010). Moreover, they discovered 211 additional candidate genes for lateral root development including known regulators of lateral root development (Parizot et al., 2010). Furthermore, they identified 19 pericycle-specific genes. Most of them were of unknown function and nearly all were down

regulated by auxin (Parizot et al., 2010). In another *in silico* transcriptome analysis of pericycle cell populations and their associated vascular phloem or xylem poles tissues, only minorities of genes were either enriched in phloem pole or xylem pole pericycle cells (Parizot et al., 2012). Furthermore, these researchers observed a substantial overlap between the expression of pericycle cells and their respective adjacent vasculature tissue. In phloem pole pericycle and phloem pole cells, this overlap was higher than in xylem pole pericycle cells and xylem pole cells. The authors explained this observation by the meristematic identity of the xylem pole pericycle cells, which distinguishes their function from the adjacent phloem pole pericycle cells (Parizot et al., 2012).

CELL TYPE-SPECIFIC TRANSCRIPTOMICS TARGETING LATERAL ROOT FORMATION IN MONOCOTS

In contrast to Arabidopsis, lateral root primordia of maize and rice are formed from two different cell types: pericycle and endodermis cells (Bell and McCully, 1970; Clowes, 1978). Furthermore, in maize, lateral roots emerge from phloem pole pericycle cells compared to xylem pole pericycle cells in Arabidopsis [reviewed in: Hochholdinger and Zimmermann (2008)].

In rice (*Oryza sativa*), the combination of LCM and microarray profiling was used to create a cell type-specific transcriptome atlas of 40 cell types from shoot, root and germinating seeds at several developmental stages. The aim of this study was to identify cell type-specific genes and gene classes as well as cell-specific promoter motifs (Jiao et al., 2009). Through the application of LCM-assisted microarray experiments the transcriptome of three cell type clusters: (1) epidermis, exodermis and sclerenchyma, (2) cortex, and (3) endodermis, pericycle, and stele termed endstele were compared in rice crown roots, at different developmental stages. In total, 232 genes were up regulated in cluster (3) comprising endodermis, pericycle and stele cells in comparison to the other two clusters and in comparison to stele tissue collected further away from the root tip (Takehisa et al., 2012). 71 genes associated with cell division and elongation as well as numerous transcription factors were only expressed in the region of 1–3 mm from the root tip emphasizing a role particularly in priming and initiation of lateral roots (Takehisa et al., 2012). An *AP2/EREBP* gene (Os07g0669500), which was assorted to this group, is a homolog of Arabidopsis gene *PUCHI*. The *PUCHI* gene is involved in specific patterning of cell division during the early stages of lateral root primordium development (Hirota et al., 2007). Another member of this gene cluster (Os03g0659700) shares similarities with *Arabidopsis AS2−LIKE 18* (*ASL18/LBD 16*), *ASL16/LBD29*, *ASL20/LBD18*, and rice *CROWN ROOTLESS 1/ADVENTITIOUS ROOTLESS 1* (*CRL1/ARL1*), which are linked to lateral root initiation (Inukai et al., 2005; Okushima et al., 2007; Lee et al., 2009; Coudert et al., 2015). In addition, the homolog (Os09g0531600) of the Arabidopsis gene *LATERAL ROOT PRIMORDIUM 1*, which has been previously linked to the early development of the lateral root meristem (Smith and Fedoroff, 1995), was specifically expressed in the endodermis, pericycle and stele cluster (Takehisa et al., 2012). Furthermore, the preferential expression of auxin biosynthesis and signaling−related genes in the endstele tissue that is positioned 1–3 mm away from the root tip was observed in this study, supporting the notion of an auxin−associated mechanisms of lateral root initiation similar to Arabidopsis (Takehisa et al., 2012).

In maize (*Zea mays*), LCM was utilized to isolate pericycle cells from primary roots of the lateral root deficient mutant *rootless with undetectable meristem 1* (*rum1*) and subjecting them to a subsequent transcriptome comparison with wild type pericycle cells. In this study, 90 genes preferentially expressed in wild type and 73 genes preferentially expressed in *rum1* pericycle cells were identified (Woll et al., 2005). Among the annotated genes, genes involved in signal transduction, transcription, and cell cycle were identified, indicating a link between these protein coding genes and lateral root initiation (Woll et al., 2005). Two of the genes preferentially expressed in wild type pericycle cells were helix-loop-helix transcription factors (NP_194827.1 and AAO72577.1), known to control the proliferation and development of specific cell lineages (Heim et al., 2003) undermining their possible involvement in lateral root initiation. In this study, the gene *Cyclin T2* (BAD17160.1), which is involved in the regulation of eukaryotic cell cycle progression was up regulated in wild type pericycle cells (Wang et al., 2004).

To survey the transcriptome of pericycle cells of the maize primary root before lateral root initiation, pericycle and non-pericycle cells isolated via LCM were compared (Dembinsky et al., 2007). This experiment resulted in the identification of 32 genes significantly higher expressed in pericycle cells compared to the non-pericycle cells (Dembinsky et al., 2007). These genes belonged to multiple functional classes including transcription, protein synthesis, disease/defense, signal transduction, metabolism, protein fate and subcellular localization. To identify genes preferentially expressed in pericycle cells that might not have been included in the 12 k microarray chip used in this study, suppression subtractive hybridization (SSH) and sequencing of expressed sequence tags (ESTs) were performed (Dembinsky et al., 2007). SSH led to the identification and validation of seven genes preferentially expressed in pericycle cells belonging to the functional categories of protein synthesis, cellular transport, disease/defense, signal transduction and metabolism. Moreover, 377 ESTs were sequenced from pericycle and 324 from non-pericycle central cylinder cells. Among those, the category protein synthesis was overrepresented and the category cell fate was underrepresented in pericycle compared to non-pericycle central cylinder cells (Dembinsky et al., 2007).

To identify distinct and shared components of the lateral root initiation pathway in maize primary and adventitious roots, pericycle cells were isolated via LCM from the different root types at multiple time points using a lateral root inducible

system (Jansen et al., 2013). The authors discovered a shared core regulation system between primary and adventitious roots. This regulatory system was shown to be enriched for genes of the functional categories DNA binding and microtubule movement, indicating functions in gene regulation and cell division (Jansen et al., 2013). Moreover, in this study 14 genes from monocot-specific gene families, which might be involved in the positioning of lateral root initiation, were discovered. These genes might be involved in the different positioning of lateral root founder cells between Arabidopsis and maize (Jansen et al., 2013). This analysis also led to the identification of root type-specific transcription factors, of the MYB and MYB-related, homeobox and bHLH families (Jansen et al., 2013). A comparative study of maize (Jansen et al., 2013) and previously published Arabidopsis (Vanneste et al., 2005; De Smet et al., 2008) transcriptome datasets led to the identification of a shared core set of 60 genes. Moreover, these authors compared the phloem pole pericycle cell transcriptome of maize with transcriptomic profiles of xylem and phloem pole pericycle cells in Arabidopsis (Jansen et al., 2013). They showed that multiple genes including the gene *LBD16/ASL18* were underrepresented in phloem pole pericycle cells of Arabidopsis, while the corresponding orthologs were induced upon lateral root induction in phloem pole pericycle cells of maize (Jansen et al., 2013). These findings indicated a shared identity between xylem pole pericycle cells of Arabidopsis and phloem pole pericycle cells of maize (Jansen et al., 2013). In addition, the existence of a conserved regulatory network among maize and Arabidopsis was further substantiated by the observed intersection of expression profiles of auxin-related genes (Jansen et al., 2013).

CELL TYPE-SPECIFIC RESPONSES TO NITRATE LINKED TO LATERAL ROOT FORMATION

Lateral roots shape overall root architecture based on the availability of nutrients such as nitrate and phosphate (Araya et al., 2014; Péret et al., 2014). Genotypes with sparsely spaced and long lateral roots are optimal for nitrate acquisition, while genotypes with densely spaced and short lateral roots are optimal for phosphate acquisition in crops (Lynch, 2011, 2013). Cell type-specific experiments have been performed to uncover transcriptomic changes in different cell types, which might regulate the adaptation observed upon nitrate treatment. Cell type-specific transcriptome analyses showed that nitrogen responses are to a large extent cell type-specific (Gifford et al., 2008). One of these cell type-specific nitrogen response genes, *ARF8,* which has been linked to root development before (Gutierrez et al., 2009), was induced in pericycle cells through nitrogen (Gifford et al., 2008). Furthermore, *miR167a* was down regulated in pericycle cells in response to nitrogen treatment, resulting in the up regulation of *ARF8*, which is a target of *miR167a* (Gifford et al., 2008; Gutierrez et al., 2009).

Similarly, nitrate treatment induced the expression of the *Auxin Receptor F-Box Protein 3* (*AFB3*), a target of *miR393* in pericycle cells of Arabidopsis (Vidal et al., 2010). This suggests that both are part of a network regulating lateral root formation as a response to high nitrate availability. Later, it was demonstrated that *AFB3* regulates the expression of NAM/ATAF/CUC transcription factor NAC4 and DNA-binding-with-one-finger (*DOF*) transcription factor binding protein 4 (OBP4) upon nitrogen treatment (Vidal et al., 2013). This emphasizes the existence of a regulatory module, which acts downstream of an auxin signal leading to the initiation of lateral roots through regulation of cell cycle progression in the pericycle (Vidal et al., 2013). This is in line with previous reports of *OBP4* gene function in cell cycle regulation in Arabidopsis (Skirycz et al., 2008).

By utilizing FACS and GFP marker lines specific to Arabidopsis xylem pole pericycle cells, it was possible to observe the response of this cell type under nitrate influence over a time period of 48 h (Walker et al., 2017). In this experiment, NITRITE REDUCTASE (NIA1) and other NITRATE TRANSPORTERS (NRT2.3 and NRT2.5) were down regulated in the pericycle as an immediate response to the treatment (Walker et al., 2017). In the same context, the gene *SENESCENCE-ASSOCIATED GENE 21 (SAG21)*, which has been previously linked to regulation of lateral root development and biotic responses (Salleh et al., 2012), was shown to be down regulated in the pericycle cells as a late response to nitrogen (Walker et al., 2017). In contrast, *WRKY75*, previously reported to regulate lateral root development (Devaiah et al., 2007), was strongly and directly up regulated in pericycle cells upon nitrogen treatment (Walker et al., 2017). Through the utilization of FACS and GFP-tagged lines, an induction of *TGA1*, *TGA4*, *NRT2.1*, and *NRT2.2* in pericycle cells in response to nitrate was observed, indicating a possible involvement in the regulation of nitrogen-induced lateral root initiation in Arabidopsis (Alvarez et al., 2014).

In maize phloem pole pericycle cells of shoot-borne brace roots, local high nitrate induces the expression of *B-type cyclin-dependent kinases* (*CDKB*) and *cyclin B* (*CYCB*) genes, while simultaneously inhibiting the expression of Kip-related proteins (Yu et al., 2015). *CDKB* and *CYCB* genes are positive regulators of cell cycle progression (Schnittger et al., 2002; Boudolf et al., 2004), while Kip-related proteins (KRPs) are repressors of the cell cycle (De Veylder et al., 2001), linking the observed expression pattern to a reactivation of the cell cycle in the pericycle (Yu et al., 2015). Furthermore, local nitrate influence led to a strong up regulation of *ZmPIN9* in phloem pole cells compared to endodermis and pericycle cells, indicating that this protein serves in the transport of auxin to adjacent pericycle cells (Yu et al., 2015). While *PIN*-formed genes have for long been known as auxin efflux carriers (Gälweiler et al., 1998), similar cell type-specific findings in rice emphasize that these monocot-specific *PIN* formed genes might also regulate the formation of the complex root systems developed by monocots (Wang et al., 2009; Yu et al., 2015).

Cell type-specific transcriptomics also enables comparisons between similar cell types in different root types within a species. In maize, it was shown that some nitrate-dependent expression patterns are conserved between the different root types (Yu et al., 2016a). Conversely, in brace roots the number of genes

exclusively expressed in pericycle cells exceeded the amount of exclusively expressed genes in seedling root types under homogeneous low or local high nitrate conditions (Yu et al., 2016a). This indicates a root type-specific regulation of these genes during early lateral root initiation as well as a different response to nitrate influence (Yu et al., 2016a). Multiple nitrate-responsive genes specific to brace roots were shown to be involved in the assembly of nucleosomes/chromatin and in the microtubule motor activity needed for the movement of these during mitosis (Yu et al., 2016a).

CONCLUSION AND PROSPECTS

Tissue and cell type-specific transcriptomics have promoted the understanding of the molecular networks involved in lateral root formation. Moreover, these studies identified regulators of lateral root formation and regulators of pericycle founder cell identity. Integration of transcriptome datasets was useful for mechanistic comparisons between dicots and monocots during lateral root development. In addition, cell type-specific transcriptomics accelerated a deeper understanding of nitrate induced functional networks of lateral root formation in Arabidopsis and maize at the cellular level. In the future, it will be desirable to integrate *in situ* root visualization techniques such as micro x-ray computer tomography with cell type-specific transcriptome analyses, although it is still challenging to apply FACS and LCM techniques to roots grown in natural soil environments. Single-cell RNA-seq (Birnbaum, 2018), will further increase the spatial and temporal resolution of cells involved in lateral root formation. This technique will for instance enable the identification of differences within pericycle cells that acquire lateral root founder cell identity and will reveal the details of the fine-tuned processes underlying lateral root organization and development.

AUTHOR CONTRIBUTIONS

AK, FH, and PY contributed to the writing of this review.

FUNDING

This work was supported by the Deutsche Forschungsgemeinschaft (DFG) grant no. YU 272/1-1 to PY and DFG grant no. HO2249/12-1 to FH.

REFERENCES

Alvarez, J. M., Riveras, E., Vidal, E. A., Gras, D. E., Contreras-López, O., Tamayo, K. P., et al. (2014). Systems approach identifies TGA1 and TGA4 transcription factors as important regulatory components of the nitrate response of *Arabidopsis thaliana* roots. *Plant J.* 80, 1–13. doi: 10.1111/tpj.12618

Araya, T., Miyamoto, M., Wibowo, J., Suzuki, A., Kojima, S., Tsuchiya, Y. N., et al. (2014). CLE-CLAVATA1 peptide-receptor signaling module regulates the expansion of plant root systems in a nitrogen-dependent manner. *Proc. Natl. Acad. Sci. U.S.A.* 111, 2029–2034. doi: 10.1073/pnas.1319953111

Bell, J. K., and McCully, M. E. (1970). A histological study of lateral root initiation and development in *Zea mays*. *Protoplasma* 70, 179–205. doi: 10.1007/BF01276979

Birnbaum, K., Shasha, D. E., Wang, J. Y., Jung, J. W., Lambert, G. M., Galbraith, D. W., et al. (2003). A gene expression map of the *Arabidopsis* root. *Science* 302:1956. doi: 10.1126/science.1090022

Birnbaum, K. D. (2018). Power in numbers: single-cell RNA-Seq strategies to dissect complex tissues. *Annu. Rev. Genet.* 52, 203–221. doi: 10.1146/annurev-genet-120417-031247

Boudolf, V., Vlieghe, K., Beemster, G. T. S., Magyar, Z., Acosta, J. A. T., Maes, S., et al. (2004). The plant-specific cyclin-dependent kinase CDKB1;1 and transcription factor E2Fa-DPa control the balance of mitotically dividing and endoreduplicating cells in *Arabidopsis*. *Plant Cell* 16, 2683–2692. doi: 10.1105/tpc.104.024398

Brady, S. M., Orlando, D. A., Lee, J.-Y., Wang, J. Y., Koch, J., Dinneny, J. R., et al. (2007). A high-resolution root spatiotemporal map reveals dominant expression patterns. *Science* 318, 801–806. doi: 10.1126/science.1146265

Clowes, F. A. L. (1978). Chimeras and the origin of lateral root primordia in *Zea mays*. *Ann. Bot.* 42, 801–807. doi: 10.1093/oxfordjournals.aob.a085519

Coudert, Y., Le, V. A., Adam, H., Bès, M., Vignols, F., Jouannic, S., et al. (2015). Identification of CROWN ROOTLESS1-regulated genes in rice reveals specific and conserved elements of postembryonic root formation. *New Phytol.* 206, 243–254. doi: 10.1111/nph.13196

De Smet, I., Vassileva, V., de Rybel, B., Levesque, M. P., Grunewald, W., Van Damme, D., et al. (2008). Receptor-like kinase ACR4 restricts formative cell divisions in the *Arabidopsis* root. *Science* 322, 594–597. doi: 10.1126/science.1160158

De Veylder, L., Beeckman, T., Beemster, G. T. S., Krols, L., Terras, F., Landrieu, I., et al. (2001). Functional analysis of cyclin-dependent kinase inhibitors of *Arabidopsis*. *Plant Cell* 13, 1653–1668. doi: 10.1105/TPC.010087

Dembinsky, D., Woll, K., Saleem, M., Liu, Y., Fu, Y., Borsuk, L. A., et al. (2007). Transcriptomic and proteomic analyses of pericycle cells of the maize primary root. *Plant Physiol.* 145, 575–588. doi: 10.1104/pp.107.106203

Devaiah, B. N., Karthikeyan, A. S., and Raghothama, K. G. (2007). WRKY75 transcription factor is a modulator of phosphate acquisition and root development in *Arabidopsis*. *Plant Physiol.* 143, 1789–1801. doi: 10.1104/pp.106.093971

Dolan, L., Janmaat, K., Willemsen, V., Linstead, P., Poethig, S., Roberts, K., et al. (1993). Cellular organisation of the *Arabidopsis thaliana* root. *Development* 119, 71–84.

Emmert-Buck, M. R., Bonner, R. F., Smith, P. D., Chuaqui, R. F., Zhuang, Z., Goldstein, S. R., et al. (1996). Laser capture microdissection. *Science* 274, 998–1001. doi: 10.1126/science.274.5289.998

Galbraith, D. W. (2010). Flow cytometry and fluorescence-activated cell sorting in plants: the past, present, and future. *Biomédica* 30, 61–69. doi: 10.7705/biomedica.v30i0.824

Gälweiler, L., Guan, C., Müller, A., Wisman, E., Mendgen, K., Yephremov, A., et al. (1998). Regulation of polar auxin transport by AtPIN1 in *Arabidopsis* vascular tissue. *Science* 282, 2226–2230. doi: 10.1126/science.282.5397.2226

Gautam, V., and Sarkar, A. K. (2015). Laser assisted microdissection, an efficient technique to understand tissue specific gene expression patterns and functional genomics in plants. *Mol. Biotechnol.* 57, 299–308. doi: 10.1007/s12033-014-9824-3

Gifford, M. L., Dean, A., Gutierrez, R. A., Coruzzi, G. M., and Birnbaum, K. D. (2008). Cell-specific nitrogen responses mediate developmental plasticity. *Proc. Natl. Acad. Sci. U.S.A.* 105, 803–808. doi: 10.1073/pnas.0709559105

Gutierrez, L., Bussell, J. D., Păcurar, D. I., Schwambach, J., Păcurar, M., and Bellini, C. (2009). Phenotypic plasticity of adventitious rooting in *Arabidopsis* is controlled by complex regulation of AUXIN RESPONSE FACTOR transcripts and microRNA abundance. *Plant Cell* 21, 3119–3132. doi: 10.1105/tpc.108.064758

Gutjahr, C., Sawers, R. J., Marti, G., Andrés-Hernández, L., Yang, S. Y., Casieri, L., et al. (2015). Transcriptome diversity among rice root types during asymbiosis and interaction with arbuscular mycorrhizal fungi. *Proc. Natl. Acad. Sci. U.S.A.* 112, 6754–6759. doi: 10.1073/pnas.1504142112

Heim, M. A., Jakoby, M., Werber, M., Martin, C., Weisshaar, B., and Bailey, P. C. (2003). The basic Helix–Loop–Helix transcription factor family in plants: a genome-wide study of protein structure and functional diversity. *Mol. Biol. Evol.* 20, 735–747. doi: 10.1093/molbev/msg088

Hirota, A., Kato, T., Fukaki, H., Aida, M., and Tasaka, M. (2007). The auxin-regulated AP2/EREBP gene PUCHI is required for morphogenesis in the early lateral root primordium of *Arabidopsis*. *Plant Cell* 19, 2156–2168. doi: 10.1105/tpc.107.050674

Hochholdinger, F., and Zimmermann, R. (2008). Conserved and diverse mechanisms in root development. *Curr. Opin. Plant Biol.* 11, 70–74. doi: 10.1016/j.pbi.2007.10.002

Hulett, H. R., Bonner, W. A., Barrett, J., and Herzenberg, L. A. (1969). Cell sorting: automated separation of mammalian cells as a function of intracellular fluorescence. *Science* 166, 747–749. doi: 10.1126/science.166.3906.747

Inukai, Y., Sakamoto, T., Ueguchi-Tanaka, M., Shibata, Y., Gomi, K., Umemura, I., et al. (2005). Crown rootless1, which is essential for crown root formation in rice, is a target of an AUXIN RESPONSE FACTOR in auxin signaling. *Plant Cell* 17, 1387–1396. doi: 10.1105/tpc.105.030981

Iyer-Pascuzzi, A. S., and Benfey, P. N. (2010). Fluorescence-activated cell sorting in plant developmental biology. *Methods Mol. Biol.* 655, 313–319. doi: 10.1007/978-1-60761-765-5_21

Jansen, L., Hollunder, J., Roberts, I., Forestan, C., Fonteyne, P., van Quickenborne, C., et al. (2013). Comparative transcriptomics as a tool for the identification of root branching genes in maize. *Plant Biotechnol. J.* 11, 1092–1102. doi: 10.1111/pbi.12104

Jiao, Y., Lori Tausta, S., Gandotra, N., Sun, N., Liu, T., Clay, N. K., et al. (2009). A transcriptome atlas of rice cell types uncovers cellular, functional and developmental hierarchies. *Nat. Genet.* 41, 258–263. doi: 10.1038/ng.282

Lavenus, J., Goh, T., Roberts, I., Guyomarc'h, S., Lucas, M., De Smet, I., et al. (2013). Lateral root development in *Arabidopsis*: fifty shades of auxin. *Trends Plant Sci.* 18, 450–458. doi: 10.1016/j.tplants.2013.04.006

Lee, H. W., Kim, N. Y., Lee, D. J., and Kim, J. (2009). LBD18/ASL20 regulates lateral root formation in combination with LBD16/ASL18 downstream of ARF7 and ARF19 in *Arabidopsis*. *Plant Physiol.* 151, 1377–1389. doi: 10.1104/pp.109.143685

Ludwig, Y., and Hochholdinger, F. (2014). "Laser microdissection of plant cells," in *Plant Cell Morphogenesis: Methods and Protocols*, eds V. Žárský, and F. Cvrčková (Totowa, NJ: Humana Press), 249–258. doi: 10.1007/978-1-62703-643-6_21

Lynch, J. P. (2011). Root phenes for enhanced soil exploration and phosphorus acquisition: tools for future crops. *Plant Physiol.* 156, 1041–1049. doi: 10.1104/pp.111.175414

Lynch, J. P. (2013). Steep, cheap and deep: an ideotype to optimize water and N acquisition by maize root systems. *Ann. Bot.* 112, 347–357. doi: 10.1093/aob/mcs293

Nelson, T., Tausta, S. L., Gandotra, N., and Liu, T. (2006). Laser microdissection of plant tissue: what you see is what you get. *Annu. Rev. Plant Biol.* 57, 181–201. doi: 10.1146/annurev.arplant.56.032604.144138

Okushima, Y., Fukaki, H., Onoda, M., Theologis, A., and Tasaka, M. (2007). ARF7 and ARF19 regulate lateral root formation via direct activation of LBD/ASL genes in *Arabidopsis*. *Plant Cell* 19, 118–130. doi: 10.1105/tpc.106.047761

Parizot, B., Laplaze, L., Ricaud, L., Boucheron-Dubuisson, E., Bayle, V., Bonke, M., et al. (2008). Diarch symmetry of the vascular bundle in *Arabidopsis* root encompasses the pericycle and is reflected in distich lateral root initiation. *Plant Physiol.* 146, 140–148. doi: 10.1104/pp.107.107870

Parizot, B., Roberts, I., Raes, J., Beeckman, T., and De Smet, I. (2012). *In silico* analyses of pericycle cell populations reinforce their relation with associated vasculature in *Arabidopsis*. *Philos. Trans. R. Soc. B* 367, 1479–1488. doi: 10.1098/rstb.2011.0227

Parizot, B., Rybel, B., and de Beeckman, T. (2010). VisuaLRTC: a new view on lateral root initiation by combining specific transcriptome data sets. *Plant Physiol.* 153, 34–40. doi: 10.1104/pp.109.148676

Péret, B., Desnos, T., Jost, R., Kanno, S., Berkowitz, O., and Nussaume, L. (2014). Root architecture responses: in search of phosphate. *Plant Physiol.* 166, 1713–1723. doi: 10.1104/pp.114.244541

Salleh, F. M., Evans, K., Goodall, B., Machin, H., Mowla, S. B., Mur, L. A. J., et al. (2012). A novel function for a redox-related LEA protein (SAG21/AtLEA5) in root development and biotic stress responses. *Plant Cell Environ.* 35, 418–429. doi: 10.1111/j.1365-3040.2011.02394.x

Schnable, P. S., Hochholdinger, F., and Nakazono, M. (2004). Global expression profiling applied to plant development. *Curr. Opin. Plant Biol.* 7, 50–56. doi: 10.1016/j.pbi.2003.11.001

Schnittger, A., Schöbinger, U., Stierhof, Y.-D., and Hülskamp, M. (2002). Ectopic B-type cyclin expression induces mitotic cycles in endoreduplicating *Arabidopsis* trichomes. *Curr. Biol.* 12, 415–420. doi: 10.1016/S0960-9822(02)00693-0

Skirycz, A., Radziejwoski, A., Busch, W., Hannah, M. A., Czeszejko, J., Kwaśniewski, M., et al. (2008). The DOF transcription factor OBP1 is involved in cell cycle regulation in *Arabidopsis thaliana*. *Plant J.* 56, 779–792. doi: 10.1111/j.1365-313X.2008.03641.x

Smith, D. L., and Fedoroff, N. V. (1995). LRP1, a gene expressed in lateral and adventitious root primordia of *Arabidopsis*. *Plant Cell* 7, 735–745. doi: 10.1105/tpc.7.6.735

Stelpflug, S. C., Sekhon, R. S., Vaillancourt, B., Hirsch, C. N., Buell, C. R., de Leon, N., et al. (2016). An expanded maize gene expression atlas based on RNA sequencing and its use to explore root development. *Plant Genome* 9, 1–16. doi: 10.3835/plantgenome2015.04.0025

Takehisa, H., Sato, Y., Igarashi, M., Abiko, T., Antonio, B. A., Kamatsuki, K., et al. (2012). Genome-wide transcriptome dissection of the rice root system: implications for developmental and physiological functions. *Plant J.* 69, 126–140. doi: 10.1111/j.1365-313X.2011.04777.x

van Norman, J. M., Xuan, W., Beeckman, T., and Benfey, P. N. (2013). To branch or not to branch: the role of pre-patterning in lateral root formation. *Development* 140, 4301–4310. doi: 10.1242/dev.090548

Vanneste, S., De Rybel, B., Beemster, G. T. S., Ljung, K., De Smet, I., van Isterdael, G., et al. (2005). Cell cycle progression in the pericycle is not sufficient for SOLITARY ROOT/IAA14-mediated lateral root initiation in *Arabidopsis thaliana*. *Plant Cell* 17, 3035–3050. doi: 10.1105/tpc.105.035493

Vidal, E. A., Araus, V., Lu, C., Parry, G., Green, P. J., Coruzzi, G. M., et al. (2010). Nitrate-responsive miR393/AFB3 regulatory module controls root system architecture in *Arabidopsis thaliana*. *Proc. Natl. Acad. Sci. U.S.A.* 107, 4477–4482. doi: 10.1073/pnas.0909571107

Vidal, E. A., Moyano, T. C., Riveras, E., Contreras-López, O., and Gutiérrez, R. A. (2013). Systems approaches map regulatory networks downstream of the auxin receptor AFB3 in the nitrate response of *Arabidopsis thaliana* roots. *Proc. Natl. Acad. Sci. U.S.A.* 110, 12840–12845. doi: 10.1073/pnas.1310937110

Walker, L., Boddington, C., Jenkins, D., Wang, Y., Grønlund, J. T., Hulsmans, J., et al. (2017). Changes in gene expression in space and time orchestrate environmentally mediated shaping of root architecture. *Plant Cell* 29, 2393–2412. doi: 10.1105/tpc.16.00961

Wang, G., Kong, H., Sun, Y., Zhang, X., Zhang, W., Altman, N., et al. (2004). Genome-wide analysis of the cyclin family in *Arabidopsis* and comparative phylogenetic analysis of plant cyclin-like proteins. *Plant Physiol.* 135, 1084–1099. doi: 10.1104/pp.104.040436

Wang, J., Hu, H., Wang, G., Li, J., Chen, J., and Wu, P. (2009). Expression of PIN genes in rice (*Oryza sativa* L.): tissue specificity and regulation by hormones. *Mol. Plant* 2, 823–831. doi: 10.1093/mp/ssp023

Woll, K., Borsuk, L. A., Stransky, H., Nettleton, D., Schnable, P. S., and Hochholdinger, F. (2005). Isolation, characterization, and pericycle-specific transcriptome analyses of the novel maize lateral and seminal root initiation mutant *rum1*. *Plant Physiol.* 139, 1255–1267. doi: 10.1104/pp.105.067330

Yu, P., Eggert, K., Wirén, N., von Li, C., and Hochholdinger, F. (2015). Cell type-specific gene expression analyses by RNA sequencing reveal local high nitrate-triggered lateral root initiation in shoot-borne roots of maize by modulating auxin-related cell cycle regulation. *Plant Physiol.* 169, 690–704. doi: 10.1104/pp.15.00888

Yu, P., Baldauf, J. A., Lithio, A., Marcon, C., Nettleton, D., Li, C., et al. (2016a). Root type-specific reprogramming of maize pericycle transcriptomes by local high nitrate results in disparate lateral root branching patterns. *Plant Physiol.* 170, 1783–1798. doi: 10.1104/pp.15.01885

Yu, P., Gutjahr, C., Li, C., and Hochholdinger, F. (2016b). Genetic control of lateral root formation in cereals. *Trends Plant Sci.* 21, 951–961. doi: 10.1016/j.tplants.2016.07.011

Yu, P., Wang, C., Baldauf, J. A., Tai, H., Gutjahr, C., Hochholdinger, F., et al. (2018). Root type and soil phosphate determine the taxonomic landscape of colonizing fungi and the transcriptome of field-grown maize roots. *New Phytol.* 217, 1240–1253. doi: 10.1111/nph.14893

Zhang, Y., Paschold, A., Marcon, C., Liu, S., Tai, H., Nestler, J., et al. (2014). The *Aux/IAA* gene *rum1* involved in seminal and lateral root formation controls vascular patterning in maize (*Zea mays* L.) *primary roots*. *J. Exp. Bot.* 65, 4919–4930. doi: 10.1093/jxb/eru249

Zhao, H., Ma, T., Wang, X., Deng, Y., Ma, H., Zhang, R., et al. (2015). OsAUX1 controls lateral root initiation in rice (*Oryza sativa* L.). *Plant Cell Environ.* 38, 2208–2222. doi: 10.1111/pce.12467

Conflict of Interest Statement: The authors declare that the research was conducted in the absence of any commercial or financial relationships that could be construed as a potential conflict of interest.

frontiers in Plant Science

ORIGINAL RESEARCH
published: 20 February 2019
doi: 10.3389/fpls.2019.00154

Root Branching Is Not Induced by Auxins in *Selaginella moellendorffii*

Tao Fang[1,2], *Hans Motte*[1,2], *Boris Parizot*[1,2] *and Tom Beeckman*[1,2]*

[1] Department of Plant Biotechnology and Bioinformatics, Ghent University, Ghent, Belgium, [2] VIB Center for Plant Systems Biology, Ghent, Belgium

Angiosperms develop intensively branched root systems that are accommodated with the high capacity to produce plenty of new lateral roots throughout their life-span. Root branching can be dynamically regulated in response to edaphic conditions and provides the plants with a soil-mining potential. This highly specialized branching capacity has most likely been key in the colonization success of the present flowering plants on our planet. The initiation, formation and outgrowth of branching roots in Angiosperms are dominated by the plant hormone auxin. Upon auxin treatment root branching through the formation of lateral roots can easily be induced. In this study, we questioned whether this strong branching-inducing action of auxin is part of a conserved mechanism that was already active in the earliest diverging lineage of vascular plants with roots. In Selaginella, an extant representative species of this early clade of root forming plants, components of the canonical auxin signaling pathway are retrieved in its genome. Although we observed a clear physiological response and an indirect effect on root branching, we were not able to directly induce root branching in this species by application of different auxins. We conclude that the structural and developmental difference of the Selaginella root, which branches via bifurcation of the root meristem, or the absence of an auxin-mediated root development program, is most likely causative for the absence of an auxin-induced branching mechanism.

Keywords: root branching, *Selaginella*, evolution, auxin, bifurcation

OPEN ACCESS

Edited by:
Joseph G. Dubrovsky, National Autonomous University of Mexico, Mexico

Reviewed by:
Alexander John Hetherington, University of Oxford, United Kingdom
Guichuan Hou, Appalachian State University, United States

***Correspondence:**
Tom Beeckman
tom.beeckman@psb.vib-ugent.be

Specialty section:
This article was submitted to Plant Development and EvoDevo, a section of the journal Frontiers in Plant Science

Received: *29 November 2018*
Accepted: *29 January 2019*
Published: *20 February 2019*

Citation:
Fang T, Motte H, Parizot B and Beeckman T (2019) Root Branching Is Not Induced by Auxins in Selaginella moellendorffii. Front. Plant Sci. 10:154. doi: 10.3389/fpls.2019.00154

INTRODUCTION

Roots, the hidden half of plants, anchor the plant body to the ground and absorb water and nutrients. The evolution of roots has been a very important innovation for plants to successfully colonize the terrestrial environment over about 400 million years ago (Raven and Edwards, 2001). The branching capacity of roots was of utmost importance in the colonization of plants, as it allows, beside a strong anchor, exploration of the soil and foraging of nutrients and water.

In angiosperms such as *Arabidopsis*, roots branch by the formation of lateral roots, which initiate from specialized pericycle cells. Auxin, a powerful plant growth regulator, plays a key role in this biological process by stimulating and activating pericycle cells to specify lateral root founder cells (Himanen et al., 2002; Dubrovsky et al., 2008; De Rybel et al., 2010; Möller et al., 2017). The importance of auxin signaling in promoting lateral root formation through several Aux/IAA-ARF modules has been well studied (Fukaki et al., 2002; De Rybel et al., 2010; De Smet et al., 2010; Moreno-Risueno et al., 2010; Goh et al., 2012; Du and Scheres, 2018). Accordingly, polar auxin transport inhibitors, such as 1-n-naphthylphthalamic acid (NPA) and 2,3,5-triiodobenzoic acid (TIBA), were found to inhibit lateral root branching through blocking auxin efflux

(Karabaghli-Degron et al., 1998; Reed et al., 1998; Casimiro et al., 2001; Himanen et al., 2002). In addition to polar auxin transport inhibitors, cytokinin can also inhibit lateral root initiation possibly through a separate signaling pathway (Li et al., 2006; Chang et al., 2013). Similar to lateral root initiation, auxin signaling and auxin transport are crucial in root meristem and lateral root meristem establishment (Sabatini et al., 1999; Benkova et al., 2003; Blilou et al., 2005; Dello Ioio et al., 2008; Du and Scheres, 2017, 2018).

In contrast to lateral branching roots, lycophyte roots branch via bifurcation of the root tip, also called dichotomous branching (Webster and Steeves, 1964; Otreba and Gola, 2011; Gola, 2014). The lycophyte clade is the most ancient clade with rooting plants. Selaginella is an important representative of the lycophytes (Banks, 2009), in particular as it includes *Selaginella moellendorffii*, the first lycophyte with a sequenced genome (Banks et al., 2011). Roots of Selaginella originate from rhizophores, root primordia-bearing organs that develop on stems. The root meristem originates from a single tetrahedral apical stem cell and is anatomically similar to the root meristem in ferns. This meristem is however very different to seed plants (Motte and Beeckman, 2018). Root dichotomous branching occurs through the bifurcation of the meristem, presumably via the activation of two new apical stem cells (Gola, 2014). As such, two new root meristems establish within the root tip (Imaichi and Kato, 1989; Otreba and Gola, 2011).

Auxin signaling and auxin transport are highly conserved within land plants and key components of these pathways are already present in Selaginella (Viaene et al., 2013, 2014; Bennett et al., 2014; Kato et al., 2018; Mutte et al., 2018). In addition, the auxin flow toward the Selaginella root apex (Wochok and Sussex, 1974) suggests an important role of auxin in the root meristem as well. Considering its importance in root initiation and root meristem establishment in many land plants, a role of auxin in the initiation of dichotomous root branching in Selaginella could be anticipated as well. This putative role was previously suggested based on heavily branching roots upon auxin treatment in *Selaginella kraussiana* (Sanders and Langdale, 2013), but to our knowledge, no data on the induction of root branching are available up to date. To fill this gap, we report here on the effect of auxin on root initiation and dichotomous branching in *Selaginella moellendorffii*. Surprisingly, we found that auxin does not induce the root bifurcation itself.

MATERIALS AND METHODS

Plant Material and Growth Conditions

Selaginella moellendorffii (Selaginella) plants were obtained from the lab of Jo Ann Banks at Purdue University. Plants are routinely propagated on sterile half-strength Murashige and Skoog (1/2MS) medium (Duchefa Biochemie) supplemented with 0.8% (w/v) agar, pH 5.8, in Sterivent boxes (Duchefa Biochemie) in a growth room at 24°C with light intensity 20.25–43.2 μmol/m^2/s (cool white fluorescent lamps) and regime of 16 h light and 8 h dark. To induce rhizophores or roots, shoot apical segments, presenting two branches (further referred as explants), were transferred into Petri dish plates with 1/2MS. After a few days, rhizophores and roots started to emerge, as illustrated in **Figure 1** and **Video S1** showing growth of an explant from 8 days post transfer onwards.

To test the promotive/inhibitory effect of auxin compounds as well as potential inhibitors on the root bifurcation, explants incubated for 12 days on 1/2MS were transferred to the treatment medium and only roots that just underwent a new branching event were used for analysis. For this purpose, all roots were preliminary screened at 11 and 12 days of incubation with a stereomicroscope. Roots that bifurcated between day 11 and day 12 were annotated as newly branched roots (**Figure 1D** or **Figure 1E**). Microscopic analysis of these roots showed that the newly formed tips never contained two meristems ($n = 58$), i.e., the next dichotomous branching was not initiated yet (**Figures 1G,H**). After transfer to the treatment medium, each root tip was observed daily with a stereomicroscope to evaluate bifurcation. The branching percentage was calculated as the number of bifurcated apices divided by the total number of root apices coming from newly branched roots. The number of branching events in a period of 13 days was counted per root apex coming from a newly branched root. In case of indole-3-acetic acid (IAA) treatments, yellow plastic sheets covering the plates were used to prevent IAA degradation from light.

Root Morphology

Explants or roots were subjected to daily stereomicroscopic observation to record the number of new emerging rhizophores and bifurcating roots. To determine root length elongation, the Petridish plates were scanned with a flatbed scanner (EPSON Expression 11000XL) and the length of the root segment between two branching sites was measured with ImageJ software (Abramoff et al., 2004). The elongation rate was calculated by dividing the length between two branching sites by the time in days between the two branching events.

Microscopy

Selaginella root tips were first fixed in 50% methanol and 10% acetic acid and after clearing subjected to a modified pseudo-Schiff propidium iodide staining as described previously (Truernit et al., 2008). Analysis was done with a Zeiss LSM5 Exciter confocal microscope with an argon ion laser at 488 nm as the excitation source and a detection filter at 505 nm. For all samples, z-stacks were taken to ensure the possible detection of meristematic regions in different planes.

RESULTS

Auxins Do Not Affect the Formation of Root-Bearing Rhizophores in Selaginella

In *Selaginella moellendorffii* (Selaginella), new roots are derived from rhizophores, root-like organs forming on the stem (**Figure 1A**). In accordance with the positive effect of auxin on adventitious rooting in seed plants, an auxin-dependent effect on the formation of new rhizophores in Selaginella might be anticipated as well. In order to evaluate this putative effect, we investigated the effect of auxins on the formation of

rhizophores on Selaginella shoot explants. Hitherto, Selaginella shoot explants of approximately 1 cm were isolated from *in vitro* growing plants and transferred to growth media with different auxins. The number of rhizophores on explants after 13 days of auxin treatments does not significantly differ from the control (**Figure 2**). Thus, auxins do not promote the formation of rhizophores in Selaginella. Consistently, treatments with auxin transport inhibitors or a cytokinin, which mostly work antagonistically toward auxin in seed plants, did not or only in a limited extent affect rhizophore formation (**Figure 2**). NPA treatments showed a significant but very modest decrease in rhizophores, indicating rather an indirect role of auxin and auxin transport during rhizophore establishment and emergence.

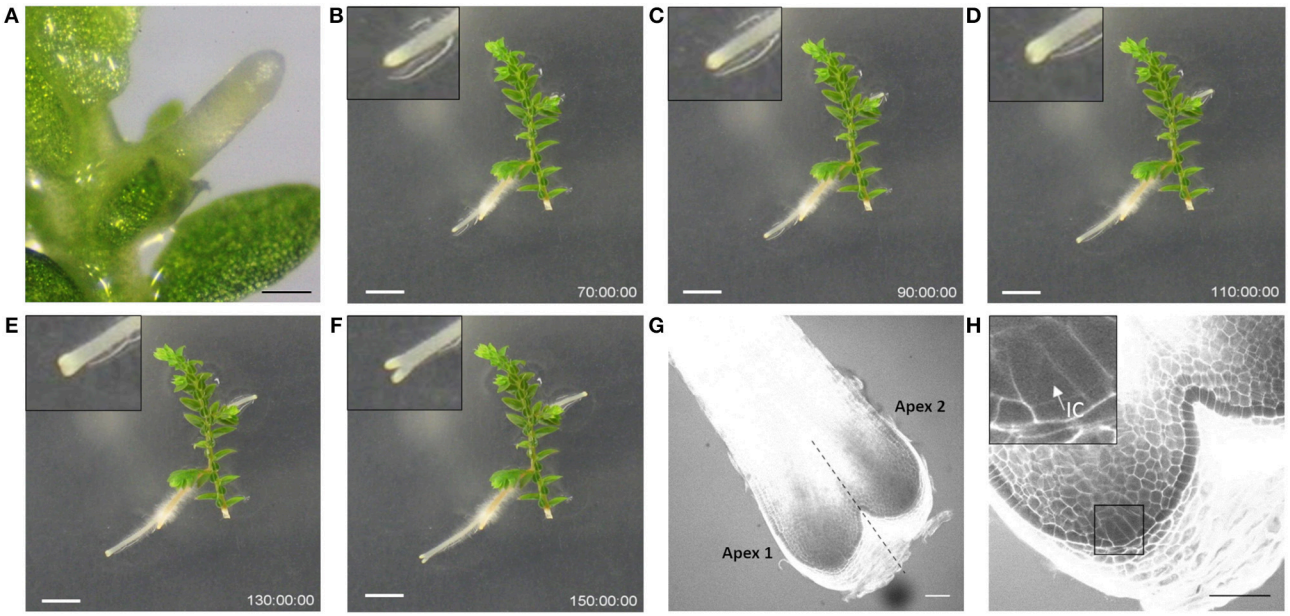

FIGURE 1 | Rhizophore and dichotomous root branching in Selaginella. **(A)** Rhizophore emerged from the stem. **(B–F)** Frames from **Video S1** showing the process of dichotomous root branching. Newly branched roots as in **(D,E)** were used as starting material in the branching experiments. The time is indicated in hours. Scale bars: 1 mm. **(G)** Representative confocal image of a newly branched root. **(H)** Magnification of apex 1 in **(G)** shows one single IC. The inset is a magnification of the square. IC, initial cell. Scale bars: 50 μm.

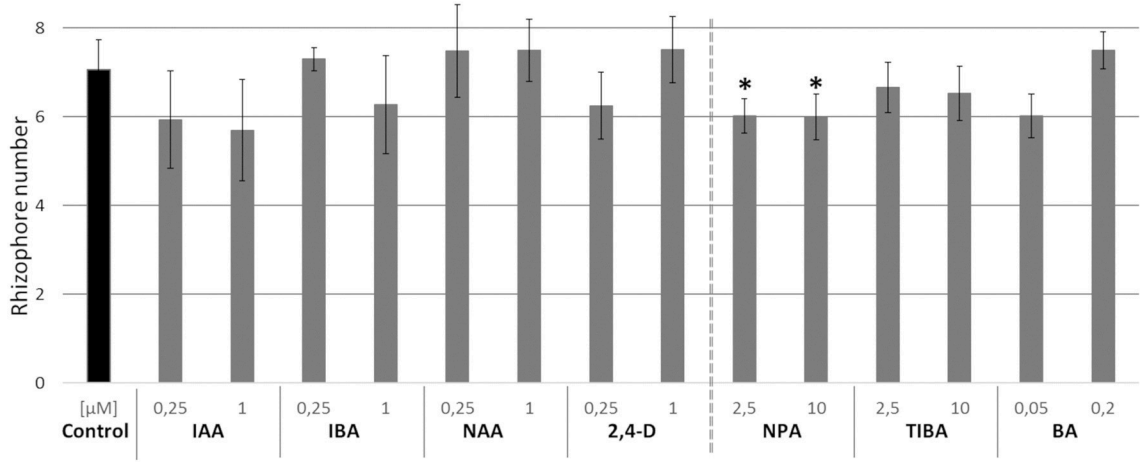

FIGURE 2 | Effects of auxins, polar auxin transport inhibitors and a cytokinin on rhizophore emergence. Selaginella explants with newly branched roots were incubated with dimethyl sulphoxide (DMSO) or different concentrations of treatments for 13 days: indole-3-acetic acid (IAA), indole-3-butyric acid (IBA), 1-naphthaleneacetic acid (NAA), 2,4-dichlorophenoxyacetic acid (2,4-D), naphthylphthalamic acid (NPA), 2,3,5-triiodobenzoic acid (TIBA) or 6-benzylaminopurine (BA). Number of rhizophores emerging post treatments was recorded on 13 d post treatments. Error bars represent SD. *n* (number of plates) = 4 (except for 10 μM TIBA, *n* = 3) with on average 5 explants per plate. *represents *p*-value ≤ 0.05 (Kruskal-Wallis test).

Auxins Affect Root Development in Selaginella

In Selaginella, roots branch dichotomously (**Figures 1B–H**, **Video S1**). To examine the effect of auxins on root development, shoot explants were first isolated and incubated on hormone-free growth medium to allow the spontaneous formation of rhizophores and roots. To standardize the starting material, explants with a root that recently bifurcated were selected and transferred to an auxin-containing medium. Microscopic inspection of newly formed root tips after bifurcation shows

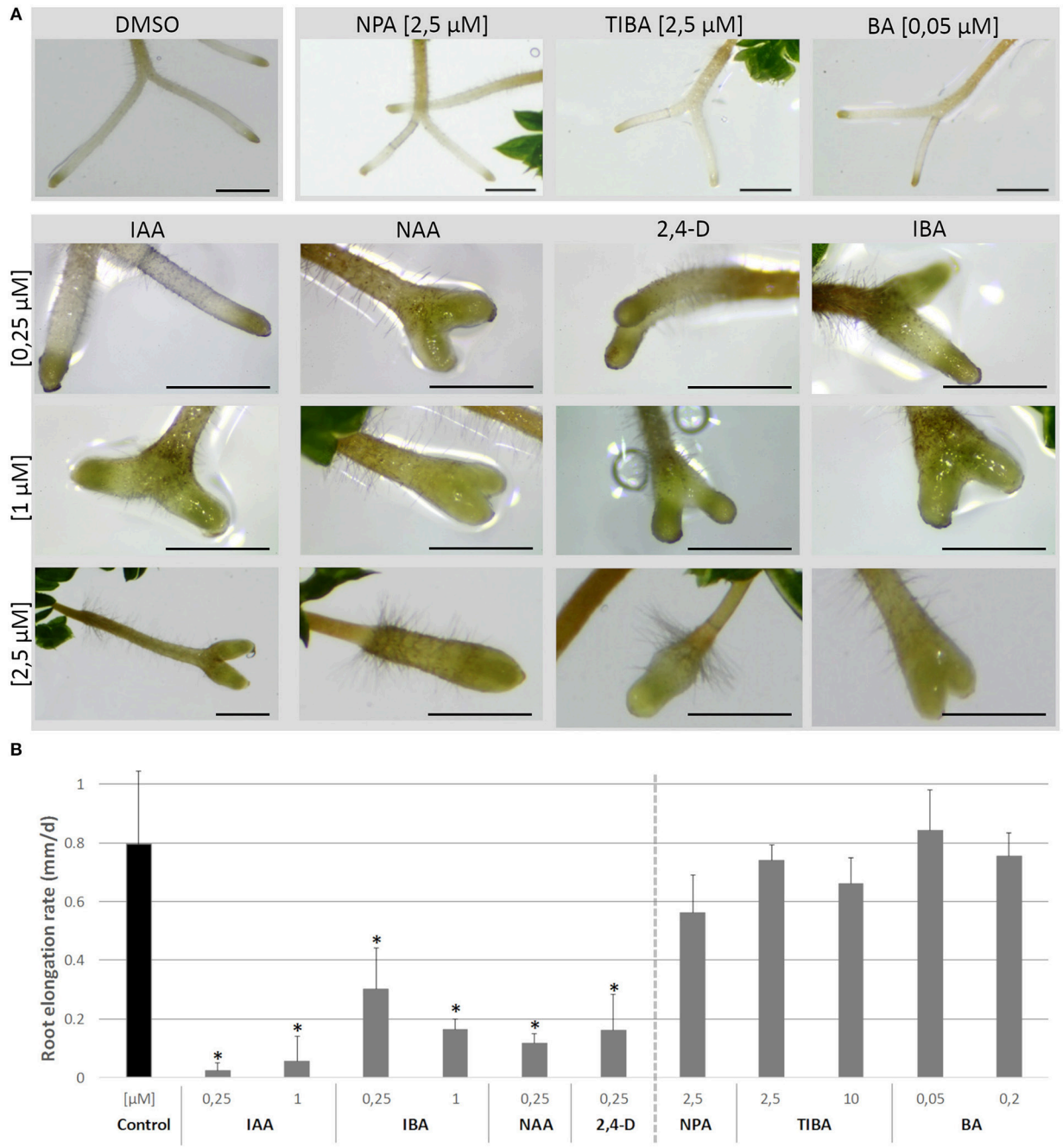

FIGURE 3 | Root growth after treatments with auxins, NPA, TIBA, and BA. **(A)** Explants with newly branched roots were treated with different concentrations of auxins, auxin transport inhibitors or the cytokinin BA for 4 days and root morphology was observed. Scale bars: 1 mm. **(B)** shows the effects of treatments on root elongation rate over the time frame between two branching events. Data is not presented for the treatments that severely inhibited branching or obstructed the observation of possible branching events. Error bars represent SD. *n* (number of plates) = 4 (except for 10 µM TIBA, *n* = 3) with on average 10 root samples per plate. *represents *p*-value ≤ 0.05 (Kruskal-Wallis test).

that these apices, without exception, only contain one single meristem. We were able to clearly recognize the described tetrahedral initial cell (IC) and its derivatives form the root meristem in root anatomy of Selaginella (**Figures 1G,H**). The presence of recently branched root tips in the starting material was thus crucial to dispose of a clear definable stage 0 that can be used for all the treatments.

On the short term, the auxin treatments, especially at higher concentrations, inhibited root elongation, caused thickening of the root tips, induced callus-like tissue and stimulated root hair elongation (**Figure 3**). The root elongation rate, calculated between two consecutive branching events, was severely inhibited even at low auxin concentrations. In contrast, the auxin transport inhibitor TIBA and a low concentration (2.5 μM) of NPA showed no or a limited effect on the root elongation and morphology. Only high concentrations (10 μM; 25 μM) of NPA did more severely affect the root morphology (**Figure S1**). None of the treatments induced laterally positioned root

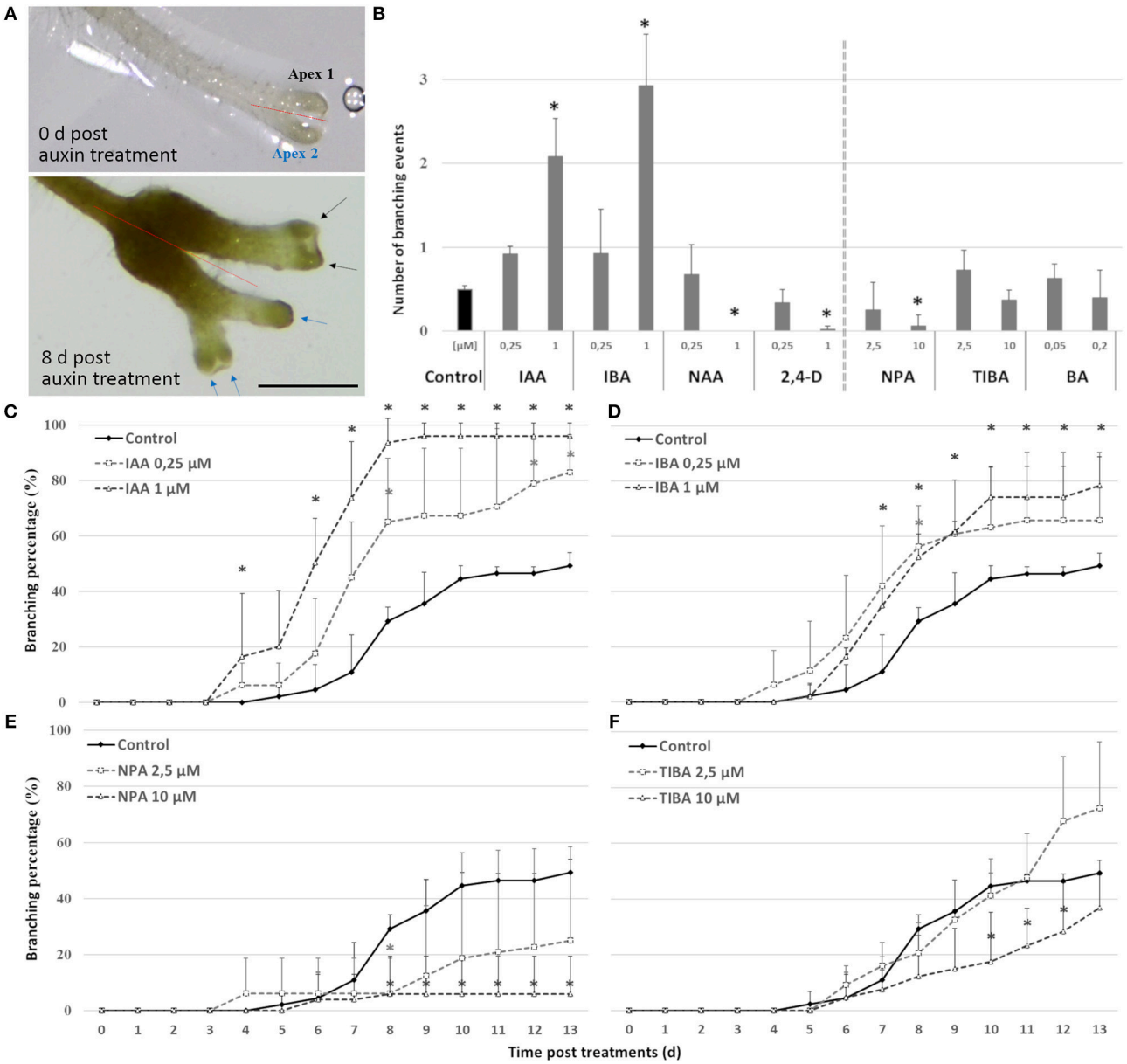

FIGURE 4 | Effect of auxins, polar auxin transport inhibitors and a cytokinin on Selaginella dichotomous root branching. Selaginella explants with newly branched roots were incubated with different concentrations of auxins, auxin transport inhibitors, or the cytokinin BA. **(A)** Selaginella root on 0 and 8 days after IAA (2.5 μM) treatment. Arrows of different colors indicate branching derived from different apices. Scale bar: 1 mm. **(B)** Number of branching events per root tip after 13 days. **(C–F)** Percentage of root tips that branched during 13 days of treatments. Error bars represent SD. *n* (number of plates) = 4 (except for 10 μM TIBA, *n* = 3) with on average 10 root samples per plate. *represents *p*-value ≤ 0.05 (Kruskal-Wallis test).

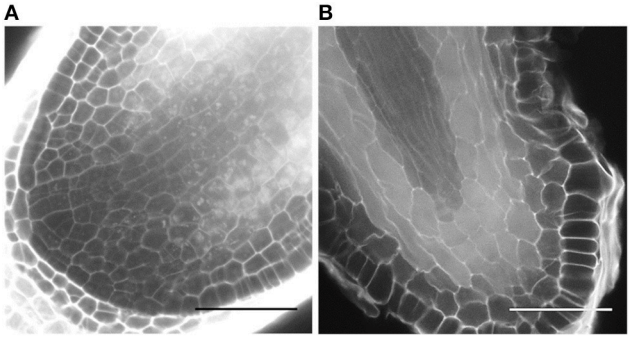

FIGURE 5 | Selaginella root meristem of **(A)** a DMSO-treated root or **(B)** a root treated with 25 μM NPA for 7 days. Scale bars: 50 μm.

branches, showing that the absence of lateral roots in Selaginella is not due to a limited auxin availability. There was, however, a positive effect on the bifurcation of roots. In accordance to the previous observations of (Sanders and Langdale, 2013), auxin treatment resulted in more branching and a higher branching frequency (**Figures 4A,B**). When we followed the first branching of individual root tips, in particular IAA and IBA induced much more root tips to bifurcate (**Figures 4C,D**). NAA and 2,4-D, even at a concentration of 0.25 μM, and all auxins at higher concentrations induced callus, which obstructed the observation of possible branching events (**Figure 3A**, **Figure S2**). The auxin transport inhibitors had in most cases no or only a weak effect on the branching (**Figures 4B,E,F**). Only at higher NPA concentrations, we noticed a strong inhibition of the root branching (**Figures 4B,E**), with a complete inhibition at 25 μM (data not shown). This however concurred with a growth arrest of the root tip and completely degenerated root meristem (**Figure 5**). Hence, it seems that auxin transport only affects the root meristem bifurcation when it is almost completely blocked, which in particular disturbs the meristem organization.

Auxin treatments induce only branches after 4 days, which is the same time required to obtain a bifurcation in the hormone-free control. If auxin would be capable in inducing the root meristem bifurcation itself, a much faster induction would have been anticipated.

Auxins Do Not Induce Root Meristem Bifurcation in Selaginella

To ascertain whether the bifurcation-promoting effect of auxin is direct or not, the effect of transient auxin treatments on root branching was assessed. 1 μM IAA was selected for this experiment as it had shown the highest potency in accelerating branching over long treatments. Shoot explants with a newly branched root were transferred to 1 μM IAA for either 1 or 2 days and then transferred back to either hormone-free or IAA medium. In contrast to continuous auxin application (transfer IAA to IAA), none of the transient treatments (IAA to 1/2MS) induced extra root branching compared to the untreated samples (1/2MS to 1/2MS) (**Figure 6**). This observation strengthens our previous observation that auxins do not induce the bifurcation of the root meristem itself in Selaginella but shorten the timing between two branching events.

To further confirm that auxins do not induce root branching in Selaginella, microscopic analysis at earlier time points was performed using a modified pseudo-Schiff propidium iodide staining and confocal microscopy. We were able to clearly recognize the described Selaginella root anatomy in which one tetrahedral initial cell (IC) and its derivatives form the root meristem (**Figures 1G,H**). To observe early stages in the meristem bifurcation process, we first collected multiple DMSO-treated root samples at different days after a new branch was formed. Several samples showed an early stage of meristem bifurcation at 3 days (**Figure 7A**). However, newly branched roots treated for 3 days with 1 μM IAA did not show any meristem bifurcation ($n = 11$). Conversely, a higher auxin concentration hardly affected the induction of meristem bifurcation: either a concentration of 2.5 μM (**Figure 7B**, $n = 13$) or 5 μM ($n = 5$) IAA yielded only 1 divided meristem after 3 days. Hence, auxins and auxin signaling seem to advance root branching most likely by promoting processes taking place after the early events during root meristem bifurcation and do not directly induce the bifurcation event itself in Selaginella.

DISCUSSION

Auxin is, in particular regarding to root development, a predominant plant growth regulator with a highly conserved signaling pathway within land plants (Kato et al., 2018; Mutte et al., 2018). Auxins were also reported to induce root cultures in *Selaginella microphylla* (Bandyopadhyay et al., 2013). In accordance with these findings, we did find evidence of a certain level of physiological conservation. Indeed, typical auxin responses such as root hair elongation, callus induction or root elongation inhibition occurred in *Selaginella moellendorffii* as well. In contrast, auxins did not induce root-bearing rhizophores formation nor dichotomous root branching in this species. This is suggestive for the existence of an auxin independent meristem initiation and branching mechanism. Polar auxin transport mechanisms are conserved as well (Viaene et al., 2013, 2014; Bennett et al., 2014; Bennett, 2015) and clearly have an important impact on the growth of Selaginella species (Wochok and Sussex, 1973, 1974, 1975; Sanders and Langdale, 2013; Matsunaga et al., 2017). However, the inhibition of polar auxin transport is not able to block root branching in *Selaginella moellendorffii*, which further supports a potential auxin-independent root branching mechanism. Only high concentrations of NPA resulted in a reduction in root branching, but does not delay the timing in branching, and can be interpreted as a presumably indirect effect.

Sanders and Langdale (2013) previously showed strongly branching root tips upon auxin treatment and hence suggested a role of auxin in this branching. Similarly, we also observed on the long term, in particular with high auxin concentrations, consecutive branches with shorter time intervals. However, as there is no difference in meristem formation, as shown by our microscopic observations, and as transient auxin treatments up

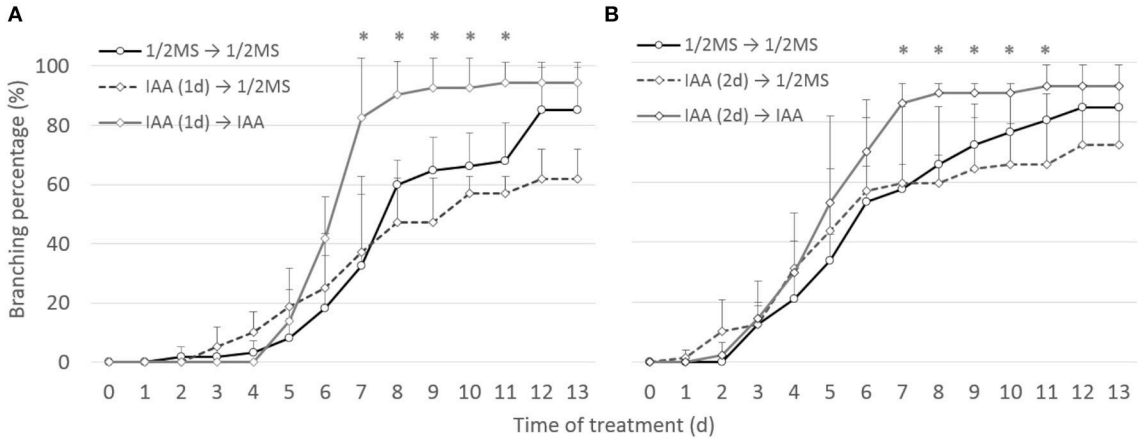

FIGURE 6 | Effect of short auxin treatment on dichotomous root branching. Selaginella explants with newly branched roots were treated with DMSO or 1 μM IAA for 1 **(A)** or 2 **(B)** days. Explants were then transferred to hormone-free or 1 μM IAA-containing media. Error bars represent SD. *n* (number of plates) = 3 with on average 15 root samples per plate. *represents *p*-value ≤ 0.05 (Kruskal-Wallis test).

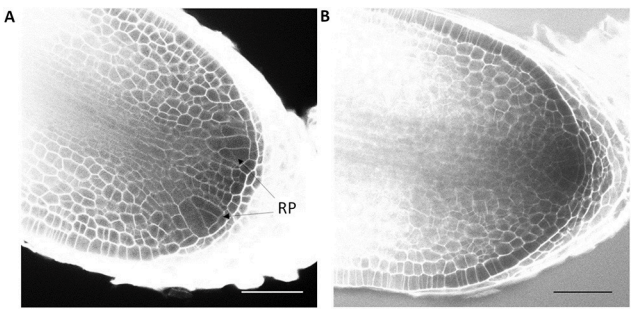

FIGURE 7 | Effect of auxin treatment on bifurcation of root apical meristem. Newly branched roots of Selaginella explants treated by DMSO and IAA were sampled for confocal microscopy daily from 0 to 3 d post treatment. **(A)** A newly bifurcated root meristem 3 days post DMSO treatment. Two new meristems could be clearly recognized. **(B)** A root meristem treated for 3 days with 2.5 μM IAA. RP, root primordium. Scale bar: 50 μm.

to 48 h do not result in an increased branching, the induction of root branching is clearly not directly affected by auxin. Hence, the increased root branching rather seems to be the consequence of an acceleration in development after branching which could have been resulted from shorter cell division cycles.

Possibly, the fundamental structural differences of Selaginella roots (Motte and Beeckman, 2018) are causative for the absence of an auxin-induced branching mechanism. The root meristem and cell divisions within the meristem are patterned differently in lycophytes compared to seed plants and therefore possibly adopted a different controlling program as well. The strong branching capacity of roots in the angiosperms moreover required the development of pluripotent pericycle cells. Although a pericycle layer is present in Selaginella species (Webster and Steeves, 1964), our observations suggests the absence of such pluripotency in the early land plants.

The fossil record shows that Lycophyte roots evolved independently from other clades (Raven and Edwards, 2001; Kenrick, 2002; Friedman et al., 2004; Boyce, 2005, 2010; Doyle, 2013; Hetherington and Dolan, 2018, 2019), but gene expression profiles suggested the presence of a root developmental program in a common ancestor or at least a parallel recruitment of largely the same root developmental program from a common ancestor (Huang and Schiefelbein, 2015). Based on our observations, this common program did, however, not contain the elements for the auxin-mediated meristem induction or root branching, which might only have been evolved later on. Supportive for this, lateral root formation in the fern *Ceratopteris richardii*, an earlier diverging lineage than the angiosperms, occurs also independently from auxin (Hou et al., 2004). Moreover, orthologs of important root meristem or lateral root factors downstream of auxin such as *WOX5* or *LBD16* are not found in the lycophyte clade (Nardmann et al., 2009; Coudert et al., 2013; Zhang et al., 2017). Hence, it seems that at least the root branching mechanisms downstream of auxin were only introduced during evolution after the origin of lycophytes, and further corroborates that roots originated multiple times during evolution.

In conclusion, by providing the first extensive evaluation of the effect of auxins on Selaginella root branching, we showed that root branching is not induced by auxins in this representative of an early diverging lineage of land plants. Despite conserved auxin signaling genes and conserved auxin responses, auxin itself seems to be not important for the root branching program and only acquired this role later during evolution.

AUTHOR CONTRIBUTIONS

TF, HM, and BP designed the experiments. TF performed the experiments. TF, HM, BP, and TB analyzed the data and wrote the manuscript. All the authors read and approved the final manuscript.

ACKNOWLEDGMENTS

We thank Davy Opdenacker for technical support. This study was financially supported by the Fonds voor Wetenschappelijk Onderzoek - Vlaanderen (FWO)-project G027313N. TF was financially supported by China Scholarship Council (CSC).

SUPPLEMENTARY MATERIAL

The Supplementary Material for this article can be found online at: https://www.frontiersin.org/articles/10.3389/fpls.2019.00154/full#supplementary-material

Figure S1 | Root growth after NPA, TIBA and BA treatments. Explants with newly branched roots were treated for 4 days and root morphology was observed. Scale bars: 1 mm.

Figure S2 | Effect of applied NAA, 2,4-D and BA on dichotomous root branching. Selaginella explants with newly branched roots were incubated with DMSO or different concentrations of treatments for 13 days: NAA **(A)**, 2,4-D **(B)**, and BA **(C)**. Error bars represent SD. *n* (number of plates) = 4 with on average 10 root samples per plate. *represents *p*-value ≤ 0.05 (Kruskal-Wallis test).

Video S1 | Selaginella shoot explant transferred to 1/2MS. The video shows the emergence of rhizophores and the subsequent development of roots from 8 days onwards.

REFERENCES

Abramoff, M., Magalhaes, P., and Ram, S. (2004). Image processing with ImageJ. *Biophoton. Intern.* 11, 36–42. Available online at: https://imagej.nih.gov/ij/

Bandyopadhyay, S., Nandagopal, K., and Jha, T. B. (2013). Characterization of RAM to SAM transitions in *Selaginella microphylla* grown *in vitro*. *Biol. Plant.* 57, 597–600. doi: 10.1007/s10535-013-0325-1

Banks, J. A. (2009). Selaginella and 400 million years of separation. *Annu. Rev. Plant. Biol.* 60, 223–238. doi: 10.1146/annurev.arplant.59.032607.092851

Banks, J. A., Nishiyama, T., Hasebe, M., Bowman, J. L., Gribskov, M., dePamphilis, C., et al. (2011). The Selaginella genome identifies genetic changes associated with the evolution of vascular plants. *Science* 332, 960–963. doi: 10.1126/science.1203810

Benkova, E., Michniewicz, M., Sauer, M., Teichmann, T., Seifertova, D., Jurgens, G., et al. (2003). Local, efflux-dependent auxin gradients as a common module for plant organ formation. *Cell* 115, 591–602. doi: 10.1016/S0092-8674(03)00924-3

Bennett, T. (2015). PIN proteins and the evolution of plant development. *Trends. Plant Sci.* 20, 498–507. doi: 10.1016/j.tplants.2015.05.005

Bennett, T. A., Liu, M. M., Aoyama, T., Bierfreund, N. M., Braun, M., Coudert, Y., et al. (2014). Plasma membrane-targeted PIN proteins drive shoot development in a moss. *Curr. Biol.* 24, 2776–2785. doi: 10.1016/j.cub.2014.09.054

Blilou, I., Xu, J., Wildwater, M., Willemsen, V., Paponov, I., Friml, J., et al. (2005). The PIN auxin efflux facilitator network controls growth and patterning in *Arabidopsis* roots. *Nature* 433, 39–44. doi: 10.1038/nature03184

Boyce, C. K. (2005). "The evolutionary history of roots and leaves," in *Vascular Transport in Plants,* eds N. M. Holbrook and M. A. Zwieniecki (Amsterdam: Elsevier Academic Press), 479–499.

Boyce, C. K. (2010). The evolution of plant development in a paleontological context. *Curr. Opin. Plant Biol.* 13, 102–107. doi: 10.1016/j.pbi.2009.10.001

Casimiro, I., Marchant, A., Bhalerao, R. P., Beeckman, T., Dhooge, S., Swarup, R., et al. (2001). Auxin transport promotes Arabidopsis lateral root initiation. *Plant Cell* 13, 843–852. doi: 10.1105/tpc.13.4.843

Chang, L., Ramireddy, E., and Schmülling, T. (2013). Lateral root formation and growth of *Arabidopsis* is redundantly regulated by cytokinin metabolism and signalling genes. *J. Exp. Bot.* 64, 5021–5032. doi: 10.1093/jxb/ert291

Coudert, Y., Dievart, A., Droc, G., and Gantet, P. (2013). ASL/LBD phylogeny suggests that genetic mechanisms of root initiation downstream of auxin are distinct in lycophytes and euphyllophytes. *Mol. Biol. Evol.* 30, 569–572. doi: 10.1093/molbev/mss250

De Rybel, B., Vassileva, V., Parizot, B., Demeulenaere, M., Grunewald, W., Audenaert, D., et al. (2010). A novel Aux/IAA28 signaling cascade activates GATA23-dependent specification of lateral root founder cell identity. *Curr. Biol.* 20, 1697–1706. doi: 10.1016/j.cub.2010.09.007

De Smet, I., Lau, S., Voss, U., Vanneste, S., Benjamins, R., Rademacher, E. H., et al. (2010). Bimodular auxin response controls organogenesis in *Arabidopsis*. *Proc. Natl. Acad. Sci. U.S.A.* 107, 2705–2710. doi: 10.1073/pnas.0915001107

Dello Ioio, R., Nakamura, K., Moubayidin, L., Perilli, S., Taniguchi, M., Morita, M. T., et al. (2008). A genetic framework for the control of cell division and differentiation in the root meristem. *Science* 322, 1380–1384. doi: 10.1126/science.1164147

Doyle, J. A. (2013). "Phylogenetic analyses and morphological innovations in land plants," in *Annual Plant Reviews,* eds A. A. Barbara and P. Michael (Hoboken: Blackwell Publishing Ltd.), 1–50.

Du, Y., and Scheres, B. (2018). Lateral root formation and the multiple roles of auxin. *J. Exp. Bot.* 69, 155–167. doi: 10.1093/jxb/erx223

Du, Y. J., and Scheres, B. (2017). PLETHORA transcription factors orchestrate de novo organ patterning during *Arabidopsis* lateral root outgrowth. *Proc. Natl. Acad. Sci. U.S.A.* 114, 11709–11714. doi: 10.1073/pnas.1714410114

Dubrovsky, J. G., Sauer, M., Napsucialy-Mendivil, S., Ivanchenko, M. G., Friml, J., Shishkova, S., et al. (2008). Auxin acts as a local morphogenetic trigger to specify lateral root founder cells. *Proc. Natl. Acad. Sci. U.S.A.* 105, 8790–8794. doi: 10.1073/pnas.0712307105

Friedman, W. E., Moore, R. C., and Purugganan, M. D. (2004). The evolution of plant development. *Am. J. Bot.* 91, 1726–1741. doi: 10.3732/ajb.91.10.1726

Fukaki, H., Tameda, S., Masuda, H., and Tasaka, M. (2002). Lateral root formation is blocked by a gain-of-function mutation in the *SOLITARY-ROOT/IAA14* gene of *Arabidopsis*. *Plant J.* 29, 153–168. doi: 10.1046/j.0960-7412.2001.01201.x

Goh, T., Kasahara, H., Mimura, T., Kamiya, Y., and Fukaki, H. (2012). Multiple AUX/IAA-ARF modules regulate lateral root formation: the role of *Arabidopsis* SHY2/IAA3-mediated auxin signalling. *Phil. Trans. R. Soc. B.* 367, 1461–1468. doi: 10.1098/rstb.2011.0232

Gola, E. M. (2014). Dichotomous branching: the plant form and integrity upon the apical meristem bifurcation. *Front Plant. Sci.* 5:263. doi: 10.3389/fpls.2014.00263

Hetherington, A. J., and Dolan, L. (2018). Stepwise and independent origins of roots among land plants. *Nature* 561, 235–238. doi: 10.1038/s41586-018-0445-z

Hetherington, A. J., and Dolan, L. (2019). Rhynie chert fossils demonstrate the independent origin and gradual evolution of lycophyte roots. *Curr. Opin. Plant Biol.* 47, 119–126. doi: 10.1016/j.pbi.2018.12.001

Himanen, K., Boucheron, E., Vanneste, S., de Almeida Engler, J., Inzé, D., and Beeckman, T. (2002). Auxin-mediated cell cycle activation during early lateral root initiation. *Plant Cell* 14, 2339–2351. doi: 10.1105/tpc.004960

Hou, G., Hill, J. P., and Blancaflor, E. B. (2004). Developmental anatomy and auxin response of lateral root formation in *Ceratopteris richardii*. *J. Exp. Bot.* 55, 685–693. doi: 10.1093/jxb/erh068

Huang, L., and Schiefelbein, J. (2015). Conserved gene expression programs in developing roots from diverse plants. *Plant Cell* 27, 2119–2132. doi: 10.1105/tpc.15.00328

Imaichi, R., and Kato, M. (1989). Developmental anatomy of the shoot apical cell, rhizophore and root of *Selaginella Uncinata*. *Bot. Mag. Tokyo* 102, 369–380. doi: 10.1007/BF02488120

Karabaghli-Degron, C., Sotta, B., Bonnet, M., Gay, G., and Le Tacon, F. (1998). The auxin transport inhibitor 2,3,5-triiodobenzoic acid (TIBA) inhibits the stimulation of *in vitro* lateral root formation and the colonization of the tap-root cortex of Norway spruce (*Picea abies*) seedlings by the ectomycorrhizal fungus *Laccaria bicolor*. *New Phytol.* 140, 723–733.

Kato, H., Nishihama, R., Weijers, D., and Kohchi, T. (2018). Evolution of nuclear auxin signaling: lessons from genetic studies with basal land plants. *J. Exp. Bot.* 69, 291–301. doi: 10.1093/jxb/erx267

Kenrick, P. (2002). "The origin of roots," in *Plant Roots: The Hidden Half, 3rd Edn.*, eds Y. Waisel, A. Eshel, T. Beeckman, and K. Uzi (New York, NY: Marcel Dekker, Inc.), 1–13.

Li, X., Mo, X., Shou, H., and Wu, P. (2006). Cytokinin-mediated cell cycling arrest of pericycle founder cells in lateral root initiation of *Arabidopsis*. *Plant Cell Physiol.* 47, 1112–1123. doi: 10.1093/pcp/pcj082

Matsunaga, K. K. S., Cullen, N. P., and Tomescu, A. M. F. (2017). Vascularization of the *Selaginella* rhizophore: anatomical fingerprints of polar auxin transport with implications for the deep fossil record. *New Phytol.* 216, 419–428. doi: 10.1111/nph.14478

Möller, B. K., Xuan, W., and Beeckman, T. (2017). Dynamic control of lateral root positioning. *Curr. Opin. Plant Biol.* 35, 1–7. doi: 10.1016/j.pbi.2016.09.001

Moreno-Risueno, M. A., Van Norman, J. M., Moreno, A., Zhang, J., Ahnert, S. E., and Benfey, P. N. (2010). Oscillating gene expression determines competence for periodic *Arabidopsis* root branching. *Science* 329, 1306–1311. doi: 10.1126/science.1191937

Motte, H., and Beeckman, T. (2018). The evolution of root branching: increasing the level of plasticity. *J. Exp. Bot.* 70, 785–793. doi: 10.1093/jxb/ery409

Mutte, S. K., Kato, H., Rothfels, C., Melkonian, M., Wong, G. K., and Weijers, D. (2018). Origin and evolution of the nuclear auxin response system. *Elife* 7:e33399. doi: 10.7554/eLife.33399

Nardmann, J., Reisewitz, P., and Werr, W. (2009). Discrete shoot and root stem cell-promoting *WUS/WOX5* functions are an evolutionary innovation of angiosperms. *Mol. Biol. Evol.* 26, 1745–1755. doi: 10.1093/molbev/msp084

Otreba, P., and Gola, E. M. (2011). Specific intercalary growth of rhizophores and roots in *Selaginella kraussiana* (Selaginellaceae) is related to unique dichotomous branching. *Flora* 206, 227–232. doi: 10.1016/j.flora.2010.07.001

Raven, J. A., and Edwards, D. (2001). Roots: evolutionary origins and biogeochemical significance. *J. Exp. Bot.* 52, 381–401. doi: 10.1093/jexbot/52.suppl_1.381

Reed, R. C., Brady, S. R., and Muday, G. K. (1998). Inhibition of auxin movement from the shoot into the root inhibits lateral root development in Arabidopsis. *Plant Physiol.* 118, 1369–1378. doi: 10.1104/pp.118.4.1369

Sabatini, S., Beis, D., Wolkenfelt, H., Murfett, J., Guilfoyle, T., Malamy, J., et al. (1999). An auxin-dependent distal organizer of pattern and polarity in the *Arabidopsis* root. *Cell* 99, 463–472. doi: 10.1016/S0092-8674(00)81535-4

Sanders, H. L., and Langdale, J. A. (2013). Conserved transport mechanisms but distinct auxin responses govern shoot patterning in *Selaginella kraussiana*. *New Phytol.* 198, 419–428. doi: 10.1111/nph.12183

Truernit, E., Bauby, H., Dubreucq, B., Grandjean, O., Runions, J., Barthélémy, J., et al. (2008). High-resolution whole-mount imaging of three-dimensional tissue organization and gene expression enables the study of phloem development and structure in *Arabidopsis*. *Plant Cell* 20, 1494–1503. doi: 10.1105/tpc.107.056069

Viaene, T., Delwiche, C. F., Rensing, S. A., and Friml, J. (2013). Origin and evolution of PIN auxin transporters in the green lineage. *Trends. Plant Sci.* 18, 5–10. doi: 10.1016/j.tplants.2012.08.009

Viaene, T., Landberg, K., Thelander, M., Medvecka, E., Pederson, E., Feraru, E., et al. (2014). Directional auxin transport mechanisms in early diverging land plants. *Curr. Biol.* 24, 2786–2791. doi: 10.1016/j.cub.2014.09.056

Webster, T. R., and Steeves, T. A. (1964). Developmental morphology of the root of *Selaginella kraussiana* A. Br. and *Selaginella wallacei* Hieron. *Can. J. Bot.* 42, 1665–1676. doi: 10.1139/b64-165

Wochok, Z. S., and Sussex, I. M. (1973). Morphogenesis in *Selaginella*: auxin transport in stem. *Plant Physiol.* 51, 646–650. doi: 10.1104/pp.51.4.646

Wochok, Z. S., and Sussex, I. M. (1974). Morphogenesis in *Selaginella*: II. Auxin transport in root (rhizophore). *Plant Physiol.* 53, 738–741. doi: 10.1104/pp.53.5.738

Wochok, Z. S., and Sussex, I. M. (1975). Morphogenesis in *Selaginella*. III. Meristem determination and cell-differentiation. *Dev. Biol.* 47, 376–383. doi: 10.1016/0012-1606(75)90291-2

Zhang, Y., Jiao, Y., Jiao, H., Zhao, H., and Zhu, Y. (2017). Two-step functional innovation of the stem-cell factors WUS/WOX5 during plant evolution. *Mol. Biol. Evol.* 34, 640–653. doi: 10.1093/molbev/msw263

Conflict of Interest Statement: The authors declare that the research was conducted in the absence of any commercial or financial relationships that could be construed as a potential conflict of interest.

frontiers in Plant Science

REVIEW
published: 04 March 2019
doi: 10.3389/fpls.2019.00237

Root Branching and Nutrient Efficiency: Status and Way Forward in Root and Tuber Crops

*Luis O. Duque[1] and Arthur Villordon[2]**

[1] Department of Plant Science, The Pennsylvania State University, University Park, PA, United States, [2] Sweet Potato Research Station, Louisiana State University Agricultural Center, Chase, LA, United States

Plants are immobile organisms that require roots to efficiently and cost-effectively exploit their habitat for water and nutrients. Plant root systems are dynamic structures capable of altering root branching, root angle, and root growth rates determining overall architecture. This plasticity involves belowground plant-root mediated synergies coupled through a continuum of environmental interactions and endogenous developmental processes facilitating plants to adapt to favorable or adverse soil conditions. Plant root branching is paramount to ensure adequate access to soil water and nutrients. Although substantial resources have been devoted toward this goal, significant knowledge gaps exist. In well-studied systems such as rice and maize, it has become evident that root branching plays a significant role in the acquisition of nutrients and other soil-based resources. In these crop species, specific root branching traits that confer enhanced nutrient acquisition are well-characterized and are already being incorporated into breeding populations. In contrast, the understanding of root branching in root and tuber crop productivity has lagged behind. In this review article, we highlight what is known about root branching in root and tuber crops (RTCs) and mark new research directions, such as the use novel phenotyping methods, examining the changes in root morphology and anatomy under nutrient stress, and germplasm screening with enhanced root architecture for more efficient nutrient capture. These directions will permit a better understanding of the interaction between root branching and nutrient acquisition in these globally important crop species.

Keywords: root system architecture (RSA), root and tuber crops, nutrient efficiency, sweetpotato, potato, yam, cassava

OPEN ACCESS

Edited by:
Joseph G. Dubrovsky, National Autonomous University of Mexico, Mexico

Reviewed by:
Johannes Auke Postma, Forschungszentrum Jülich, Germany
Peter John Gregory, University of Reading, United Kingdom

****Correspondence:***
Arthur Villordon
avillordon@agcenter.lsu.edu

Specialty section:
This article was submitted to Plant Development and EvoDevo, a section of the journal Frontiers in Plant Science

Received: *01 November 2018*
Accepted: *12 February 2019*
Published: *04 March 2019*

Citation:
Duque LO and Villordon A (2019) Root Branching and Nutrient Efficiency: Status and Way Forward in Root and Tuber Crops. Front. Plant Sci. 10:237. doi: 10.3389/fpls.2019.00237

INTRODUCTION

A plant's ability to explore the soil and to compete for soil resources is largely dependent on the architecture of its root system (Lynch, 1995). Root system architecture (RSA) is determined by the pattern of root branching and by the rate and trajectory of growth of individual roots (Zhang et al., 1999). There is scientific consensus that root branching is subject to genetic control and influenced by biotic and abiotic factors. Therefore, manipulating RSA has emerged as a fundamental strategy to enhance nutrient acquisition especially in low input agricultural systems. For example, Gamuyao et al. (2012) documented the presence of a Pup1-specific protein kinase gene, the phosphorus-starvation tolerance 1 (PSTOL1) derived from the traditional aus-type rice

variety Kasalath. This protein kinase was shown to enhance early root growth, thereby enabling plants to acquire more phosphorus and other nutrients under phosphorus-deficient soils. Gamuyao et al. (2012) suggested that introduction of this quantitative trait locus into locally adapted rice cultivars in Asia and Africa could enhance productivity under low nutrient conditions. Follow-up work by Neelam et al. (2017) documents novel alleles of *PSTOL1* in *Oryza rufipogon*, the Asian wild rice, and work is already ongoing to introduce these alleles in elite rice cultivars. This and other similar examples underscore the importance of gaining a comprehensive understanding of root architecture adaptations that could contribute to productivity under marginal or low-input growing conditions. Low soil fertility in developing countries is a primary constraint to food security and economic development (Rao et al., 2016). In Africa in particular, depletion of soil fertility is a major biophysical cause of low per capita food production, contributing to food insecurity in the region (Sanchez, 2002). Increasing the capacity of plants to acquire soil resources is a key approach to improve crop yields and reduce farmer's dependence on fertilizers (Bishopp and Lynch, 2015). The cereal species wheat and rice provide more than 50% of the calories consumed by humans (Rich and Watt, 2013). However, root and tuber crops (RTCs) are second in importance to cereals as a global source of carbohydrates, and grown in regions not suitable for cereal production[1]. In this work, we focus mainly on cassava (*Manihot esculenta*), potato (*Solanum tuberosum*), sweetpotato (*Ipomoea batatas*) and yams (*Dioscorea sp*), which the Food and Agriculture Organization defines as among the primary root and tuber crops of global importance[2].

ROOT ARCHITECTURE AND NUTRIENT EFFICIENCY IN ROOT AND TUBER CROPS: THE CURRENT STATE OF KNOWLEDGE

Two comprehensive reviews of literature regarding root architecture in RTCs were conducted in 2014 and 2016 (Villordon et al., 2014; Khan et al., 2016). Curiously enough, in a comprehensive review of the subject matter, it was determined that between 2004 and 2014, there was only one published work on the subject of root morphological description for each of the RTCs compared to 12 for maize (Villordon et al., 2014). In the current work, we surveyed articles published within the past 10 years that specifically address the relationship of root architecture in response to heterogenous nutrient environments in RTCs (**Table 1**).

Crops frequently alter both their aboveground as well as their belowground structures morphologically and physiologically in response to heterogeneous nutrient environments (Drew, 1975; Fransen et al., 1999; Hodge, 2004), in which yield and nutrient uptake capabilities surpass those in nutrient-homogeneous environments. Of these soil mineral nutrients, nitrogen (N), phosphorus (P) and potassium (K) are considered the most important for crop growth, development and subsequent yield. However, phytoavailability of NPK often limits low-input agriculture (Mueller et al., 2012; White et al., 2013). For comparison, we included references available for the relationship between root architecture manipulation and NPK uptake in rice. The survey reveals a disturbing trend: the number of publications on rice exceeds the combined scientific output of the RTCs. Relative to the rice knowledge base, there is a substantial knowledge gap in RTCs about the role of RSA in the exploration and acquisition of nutrients in low-input environments. The survey reveals that rice RSA research has focused on N and P. This is consistent with current understanding that N and P availability are the primary global constraints and particularly severe in low-input agriculture characteristic of many developing nations (Lynch, 2007). N compounds are mobile and prone to leaching into deeper soils. In contrast, P accumulates mainly in the topsoil in part due to its low mobility. Among the RTCs, potato leads in terms of research output, primarily focusing on P. This is in part due to the large P requirement in the crop, about two-fold higher compared to that of cereal crops such as wheat and barley and 1/3 higher compared to most vegetable crops (White et al., 2018). The published studies on potato RSA and P, although relatively fewer compared to rice, has led to direct applications in terms of identifying desirable root traits for improved P acquisition and the identification of cultivars and genotypes with improved P efficiency in low nutrient conditions (White et al., 2005, 2018; Wang et al., 2015; Krell et al., 2018).

In sweetpotato, the published reports on N and P represent translational research of key findings from model systems (i.e., *Arabidopsis*, maize and rice). First, Villordon et al. (2013) demonstrated that lateral root branching jointly measured as lateral root length, number of lateral roots and lateral root density in sweetpotato cv. Beauregard was altered in response to variation in overall available N. The variation in RSA in response to different available N was consistent with prior work in *Arabidopsis* where external N presence had stimulatory effect on lateral root elongation, whereas high N concentrations inhibited lateral root meristem activity (Zhang et al., 2007). The data regarding relationship between

TABLE 1 | Survey of articles published within the past 10 years that address root architecture and NPK acquisition in rice, cassava, sweetpotato, potato, and yams.

Nutrient	Crop species	Reference
Nitrogen	Rice	Obara et al., 2010; Ji et al., 2012; Ogawa et al., 2014; Ju et al., 2015; Kim et al., 2015; Selvaraj et al., 2017
	Sweetpotato	Villordon et al., 2013, 2014
Phosphorus	Rice	Shimizu et al., 2008; Fang et al., 2009; Li et al., 2009; Dai et al., 2012; Gamuyao et al., 2012; Shen et al., 2013; Takehisa et al., 2013; Topp et al., 2013; Vejchasarn et al., 2016
	Potato	Balemi and Schenk, 2009; Wang et al., 2015; Krell et al., 2018; White et al., 2018
	Sweetpotato	Villordon et al., 2018
Potassium	Rice	Jia et al., 2008; Ma et al., 2012

[1]http://www.fao.org/docrep/x5415e/x5415e01.htm

[2]http://www.fao.org/docrep/005/y9422e/y9422e0d.htm

spatial N availability and RSA modifications were similar to findings in *Arabidopsis* model systems that localized N availability is critical for lateral root signaling and development (Zhang and Forde, 2000; Zhang et al., 2007; Lima et al., 2010). Second, Villordon et al. (2018) reported that storage root length in sweetpotato cvs. Bayou Belle and Beauregard varied in response to experimental P deficiency. These findings corroborate available experimental evidence in *Arabidopsis* model systems that support the hypothesis that the root tip is the site of P sensing and that optimal or low P is involved in the growth or arrest of primary root growth (Svistoonoff et al., 2007; Kellermeier et al., 2014; Medici et al., 2015; Abel, 2017).

With regards to K, Liu et al. (2017) showed differences in root morphology under controlled K and deficient K treatments in two representative sweetpotato cultivars, Ningzishu 1 (sensitive to K deficiency) and Xushu 32 (tolerant to K deficiency). Under K deficiency, root length, surface area, root volume and average root diameter was reduced in Ningzishu 1 compared to Xushu 32. Interestingly, the proportion of fine roots (Ø < 0.5 mm) and thick root (Ø > 1.0 mm) of Xushu 32 seedlings increased significantly under condition of K deficiency. These results indicate potential genotypic differences in RSA and K absorption ability under K deficiency. Similarly, Wang et al. (2017) under field conditions, indicated that increased K application increased total root length, average root diameter and significantly increased the differentiation from adventitious roots to fibrous roots and tuberous roots. This root traits coupled with added K is beneficial to the early formation of storage roots and number of storage roots per plant, overall root biomass and yield.

However, limited work on the relationship between RSA and NPK can be found for cassava and yams, the most important RTC species in sub-Saharan Africa[3]. In cassava, Izumi et al. (1999) provided evidence that well-developed branching pattern (i.e., number and length of axile roots and lateral roots) and total root length was associated with water and nutrient absorption and essential for storage root bulking. There has been some follow-up work on the role of cassava RSA and drought tolerance but none for nutrient acquisition (Pardales and Esquibel, 1996; Subere et al., 2009). Adu et al. (2018) corroborated earlier findings and documented root genotypic variation in relative root growth rate, root length, number of nodal roots, root diameter and root branching density in a panel of cassava cultivars bred for high carotenoid content and resistance to cassava mosaic disease (CMD), recommending further studies regarding manipulating cassava RSA for nutrient use efficiency and yield.

Charles-Dominique et al. (2009) conducted an analysis of the tuber monocot, white yam (*Dioscorea cayennensis* subsp. *rotundata* Poir., *Dioscoreaceae*) root system derived from both sexually and vegetatively propagated yams and demonstrated that both seedlings and plants derived from tubers have two distinct root systems that are highly organized. The first type of root system (seminal) is considered transitory (i.e., short-lived) consisting of two root axis categories. The second type of root system (adventitious) is considered permanent and is larger in weight and volume compared to the transitory root system. This adventitious root system is made up of three root axis categories and this is the site for initial tuber formation. Charles-Dominique et al. (2009) concluded the importance of studying the yam root system architecture as a whole and simultaneously in order to understand its growth, development and tuber formation. In a similar study, Hgaza et al. (2012) documented the response of the RSA of water yam (*Dioscorea alata*) and white yam (*Dioscorea cayennensis* subsp. *rotundata*) to mineral fertilizer application under field conditions. Researchers used sequential root coring to assess horizontal and vertical root distribution. Results revealed three root types (seminal, adventitious and tuber roots) and differences in root length density, root mass density and specific root length correlated directly with higher temperature and not with fertilizer application when compared to controls. Hgaza et al. (2012) concluded that tuber formation was independent from seminal and adventitious root development and mineral nutrition did not affect final tuber yield.

The significant resources devoted to the investigation of RSA in cereal crops has led to advances in breeding and selecting RSA for improved NPK acquisition in low-input production environments. **Table 2** summarizes the root traits necessary for adaptation to low NPK conditions in rice, maize, and the common bean (*Phaseolus vulgaris* L.) (Lynch and Brown, 1998; Kong et al., 2014). In maize, it has been determined that deeper roots are associated with increased acquisition of N that may leach to lower soil layers (Lynch and Wojciechowski, 2015). In rice, there is evidence that *DEEPER ROOTING 1*, a quantitative trait locus for root growth angle, increased N uptake in N-deficient conditions (Arai-Sanoh et al., 2014). This knowledge has led breeding programs to screen rice and maize genotypes for this desirable trait but also to invest in management practices like nutrient amendments that could improve root growth in rice (Abiven et al., 2015; Ju et al., 2015; Qiao et al., 2018).

TABLE 2 | Summary of relevant root traits related to N and P deficiency in rice, maize, and beans.

Species	Nutrient deficiency	Root traits	Reference
Rice	N	Deeper roots	Ogawa et al., 2014; Ju et al., 2015
Maize	N	Low lateral root (LR) branching density, longer LRs	Postma et al., 2014; Yu et al., 2015a; Zhan and Lynch, 2015
		Deeper roots	Lynch and Wojciechowski, 2015; Yu et al., 2015b
		Low crown root number	Saengwilai et al., 2014
Rice	P	Early root growth	Gamuyao et al., 2012
Maize	P	High LR branching density, shorter LRs	Postma et al., 2014
Bean	P	Decreased root metabolic cost, higher root hair length and density	Strock et al., 2018

[3]www.fao.org/docrep/x5415e/x5415e01.htm

MANIPULATING ROOT SYSTEM ARCHITECTURE FOR INCREASED NUTRIENT EFFICIENCY: WAY FORWARD FOR ROOT AND TUBER CROPS

Advances in manipulating RSA in cereal crops like rice and maize can serve as a model for RTCs. Meaningful advances in rice and maize RSA were made possible by first achieving fundamental understanding of the intrinsic and environmental factors that control RSA. Some of these findings have already been translated into some RTCs, underscoring the importance of translating findings from model crop systems, such as, rice, maize and bean into non-model species, such as, sweetpotato, potato, and yams. Concomitant with the understanding of the biology of RSA, significant investments were made toward the development of minimally intrusive, non-destructive whole-root phenotyping systems (Chen et al., 2011; Kuijken et al., 2015). The development of these phenotyping platforms in turn enabled functional genomics and crop improvement applications (Yang et al., 2013). These phenotyping tools and approaches can be adapted for use in RTCs.

Recent and past advances in understanding RSA have come from the studies on the model plant *Arabidopsis thaliana* and the description of the cellular structure laid the foundation for developmental and genetic work in cereals and other well-studied crops (Dolan et al., 1993; Smith and De Smet, 2012). Similar to RTCs, the *Arabidopsis* root system undergoes secondary thickening under appropriate growth conditions (Dolan and Roberts, 1995; Chaffey et al., 2002). In these and other root crops, root secondary growth followed by starch deposition and increase in root biomass determine the harvestable agronomic yield. This particular area of research has not been extensively studied in RTC under nutrient deficiencies and merits research.

Reduced metabolic cost of soil exploration is important for P capture because continued soil probing is required to increase beyond the depletion of available P in the rhizosphere (Lynch, 2015). For example, the formation of root cortical aerenchyma (RCA) in different crop species is one of the latest advances in our understanding of the impact of nutrient deficiencies in root architecture. RCA is defined as tissue with large intercellular spaces in root cortex normally produced in plant species under hypoxia (Esau, 1977; Drew et al., 1979). However, RCA can be also formed in response to drought and edaphic stresses such as N and S deficiencies (Drew et al., 1989; Bouranis et al., 2003; Fan et al., 2003, Zhu et al., 2010). In maize, genotypes with greater RCA had greater topsoil foraging, P acquisition, growth and yield under low P environments (Galindo-Castañeda et al., 2018). Currently, there are no published studies on the formation of RCA in RTCs.

Another important change in root architecture as a result of nutrient deficiency is the presence or absence of root secondary growth. It has been hypothesized that a decrease in root secondary growth could lessen the carbon cost of producing and sustaining root length to improve the balance between soil exploration use and depletion of growth limiting nutrients (Lynch, 1995). This may be an adaptive strategy to improve the metabolic efficiency of soil foraging under sub-optimal P, where roots will favor primary growth (elongation) over secondary growth (radial swelling) to reach greater probing of soil areas that still hold available P (Lynch, 2007, 2011; Lynch and Brown, 2008; De la Riva, 2010). In bean, secondary root growth under low P is inhibited, but genotypes with higher inhibition of secondary root growth presented reduced root costs, greater P capture, and greater growth under low P environments (Strock et al., 2018). Contrary to the reduced bean secondary root growth model, sweetpotato storage and lateral root growth were not reduced under sub-optimal P levels (Duque and Lynch, 2018).

New evidence in sweetpotato RSA under low P environments both in greenhouse and field settings suggests a reduction in metabolic costs of soil exploration with the formation of RCA after root secondary growth in basal cross sections of storage roots but not in lateral roots (**Figure 1**). These preliminary results suggest a translocation of carbon resources from the storage root to the lateral roots to enhance further soil exploration and/or increase of lateral root branching (Duque and Lynch, 2018). Based on these primary results, RCA merits research on how it can potentially affect final root yield. However, this phenomenon could have profound effects on storage root size, shape and yield, thus future research should focus on the assessment of early versus late bulking genotypes, root genotypic variability and tolerance of sweetpotato under P deficiency, focusing breeding and management efforts for degraded, low input agricultural systems found in Sub-Saharan Africa where sweetpotato as well as other RTCs are staple and subsistence crops.

Indeed, for RTCs in general, species-specific RSA knowledge appears to be at the level of classical morphology and with scant information on the genetic, hormonal, and molecular

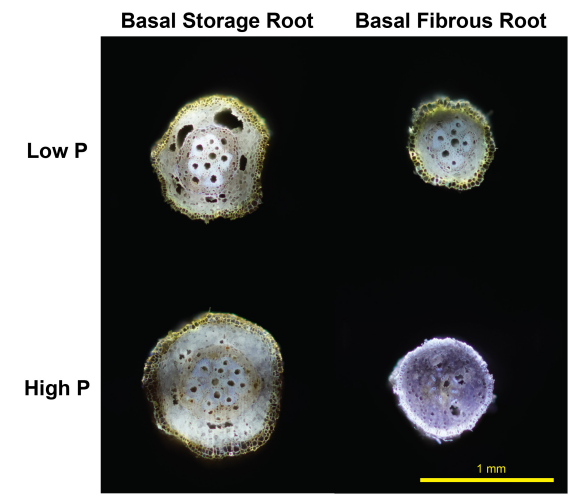

FIGURE 1 | Root cortical aerenchyma-like structure formed after secondary root growth under low phosphorus in sweetpotato storage root and fibrous root at 30 DAP. (Basal meaning root segment farthest from the attachment to the stem node). Root transversal cut sections were performed using laser ablation tomography. Ablation and picture were taken by Peter Ilhardt at Penn State University.

control of RSA. For root crops in particular, there is a general disconnect between RSA and storage root formation under nutrient deficiencies or water stress, either at the genetic, hormonal and/or molecular level. There has been crop-specific progress on the relationship between RSA and storage root formation in sweetpotato. In particular, it has been shown that lateral root development is a prerequisite to secondary cambium development in the adjacent main root tissue (Villordon et al., 2012). Previously, a cytokinin-regulated *I. batatas MADS-box 1* (*IbMADS1*) showed evidence of selective gene expression in meristematic tissue in the stele and in lateral root primordia and it has been proposed that this gene is an integrator at the onset of storage root formation in a network that involves hormones such as jasmonic acid and cytokinin as trigger factors (Ku et al., 2008). *IbMADS1* belongs to the same family as *Arabidopsis nitrate regulated* (*ANR1*), a gene previously shown to be associated with *Arabidopsis* lateral root development in response to nitrate (Zhang and Forde, 1998). In potato, it has been determined that RSA traits such as specific root length of basal roots and total root weight for various root classes are related to final tuber yield (Wishart et al., 2013). Basal roots are important for water uptake and anchorage, whereas stolon roots are connected with nutrient acquisition and tuber formation (Wishart et al., 2013). An earlier work by Sattelmacher et al. (1990) provided evidence that root length and surface area was important for nitrogen acquisition and that a large root system was associated with higher N acquisition.

Despite these efforts, the link between storage root/tuber yield and the carbon partitioning to other root types as well as the regulatory networks involved in RTCs has yet to be established (Khan et al., 2016). However, the cumulative evidence supporting the link between RSA and storage root in sweetpotato and between RSA and tuber yield in potato paves the way forward for more in depth work in sweetpotato and potato as well as similar studies in other RTCs. Root systems are inherently difficult to study and frequently overlooked in research. Due in large part to the RSA work in cereals and other model systems, novel tools and approaches have been developed to non-invasively measure root development in laboratory, greenhouse and field settings. Traditional methods for studying root systems include rhizotrons (Nagel et al., 2012), rhizoboxes (Lemming et al., 2016), and excavation (Bucksch et al., 2014). Image-based systems have been developed to overcome the phenotyping bottleneck, including X-ray computed tomography (Mairhofer et al., 2012), magnetic resonance imaging (Metzner et al., 2015; van Dusschoten et al., 2016), and ground penetrating radar (Guo et al., 2013), among others. However, wide scale adoption of some of these methods continued to be hampered by prohibitive costs and lack of accessibility. In RTCs, some of the non-destructive methods that have been used in the field with limited samples include rhizotrons or rhizotron-like methods in cassava (Tscherning et al., 1995), potato (Parker et al., 1991) and sweetpotato (Villordon et al., 2011). The use of viewing devices like minirhizotrons have actually been shown to interfere with storage root formation (Villordon et al., 2011), further limiting the options to study the relationship between RSA and storage root formation in root crops. Taken together, it appears that critical barriers to progress in understanding crop-specific RSA attributes in RTCs include the lack of a model system for interpreting the relationship between RSA and storage root and tuber yield and the current prohibitive costs of non-destructive, high-throughput image-based phenotyping tools.

One way forward to overcome these barriers is to use the sweetpotato (dicot, storage root), cassava (dicot, storage root), potato (dicot, tuber) and yam (monocot, tuber) as primary model systems for understanding the connection between RSA and agronomic yield in RTCs, respectively. These RTCs are considered the most important calorie-producing staple crops for smallholder subsistence farmers combined with low input agriculture on marginal lands typically located in underdeveloped countries.

Strategic translational research using data on RSA and NPK uptake from *Arabidopsis* and cereal model systems should continue using key RTC cultivars, as a means to rapidly validate key findings. Once validated, information on key RSA traits should be immediately forwarded to breeding programs for further studies and validation in breeding populations. These breeding programs should take advantage of available resources for adapting phenotyping methods for integrating root traits into existing breeding objectives. Finally, international agricultural research centers, as well as national institutions that have mandates in RTCs, should continue to intensify RSA research investments into their current and future research priorities, especially under the threat of climate change, vulnerable agro-ecological landscapes and poverty. During the first Green Revolution, improved rice and wheat varieties were rapidly adopted in tropical and subtropical regions that had good irrigation systems or reliable rainfall (Evenson and Gollin, 2003). The spread of these improved varieties was associated with the activity of international agricultural research centers (Evenson and Gollin, 2003). It has been suggested that a second Green Revolution, one that incorporates RSA traits, is vital to improve the yield of crops grown in infertile soils by farmers with little or no access to fertilizers (Lynch, 2007). Just like the first Green Revolution, such research centers will likely have an important role in ushering in the second Green Revolution (Zeigler and Mohanty, 2010).

CONCLUSION

The agronomic significance of understanding the regulation of RSA development is now widely accepted because of its role in soil resource acquisition under edaphic stress. In well-studied "model" crop species like rice, maize, and soybeans, the knowledge of RSA has already led to measurable gains in the ability of these crops to exploit soil resources under low-input conditions. For example, Zhao et al. (2004) reviewed by Li et al. (2016), showed that an applied core collection of soybeans

with shallow root architecture presented improved spatial root aggregations enhancing P explorations resulting in higher P efficiency and yield. In maize, Liu et al. (2018) showed a positive and significant correlation between grain yield and both total root number and total root length. The tools and approaches that have been used in cereals can be applied to RTCs, potentially reducing the costs of research and development, however, these novel tools and approaches have to be sufficiently modified to account for real-time tuber and storage root development and growth as no single phenotyping platform nor specialized analytical software exists at the moment for RTCs. Unraveling the role of RSA in RTC nutrient uptake will improve global food security, especially in regions with marginal soil fertility and low-input agricultural conditions.

DATA AVAILABILITY

All datasets generated for this study are included in the manuscript and/or the supplementary files.

AUTHOR CONTRIBUTIONS

LD and AV conceptualized and wrote the review.

FUNDING

This work was supported by the USDA National Institute of Food and Agriculture and Hatch Appropriations under Project #PEN04582 and Accession #1005492. The Louisiana Sweetpotato Advertising and Development Fund supported portions of this work.

ACKNOWLEDGMENTS

Laser Ablation Tomography analyses were performed at the Roots Lab (Penn State University, University Park, PA, United States). LD would like to thank Dr. Jonathan Lynch and the Roots Labs for their practical advice and technical assistance.

REFERENCES

Abel, S. (2017). Phosphate scouting by root tips. *Curr. Opin. Plant Biol.* 39, 168–177. doi: 10.1016/j.pbi.2017.04.016

Abiven, S., Hund, A., Martinsen, V., and Cornelissen, G. (2015). Biochar amendment increases maize root surface areas and branching: a shovelomics study in Zambia. *Plant Soil* 395, 45–55. doi: 10.1007/s11104-015-2533-2

Adu, M. O., Asare, P. A., Asare-Bediako, E., Amenorpe, G., Ackah, F. K., Afutu, E., et al. (2018). Characterising shoot and root system trait variability and contribution to genotypic variability in juvenile cassava (*Manihot esculenta* Crantz) plants. *Heliyon* 4:e00665. doi: 10.1016/j.heliyon.2018.e00665

Arai-Sanoh, Y., Takai, T., Yoshinaga, S., Nakano, H., Kojima, M., Sakakibara, H., et al. (2014). Deep rooting conferred by DEEPER ROOTING 1 enhances rice yield in paddy fields. *Sci. Rep.* 4:5563. doi: 10.1038/srep05563

Balemi, T., and Schenk, M. K. (2009). Genotypic variation of potato for phosphorus efficiency and quantification of phosphorus uptake with respect to root characteristics. *J. Plant Nutr. Soil Sci.* 172, 669–677. doi: 10.1002/jpln.200800246

Bishopp, A., and Lynch, J. P. (2015). The hidden half of crop yields. *Nat. Plants* 1, 10–38. doi: 10.1038/nplants.2015.117

Bouranis, D. L., Chorianopoulou, S. N., Siyiannis, V. F., Protonotarios, V. E., and Hawkesford, M. J. (2003). Aerenchyma formation in roots of maize during sulphate starvation. *Planta* 217, 382–391. doi: 10.1007/s00425-003-1007-6

Bucksch, A., Burridge, J., York, L. M., Das, A., Nord, E., Weitz, J. S., et al. (2014). Image-based high-throughput field phenotyping of crop roots. *Plant Physiol.* 166, 470–486. doi: 10.1104/pp.114.24351

Chaffey, N., Cholewa, E., Regan, S., and Sundberg, B. (2002). Secondary xylem development in *Arabidopsis*: a model for wood formation. *Physiol. Plant.* 114, 594–600. doi: 10.1034/j.1399-3054.2002.1140413.x

Charles-Dominique, T., Mangenet, T., Rey, H., Jourdan, C., and Edelin, C. (2009). Architectural analysis of root system of sexually vs. vegetatively propagated yam (*Dioscorea rotundata* Poir.), a tuber monocot. *Plant Soil* 317, 61–77. doi: 10.1007/s11104-008-9788-9

Chen, Y. L., Dunbabin, V. M., Diggle, A. J., Siddique, K. H. M., and Rengel, Z. (2011). Development of a novel semi-hydroponic phenotyping system for studying root architecture. *Funct. Plant Biol.* 38, 355–363.

Dai, X., Wang, Y., Yang, A., and Zhang, W. H. (2012). OsMYB2P-1, a R2R3 MYB transcription factor, is involved in regulation of phosphate-starvation responses and root architecture in rice. *Plant Physiol.* 159, 169–183. doi: 10.1104/pp.112.194217

De la Riva, L. (2010). *Root Etiolation as a Strategy for Phosphorus Acquisition in Common Bean*. Master's thesis, Pennsylvania State University, University Park, PA.

Dolan, L., Janmaat, K., Willemsen, V., Linstead, P., Poethig, S., Roberts, K., et al. (1993). Cellular organisation of the *Arabidopsis thaliana* root. *Development* 119, 71–84.

Dolan, L., and Roberts, K. (1995). Secondary thickening in roots of *Arabidopsis thaliana*: anatomy and cell surface changes. *New Phytol.* 131, 121–128. doi: 10.1111/j.1469-8137.1995.tb03061.x

Drew, M. C. (1975). Comparison of the effects of a localised supply of phosphate, nitrate, ammonium and potassium on the growth of the seminal root system, and the shoot, in barley. *New Phytol.* 75, 479–490.

Drew, M. C., He, C. J., and Morgan, P. W. (1989). Decreased ethylene biosynthesis, and induction of aerenchyma, by nitrogen- or phosphate-starvation in adventitious roots of *Zea mays* L. *Plant Physiol.* 91, 266–271. doi: 10.1104/pp.91.1.266

Drew, M. C., Jackson, M. B., and Giffard, S. (1979). Ethylene-promoted adventitious rooting and development to flooding in *Zea mays* L. *Planta* 88, 83–88. doi: 10.1007/BF00384595

Duque, L., and Lynch, J. (2018). "Genetic variability of root system architectural traits under phosphorus deficiency in sweet potato: interpreting efficiency, utilization and physiological performance," in *Proceedings of the 18th Triennial Symposium of the International Society for Tropical Root Crops; 2018 Oct 22-25*, (Cali: CIAT Publication).

Esau, K. (1977). *Anatomy of Seed Plants*, 2nd Edn. New York, NY: Wiley.

Evenson, R. E., and Gollin, D. (2003). Assessing the impact of the green revolution 1960 to 2000. *Science* 300, 758–762. doi: 10.1126/science.1078710

Fan, M., Zhu, J., Richards, C., Brown, K. M., and Lynch, J. P. (2003). Physiological roles for aerenchyma in phosphorus-stressed roots. *Funct. Plant Biol.* 30, 493–506. doi: 10.1071/FP03046

Fang, S., Yan, X., and Liao, H. (2009). 3D reconstruction and dynamic modeling of root architecture in situ and its application to crop phosphorus research. *Plant J.* 60, 1096–1108. doi: 10.1111/j.1365-313X.2009.04009.x

Fransen, B., Blijjenberg, J., and de Kroon, H. (1999). Root morphological and physiological plasticity of perennial grass species and the exploitation of spatial and temporal heterogeneous nutrient patches. *Plant Soil* 211, 179–189.

Galindo-Castañeda, T., Brown, K. M., and Lynch, J. P. (2018). Reduced root cortical burden improves growth and grain yield under low phosphorus availability in maize. *Plant Cell Environ.* 41, 1579–1592. doi: 10.1111/pce.13197

Gamuyao, R., Chin, J. H., Pariasca-Tanaka, J., Pesaresi, P., Catausan, S., Dalid, C., et al. (2012). The protein kinase Pstol1 from traditional rice confers tolerance of phosphorus deficiency. *Nature* 488, 535–539. doi: 10.1038/nature11346

Guo, L., Chen, J., Cui, X., Fan, B., and Lin, H. (2013). Application of ground penetrating radar for coarse root detection and quantification: a review. *Plant Soil* 362, 1–23. doi: 10.1007/s11104-012-1455-5

Hgaza, V. K., Diby, L. N., Herrera, J. M., Sangakkara, U. R., and Frossard, E. (2012). Root distribution patterns of white yam (*Dioscorea rotundata* Poir.): a field study. *Acta Agric. Scand. B Soil Plant Sci.* 62, 616–626. doi: 10.1080/09064710.2012.682734

Hodge, A. (2004). The plastic plant: root responses to heterogeneous supplies of nutrients. *New Phytol.* 162, 9–24.

Izumi, Y., Yuliadi, E., and Iijima, M. (1999). Root system development including root branching in cuttings of cassava with reference to shoot growth and tuber bulking. *Plant Prod. Sci.* 2, 267–272. doi: 10.1626/pps.2.267

Ji, L., Li, T. X., Zhang, X. Z., and Yu, H. Y. (2012). Root morphological and activity characteristics of rice genotype with high nitrogen utilization efficiency. *Sci. Agric. Sin.* 45, 4770–4781.

Jia, Y. B., Yang, X. E., Feng, Y., and Jilani, G. (2008). Differential response of root morphology to potassium deficient stress among rice genotypes varying in potassium efficiency. *J. Zhejiang Univ. Sci. B* 9, 427–434. doi: 10.1631/jzus.B0710636

Ju, C., Buresh, R. J., Wang, Z., Zhang, H., Liu, L., Yang, J., et al. (2015). Root and shoot traits for rice varieties with higher grain yield and higher nitrogen use efficiency at lower nitrogen rates application. *Field Crops Res.* 175, 47–55. doi: 10.1016/j.fcr.2015.02.007

Kellermeier, F., Armengaud, P., Seditas, T. J., Danku, J., Salt, D. E., and Amtmann, A. (2014). Analysis of the root system architecture of *Arabidopsis* provides a quantitative readout of crosstalk between nutritional signals. *Plant Cell* 26, 1480–1496. doi: 10.1105/tpc.113.122101

Khan, M. A., Gemenet, D. C., and Villordon, A. (2016). Root system architecture and abiotic stress tolerance: current knowledge in root and tuber crops. *Front. Plant Sci.* 7:1584. doi: 10.3389/fpls.2016.01584

Kim, P. S., Kim, D. M., Kang, J. W., Lee, H. S., and Ahn, S. N. (2015). QTL mapping of rice root traits at different NH4+ levels in hydroponic condition. *Plant Breed. Biotechnol.* 3, 244–252. doi: 10.9787/PBB.2015.3.3.244

Kong, X., Zhang, M., De Smet, I., and Ding, Z. (2014). Designer crops: optimal root system architecture for nutrient acquisition. *Trends Biotechnol.* 32, 597–598. doi: 10.1016/j.tibtech.2014.09.008

Krell, V., Unger, S., Jakobs-Schoenwandt, D., and Patel, A. V. (2018). Importance of phosphorus supply through endophytic *Metarhizium brunneum* for root: shoot allocation and root architecture in potato plants. *Plant Soil* 1, 87–97. doi: 10.1007/s11104-018-3718-2

Ku, A. T., Huang, Y. S., Wang, Y. S., Ma, D., and Yeh, K. W. (2008). IbMADS1 (*Ipomoea batatas* MADS-box 1 gene) is involved in tuberous root initiation in sweet potato (*Ipomoea batatas*). *Ann. Bot.* 102, 57–67. doi: 10.1093/aob/mcn067

Kuijken, R. C. P., van Eeuwijk, F. A., Marcelis, L. F. M., and Bouwmeester, H. J. (2015). Root phenotyping: from component trait in the lab to breeding. *J. Exp. Bot.* 66, 5389–5401. doi: 10.1093/jxb/erv239

Lemming, C., Oberson, A., Hund, A., Jensen, L. S., and Magid, J. (2016). Opportunity costs for maize associated with localised application of sewage sludge derived fertilisers, as indicated by early root and phosphorus uptake responses. *Plant Soil* 406, 201–217. doi: 10.1007/s11104-016-2865-6

Li, J., Xie, Y., Dai, A., Liu, L., and Li, Z. (2009). Root and shoot traits responses to phosphorus deficiency and QTL analysis at seedling stage using introgression lines of rice. *J. Genet. Genomics* 36, 173–183. doi: 10.1016/S1673-8527(08)60104-6

Li, X., Zeng, R., and Liao, H. (2016). Improving crop nutrient efficiency through root architecture modifications. *J. Integr. Plant Biol.* 58, 193–202. doi: 10.1111/jipb.12434

Lima, J. E., Kojima, S., Takahashi, H., and von Wiren, N. (2010). Ammonium triggers lateral root branching in *Arabidopsis* in an ammonium transporter 1:3-dependent manner. *Plant Cell* 22, 3621–3633. doi: 10.1105/tpc.110.076216

Liu, K., He, A., Ye, C., Liu, S., Lu, J., Gao, M., et al. (2018). Root morphological traits and spatial distribution under different nitrogen treatments and their relationship with grain yield in super hybrid rice. *Sci. Rep.* 8:131. doi: 10.1038/s41598-017-18576-4

Liu, M., Zhang, A. J., Chen, X. G., Jin, R., Li, H. M., Tang, Z. H., et al. (2017). Effects of potassium deficiency on root morphology, ultrastructure and antioxidant enzyme system in sweet potato (*Ipomoea batatas* [L.] Lam.) during early growth. *Acta Physiol. Plant.* 39:211.

Lynch, J. P. (1995). Root architecture and plant productivity. *Plant Physiol.* 109, 7–13.

Lynch, J. P. (2007). Roots of the second green revolution. *Aust. J. Bot.* 55, 493–512. doi: 10.1071/BT06118

Lynch, J. P. (2011). Root phenes for enhanced soil exploration and phosphorus acquisition: tools for future crops. *Plant Physiol.* 156, 1041–1049. doi: 10.1104/pp.111.175414

Lynch, J. P. (2015). Root phenes that reduce the metabolic costs of soil exploration: opportunities for 21st century agriculture. *Plant Cell Environ.* 38, 1775–1784. doi: 10.1111/pce.12451

Lynch, J., and Brown, K. (1998). "Regulation of root architecture by phosphorus availability," in *Phosphorus in Plant Biology: Regulatory Roles in Ecosystem, Organismic, Cellular, and Molecular Processes*, eds J. Lynch, J. Deikman, U. Kafkaki, and R. Munns (Rockville, MD: American Society of Plant Physiologists), 148–156.

Lynch, J. P., and Brown, K. M. (2008). "Root strategies for phosphorus acquisition," in *The Ecophysiology of Plant–Phosphorus Interactions*, eds P. White and J. Hammond (Berlin: Springer), 83–116.

Lynch, J. P., and Wojciechowski, T. (2015). Opportunities and challenges in the subsoil: pathways to deeper rooted crops. *J. Exp. Bot.* 66, 2199–2210. doi: 10.1093/jxb/eru508

Ma, T. L., Wu, W. H., and Wang, Y. (2012). Transcriptome analysis of rice root responses to potassium deficiency. *BMC Plant Biol.* 12:161. doi: 10.1186/1471-2229-12-161

Mairhofer, S., Zappala, S., Tracy, S. R., Sturrock, C., Bennett, M., Mooney, S. J., et al. (2012). RooTrak: automated recovery of three-dimensional plant root architecture in soil from X-ray microcomputed tomography images using visual tracking. *Plant Physiol.* 158, 561–569. doi: 10.1104/pp.111.186221

Medici, A., Marshall-Colon, A., Ronzier, E., Szponarski, W., Wang, R., Gojon, A., et al. (2015). AtNIGT1/HRS1 integrates nitrate and phosphate signals at the *Arabidopsis* root tip. *Nat. Commun.* 6:6274. doi: 10.1038/ncomms7274

Metzner, R., Eggert, A., van Dusschoten, D., Pflugfelder, D., Gerth, S., Schurr, U., et al. (2015). Direct comparison of MRI and X-ray CT technologies for 3D imaging of root systems in soil: potential and challenges for root trait quantification. *Plant Methods* 11:17. doi: 10.1186/s13007-015-0060-z

Mueller, N. D., Gerber, J. S., Johnston, M., Ray, D. K., Ramankutty, N., and Foley, J. A. (2012). Closing yield gaps through nutrient and water management. *Nature* 490, 254–257. doi: 10.1038/nature11420

Nagel, K. A., Putz, A., Gilmer, F., Heinz, K., Fischbach, A., Pfeifer, J., et al. (2012). GROWSCREEN-Rhizo is a novel phenotyping robot enabling simultaneous measurements of root and shoot growth for plants grown in soil-filled rhizotrons. *Funct. Plant Biol.* 39, 891–904. doi: 10.1071/FP12023

Neelam, K., Thakur, S., Yadav, I. S., Kumar, K., Dhaliwal, S. S., and Singh, K. (2017). Novel alleles of phosphorus-starvation tolerance 1 gene (PSTOL1) from *Oryza rufipogon* confers high phosphorus uptake efficiency. *Front. Plant Sci.* 8:509. doi: 10.3389/fpls.2017.00509

Obara, M., Tamura, W., Ebitani, T., Yano, M., Sato, T., and Yamaya, T. (2010). Fine-mapping of qRL6. 1, a major QTL for root length of rice seedlings grown under a wide range of NH4+ concentrations in hydroponic conditions. *Theor. Appl. Genet.* 121, 535–547. doi: 10.1007/s00122-010-1328-3

Ogawa, S., Valencia, M. O., Ishitani, M., and Selvaraj, M. G. (2014). Root system architecture variation in response to different NH 4+ concentrations and its association with nitrogen-deficient tolerance traits in rice. *Acta Physiol. Plant.* 36, 2361–2372. doi: 10.1007/s11738-014-1609-6

Pardales, J. R. Jr., and Esquibel, C. B. (1996). Effect of drought during the establishment period on the root system development of cassava. *Jpn. J. Crop Sci.* 65, 93–97. doi: 10.1626/jcs.65.93

Parker, C. J., Carr, M. K. V., Jarvis, N. J., Puplampu, B. O., and Lee, V. H. (1991). An evaluation of the minirhizotron technique for estimating root distribution in potatoes. *J. Agric. Sci.* 116, 341–350. doi: 10.1017/S0021859600078151

Postma, J. A., Dathe, A., and Lynch, J. (2014). The optimal lateral root branching density for maize depends on nitrogen and phosphorus availability. *Plant Physiol.* 166, 590–602. doi: 10.1104/pp.113.233916

Qiao, S., Fang, Y., Wu, A., Xu, B., Zhang, S., Deng, X., et al. (2018). Dissecting root trait variability in maize genotypes using the semi-hydroponic phenotyping platform. *Plant Soil* 1–16. doi: 10.1007/s11104-018-3803-6

Rao, I. M., Miles, J. W., Beebe, S. E., and Horst, W. J. (2016). Root adaptations to soils with low fertility and aluminium toxicity. *Ann. Bot.* 118, 593–605. doi: 10.1093/aob/mcw073

Rich, S. M., and Watt, M. (2013). Soil conditions and cereal root system architecture: review and considerations for linking Darwin and Weaver. *J. Exp. Bot.* 64, 1193–1208. doi: 10.1093/jxb/ert043

Saengwilai, P., Tian, X., and Lynch, J. (2014). Low crown root number enhances nitrogen acquisition from low nitrogen soils in maize (*Zea mays* L.). *Plant Physiol.* 166, 581–589. doi: 10.1104/pp.113.232603

Sanchez, P. A. (2002). Soil fertility and hunger in Africa. *Science* 295, 2019–2020. doi: 10.1126/science.1065256

Sattelmacher, B., Klotz, F., and Marschner, H. (1990). Influence of the nitrogen level on root growth and morphology of two potato varieties differing in nitrogen acquisition. *Plant Soil* 132, 131–137. doi: 10.1007/BF00011258

Selvaraj, M. G., Valencia, M. O., Ogawa, S., Lu, Y., Wu, L., Downs, C., et al. (2017). Development and field performance of nitrogen use efficient rice lines for Africa. *Plant Biotechnol. J.* 15, 775–787. doi: 10.1111/pbi.12675

Shen, C., Wang, S., Zhang, S., Xu, Y., Qian, Q., Qi, Y., et al. (2013). OsARF16, a transcription factor, is required for auxin and phosphate starvation response in rice (*Oryza sativa* L.). *Plant Cell Environ.* 36, 607–620. doi: 10.1111/pce.12001

Shimizu, A., Kato, K., Komatsu, A., Motomura, K., and Ikehashi, H. (2008). Genetic analysis of root elongation induced by phosphorus deficiency in rice (*Oryza sativa* L.): fine QTL mapping and multivariate analysis of related traits. *Theor. Appl. Genet.* 117, 987–996. doi: 10.1007/s00122-008-0838-8

Smith, S., and De Smet, I. (2012). Root system architecture: insights from *Arabidopsis* and cereal crops. *Philos. Trans. R. Soc. Lond. B Biol. Sci.* 367, 1441–1452. doi: 10.1098/rstb.2011.0234

Strock, C. F., De la Riva, L. M., and Lynch, J. P. (2018). Reduction in root secondary growth as a strategy for phosphorus acquisition. *Plant Physiol.* 176, 691–703. doi: 10.1104/pp.17.01583

Subere, J. O., Bolatete, D., Bergantin, R., Pardales, A., Belmonte, J. J., Mariscal, A., et al. (2009). Genotypic variation in responses of cassava (*Manihot esculenta* Crantz) to drought and rewatering: root system development. *Plant Prod. Sci.* 12, 462–474. doi: 10.1626/pps.12.462

Svistoonoff, S., Creff, A., Reymond, M., Sigoillot-Claude, C., Ricaud, L., Blanchet, A., et al. (2007). Root tip contact with low-phosphate media reprograms plant root architecture. *Nat. Genet.* 39, 792–796.

Takehisa, H., Sato, Y., Antonio, B. A., and Nagamura, Y. (2013). Global transcriptome profile of rice root in response to essential macronutrient deficiency. *Plant Signal. Behav.* 8:e24409. doi: 10.4161/psb.24409

Topp, C. N., Iyer-Pascuzzi, A. S., Anderson, J. T., Lee, C. R., Zurek, P. R., Symonova, O., et al. (2013). 3D phenotyping and quantitative trait locus mapping identify core regions of the rice genome controlling root architecture. *Proc. Natl. Acad. Sci. U.S.A.* 110, E1695–E1704. doi: 10.1073/pnas.1304354110

Tscherning, K., Leihner, D. E., Hilger, T. H., Müller-Sämann, K. M., and El Sharkawy, M. A. (1995). Grass barriers in cassava hillside cultivation: rooting patterns and root growth dynamics. *Field Crops Res.* 43, 131–140. doi: 10.1016/0378-4290(95)00028-O

van Dusschoten, D., Metzner, R., Kochs, J., Postma, J. A., Pflugfelder, D., Bühler, J., et al. (2016). Quantitative 3D analysis of plant roots growing in soil using magnetic resonance imaging. *Plant Physiol.* 170, 1176–1188. doi: 10.1104/pp.15.01388

Vejchasarn, P., Lynch, J. P., and Brown, K. M. (2016). Genetic variability in phosphorus responses of rice root phenotypes. *Rice* 9:29. doi: 10.1186/s12284-016-0102-9

Villordon, A., Gregorie, J. C., LaBonte, D., Khan, A., and Selvaraj, M. (2018). Variation in 'Bayou Belle'and 'Beauregard'Sweetpotato Root length in response to experimental phosphorus deficiency and compacted layer treatments. *Hortscience* 53, 1534–1540. doi: 10.21273/HORTSCI13305-18

Villordon, A., LaBonte, D., Solis, J., and Firon, N. (2012). Characterization of lateral root development at the onset of storage root initiation in 'Beauregard' sweetpotato adventitious roots. *HortScience* 47, 961–968. doi: 10.21273/HORTSCI.47.7.961

Villordon, A., LaBonte, D., Firon, N., and Carey, E. (2013). Variation in nitrogen rate and local availability alter root architecture attributes at the onset of storage root initiation in 'Beauregard' sweetpotato. *Hortscience* 48, 808–815.

Villordon, A., LaBonte, D., and Solis, J. (2011). Using a scanner-based minirhizotron system to characterize sweetpotato adventitious root development during the initial storage root bulking stage. *Hortscience* 46, 513–517.

Villordon, A. Q., Ginzberg, I., and Firon, N. (2014). Root architecture and root and tuber crop productivity. *Trends Plant Sci.* 19, 419–425. doi: 10.1016/j.tplants.2014.02.002

Wang, S.-Y., Li, H., Liu, Q., and Shi, Y.-X. (2017). Effect of potassium application on root grow and yield of sweet potato and its physiological mechanism. *Acta Agron. Sin.* 43, 1057–1066.

Wang, Y. L., Almvik, M., Clarke, N., Eich-Greatorex, S., Øgaard, A. F., Krogstad, T., et al. (2015). Contrasting responses of root morphology and root-exuded organic acids to low phosphorus availability in three important food crops with divergent root traits. *AoB Plants* 7:lv097. doi: 10.1093/aobpla/plv097

White, P. J., Bradshaw, J. E., Brown, L. K., Dale, M. F. B., Dupuy, L. X., George, T. S., et al. (2018). Juvenile root vigour improves phosphorus use efficiency of potato. *Plant Soil* 432, 45–63. doi: 10.1007/s11104-018-3776-5

White, P. J., Broadley, M. R., Hammond, J. P., and Thompson, A. J. (2005). Optimising the potato root system for phosphorus and water acquisition in low-input growing systems. *Aspects Appl. Biol.* 73, 111–118.

White, P. J., George, T. S., Dupuy, L. X., Karley, A. J., Valentine, T. A., Wiesel, L., et al. (2013). Root traits for infertile soils. *Front. Plant Sci.* 4:193. doi: 10.3389/fpls.2013.00193

Wishart, J., George, T. S., Brown, L. K., Ramsay, G., Bradshaw, J. E., White, P. J., et al. (2013). Measuring variation in potato roots in both field and glasshouse: the search for useful yield predictors and a simple screen for root traits. *Plant Soil* 368, 231–249. doi: 10.1007/s11104-012-1483-1

Yang, W., Duan, L., Chen, G., Xiong, L., and Liu, Q. (2013). Plant phenomics and high-throughput phenotyping: accelerating rice functional genomics using multidisciplinary technologies. *Curr. Opin. Plant Biol.* 16, 180–187. doi: 10.1016/j.pbi.2013.03.005

Yu, P., Eggert, K., von Wirén, N., Li, C., and Hochholdinger, F. (2015a). Cell type-specific gene expression analyses by RNA sequencing reveal local high nitrate-triggered lateral root initiation in shoot-borne roots of maize by modulating auxin-related cell cycle regulation. *Plant Physiol.* 169, 690–704. doi: 10.1104/pp.15.00888

Yu, P., Hochholdinger, F., and Li, C. (2015b). Root-type-specific plasticity in response to localized high nitrate supply in maize (Zea mays). *Ann. Bot.* 116, 751–762. doi: 10.1093/aob/mcv127

Zeigler, R. S., and Mohanty, S. (2010). Support for international agricultural research: current status and future challenges. *New Biotechnol.* 27, 566–572. doi: 10.1016/j.nbt.2010.08.003

Zhan, A., and Lynch, J. P. (2015). Reduced frequency of lateral root branching improves N capture from low-N soils in maize. *J. Exp. Bot.* 66, 2055–2065. doi: 10.1093/jxb/erv007

Zhang, H., and Forde, B. (1998). An *Arabidopsis* MADS box gene that controls nutrient-induced changes in root architecture. *Science* 279, 407–409. doi: 10.1126/science.279.5349.407

Zhang, H., and Forde, B. G. (2000). Regulation of *Arabidopsis* root development by nitrate availability. *J. Exp. Bot.* 51, 51–59. doi: 10.1093/jexbot/51.342.51

Zhang, H., Jennings, A., Barlow, P. W., and Forde, B. G. (1999). Dual pathways for regulation of root branching by nitrate. *Proc. Nat. Acad. Sci. U.S.A.* 96, 6529–6534. doi: 10.1073/pnas.96.11.6529

Zhang, H., Rong, H., and Pilbeam, D. (2007). Signalling mechanisms underlying the morphological responses of the root system to nitrogen in *Arabidopsis*. *J. Exp. Bot.* 58, 2329–2338. doi: 10.1093/jxb/erm114

Zhao, J., Fu, J., Liao, H., He, Y., Nian, H., Hu, Y., et al. (2004). Characterization of root architecture in an applied core collection for phosphorus efficiency of soybean germplasm. *Chin. Sci. Bull.* 49, 1611–1620.

Zhu, J., Brown, K. M., and Lynch, J. P. (2010). Root cortical aerenchyma improves the drought tolerance of maize (*Zea mays* L.). *Plant Cell Environ.* 33, 740–749. doi: 10.1111/j.1365-3040.2009.02099.x

Conflict of Interest Statement: The authors declare that the research was conducted in the absence of any commercial or financial relationships that could be construed as a potential conflict of interest.

frontiers in Plant Science

ORIGINAL RESEARCH
published: 15 March 2019
doi: 10.3389/fpls.2019.00311

A Genome-Wide Association Study Identifies New Loci Involved in Wound-Induced Lateral Root Formation in *Arabidopsis thaliana*

*María Salud Justamante[1], Sergio Ibáñez[1], Adrián Peidró[2] and José Manuel Pérez-Pérez[1]**

[1] Instituto de Bioingeniería, Universidad Miguel Hernández de Elche, Elche, Spain, [2] Departamento de Ingeniería de Sistemas y Automatización, Universidad Miguel Hernández de Elche, Elche, Spain

Root systems can display variable architectures that contribute to nutrient foraging or to increase the tolerance of abiotic stress conditions. Root tip excision promotes the developmental progression of previously specified lateral root (LR) founder cells, which allows to easily measuring the branching capacity of a given root as regards its genotype and/or growth conditions. Here, we describe the natural variation among 120 *Arabidopsis thaliana* accessions in root system architecture (RSA) after root tip excision. Wound-induced changes in RSA were associated with 19 genomic loci using genome-wide association mapping. Three candidate loci associated with wound-induced LR formation were investigated. Sequence variation in the hypothetical protein encoded by the At4g01090 gene affected wound-induced LR development and its loss-of-function mutants displayed a reduced number of LRs after root tip excision. Changes in a histidine phosphotransfer protein putatively involved in cytokinin signaling were significantly associated with LR number variation after root tip excision. Our results provide a better understanding of some of the genetic components involved in LR capacity variation among accessions.

Keywords: wound-induced lateral root formation, root system architecture, genome-wide association mapping, single nucleotide polymorphism, natural variation, histidine phosphotransfer protein

OPEN ACCESS

Edited by:
Laurent Laplaze, Institut de Recherche pour le Développement (IRD), France

Reviewed by:
Magdalena Maria Julkowska, King Abdullah University of Science and Technology, Saudi Arabia
Boris Parizot, VIB-UGent Center for Plant Systems Biology, Belgium

***Correspondence:**
José Manuel Pérez-Pérez
jmperez@umh.es; arolab.edu.umh.es

Specialty section:
This article was submitted to Plant Development and EvoDevo, a section of the journal Frontiers in Plant Science

Received: *05 November 2018*
Accepted: *26 February 2019*
Published: *15 March 2019*

Citation:
Justamante MS, Ibáñez S, Peidró A and Pérez-Pérez JM (2019) A Genome-Wide Association Study Identifies New Loci Involved in Wound-Induced Lateral Root Formation in Arabidopsis thaliana. Front. Plant Sci. 10:311. doi: 10.3389/fpls.2019.00311

INTRODUCTION

Strong modulation of root system architecture (RSA) by environmental cues, such as nutrient and water availability has been a well-documented process in *Arabidopsis thaliana* (Giehl and von Wirén, 2014; Giehl et al., 2014; Robbins and Dinneny, 2015). In primary roots (PRs) (PRs), a regular pre-branching pattern of lateral roots (LRs) is established by an endogenous periodic oscillation in gene expression near the root tip (Moreno-Risueno et al., 2010). A subset of xylem pole pericycle cells within the pre-branch sites becomes specified as LR founder cells. Subsequently, LR founder cells undergo a self-organizing and non-deterministic cell division patterning (Lucas et al., 2013; von Wangenheim et al., 2016) to initiate a LR primordium that eventually emerges through the PR tissues (Peret et al., 2009; Du and Scheres, 2018). However, the developmental progression of individual LR primordia is dependent on environmental cues, such as water distribution within the soil (Bao et al., 2014). In addition, a local auxin source from the LR cap of the PR, which is

derived from the auxin precursor indole-3-butyric acid (IBA), determines whether a pre-branch site is specified or not (Xuan et al., 2015). The spatial distribution of LRs is not fixed, yet the total number of LR competent sites was stable with time. Root tip excision promotes the developmental progression of nearly all pre-branch sites toward LR emergence, providing an accurate measure for LR branching capacity. This later approach will allow assessing whether changes in LR pre-patterning have occurred in different genotypes and/or growth conditions (Van Norman et al., 2014). These results are in agreement with the current view that cells at the root tip are capable of integrating information about the local soil environment, tailoring the RSA for optimal nutrient and water uptake or after PR damage (Robbins and Dinneny, 2015).

Genome-wide association (GWA) studies have contributed to the identification of natural variation in key genes controlling PR growth under control and abiotic stress conditions (Meijon et al., 2014; Slovak et al., 2014; Satbhai et al., 2017; Bouain et al., 2018). Natural variation in RSA has also been reported (Rosas et al., 2013). Salt-induced changes in RSA were associated with more than 100 genetic loci identified by GWA mapping, some of which are involved in ethylene and abscisic acid (ABA) signaling (Julkowska et al., 2017). In addition, strong additive effects of phosphate starvation on LR density and salt stress on LR length were found in a recent study with a large number of Arabidopsis accessions (Kawa et al., 2016). Their results suggested that the integration of signals from phosphate starvation and salt stress might partially rely on endogenous ABA signaling. One of the candidate genes identified in these studies was *HIGH-AFFINITY* K^+ *TRANSPORTER1* (*HKT1*), previously identified for its role in salinity tolerance by modulating sodium/potassium homeostasis (Munns et al., 2012). The targeted HKT1 expression to pericycle cells reduced LR formation under salt stress (Julkowska et al., 2017). Recently, Ristova et al. (2018) reported a comprehensive atlas of RSA variation upon treatment with auxin, cytokinin (CK) and ABA in a large number of *A. thaliana* accessions. In that study, hierarchical clustering analyses identified groups of accessions sharing similar or diverse responses to a particular hormone perturbation that can be very useful to identify accessions that behave differently than the bulk and to use them as parents for QTL mapping.

To explore the natural variation of LR branching capacity in Arabidopsis (Van Norman et al., 2014), we performed a wound-induced LR formation assay in 174 accessions from the Haplotype Map (HapMap) collection (Weigel and Mott, 2009). GWA mapping using data from 120 accessions revealed 162 SNP associations with several RSA traits measured after root tip excision. SNPs affecting six genes were found significantly associated with LR number variation.

MATERIALS AND METHODS

Plant Materials and Growth Conditions

Our population for GWA mapping consisted of 174 natural inbred lines (i.e., accessions) of *A. thaliana* (L.) Heyhn. selected from the 1001 Genomes Project (Weigel and Mott, 2009) based on marker information and seed availability (**Supplementary Table S1**). The laboratory strain Columbia-0 (Col-0) was chosen as the reference. The following lines (in the Col-0 background) were used to isolate T-DNA homozygous mutants of the studied genes: N572850, N586312, N616200, and N620707 (**Supplementary Table S2**). The *ahp1 ahp2 ahp3* (Hutchison et al., 2006) mutants were also used. All lines used were obtained from the Nottingham Arabidopsis Stock Centre (NASC[1]). Seeds were stored at 4°C for several weeks (>12) to break dormancy.

Seeds were surface-sterilized in 2% (w/v) NaClO and rinsed with sterile water before being transferred to 120 mm × 120 mm × 10 mm Petri dishes containing 75 mL of one-half-Murashige & Skoog (MS) medium with 2% sucrose, 8 g/L plant agar (Duchefa Biochemie, Netherlands) and 1× Gamborg B5 vitamin mixture (Duchefa Biochemie). After 4 days of stratification at 4°C in darkness, plates were wrapped in aluminum foil and were transferred (0 days after sowing) to an MLR-352-PE growth chamber (Panasonic, Japan) at 22 ± 1°C during 3 days in a nearly vertical position. Plates were unwrapped (3 days after sowing) and grew during another 3 days with continuous light (50 $\mu mol \cdot m^{-2} \cdot s^{-1}$). For each accession, 12 seeds were sown per petri dish in triplicate (36 samples/line). Sixteen consecutive sowings including 11 accessions each were established. Additionally, Col-0 was also included in all the sowings to be used as the growth reference accession and for normalization purposes (**Supplementary Figure S1A**). Lines with germination percentage lower than 80% and with ambiguous marker information were discarded for further analysis (**Supplementary Table S1**).

Induction of Lateral Root Formation

To induce LR development during early seedling growth (Van Norman et al., 2014), we excised about 2 mm of the root tip using a sterile scalpel on a laminar flow hood at 6 days after sowing (**Figure 1A**). Next, samples were transferred back to the growth chamber and followed during 4 days for the analysis of several root traits as described below.

Image Processing and Parameter Measurement

Petri dishes were daily imaged from 6 to 10 days after sowing using an Epson Perfection V330 Photo scanner (Seiko Epson Corporation, Nagano, Japan), at a resolution of 600 dpi, and saved as RGB color images in JPEG file format. Scanned images were processed using EZ-Rhizo (Armengaud et al., 2009) with available plug-in macros to convert them into binary images, remove noise, gap-filling, and skeletonize them prior to automated root detection (**Supplementary Figures S1B–S1E**). PR length was directly obtained from the EZ-Rhizo output files from scanned images of 6 days after sowing. A highly significant and positive correlation was found for PR length estimated by EZ-Rhizo and directly measured by ImageJ software[2] from hand-drawn roots (**Supplementary Figure S1F**). LR number was visually counted from the scanned images between 6 and 10 days after sowing.

[1] http://arabidopsis.info/

[2] http://rsb.info.nih.gov/ij/

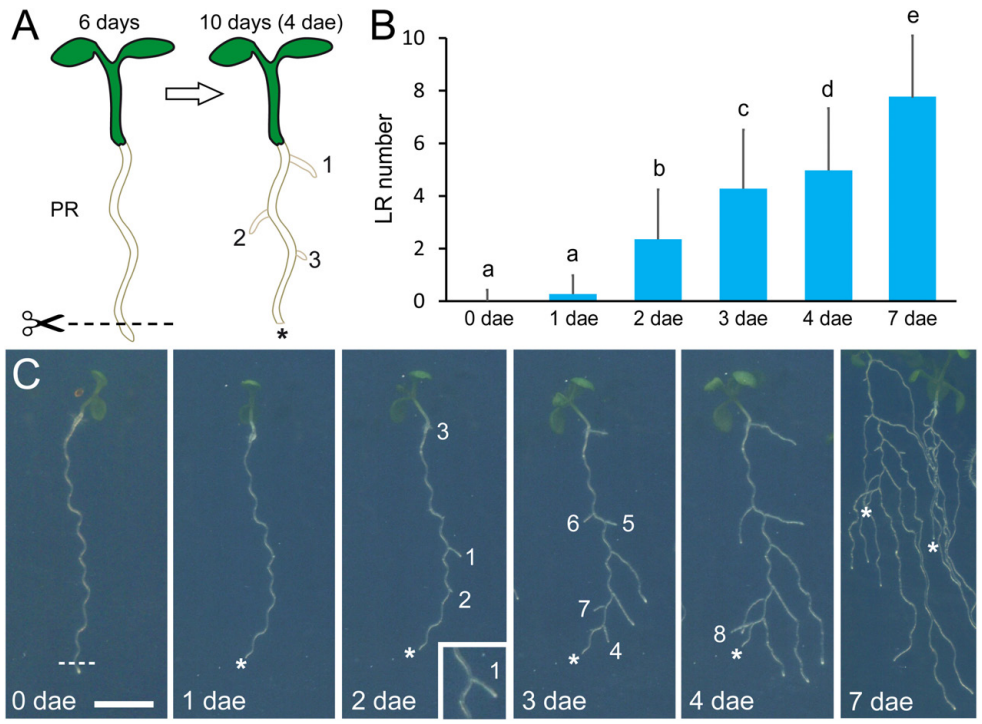

FIGURE 1 | Wound-induced lateral root (LR) development. **(A)** Schematic representation of LR induction by root tip excision (the excision site is indicated by the scissors). dae, days after excision; PR, primary root. **(B)** Average LR number observed in the Columbia-0 (Col-0) reference accession after root tip excision. Different letters indicate significant differences (LSD, *P*-value < 0.01). **(C)** Time course of LR development in Col-0 after root tip excision. Scale bar: 5 mm. Numbers in **(A,C)** indicate order of LR emergence (1, first; 2, second; etc.). Asterisks mark the PR tips after excision.

LR emergence onset corresponds to the day when the first newly emerged LR was visible. LR density was estimated at 8 and 10 days after sowing by the LR number/PR length ratio. Data values were normalized relative to Col-0 values in each sowing dividing each individual value by the Col-0 average (**Supplementary Table S3**).

Statistical Analyses and Heritability Estimation

Statistical analyses of the data was performed by using StatGraphics Centurion XV (StatPoint Technologies, United States) and SPSS 21.0.0 (SPSS Inc., United States) software packages. Data outliers were identified based on aberrant standard deviation values and were excluded for posterior analyses as described elsewhere (Aguinis et al., 2013). One-sample Kolmogorov–Smirnov tests were performed to analyze the goodness-of-fit between the distribution of the data and a theoretical normal distribution. Non-parametric tests and data transformation were applied when needed. To compare the data for a given variable, we performed multiple testing analyses with the ANOVA F-test or the Fisher's LSD (Least Significant Differences) methods. Significant differences were collected with 5% level of significance (*P*-value < 0.05) unless otherwise indicated.

The broad-sense heritability (H^2) for the studied dataset was calculated as $H^2 = \sigma_G{}^2/(\sigma_G{}^2 + \sigma_{GE}{}^2/e + \sigma^2{}_e 2/re)$, in which $\sigma_G{}^2$, $\sigma_{GE}{}^2$, $\sigma_e{}^2$, r, and e represent the estimated variances for the genetic effects, genotype-environment interactions, random errors, number of replications (12) and number of environments (three), respectively. The estimated variances for $\sigma_G{}^2$, $\sigma_{GE}{}^2$, and $\sigma_e{}^2$ were obtained by ANOVA using normalized data values as regards to the Col-0 reference accession from 106 of the studied lines.

Population Structure Analysis

The population structure of the selected accessions was estimated using the Bayesian model-based clustering algorithm (Porras-Hurtado et al., 2013) implemented in Structure v2.3.4 software[3] (Falush et al., 2003). To this end, we used a collection of 319 randomly selected bi-allelic synonymous (likely evolutionary-neutral) SNP markers from available sequence data (Atwell et al., 2010; Cao et al., 2011; Seren et al., 2012). An in-house Matlab script (**Supplementary Table S4**) was used for single nucleotide polymorphism (SNP) data selection and file formatting. Structure analysis was performed for $K = 1$ to $K = 10$ clusters with 20 replicates and 50,000 burn-in period iterations, followed by 50,000 Markov chain Monte Carlo iterations while using a population admixture ancestry model. To determine the most likely number of subpopulations (K) we applied the ΔK method, as described elsewhere (Evanno et al., 2005).

[3]https://web.stanford.edu/group/pritchardlab/structure.html

Genome-Wide Association Studies

Genome-wide association mapping was performed using the GWAPP web interface[4], which contains genotypic information for up to 250,000 bi-allelic SNP markers (Seren et al., 2012). GWAS was conducted for the studied traits using the linear regression model (LM) to identify associations between the phenotype of 120 studied accessions and the 205,978 SNPs available in the database. Relative LR numbers were transformed using the $y = \sqrt{x}$ function to fit the theoretical normal distribution. Association mapping was obtained excluding from the analyses all SNPs with a frequency <0.12. SNPs with a $-\log_{10}(P\text{-value}) > 6.5$ were considered significantly associated to the studied trait (**Supplementary Table S5**). Manhattan plots, representing the genomic position of each SNP and its association [$-\log_{10}(P$-value)] with the studied trait, were downloaded from the GWAPP web interface. We analyzed the sampling bias on GWAS by systematically removing one or several geographically isolated accessions and found that it did not make any difference to the detected SNP associations (**Supplementary Table S6**). We selected non-synonymous SNPs with a $-\log_{10}(P\text{-value}) > 6.5$ (P-value = 3.16×10^{-7}) for further studies.

Genotyping

Seedlings with T-DNA homozygous insertions in the annotated genes were identified by PCR verification with T-DNA specific primers and a pair of gene-specific primers (**Supplementary Table S2**). Genomic DNA isolation and genotyping of T-DNA insertion loci PCR were performed as described elsewhere (Pérez-Pérez et al., 2004).

Gene Expression Analysis by Real-Time Quantitative PCR

Primers amplified 81–178 bp of the cDNA sequences (**Supplementary Table S2**). To avoid amplifying genomic DNA, forward and reverse primers bound different exons and hybridized across consecutive exons.

RNA extraction and cDNA synthesis were performed as described elsewhere (Villacorta-Martín et al., 2015). For real-time quantitative PCR, 14 μl reactions were prepared with 7 μl of the SsoAdvanced Universal SYBR Green Supermix (Bio-Rad, United States), 4 μM of specific primer pairs, and 1 μl of cDNA- and DNase-free water (up to 14 μl of total volume reaction). PCR amplifications were carried out in 96-well optical reaction plates on a Step One Plus Real-Time PCR System (Applied Biosystems, United States). Three biological and two technical replicates were performed for each gene. The thermal cycling program started with a step of 10 s at 95°C, followed by 40 cycles (15 s at 95°C and 60 s at 60°C), and the melt curve (from 60 to 95°C, with increments of 0.3°C every 5 s). Dissociation kinetics of the amplified products confirmed their specificity.

Primer validation and gene expression analyses were performed by the absolute quantification method (Lu et al., 2012) by using a standard curve that comprised equal amounts from each cDNA sample. The housekeeping At4g26410 gene (*RGS1-HXK1 INTERACTING PROTEIN 1*, *RHIP1*) (Czechowski et al., 2005) was chosen as an internal control and to ensure reproducibility. In each gene, the mean of fold-change values relative to the Col-0 reference genotype was used for graphic representation. Relative expression values were analyzed using SPSS 21.0.0 (SPSS Inc., United States) by applying the Mann–Whitney U-test for statistical differences between cDNA samples (P-value < 0.05).

[4]http://gwas.gmi.oeaw.ac.at

RESULTS

Natural Variation of Wound-Induced Lateral Root Formation

To validate our experimental approach (**Figure 1A**), we studied wound-induced LR formation in Columbia-0 (Col-0) during 7 days. PR length remained almost invariable after root tip excision during the whole experiment (**Supplementary Figure S1G**). The new LRs were already visible at 1 day after PR tip excision (1 dae) and reached 4.97 ± 2.36 (n = 467) LRs at 4 dae (**Figure 1B**). At 7 dae, the number of LRs slightly increased but it was not possible to measure it unambiguously due to overlap between the LRs of adjacent seedlings (**Figures 1B,C**). We did not observe a clear spatial pattern of LR emergence from the PRs except that, in all cases, the new LRs emerged from its convex side (**Figure 1C**, inset). We found a slight variation in PR length and LR number between the different sowings (**Supplementary Figures S2A,B**), which might be caused by subtle environmental differences at the growth chamber.

We studied wound-induced LR formation in a collection of 173 additional accessions selected from the 1001 Genomes Project (Weigel and Mott, 2009; **Supplementary Table S1**). In 34 of the studied accessions, the germination percentage at 6 days after sowing was lower than 80% and were discarded for further analysis; other 20 accessions were also discarded because of ambiguous genotypes at the GWAPP web interface (Seren et al., 2012) (**Supplementary Table S1**). We found variation in all the studied traits (**Supplementary Figure S2B**). Exceptionally, one or two LRs were observed before root tip excision (0 dae) in some samples, but these were not considered. The broad-sense heritability (H^2) was calculated for each of the studied traits (see section "Materials and Methods"). Heritability estimates ranged between 0.90 (LR emergence onset and LR density) and 0.95 (LR number). Broad-sense heritability for PR length was 0.93. Interestingly, we found a positive and significant correlation between LR number and PR length at 4 dae (r = 0.83; **Figure 2A**), as well as a negative and significant correlation between LR number at 4 dae and LR emergence onset (r = −0.69; **Figure 2B**). LR number ranged from 1.38 ± 0.82 in Ru3.1-31 (PR length: 0.28 ± 0.07 cm; n = 24) and 9.42 ± 4.84 in Kidr-1 (PR length: 1.90 ± 0.50 cm; n = 24). Hence, reduced LR number in Ru3.1-31 compared to Kidr-1 was likely caused by its reduced PR length. Some accessions, such as Leo-1 and Voeran-1 displayed contrasting phenotypes as regards their LR number (7.07 ± 1.41 and 3.14 ± 1.48 LRs, respectively; n = 29) although they displayed similar PR lengths (**Figures 2A,C**). On the other hand, Leo-1 and Aitba-2 displayed similar LR number which were larger in Leo-1

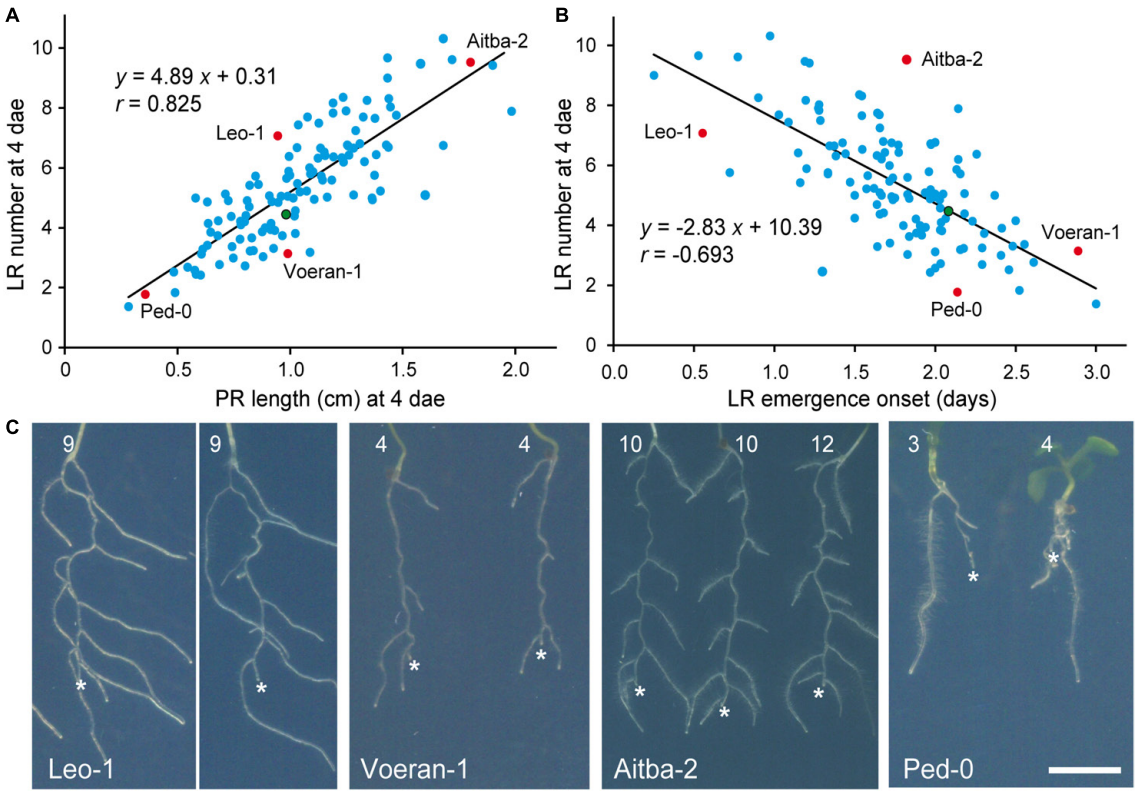

FIGURE 2 | Phenotypic variation of LR architecture after root tip excision. **(A,B)** Scatter plots of average values for LR number and PR length, or LR number and LR emergence onset among the studied accessions. **(C)** Some accessions with extreme LR architecture phenotypes after root tip excision. Asterisk marks the PR tip after excision and numbers refer to LR number at 4 dae. Scale bar: 5 mm. Red dots indicate the accessions with contrasting phenotypes shown in **(C)** and green dots correspond to Col-0.

likely due to its earlier LR emergence onset (0.55 ± 0.57 days in Leo-1 and 1.82 ± 0.50 days in Aitba-2; n = 29; **Figures 2B,C**). Ped-0 displayed very short PRs while their wound-induced LRs were much longer (**Figure 2C**). As regards LR density, Castelfed4.2 and Leo-1 displayed extreme phenotypes, with 2.98 ± 1.35 and 8.05 ± 2.37 roots/cm (n = 29), respectively.

Assessment of Population Structure

The observed phenotypic distribution for the studied traits (PR length, LR emergence onset, LR number and LR density) suggested that these traits were controlled by multiple genes, that some of the causal alleles are pleiotropic (i.e., affect several of these traits), and that the studied population (n = 120 accessions) was polymorphic for those causal alleles. We determined the genetic relationship among the studied accessions using a Structure analysis with 319 genome-wide randomly selected and synonymous (likely evolutionary neutral) SNP markers already available (see section "Materials and Methods"). Structure analysis of these accessions identified two distinct genetic groups (**Figure 3A**) that closely correspond to their geographic regions of origin (**Figure 3B**): The so-called "West" subpopulation including 101 accessions, and the "East" subpopulation with the remaining 19 accessions. However, a detailed analysis of these results indicated a continuous genetic shift from "East" to "West" accessions that follow *A. thaliana* geographical distribution and that likely arose by local haplotypes, as it has been previously proposed (Platt et al., 2010).

We found a significant variation range for the studied traits between these two genetically distinct subpopulations (**Figure 3C**). Altogether, accessions belonging to the "East" subpopulation displayed longer PRs and an increasing number of LRs as regards the "West" subpopulation. However, some accessions of the "East" subpopulation, such as Shigu-1, displayed lower phenotypic values for the studied traits than most of their relatives (**Figure 4**). On the other hand, accessions of the "West" subpopulation and highly genetically divergent from those in the "East" subpopulation (i.e., Aitba-2, HKT2-4, Leo-1, Mrk-0, and Pra-6) displayed higher number of LRs compared with their closest relatives (**Figure 4**). Despite some population structure among the studied lines and due to high heritability estimates, there is potential for the identification of natural alleles affecting wound-induced LR formation responses through GWA mapping with our dataset.

Genome-Wide Association Mapping of Wound-Induced LR Formation

To obtain insight into the genetic basis of the observed variation in wound-induced responses in young *A. thaliana*

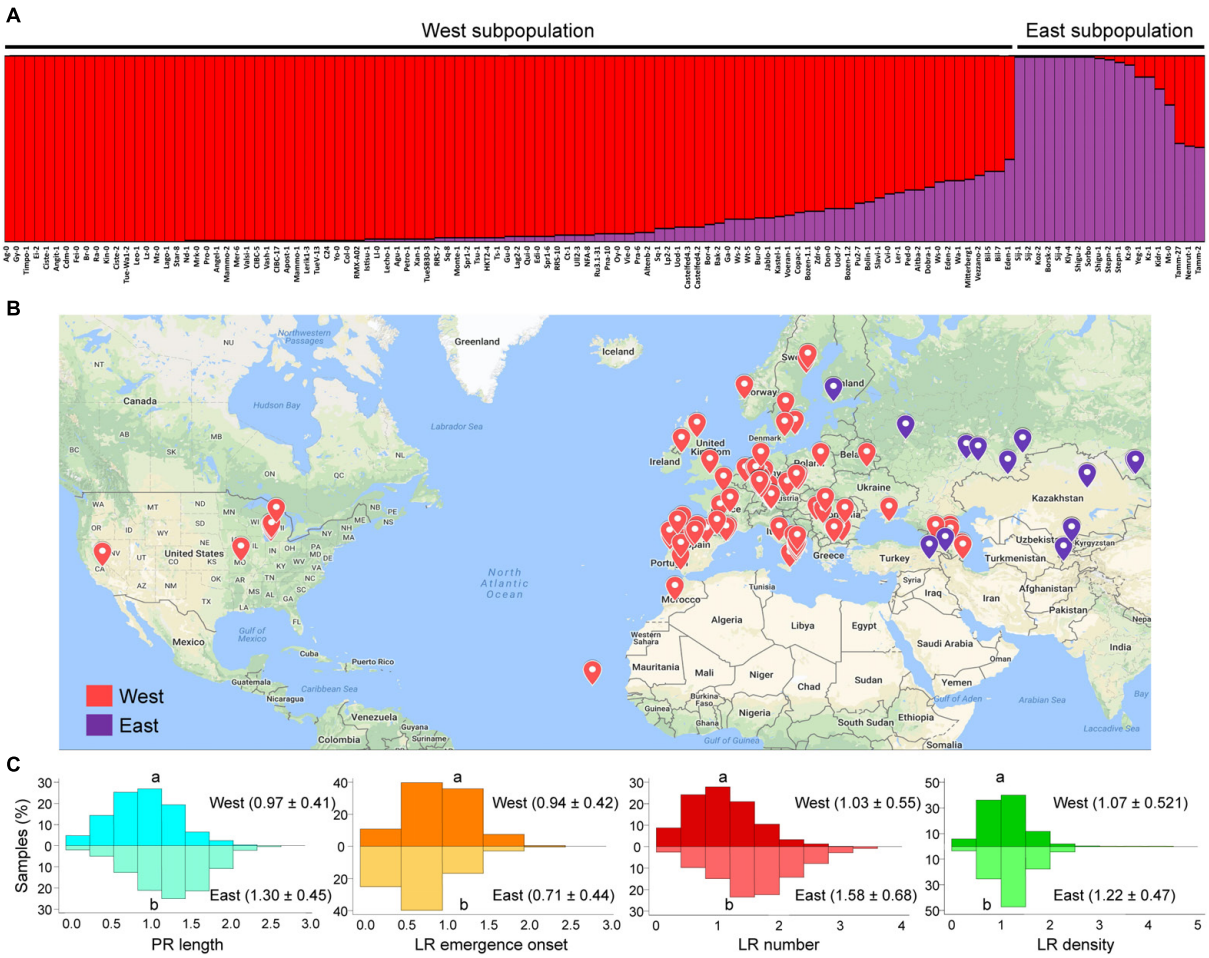

FIGURE 3 | Population structure of the studied accessions. **(A)** Population structure for the studied accessions using a collection of 319 whole-genome distributed and randomly selected synonymous single nucleotide polymorphism (SNP) markers. **(B)** Geographical localization of the studied accessions. Accessions from the "West" subpopulation are labeled in red; those from the "East" subpopulation are labeled in purple. **(C)** Histograms for the studied parameters. Relative data values at 4 dae as compared with the Col-0 reference accession from the "West" subpopulation are represented in the top histograms, while those from the "East" subpopulation are represented in the bottom histograms. Different letters indicate significant differences (LSD, P-value < 0.05).

roots, we performed GWA mapping (see section "Materials and Methods"). The significance of association was first evaluated with three different statistical models (LM, KW and AMM; **Supplementary Figures S3A–C**) and no significant SNP associations were identified by randomization of the phenotypic values within the studied lines (**Supplementary Figure S3D**). Although LM, and KW usually include more false positives than AMM, they do not present any risk of overcorrection in P-value when applied to traits correlated with population structure (Filiault and Maloof, 2012). We used a conservative threshold of $-\log_{10}(P\text{-value}) > 6.5$ and minor allele frequency (MAF) $> 12\%$ to select the SNPs being associated with a given trait. A total of 162 SNP associations were found with the LM method for the studied parameters (**Supplementary Table S5**). We found 32 SNPs associated with PR length with P-values ranging from 1.41×10^{-10} to 3.04×10^{-7}. Thirty-two SNPs were significantly associated with LR emergence onset (P-values ranging from 1.22×10^{-8} to 3.09×10^{-7}) and only one SNP was found associated with LR density. The larger number of significantly associated SNPs was found for LR number ($n = 114$), with P-values ranging from 8.27×10^{-11} to 3.15×10^{-7}. Consistently with our previous observation that PR length and LR number are significantly correlated, 11 SNPs were significantly associated with both traits; similarly, six significantly associated SNPs were shared between LR emergence onset and LR number (**Supplementary Figure S4A**).

Next, we classified the selected SNPs based on its molecular effect (**Supplementary Figure S4B**). About 36% of the significantly associated SNPs were located in intergenic regions and 17.2% of the SNPs laid in the coding region of the annotated gene causing amino acid changes in the protein (**Supplementary Figure S4B**). Previous reports have shown that, due to linkage disequilibrium, multiple significantly associated SNPs should be found within a small chromosome region for true associations (Rajarammohan et al., 2018). To reduce the number of selected loci for further studies, we focused

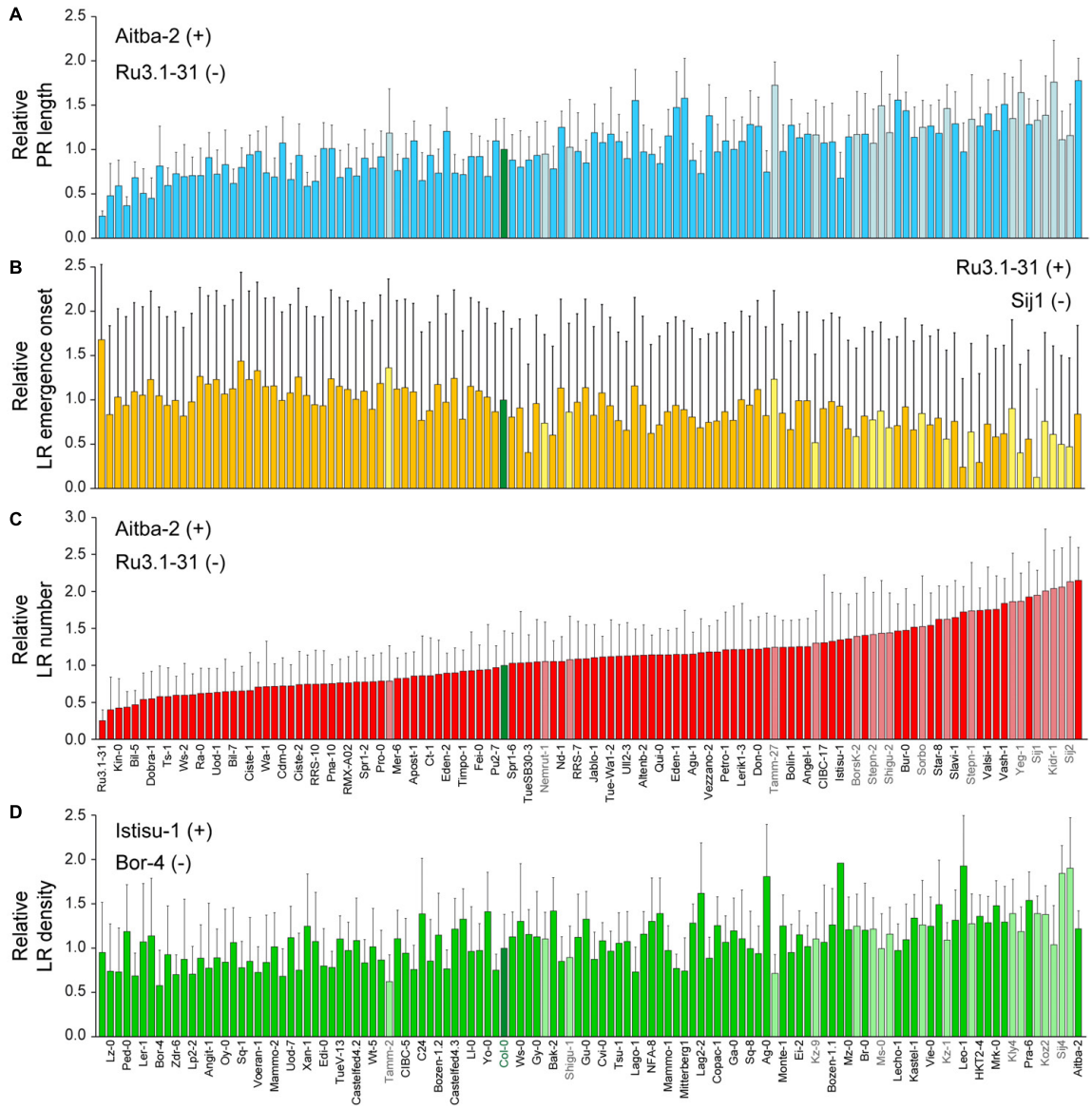

FIGURE 4 | Natural variation of LR architecture after root tip excision in 120 accessions of *Arabidopsis thaliana*. Average ± standard deviation (SD) values of **(A)** relative PR length, **(B)** relative LR emergence onset, **(C)** relative LR number, and **(D)** relative LR density at 4 dae as compared with the Col-0 reference accession. Light-colored bars indicate accessions belonging to the "East" subpopulation (names indicated in gray). The Col-0 reference is shown in green. Accessions are sorted based on their relative LR numbers. Those accessions with extreme phenotypes (+, maximum; –, minimum) are also indicated.

on 19 candidate genomic regions based on the following criteria (**Supplementary Figure S4C**): (1) *P*-value of associated SNPs $< 3.16 \times 10^{-7}$ (which corresponded to a LOD score > 6.5), (2) presence of multiple significantly associated SNPs within an average of 10 Kpb genomic window, and (3) presence of, at least, one non-synonymous SNP within the selected region. We found five genomic regions putatively contributing to PR length variation in the studied population (**Figure 5A**), with one (At1g04260), two (At1g04470), three (At2g22660), one (At4g01090), and two (At4g22920, At4g22940) non-synonymous SNPs each (**Supplementary Table S5**). Three genomic regions were identified as regards their effect on variation in LR emergence onset (**Figure 5B**), each with one non-synonymous SNP (At1g72250, At1g72300 and At5g20980, respectively; **Supplementary Table S5**). We found 14 genomic regions putatively involved in the observed variation in LR number among the studied accessions (**Figure 5C**). Interestingly, the non-synonymous SNPs of three of these regions (dubbed as 2′, 4′, and 5′) overlapped with three genomic regions also selected as being involved in PR length variation (**Supplementary Table S5**). Hence, the affected genes in these cases, At1g04470, At4g01090, and At4g22940, might indirectly contribute to the LR number differences likely due to their direct effect on PR length before root tip excision. The remaining regions identified in the

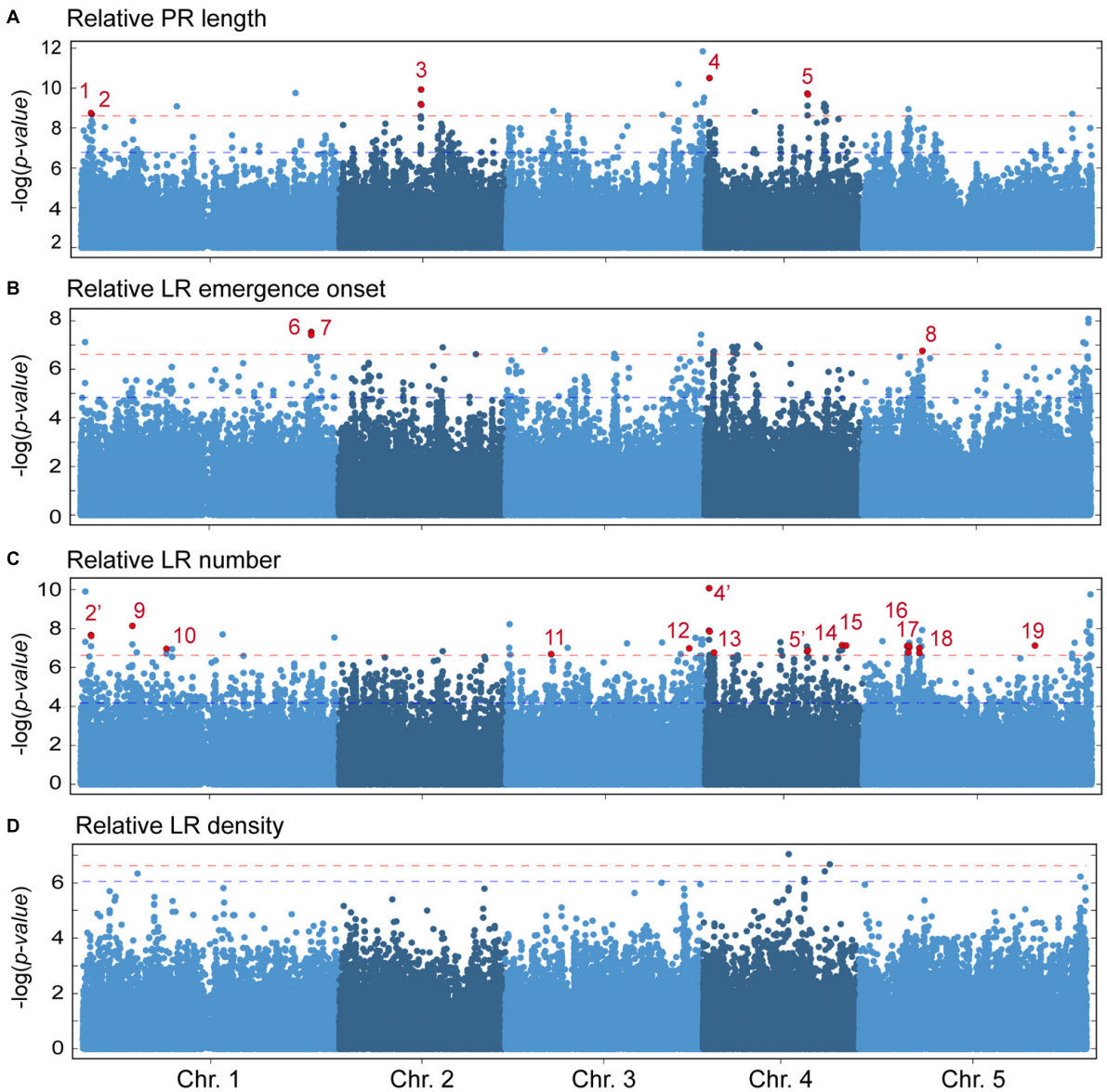

FIGURE 5 | Manhattan plots of associations between SNPs and the studied parameters using a linear regression model (LM). **(A)** Relative PR length, **(B)** relative LR emergence onset, **(C)** relative LR number, and **(D)** relative LR density at 4 dae as compared with the Col-0 reference accession. Dashed horizontal red lines indicate threshold for significance in genome-wide association (GWA) mapping set at $-\log_{10}(P\text{-value}) > 6.5$. Red dots indicate the position of non-synonymous significantly associated SNPs. Numbers 1–19 indicate the genomic regions considered for further studies. Some statistically significant SNP were found both in PR length and LR number (2 and 2′, 4 and 4′, 5 and 5′).

GWA analysis for LR number might include genes that directly contribute to wound-induced LR formation (**Supplementary Table S5**) and therefore deserve further studies. On the contrary, no other genomic region fulfilled our selection criteria as regards LR density and this trait was not considered (**Figure 5D**).

Selection of Candidate Genes Involved in Wound-Induced LR Formation

To identify allelic variation in genes contributing to the observed differences in LR number after root tip excision, we selected 20 non-synonymous SNPs for further studies (**Supplementary Table S6**). Although SNPs in intergenic regions could also be causative, we decided to focus on non-synonymous polymorphisms as their later characterization can be performed on an easier way using reverse genetics tools. Based on both geographic distribution and genotype (**Figure 3**), we hypothesized that Nemrut-1 and Yeg-1 might represent atypical accessions due to ancient migration and genetic isolation. To discard the false-positive SNPs of this spurious association, we repeated the GWA mapping by removing either one or both accessions, which allowed us to reduce to 11 the number of significantly associated SNPs contributing to LR number

(**Supplementary Table S6**). Due to the genetic structure of the studied accessions, we performed ANOVA analyses as regards the "East" and "West" subpopulations independently. Polymorphisms at eight SNPs affecting six genes (At1g17700, At3g58220, At4g01090, At4g33530, At5g16220, and At5g19710; **Table 1**) were found significantly associated with LR number variation (**Supplementary Table S6**). Four haplotypes were detected for selected SNPs within the At4g01090 gene (CAA, CAT, CTA, and TAT). The accessions containing the TAT haplotype displayed a significant increase in LR number, irrespectively of their subpopulation of origin (**Supplementary Figure S5A**). Indeed, the T to A polymorphism at Chr4:472726 accounted for the quantitative differences in LR number by its own. In addition, we observed a haplotype-dependent relationship between SNPs at At5g16220, and At5g19710, which are separated by 1.4 Mb and were previously assigned to two different candidate genomic regions (**Figure 5C**). The GA haplotype for these two genes corresponded to the higher phenotypic values for LR number (**Supplementary Figure S5B**). To our knowledge, this is the first example of two-linked quantitative trait nucleotides (QTNs) detected through GWA mapping and further experiments will account for the functional relationship between the two genes and wound-induced LR number.

Experimental Validation of Candidate Genes

To validate the identification of novel genes involved in wound-induced LR formation in *A. thaliana* seedlings, we chose At4g01090, At4g33530, and At5g19710 for further studies. We searched for available T-DNA insertions in those three genes and identified homozygous mutants by means of PCR and sequencing (**Supplementary Table S1**). Based on haplotype studies, we found that the Chr4:472726 C/T polymorphism at the At4g01090 gene (**Supplementary Figure S6A**) was significantly associated with LR number variation, even in those accessions belonging to the same subpopulation such as Fei-0 (5.19 ± 1.88; $n = 36$) and Star-8 (8.36 ± 2.33; $n = 36$; **Supplementary Figures S6B,C**). Additionally, T-DNA homozygotes from the Salk_086312 segregating line displayed a reduced number of wound-induced LR at 4 dae (2.82 ± 1.27; $n = 34$) in comparison to their wild-type siblings (6.68 ± 1.87; $n = 63$; **Supplementary Figures 6D,E**). The homozygous seedlings were also characterized by their longer hypocotyl and shorter PRs (**Supplementary Figure 6D**). Our results confirmed that the hypothetical protein encoded by the At4g01090 gene participates in wound-induced LR development and that the observed natural variation in their protein sequence might affect their biochemical activity.

At4g33530 (**Supplementary Figure S7A**) encodes a potassium (K^+) uptake transporter which is highly expressed in root hairs (Ahn et al., 2004). We found a statistically significant and non-synonymous SNP (Chr4:16128906) correlated with wound-induced LR phenotype variation (**Supplementary Figure S7B**). The accessions Pu2-7 and Aitba-2 differed in their LR number (6.44 ± 1.95; $n = 32$ and 9.53 ± 1.94; $n = 34$, respectively) and carried alternative alleles of the Chr4:16128906 marker (**Supplementary Figure S7C**). We identified T-DNA homozygotes from two Salk insertion lines interrupting the coding region of this gene (**Supplementary Figure S7A**). None of the studied homozygous mutants from Salk_120707 and Salk_072850 lines displayed significant differences in wound-induced LR number as regards their wild-type siblings (**Supplementary Figures S7D,E**).

The At5g19710 gene (**Figure 6A**) encodes a histidine phosphotransfer protein (AHP) whose function on the CK

TABLE 1 | Candidate genes for LR number identified in the genome-wide association (GWA) mapping.

Gene	SNP coordinate	-log(*P*-value)	Description (domain/name)	Root expression[a]	Reference
At1g04470	Chr1:1214221	7.660	Hypothetical protein (DUF810)	N/A	Hanada et al., 2011
	Chr1:1214425	7.660			
At1g17700	Chr1:6089805	8.130	Prenylated RAB acceptor 1.F1	Elongation zone (EZ) and mature endodermis	Alvim Kamei et al., 2008
At3g58220	Chr3:21566092	6.980	TRAF-like family protein/ MATH domain RTM3-like protein	N/A	N/A
At4g01090	Chr4:472438	7.876	Hypothetical protein (DUF3133)	EZ and LR primordium	Ascencio-Ibáñez et al., 2008
	Chr4:472726	10.082			
	Chr4:473027	7.889			
At4g33530	Chr4:16128906	7.143	Potassium transporter (KUP5)	EZ and mature cortex	Ahn et al., 2004
At5g16220	Chr5:5299807	7.080	Octicosapeptide/Phox/Bem1p family protein	Columella stem cells	N/A
At5g19710	Chr5:6665363	7.000	Histidine containing phosphotransfer protein	Lateral root cap	Nishizawa et al., 2006
At5g49880	Chr5:20286041	7.129	Spindle assembly checkpoint protein (MAD1)	Meristem and LR primordium	Du and Scheres, 2018

[a]*Gene expression was obtained from the eFP browser (Winter et al., 2007). N/A: not available.*

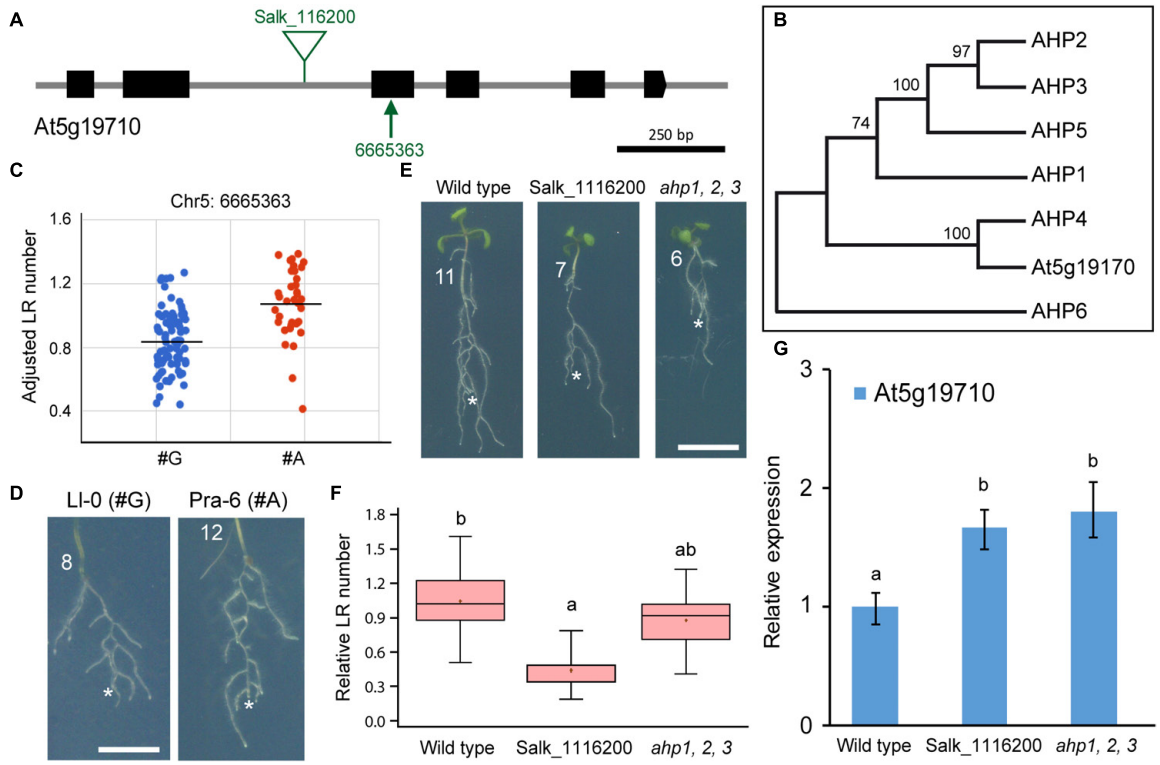

FIGURE 6 | Functional analysis of At5g19710 variation concerning LR number. **(A)** Gene structure of At5g19710. Exons are represented by black boxes and introns are depicted as gray lines. The studied non-synonymous SNP markers (arrows) and annotated T-DNA insertions (triangles) are indicated. **(B)** Phylogenetic analyses of the AHP gene family. Trees were drawn to scale, with branch lengths representing the number of substitutions per site. These analyses were conducted in MEGA7 as described elsewhere (Sánchez-García et al., 2018). **(C)** Scatterplot of average LR number values used for GWA mapping, sorted by the alleles, G and A, at Chr5:6665363 position. **(D)** Some accessions of the studied haplotypes with contrasting LR number values. **(E)** Representative images of wild-type and homozygous seedlings of indicated Salk and mutant lines at 4 dae. Asterisk marks the PR tip after excision and numbers refer to LR number at 4 dae. Scale bars: 5 mm. **(F)** Boxplot showing relative LR number values of wild type and homozygous T-DNA mutants of the indicated Salk lines. Different letters indicate significant differences (LSD, *P*-value < 0.01). (G) RT-qPCR of the expression of At5g19710 in wild-type and mutant seedlings at 7 dae. Bars indicate normalized expression levels ± standard deviation relative to the wild type. Asterisks indicate significant differences between the assayed genotypes and the reference (LSD; *P*-value < 0.05).

transduction pathway has not yet been elucidated. There are six other known AHPs involved in CK responses (Hutchison et al., 2006). Phylogenetic tree reconstruction of AHPs including At5g19710 (**Figure 6A**), suggested that the annotated AHP protein encoded by this gene was incorrectly predicted due to an exon skipping, and clustered together with the AHP4 negative regulator of CK signaling (**Figure 6B**; Moreira et al., 2013). We found that the Chr5:6665363 G/A polymorphism at the third exon of this gene (**Figure 6A**) was significantly associated with LR number variation (**Figure 6C**), even in those accessions belonging to the same subpopulation such as Ll-0 (3.91 ± 2.20; n = 32) and Pra-6 (7.91 ± 1.91; n = 33; **Figure 6D**). We identified a homozygous T-DNA insertion line for the At5g19710 gene whose seedlings showed a reduced number of wound-induced LRs (**Figures 6E,F**) due to a significant miss-regulation of At5g19710 gene expression (**Figure 6G**). We also confirmed that the triple *ahp1 ahp2 ahp3* mutants, which was defective in CK root responses (Hutchison et al., 2006), displayed a significant reduction in wound-induced LRs at 4 dae compared to their wild-type background (**Figures 6E,F**). Taken together, our results seem to indicate that altered homeostasis of AHP proteins required for CK signaling interferes with wound-induced LR formation, a statement that requires further investigation.

Finally, we wondered whether there was an epistatic interaction between the allelic variants for some of the studied non-synonymous SNP markers (Chr4:472726, Chr4:16128906 and Chr5:6665363, respectively) that contributed to the observed variation in wound-induced LR formation in the studied population. Accessions sharing the CCG haplotype for these three markers displayed the smallest number of wound-induced LRs (**Supplementary Figure S8A**), while only the accessions with the haplotype containing a single polymorphism in the At4g01090 gene showed a significant increase (LSD; *P*-value < 0.01) in LR numbers (**Supplementary Figure S8A**). The individual contribution of the SNP polymorphisms in the other two genes considered, At4g33530 and At5g19710, hardly increased wound-induced LR numbers alone but in combination (CGA haplotype) their effects on wound-induced LR formation were enhanced (**Supplementary Figure S8A**). Similar interactions were found between the other SNP pairs (TGG and TCA haplotypes).

Interestingly, we identified several accessions in the "West" subpopulation of all the haplotypes correlated with an increase in wound-induced LR numbers, such as Mrk-0 (8.17 ± 2.12; $n = 36$) and Vie-0 (6.33 ± 1.80; $n = 33$) (**Supplementary Figure S8B**). However, all accessions with the TGA haplotype combining the allelic variants that contribute to an increase of wound-induced LR formation belonged to the "East" subpopulation, which suggested that this trait might be ancestral.

DISCUSSION

The spatial configuration of the RSA allows the plant to dynamically respond to changing soil conditions (Koevoets et al., 2016). Root plasticity relies on the integration of systemic and local signals of nutrient and water availability into the core developmental program of the root (Araya et al., 2014; Bao et al., 2014). Periodic fluctuations in auxin response within the vascular region of the PR near the meristem control the patterning of LR founder cell specification (Moreno-Risueno et al., 2010). A novel IBA-to-IAA conversion pathway in the outer LR cap cells creates a local auxin source that contributes to these periodic auxin fluctuations, which in turn are essential for LR pre-patterning (Xuan et al., 2015). Our wound-induced RSA assay is simple and provides an accurate measure of LR capacity, defined as the total number of competent sites for LR formation on a given root (Van Norman et al., 2014). Interestingly, a recent study has demonstrated that *A. thaliana* PRs might use a specific pathway to activate LR formation when the PR is damaged (Sheng et al., 2017). The authors found that *WUSCHEL-related homeobox11* (*WOX11*), which is involved in *de novo* regeneration of adventitious roots from leaf explants (Liu et al., 2014), was also required for LR formation in soil conditions, likely upstream of the LATERAL ORGAN BOUNDARIES DOMAIN (LBD) genes required for LR initiation (Goh et al., 2012).

We found a wide variation for the studied wound-induced RSA traits in our GWA mapping population. There was a clear correlation between the number of wound-induced LRs (i.e., LR branching capacity) with PR length at the excision day and with the time of LR emergence after excision. Some accessions, such as Leo-1 and Voeran-1, significantly differed in their LR number because of an earlier initiation of wound-induced LRs in Leo-1, which were also longer. Hence, Leo-1 contained alleles for higher LR branching capacity that positively contributed to an enhanced root system, which might allow survival in harsh environments. It will be interesting to evaluate whether differences in *WOX11* expression between these accessions might account for the observed differences in RSA after root tip excision.

A population analysis of the studied accessions inferred two distinct genetic groups that closely corresponded to the geographic regions of *A. thaliana* native distribution and the proposed postglacial colonization routes in this species (Platt et al., 2010; Cao et al., 2011). Interestingly, the "East" subpopulation included accessions, mainly from Central Asia, with enhanced wound-induced RSA traits. In this case, genetic polymorphism may be strongly correlated with RSA traits because of demographic history, challenging the identification of the causal polymorphisms. Within the "West" subpopulation however, there was a clear longitudinal gradient of genetic polymorphisms, such as the accessions in Central Europe were also genetically close to those in the "East" subpopulation. Additionally, Nemrut-1 and Yeg-1 were included in the "East" subpopulation in our study, which is in agreement with a recently proposed migration route connecting Asia and Africa from the south (Brennan et al., 2014). Although it is well-known that population structure, among other effects, can complicate GWA studies in Arabidopsis (Filiault and Maloof, 2012), we reasoned that the studied traits showed broad phenotypic variation, globally as well as within the two subpopulations, that also exhibited continuous isolation by distance as observed earlier in this species (Platt et al., 2010). For example, some accessions from the "West" subpopulation, like Leo-1 and Pra-6, showed an enhanced root system after wounding, while other genetically and geographically close accessions (Cdm-0 and Qui-0, respectively) displayed a less complex RSA. It is well known that nutrients and other environmental signals in the soil might alter the RSA (Kellermeier et al., 2014). We thus speculate that the observed differences in wound-induced RSA traits might represent local adaptations to distinct ecological niches, and one of the environmental signals that might be involved is osmotic stress. Some accessions from the "East" subpopulation, such as Shigu-1 and Tamm-2, displayed lower RSA values than their close relatives. Hence, these contrasting accessions might be used as parents for QTL identification through conventional linkage association mapping in different soil stress conditions.

Through GWA mapping, we identified 162 SNP associations that significantly accounted for variation in wound-induced RSA traits located at 19 genomic regions, which were defined based primarily by non-synonymous SNPs. As expected by our trait correlation analyses, we found a clear overlap between three genomic regions associated for PR length and LR number (2/2′, 4/4′, and 5/5′). In all these cases, the causal polymorphism(s) might affect genes with pleiotropic effects on RSA. GWA mapping has facilitated the identification of the molecular variants underlying complex traits in crops, such as heterosis (Huang et al., 2016), grain size (Si et al., 2016), or drought resistance (Wang et al., 2016). In all these examples, hundreds of genetic variants were identified and candidate genes were assigned based on prior knowledge. In most cases, the genetic variation affected regulatory regions of candidate genes and functional validation using transgenic approaches were required for the functional validation of these genes.

Our results suggest that non-synonymous variation in the coding region of At4g01090 was significantly associated with wound-induced LR variation. At4g01090 encodes a hypothetical protein (DUF3133) of unknown function, which is expressed at higher levels in the endodermis of the elongation zone of the root and the mature xylem (Winter et al., 2007). Other ortholog genes encoding proteins with the DUF3133 domain are At4g01410, which has been annotated as a late embryogenesis abundant (LEA) protein, and *enhanced disease resistance 4* (*EDR4*), which modulates plant immunity by regulating clathrin heavy chain 2 (CHC2)-mediated vesicle trafficking (Wu et al., 2015). The protein encoded by At4g01410 has been found to interact with

EDR4 (Mukhtar et al., 2011). One intriguing possibility is that these DUF3133-containing proteins might also interact with clathrin-coated vesicles during PIN-FORMED (PIN) endocytosis (Dhonukshe et al., 2007; Kitakura et al., 2011), which could then be directly linked to LR initiation (Ditengou et al., 2008). Additional experiments will be performed in our lab to confirm the involvement of DUF3133-containing proteins in clathrin-mediated PIN endocytosis during wound-induced LR formation.

At5g19710 encodes a histidine phosphotransfer protein belonging to the AHP bridge components of the His-Asp phosphorelay transduction pathway of CK signaling (Hwang et al., 2012). Five AHPs (AHP1-5) mediate the cytoplasmic-to-nuclear transduction of the CK signal by transferring the phosphoryl group from the CK receptors to nuclear type-B (positive) and type-A (negative) Arabidopsis response regulators (ARRs). AHP6 lacks the conserved His residue and negatively interferes with CK response (Moreira et al., 2013), most likely by competing with AHP1–5 for interaction with CK-activated receptors (Mahonen et al., 2006). The AHP protein encoded by the At5g19710 gene resembled AHP4. Based on loss-of-function analysis (Hutchison et al., 2006), a negative role of AHP4 for a subset of CK responses (i.e., LR formation) has also been proposed. Interestingly, At5g19710 is specifically expressed in LR cap cells in a low nitrogen environment while it was significantly downregulated by a short nitrate treatment (Gifford et al., 2007). Despite the local inhibitory role of CKs on LR initiation (Laplaze et al., 2007), CKs are essential components of the systemic signaling network leading to the enhancement of LR formation where nitrate is available (Ruffel et al., 2016). In Arabidopsis, the adaptive root response to nitrate depends on the NRT1.1/NPF6.3 transporter/sensor system (Bouguyon et al., 2016). NRT1.1 represses LR emergence at low nitrate concentration through its auxin transport activity that lowers auxin accumulation in the LR primordia (Bouguyon et al., 2016). An additional layer of regulation of systemic N signaling involves TCP20 (Guan et al., 2014). TCP20 is a transcription factor from the TEOSINTE BRANCHED1, CYCLOIDEA, and PCF (TCP) family that binds the promoters of type-A ARR5 and ARR7 at high nitrate levels and of NRT1.1 at low nitrate only (Guan et al., 2014). We speculate that the AHP protein encoded by At5g19710 might function as a negative regulator of a subset of CK responses in LR cap cells at low nitrate, leading to a net reduction of the number of competent sites for LR formation. Interestingly, cell-specific regulation of a transcriptional circuit including ARF8 and miR167 mediates LR outgrowth in response to nitrogen (Gifford et al., 2007). Additional experiments will be required to establishing a functional link between At5g19710-encoding AHP and the ARF8/miR167 circuit.

We found a statistically significant association between a non-synonymous SNP in the coding region of *K^+ UPTAKE TRANSPORTER5 (KUP5)* that changes a Gln to His residue in a conserved transmembrane domain of the protein. Potassium is an essential element in plant growth as it affects osmotic regulation and cell water potential (Lebaudy et al., 2007). The Arabidopsis genome contains multigene families of potassium channels with distinct or redundant functions (Lebaudy et al., 2007), which might explain why the loss-of-function of kUP5 alone did not produce any effect on wound-induced RSA (this work). Consistently, loss-of-function mutations in three KUP family potassium efflux transporters, KUP6, 8 and 2, showed increased auxin responses and enhanced LR formation (Osakabe et al., 2013). As proposed earlier, these KUP transporters might coordinately control potassium homeostasis across root tissues, and the enhanced LR formation in the triple mutants might be caused by a local excess of potassium in the pericycle cells, resulting in enhanced LR formation due to its effect on cell cycle progression (Osakabe et al., 2013). We found an interesting epistatic interaction between the SNP polymorphisms in At4g33530 and At5g19710, which suggest a functional link between potassium uptake and CK signaling. CKs are fairly known to regulate uptake and metabolism of different nutrients: nitrogen, sulfate, phosphate, and iron (Brenner et al., 2012), but the roles of CKs in potassium signaling are poorly understood (Nam et al., 2012).

Through GWA mapping we have identified a number of significant non-synonymous polymorphisms that accounted for some of the variation found in wound-induced RSA. Our results highlighted new regulators of LR formation in Arabidopsis and the further dissection of the developmental mechanisms involved might help to understand the genetic basis of the natural variation of root plasticity.

AUTHOR CONTRIBUTIONS

JP-P was responsible for conceptualization and supervision and provided the funding acquisition. MJ and JP-P were responsible for methodology and performed the formal analysis. MJ, SI, and JP-P were involved in the investigation, writing of the original draft, and review and editing of the manuscript. AP was responsible for software development.

FUNDING

This work was supported by the Ministerio de Economía, Industria y Competitividad (MINECO) of Spain (Grant Nos. AGL2012-33610 and BIO2015-64255-R) and by European Regional Development Fund (ERDF) of the European Commission.

ACKNOWLEDGMENTS

We are especially indebted to Ümit Seren (Gregor Mendel Institute of Molecular Plant Biology, Austria) for sharing relevant data for this project and the two reviewers for their useful suggestions.

SUPPLEMENTARY MATERIAL

The Supplementary Material for this article can be found online at: https://www.frontiersin.org/articles/10.3389/fpls.2019.00311/full#supplementary-material

REFERENCES

Aguinis, H., Gottfredson, R. K., and Joo, H. (2013). 'Best-practice recommendations for defining, identifying, and handling outliers'. *Organ. Res. Methods* 16, 270–301. doi: 10.1177/1094428112470848

Ahn, S. J., Shin, R., and Schachtman, D. P. (2004). 'Expression of KT/KUP genes in *Arabidopsis* and the role of root hairs in K+ uptake'. *Plant Physiol.* 134, 1135–1145. doi: 10.1104/pp.103.034660

Alvim Kamei, C. L., Boruc, J., Vandepoele, K., Van den Daele, H., Maes, S., Russinova, E., et al. (2008). 'The PRA1 gene family in *Arabidopsis*'. *Plant Physiol.* 147, 1735–1749. doi: 10.1104/pp.108.122226

Araya, T., Miyamoto, M., Wibowo, J., Suzuki, A., Kojima, S., Tsuchiya, Y. N., et al. (2014). 'CLE-CLAVATA1 peptide-receptor signaling module regulates the expansion of plant root systems in a nitrogen-dependent manner'. *Proc. Natl. Acad. Sci. U.S.A.* 111, 2029–2034. doi: 10.1073/pnas.1319953111

Armengaud, P., Zambaux, K., Hills, A., Sulpice, R., Pattison, R. J., Blatt, M. R., et al. (2009). 'EZ-Rhizo: integrated software for the fast and accurate measurement of root system architecture'. *Plant J.* 57, 945–956. doi: 10.1111/j.1365-313X.2008.03739.x

Ascencio-Ibáñez, J. T., Sozzani, R., Lee, T. J., Chu, T. M., Wolfinger, R. D., Cella, R., et al. (2008). 'Global analysis of *Arabidopsis* gene expression uncovers a complex array of changes impacting pathogen response and cell cycle during geminivirus infection'. *Plant Physiol.* 148, 436–454. doi: 10.1104/pp.108.121038

Atwell, S., Huang, Y. S., Vilhjálmsson, B. J., Willems, G., Horton, M., Li, Y., et al. (2010). 'Genome-wide association study of 107 phenotypes in a common set of *Arabidopsis thaliana* inbred lines'. *Nature* 465, 627–631. doi: 10.1038/nature08800

Bao, Y., Aggarwal, P., Robbins, N. E., Sturrock, C. J., Thompson, M. C., Tan, H. Q., et al. (2014). 'Plant roots use a patterning mechanism to position lateral root branches toward available water'. *Proc. Natl. Acad. Sci. U.S.A.* 111, 9319–9324. doi: 10.1073/pnas.1400966111

Bouain, N., Satbhai, S. B., Korte, A., Saenchai, C., Desbrosses, G., Berthomieu, P., et al. (2018). 'Natural allelic variation of the AZI1 gene controls root growth under zinc-limiting condition'. *PLoS Genet.* 14:e1007304. doi: 10.1371/journal.pgen.1007304

Bouguyon, E., Perrine-Walker, F., Pervent, M., Rochette, J., Cuesta, C., Benkova, E., et al. (2016). 'Nitrate controls root development through posttranscriptional regulation of the NRT1.1/NPF6.3 transporter/sensor'. *Plant Physiol.* 172, 1237–1248.

Brennan, A. C., Méndez-Vigo, B., Haddioui, A., Martínez-Zapater, J. M., Picó, F. X., and Alonso-Blanco, C. (2014). 'The genetic structure of *Arabidopsis thaliana* in the south-western mediterranean range reveals a shared history between north africa and southern europe'. *BMC Plant Biol.* 14:17. doi: 10.1186/1471-2229-14-17

Brenner, W. G., Ramireddy, E., Heyl, A., and Schmülling, T. (2012). 'Gene regulation by cytokinin in *Arabidopsis*'. *Front. Plant Sci.* 3:8. doi: 10.3389/fpls.2012.00008

Cao, J., Schneeberger, K., Ossowski, S., Gunther, T., Bender, S., Fitz, J., et al. (2011). 'Whole-genome sequencing of multiple *Arabidopsis thaliana* populations'. *Nat. Genet.* 43, 956–963. doi: 10.1038/ng.911

Czechowski, T., Stitt, M., Altmann, T., Udvardi, M. K., and Scheible, W. R. (2005). 'Genome-wide identification and testing of superior reference genes for transcript normalization in *Arabidopsis*'. *Plant Physiol.* 139, 5–17. doi: 10.1104/pp.105.063743

Dhonukshe, P., Aniento, F., Hwang, I., Robinson, D. G., Mravec, J., Stierhof, Y. D., et al. (2007). 'Clathrin-mediated constitutive endocytosis of PIN auxin efflux carriers in *Arabidopsis*'. *Curr. Biol.* 17, 520–527. doi: 10.1016/j.cub.2007.01.052

Ditengou, F. A., Teale, W. D., Kochersperger, P., Flittner, K. A., Kneuper, I., van der Graaff, E., et al. (2008). 'Mechanical induction of lateral root initiation in *Arabidopsis thaliana*'. *Proc. Natl. Acad. Sci. U.S.A.* 105, 18818–18823. doi: 10.1073/pnas.0807814105

Du, Y., and Scheres, B. (2018). 'Lateral root formation and the multiple roles of auxin'. *J. Exp. Bot.* 69, 155–167. doi: 10.1093/jxb/erx223

Evanno, G., Regnaut, S., and Goudet, J. (2005). 'Detecting the number of clusters of individuals using the software STRUCTURE: a simulation study'. *Mol. Ecol.* 14, 2611–2620. doi: 10.1111/j.1365-294X.2005.02553.x

Falush, D., Stephens, M., and Pritchard, J. K. (2003). 'Inference of population structure using multilocus genotype data: linked loci and correlated allele frequencies'. *Genetics* 164, 1567–1587.

Filiault, D. L., and Maloof, J. N. (2012). 'A genome-wide association study identifies variants underlying the *Arabidopsis thaliana* shade avoidance response'. *PLoS Genet.* 8:e1002589. doi: 10.1371/journal.pgen.1002589

Giehl, R. F., Gruber, B. D., and von Wiren, N. (2014). 'It's time to make changes: modulation of root system architecture by nutrient signals'. *J. Exp. Bot.* 65, 769–778. doi: 10.1093/jxb/ert421

Giehl, R. F., and von Wirén, N. (2014). 'Root nutrient foraging'. *Plant Physiol.* 166, 509–517. doi: 10.1104/pp.114.245225

Gifford, M. L., Dean, A., Gutierrez, R. A., Coruzzi, G. M., and Birnbaum, K. D. (2007). 'Cell-specific nitrogen responses mediate developmental plasticity'. *Proc. Natl. Acad. Sci. U.S.A.* 105, 803–808. doi: 10.1073/pnas.0709559105

Goh, T., Joi, S., Mimura, T., and Fukaki, H. (2012). ' The establishment of asymmetry in *Arabidopsis* lateral root founder cells is regulated by LBD16/ASL18 and related LBD/ASL proteins'. *Development* 139, 883–893. doi: 10.1242/dev.071928

Guan, P., Wang, R., Nacry, P., Breton, G., Kay, S. A., Pruneda-Paz, J. L., et al. (2014). 'Nitrate foraging by *Arabidopsis* roots is mediated by the transcription factor TCP20 through the systemic signaling pathway'. *Proc. Natl. Acad. Sci. U.S.A.* 111, 15267–15272. doi: 10.1073/pnas.1411375111

Hanada, K., Sawada, Y., Kuromori, T., Klausnitzer, R., Saito, K., Toyoda, T., et al. (2011). 'Functional compensation of primary and secondary metabolites by duplicate genes in *Arabidopsis thaliana*'. *Mol. Biol. Evol.* 28, 377–382. doi: 10.1093/molbev/msq204

Huang, X., Yang, S., Gong, J., Zhao, Q., Feng, Q., Zhang, Q., et al. (2016). 'Genomic architecture of heterosis for yield traits in rice'. *Nature* 537, 629–633. doi: 10.1038/nature19760

Hutchison, C. E., Li, J., Argueso, C., Gonzalez, M., Lee, E., Lewis, M. W., et al. (2006). 'The *Arabidopsis* histidine phosphotransfer proteins are redundant positive regulators of cytokinin signaling'. *Plant Cell* 18, 3073–3087. doi: 10.1105/tpc.106.045674

Hwang, I., Sheen, J., and Muller, B. (2012). 'Cytokinin signaling networks'. *Annu. Rev. Plant Biol.* 63, 353–380. doi: 10.1146/annurev-arplant-042811-105503

Julkowska, M. M., Koevoets, I. T., Mol, S., Hoefsloot, H., Feron, R., Tester, M. A., et al. (2017). 'Genetic components of root architecture remodeling in response to salt stress'. *Plant Cell* 29, 3198–3213. doi: 10.1105/tpc.16.00680

Kawa, D., Julkowska, M. M., Sommerfeld, H. M., ter Horst, A., Haring, M. A., and Testerink, C. (2016). 'Phosphate-dependent root system architecture responses to salt stress. *Plant Physiol.* 172, 690–706. doi: 10.1104/pp.16.00712

Kellermeier, F., Armengaud, P., Seditas, T. J., Danku, J., Salt, D. E., and Amtmann, A. (2014). 'Analysis of the root system architecture of *Arabidopsis* provides a quantitative readout of crosstalk between nutritional signals'. *Plant Cell* 26, 1480–1496. doi: 10.1105/tpc.113.122101

Kitakura, S., Vanneste, S., Robert, S., Löfke, C., Teichmann, T., Tanaka, H., et al. (2011). 'Clathrin mediates endocytosis and polar distribution of PIN auxin transporters in *Arabidopsis*'. *Plant Cell* 23, 1920–1931. doi: 10.1105/tpc.111.083030

Koevoets, I. T., Venema, J. H., Elzenga, J. T. M., and Testerink, C. (2016). 'Roots withstanding their environment: exploiting root system architecture responses to abiotic stress to improve crop tolerance'. *Front. Plant Sci.* 7:1335. doi: 10.3389/fpls.2016.01335

Laplaze, L., Benkova, E., Casimiro, I., Maes, L., Vanneste, S., Swarup, R., et al. (2007). 'Cytokinins act directly on lateral root founder cells to inhibit root initiation'. *Plant Cell* 19, 3889–3900. doi: 10.1105/tpc.107.055863

Lebaudy, A., Very, A. A., and Sentenac, H. (2007). 'K+ channel activity in plants: genes, regulations and functions'. *FEBS Lett.* 581, 2357–2366. doi: 10.1016/j.febslet.2007.03.058

Liu, J., Sheng, L., Xu, Y., Li, J., Yang, Z., Huang, H., et al. (2014). 'WOX11 and 12 are involved in the first-step cell fate transition during de novo root organogenesis in *Arabidopsis*'. *Plant Cell* 26, 1081–1093. doi: 10.1105/tpc.114.122887

Lu, Y., Xie, L., and Chen, J. (2012). 'A novel procedure for absolute real-time quantification of gene expression patterns'. *Plant Methods* 8, 9–19. doi: 10.1186/1746-4811-8-9

Lucas, M., Kenobi, K., von Wangenheim, D., Vobeta, U., Swarup, K., De Smet, I., et al. (2013). 'Lateral root morphogenesis is dependent on the mechanical

properties of the overlaying tissues'. *Proc. Natl. Acad. Sci. U.S.A.* 110, 5229–5234. doi: 10.1073/pnas.1210807110

Mahonen, A. P., Bishopp, A., Higuchi, M., Nieminen, K. M., Kinoshita, K., Tormakangas, K., et al. (2006). 'Cytokinin signaling and its inhibitor AHP6 regulate cell fate during vascular development'. *Science* 311, 94–98. doi: 10.1126/science.1118875

Meijon, M., Satbhai, S. B., Tsuchimatsu, T., and Busch, W. (2014). 'Genome-wide association study using cellular traits identifies a new regulator of root development in *Arabidopsis*'. *Nat. Genet.* 46, 77–81. doi: 10.1038/ng.2824

Moreira, S., Bishopp, A., Carvalho, H., and Campilho, A. (2013). 'AHP6 inhibits cytokinin signaling to regulate the orientation of pericycle cell division during lateral root initiation'. *PLoS One* 8:e56370. doi: 10.1371/journal.pone.0056370

Moreno-Risueno, M. A., Van Norman, J. M., Moreno, A., Zhang, J., Ahnert, S. E., and Benfey, P. N. (2010). 'Oscillating gene expression determines competence for periodic *Arabidopsis* root branching'. *Science* 329, 1306–1311. doi: 10.1126/science.1191937

Mukhtar, M. S., Carvunis, A. R., Dreze, M., Epple, P., Steinbrenner, J., Moore, J., et al. (2011). 'Independently evolved virulence effectors converge onto hubs in a plant immune system network'. *Science* 333, 596–601. doi: 10.1126/science.1203659

Munns, R., James, R. A., Xu, B., Athman, A., Conn, S. J., Jordans, C., et al. (2012). 'Wheat grain yield on saline soils is improved by an ancestral Na(+) transporter gene'. *Nat. Biotechnol.* 30, 360–364. doi: 10.1038/nbt.2120

Nam, Y. J., Tran, L. S. P., Kojima, M., Sakakibara, H., Nishiyama, R., and Shin, R. (2012). 'Regulatory roles of cytokinins and cytokinin signaling in response to potassium deficiency in *Arabidopsis*'. *PLoS One* 7:e47797. doi: 10.1371/journal.pone.0047797

Nishizawa, A., Yabuta, Y., Yoshida, E., Maruta, T., Yoshimura, K., and Shigeoka, S. (2006). '*Arabidopsis* heat shock transcription factor A2 as a key regulator in response to several types of environmental stress'. *Plant J.* 48, 535–547. doi: 10.1111/j.1365-313X.2006.02889.x

Osakabe, Y., Arinaga, N., Umezawa, T., Katsura, S., Nagamachi, K., Tanaka, H., et al. (2013). 'Osmotic stress responses and plant growth controlled by potassium transporters in *Arabidopsis*'. *Plant Cell* 25, 609–624. doi: 10.1105/tpc.112.105700

Peret, B., De Rybel, B., Casimiro, I., Benkova, E., Swarup, R., Laplaze, L., et al. (2009). '*Arabidopsis* lateral root development: an emerging story'. *Trends Plant Sci.* 14, 399–408. doi: 10.1016/j.tplants.2009.05.002

Pérez-Pérez, J. M., Ponce, M. R., and Micol, J. L. (2004). 'The ULTRACURVATA2 gene of *Arabidopsis* encodes an FK506-binding protein involved in auxin and brassinosteroid signaling'. *Plant Physiol.* 134, 101–117. doi: 10.1104/pp.103.032524

Platt, A., Horton, M., Huang, Y. S., Li, Y., Anastasio, A. E., Mulyati, N. W., et al. (2010). 'The scale of population structure in *Arabidopsis thaliana*'. *PLoS Genet.* 6:e1000843. doi: 10.1371/journal.pgen.1000843

Porras-Hurtado, L., Ruiz, Y., Santos, C., Phillips, C., Carracedo, Á., and Lareu, M. V. (2013). 'An overview of STRUCTURE: applications, parameter settings, and supporting software'. *Front. Genet.* 4:98. doi: 10.3389/fgene.2013.00098

Rajarammohan, S., Pradhan, A. K., Pental, D., and Kaur, J. (2018). 'Genome-wide association mapping in *Arabidopsis* identifies novel genes underlying quantitative disease resistance to *Alternaria brassicae*'. *Mol. Plant Pathol.* 19, 1719–1732. doi: 10.1111/mpp.12654

Ristova, D., Giovannetti, M., Metesch, K., and Busch, W. (2018). 'Natural genetic variation shapes root system responses to phytohormones in *Arabidopsis*'. *Plant J.* 96, 468–481. doi: 10.1111/tpj.14034

Robbins, N. E., and Dinneny, J. R. (2015). 'The divining root: moisture-driven responses of roots at the micro- and macro-scale'. *J. Exp. Bot.* 66, 2145–2154. doi: 10.1093/jxb/eru496

Rosas, U., Cibrian-Jaramillo, A., Ristova, D., Banta, J. A., Gifford, M. L., Fan, A. H., et al. (2013). 'Integration of responses within and across *Arabidopsis* natural accessions uncovers loci controlling root systems architecture'. *Proc. Natl. Acad. Sci. U.S.A.* 110, 15133–15138. doi: 10.1073/pnas.1305883110

Ruffel, S., Poitout, A., Krouk, G., Coruzzi, G. M., and Lacombe, B. (2016). 'Long-distance nitrate signaling displays cytokinin dependent and independent branches'. *J. Integr. Plant Biol.* 58, 226–229. doi: 10.1111/jipb.12453

Sánchez-García, A. B., Ibáñez, S., Cano, A., Acosta, M., and Pérez-Pérez, J. M. (2018). 'A comprehensive phylogeny of auxin homeostasis genes involved in adventitious root formation in carnation stem cuttings'. *PLoS One* 13:e0196663. doi: 10.1371/journal.pone.0196663

Satbhai, S. B., Setzer, C., Freynschlag, F., Slovak, R., Kerdaffrec, E., and Busch, W. (2017). 'Natural allelic variation of FRO2 modulates *Arabidopsis* root growth under iron deficiency'. *Nat. Commun.* 8, 15603–15612. doi: 10.1038/ncomms15603

Seren, Ü., Vilhjálmsson, B. J., Horton, M. W., Meng, D., Forai, P., Huang, Y. S., et al. (2012). 'GWAPP: A web application for genome-wide association mapping in *Arabidopsis*. *Plant Cell* 24, 4793–4805. doi: 10.1105/tpc.112.108068

Sheng, L., Hu, X., Du, Y., Zhang, G., Huang, H., Scheres, B., et al. (2017). 'Non-canonical WOX11-mediated root branching contributes to plasticity in *Arabidopsis* root system architecture'. *Development* 144, 3126–3133. doi: 10.1242/dev.152132

Si, L., Chen, J., Huang, X., Gong, H., Luo, J., Hou, Q., et al. (2016). 'OsSPL13 controls grain size in cultivated rice. *Nat. Genet.* 48, 447–456. doi: 10.1038/ng.3518

Slovak, R., Göschl, C., Su, X., Shimotani, K., Shiina, T., and Busch, W. (2014). 'A scalable open-source pipeline for large-scale root phenotyping of *Arabidopsis*'. *Plant Cell* 26, 2390–2403. doi: 10.1105/tpc.114.124032

Van Norman, J., Zhang, J., Cazzonelli, C., Pogson, B., Harrison, P., Bugg, T., et al. (2014). 'Periodic root branching in *Arabidopsis* requires synthesis of an uncharacterized carotenoid derivative'. *Proc. Natl. Acad. Sci. U.S.A.* 111, E1300–E1309. doi: 10.1073/pnas.1403016111

Villacorta-Martín, C., Sánchez-García, A. B., Villanova, J., Cano, A., van de Rhee, M., de Haan, J., et al. (2015). 'Gene expression profiling during adventitious root formation in carnation stem cuttings'. *BMC Genomics* 16:789. doi: 10.1186/s12864-015-2003-5

von Wangenheim, D., Fangerau, J., Schmitz, A., Smith, R. S., Leitte, H., Stelzer, E. H., et al. (2016). 'Rules and self-organizing properties of post-embryonic plant organ cell division patterns'. *Curr. Biol.* 26, 439–449. doi: 10.1016/j.cub.2015.12.047

Wang, X., Wang, H., Liu, S., Ferjani, A., Li, J., Tan, J., et al. (2016). 'Genetic variation in ZmVPP1 contributes to drought tolerance in maize seedlings'. *Nat. Genet.* 48, 1233–1244. doi: 10.1038/ng.3636

Weigel, D., and Mott, R. (2009). 'The 1001 Genomes project for *Arabidopsis thaliana*'. *Genome Biol.* 10, 107–111. doi: 10.1186/gb-2009-10-5-107

Winter, D., Vinegar, B., Nahal, H., Ammar, R., Wilson, G. V., and Provart, N. J. (2007). 'An "electronic fluorescent pictograph" browser for exploring and analyzing large-scale biological data sets'. *PLoS One* 2:e718. doi: 10.1371/journal.pone.0000718

Wu, G., Liu, S., Zhao, Y., Wang, W., Kong, Z., and Tang, D. (2015). 'Enhanced disease resistance4 associates with clathrin heavy chain2 and modulates plant immunity by regulating relocation of EDR1 in *Arabidopsis*'. *Plant Cell* 27, 857–873. doi: 10.1105/tpc.114.134668

Xuan, W., Audenaert, D., Parizot, B., Moller, B. K., Njo, M. F., De Rybel, B., et al. (2015). 'Root cap-derived auxin pre-patterns the longitudinal axis of the *Arabidopsis* root'. *Curr. Biol.* 25, 1381–1388. doi: 10.1016/j.cub.2015.03.046

Conflict of Interest Statement: The authors declare that the research was conducted in the absence of any commercial or financial relationships that could be construed as a potential conflict of interest.

frontiers in Plant Science

REVIEW
published: 19 March 2019
doi: 10.3389/fpls.2019.00206

Lateral Root Primordium Morphogenesis in Angiosperms

*Héctor H. Torres-Martínez, Gustavo Rodríguez-Alonso, Svetlana Shishkova and Joseph G. Dubrovsky**

Departamento de Biología Molecular de Plantas, Instituto de Biotecnología, Universidad Nacional Autónoma de México, Cuernavaca, Mexico

Morphogenetic processes are the basis of new organ formation. Lateral roots (LRs) are the building blocks of the root system. After LR initiation and before LR emergence, a new lateral root primordium (LRP) forms. During this period, the organization and functionality of the prospective LR is defined. Thus, proper LRP morphogenesis is a decisive process during root system formation. Most current studies on LRP morphogenesis have been performed in the model species *Arabidopsis thaliana*; little is known about this process in other angiosperms. To understand LRP morphogenesis from a wider perspective, we review both contemporary and earlier studies. The latter are largely forgotten, and we attempted to integrate them into present-day research. In particular, we consider in detail the participation of parent root tissue in LRP formation, cell proliferation and timing during LRP morphogenesis, and the hormonal and genetic regulation of LRP morphogenesis. Cell type identity acquisition and new stem cell establishement during LRP morphogenesis are also considered. Within each of these facets, unanswered or poorly understood questions are identified to help define future research in the field. Finally, we discuss emerging research avenues and new technologies that could be used to answer the remaining questions in studies of LRP morphogenesis.

Keywords: root development, lateral root primordium, morphogenesis, root architecture, crop species, Arabidopsis, cell proliferation, stem cells

OPEN ACCESS

Edited by:
José Manuel Pérez-Pérez, Universidad Miguel Hernández de Elche, Spain

Reviewed by:
Juan Carlos Del Pozo, Centro de Biotecnología y Genómica de Plantas (CBGP), Spain
Franck Anicet Ditengou, University of Freiburg, Germany

***Correspondence:**
Joseph G. Dubrovsky
jdubrov@ibt.unam.mx

Specialty section:
This article was submitted to Plant Development and EvoDevo, a section of the journal Frontiers in Plant Science

Received: *29 November 2018*
Accepted: *07 February 2019*
Published: *19 March 2019*

Citation:
Torres-Martínez HH, Rodríguez-Alonso G, Shishkova S and Dubrovsky JG (2019) Lateral Root Primordium Morphogenesis in Angiosperms. Front. Plant Sci. 10:206. doi: 10.3389/fpls.2019.00206

INTRODUCTION

A key function of roots—water and mineral uptake and transport—is strongly related to the root system surface area. Root branching promotes and underlies the increase in root surface area, and therefore a single lateral root (LR) constitutes a building block of the root system. Thus, root branching is a ubiquitous and widely distributed process in vascular plants. A classic example of the abundance of roots is the extended root system of a single rye plant (*Secale cereale*). During only one growth season of approximately 4 months, a single plant formed 13,815,672 roots (Dittmer, 1937), most of which were LRs. LRs are initiated in the pericycle (Laskowski et al., 1995; Dubrovsky et al., 2000, 2008; Beeckman et al., 2001; Dubrovsky and Rost, 2012; Beeckman and De Smet, 2014), and comprehensive analysis of LR development has been performed on a model species, *Arabidopsis thaliana* (hereafter *Arabidopsis*). In this species, it has been recognized that LR formation is a process that includes multiple steps: (a) pericycle priming; (b) founder cell specification; (c) the first divisions in pericycle founder cells leading to LR formation, processes defined as LR initiation; (d) lateral root primordium (LRP) formation, comprising developmental processes from the first derivatives of the founder cells to formation of the dome-shaped LRP; (e) LR emergence,

i.e., protrusion of the LRP through the external root tissues, including ground tissues and epidermis; (f) activation of the apical meristem in the nascent LR; and (g) LR growth (Malamy and Benfey, 1997; De Smet et al., 2003; Péret et al., 2009; Malamy, 2010; Stoeckle et al., 2018). The details of these processes are studied at different levels, from developmental anatomy to hormonal and genetic control (Casimiro et al., 2003; De Smet et al., 2006a; Fukaki and Tasaka, 2009; De Smet, 2012; Atkinson et al., 2014; Du and Scheres, 2017a; Dubrovsky and Laskowski, 2017; Ötvös and Benková, 2017). However, not all these steps are equally understood. One of the less understood steps comprises morphogenetic processes from LR initiation to LR emergence (**Figure 1**). Indeed, the mechanisms underlying the remarkably stable and reproducible process of formation of the three-dimensional (3D) LRP structure from a 2D plate of founder cell derivatives are a mystery. In this review, we summarize what is known about the essential elements underlying LRP morphogenesis in angiosperms and attempt to identify the basic questions related to LRP morphogenesis that remain to be answered or better understood.

PARENT TISSUES PARTICIPATING IN PRIMORDIUM FORMATION

Although the pericycle is a principal tissue giving rise to LRs in angiosperms, other parent root tissues, including the endodermis, cortex and vascular parenchyma, participate in LRP morphogenesis.

Pericycle

The specification of pericycle founder cells and other pre-initiation events take place before LRP initiation (De Smet et al., 2007; Moreno-Risueno et al., 2010; Van Norman et al., 2013) and are therefore beyond the scope of this review. In *Arabidopsis*, two types of LRP initiation have been recognized: longitudinal unicellular and longitudinal bi-cellular, in which a single or two adjacent pericycle founder cells in the longitudinal plane, respectively, participate in LRP initiation (Dubrovsky et al., 2001, 2008). The most common type of initiation is considered to be longitudinal bi-cellular (Casero et al., 1995; Lloret and Casero, 2002; De Rybel et al., 2010; von Wangenheim et al., 2016). However, it cannot be excluded that the longitudinal bi-cellular type is a result of the cell division of the founder cell following the longitudinal unicellular type of initiation. Even for a model species such as *Arabidopsis*, it is not known how common each initiation type is.

When viewed in a transversal plane, the number of pericycle cell files that participate in the specification of the LRP founder cells varies among species; for instance, 4 to 6 phloem-adjacent files in wheat (*Triticum aestivum*; Demchenko and Demchenko, 2001) and 6–8 xylem-adjacent cell files in *Arabidopsis* (von Wangenheim et al., 2016) are involved in LRP formation. In most species, the pericycle is a unicellular tissue layer. Nevertheless, in Cucurbitaceae, two pericycle layers, internal and external, are formed in the xylem pole, and both participate in LRP formation (Dubrovsky, 1986a; Ilina et al., 2018). The most detailed analysis of pericycle participation in LRP morphogenesis has been performed in *Arabidopsis*. In this species, the first few divisions in the pericycle leading to LRP formation are anticlinal formative (asymmetrical) divisions (De Smet and Beeckman, 2011). Anticlinal divisions are perpendicular to the nearest root surface. As these divisions take place in few tangentially (i.e., in the direction perpendicular to the radius of the parent root) adjacent founder cells (Dubrovsky et al., 2001; Casimiro et al., 2003; von Wangenheim et al., 2016), a plate of on average 26 pericycle-derived cells is formed (von Wangenheim et al., 2016), corresponding to Stage (St) I, as defined by Malamy and Benfey (1997) (**Figure 1**). This cell plate has 2D organization and, at this point, the transition to the formation of the new growth axis that permits the 3D LRP organization is defined. The first event leading to this transition is the radial growth of StI LRP cells, resulting in the formation of the apical–basal axis of the new LR (**Figure 2**). This new growth direction is controlled by the adjacent endodermis through auxin signaling mediated by SHORT HYPOCOTYL2, SHY2/IAA3 (Vermeer et al., 2014). Radially expanded LRP cells eventually divide periclinally (Malamy and Benfey, 1997), i.e., parallel to the nearest root surface (**Figure 1**), starting in the central xylem-adjacent cell files of the plate. This division follows the established Errera's rule, which states that cells divide preferentially along the shortest distance between cell walls (Besson and Dumais, 2011). Concurrently, the tangentially flanking cells of the plate divide in an oblique orientation, impacting the formation of the oval-shaped basal portion of the prospective LRP (Lucas et al., 2013). Starting from the two-layered LRP, 3D morphogenesis continues along the axis of the future LR. The number of cells at a given developmental stage and the division patterns vary, even though the overall LRP shape changes are conserved (Lucas et al., 2013; von Wangenheim et al., 2016). The developmental stages recognized for *Arabidopsis* (Malamy and Benfey, 1997; Napsucialy-Mendivil and Dubrovsky, 2018), depicted in **Figure 1**, are frequently applied to other species (Yu et al., 2016). In most angiosperms examined, pericycle participation in LRP formation is similar, at least during the early stages (Lloret and Casero, 2002).

Endodermis and Cortex

As early as the 1870s, it was documented that in addition to the pericycle, other tissues participate in LRP morphogenesis (Janczewski, 1874; Van Tieghem and Douliot, 1888; Von Guttenberg, 1968). In most dicots and monocots, the endodermis is also involved in LRP formation (Van Tieghem and Douliot, 1888; Kawata and Shibayama, 1965; Bell and McCully, 1970; Seago, 1973). In some orders—for example, Poales—endodermis participation in LRP formation requires cell dedifferentiation (Danilova and Serdyuk, 1982). The first few divisions in the endodermal layer, like in the pericycle, are anticlinal (Seago, 1973; Demchenko and Demchenko, 2001). Next, in maize (*Zea mays*; Bell and McCully, 1970), *T. aestivum* (Demchenko and Demchenko, 2001), tomato (*Solanum lycopersicum*; Ivanchenko et al., 2006) and other species, the endodermal derivatives undergo periclinal divisions and form a two-layered structure. In many angiosperm taxa, even more than two layers

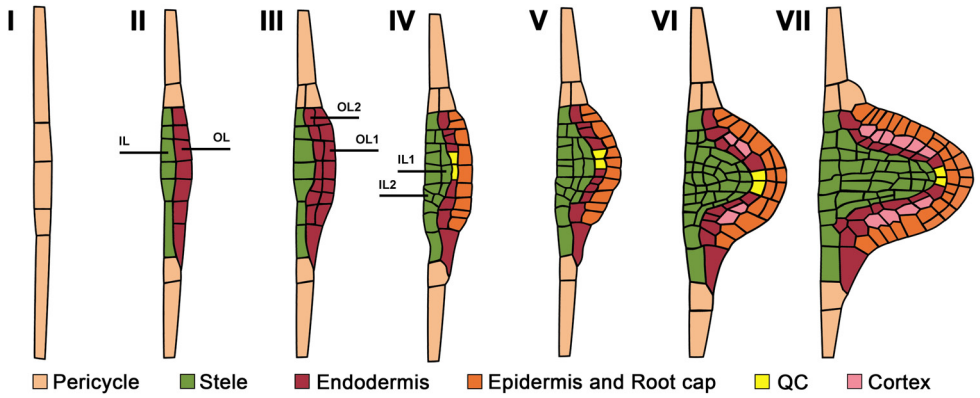

FIGURE 1 | Developmental stages and cell type identity acquisition during lateral root primordium morphogenesis from initiation to lateral root emergence. Numbers correspond to the developmental stages as defined by Malamy and Benfey (1997). Emerging cell identity recognized based on cell type reporters is color-coded. Pericycle cell identity corresponds to that of the parent root. OL and IL are outer and internal layers. See text for details.

of endodermal origin can be formed (**Figure 3**). The LRP tissues of endodermal origin form a temporary structure called *Tasche* in the German literature and *Poche* in the French (Clowes, 1978a). No specific term for this structure is used in the English literature. This temporary structure has some features of the root cap and sloughs off after LR emergence. Here we call this temporary structure the *Cap-Like Structure* (CLS). The CLS results from both anticlinal and periclinal divisions of the endodermis and sometimes cortex (see below). We should note here that in some cases the CLS is not temporary but a permanent structure (see below). Anatomical studies of *Z. mays* LRPs showed that the endodermis contributes to the formation of the LR's permanent tissues, the epidermis and the root cap (Bell and McCully, 1970; Karas and McCully, 1973; McCully, 1975). This interpretation results from the fact that the epidermis of a recently emerged LR can be traced back to the endodermis of the parent root and that endodermal derivative cells in the central apical domain of the LRP start to divide periclinally and form a root cap (Bell and McCully, 1970; Karas and McCully, 1973). Particularly, when a *Z. mays* LRP protrudes about half the width of the parent root cortex, endodermal derivatives of the LRP contain abundant starch grains (Bell and McCully, 1970). By analyzing colchicine-treated chimeric LRPs that contain cells of different ploidy, Clowes (1978a) showed that the whole LR in *Z. mays* plants is of pericyclic origin and that the endodermis forms the CLS, which is maintained only for a short period after LR emergence. Similar conclusions were reached for more complex scenarios in which not only the endodermis but also the cortex participates in LRP formation (Dubrovsky, 1986a; Demchenko et al., 2001; Ilina et al., 2018), confirming the earlier view that the permanent body of the LR is entirely of pericyclic origin (Van Tieghem and Douliot, 1888).

As it is not always possible to deduce which LRP tissues are formed from the pericycle or endodermis based on anatomical observations alone, there is a need to develop cell type identity markers for this purpose. Nevertheless, anatomical studies are of great value. Based on the classical work of Philippe Van Tieghem and Douliot (1888), Voronin (1957, 1964) analyzed the types and distribution of the CLS among angiosperms. We incorporated Voronin's data in the angiosperm phylogenetic tree proposed by the Angiosperm Phylogeny Group (Chase et al., 2016), in an effort to visualize the distribution and evolutionary trends of the appearance and types of the CLS in angiosperms (**Figure 3**). This analysis showed that the CLS is present in most angiosperm orders. The distribution of the CLS in angiosperms suggests an evolutionary trend toward CLS reduction until its complete disappearance, as inferred from the absence of a CLS in most orders of the recent Asterids clade (**Figure 3**). In *Arabidopsis*, a CLS is not found, even though it is present in other Brassicales. This 'atypical' pattern is perhaps a consequence of very simple root organization with a two-layered ground tissue composed of single layers of endodermis and cortex. It would be interesting to validate this hypothesis by analyzing LRP formation in *Arabidopsis* transgenic lines with supernumerary ground tissue layers that maintain endodermis identity (Nakajima et al., 2001).

In some species, the developing LRP is capable of inducing cell divisions in the adjacent cortex (Tschermak-Woess and Doležal, 1953; Demchenko et al., 2001) that are unrelated to LRP morphogenesis. The role of these divisions is unclear. In some taxa, cortex adjacent to the endodermis participates in CLS formation. This is commonly found in Fabaceae (Popham, 1955; Byrne et al., 1977) and Cucurbitaceae (Van Tieghem and Douliot, 1886; Dubrovsky, 1986a; Demchenko and Demchenko, 2001;

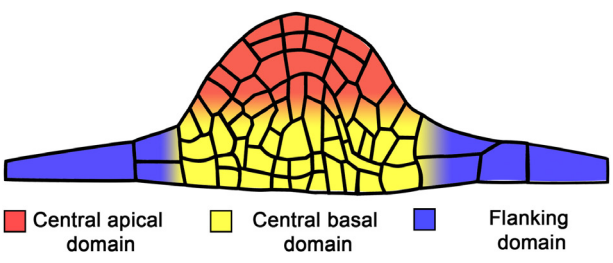

FIGURE 2 | Main domains in the developing lateral root primordium.

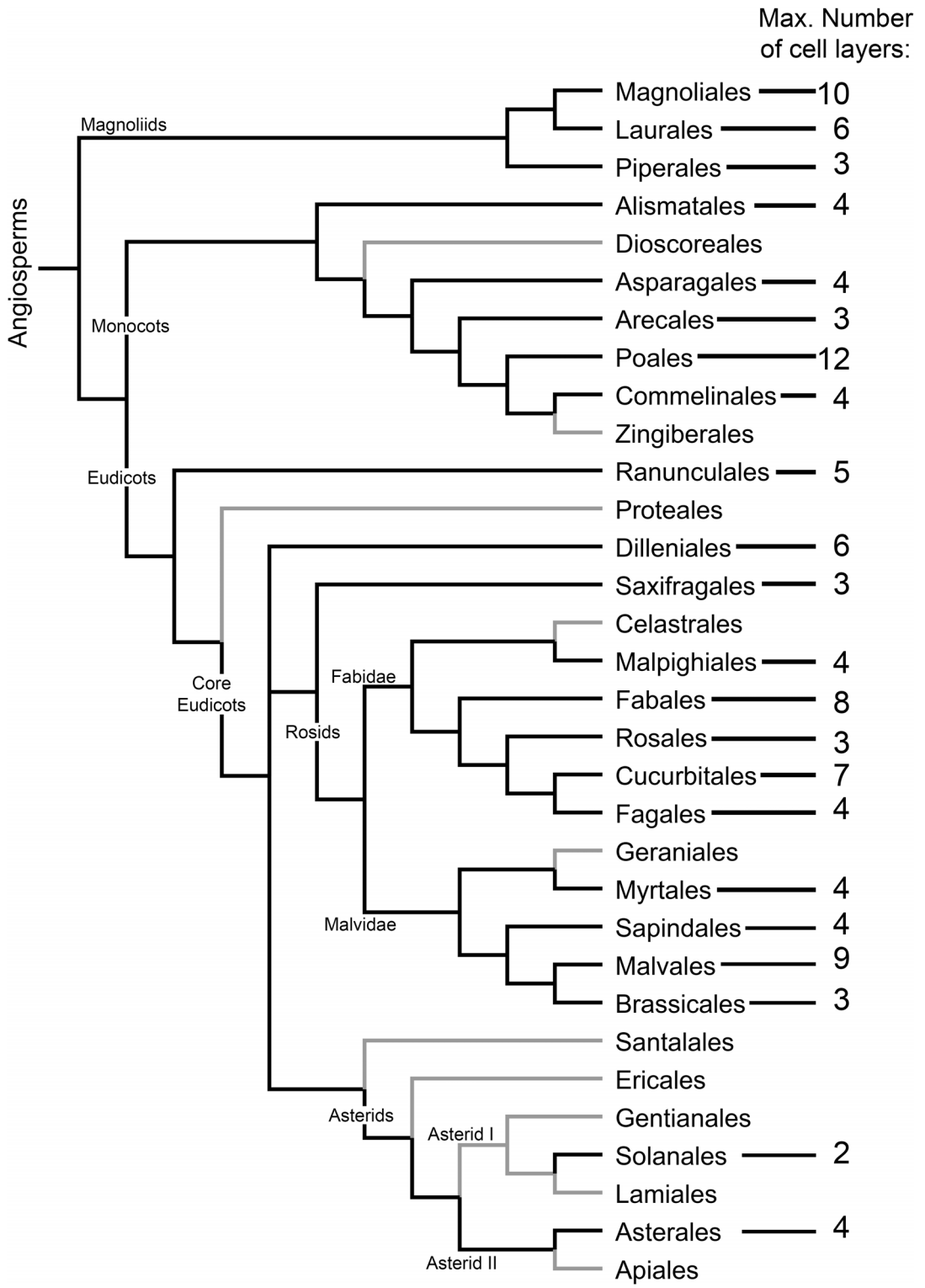

FIGURE 3 | Distribution and extent of the development of the cap-like structure (CLS) of the lateral root primordium among angiosperm orders. The maximum number of CLS cell layers is indicated. Angiosperm orders for which no CLS has been found are depicted with gray branches. Cladogram topology was depicted using FigTree (http://tree.bio.ed.ac.uk/software/figtree/) following the phylogenetic relationship among angiosperms as proposed by the Angiosperm Phylogeny Group (Chase et al., 2016). The data were taken from Voronin's (1957) analysis of Van Tieghem and Douliot (1888). Species included in the analysis were revised in accordance with contemporary taxonomic classification. Orders for which no data are available were not included in the cladogram. Additionally, data for Solanales were added (Seago, 1973; Ivanchenko et al., 2006).

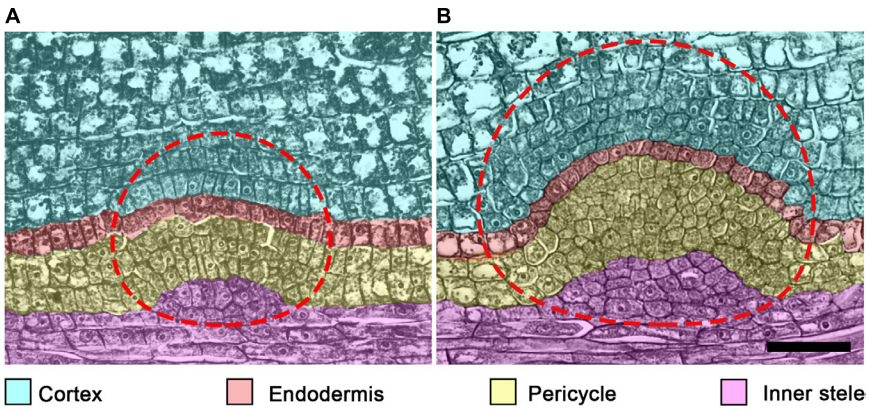

FIGURE 4 | Tissues participating in lateral root primordium (LRP) formation in cucumber (*Cucumis sativus*) root. In *C. sativus*, several embryonic LRPs are formed during embryogenesis. Within the same parent root, the more apical primordium **(A)** is developed to a lesser extent than the most basal primordium **(B)**. Note the different extent of each cell type participation in LRP morphogenesis in these primordia. The temporal cap-like structure (CLS) includes endodermis and cortex derivatives of the LRP. Cell types and their derivative cells produced within the LRP are color coded. The LRP is indicated by a dashed line. Seeds were imbibed for 18 h and fixed; histological sections of the radicle were prepared and stained as described (Dubrovsky, 1986a). Scale bar = 50 μm.

Ilina et al., 2018), which form a massive CLS (**Figure 4**). Interestingly, the cortical and endodermal cells of the same files of the parent root that constitute the developing LRP participate in CLS formation and the cells outside the LRP of the same files do not divide (Dubrovsky, 1986a; Demchenko and Demchenko, 2001; Ilina et al., 2018). This endodermis continuity between the parent and lateral roots is not always maintained, and the CLS on the flanks can be destroyed before LR emergence, as in *Z. mays* (Clowes, 1978a). Few studies have examined how the ground tissue and epidermis of endodermal and cortical origin are replaced by the same cell types produced by the pericycle (Dubrovsky, 1986a).

Surprisingly, studies of CLS function during and after LRP formation are scarce. It has been suggested that CLS cells secrete hydrolases that may facilitate LR emergence (Van Tieghem and Douliot, 1888; Bonnett, 1969; McCully, 1975). The early literature on CLSs suggests that this structure protects the pericycle derivatives from mechanical damage as the LRP protrudes through the parental root tissues before LR emergence. Despite the fact that in most angiosperms the CLS is displaced by the permanent cap of pericyclic origin post-emergence, in some hydrophytes (e.g., *Hydrocharis*, *Lemna*, *Pistia*, *Eichornia*, and *Pontederia*) the CLS is permanently maintained on the LRs (Voronin, 1957).

Another possible function of the CLS might be related to cell proliferation. Cell division in the endodermis and the pericycle start simultaneously during LRP initiation and may create a critical mass of cells required to sustain rapid cell divisions (see section "The Cell Cycle During Lateral Root Primordium Morphogenesis and Timing Aspects"). Also, cell proliferation of the CLS is important for quiescent center (QC) establishment (see Section "Cell Type Identity Acquisition"). Whether endodermal participation in LRP morphogenesis in angiosperms is evolutionarily linked to the ability of this tissue in ferns to form LRPs (Mallory et al., 1970; Hou et al., 2004) is an open question.

Vascular Parenchyma

No participation of vascular parenchyma in LRP formation has been documented in *Arabidopsis*. Therefore, this aspect of LRP morphogenesis is seldom discussed in contemporary literature. Nonetheless, the vascular parenchyma participates in primordium formation in both monocots (Rywosch, 1909; Bunning, 1952; Bell and McCully, 1970; Demchenko and Demchenko, 1996b) and eudicots (Seago, 1973; Byrne et al., 1977) by contributing to the vascular connection of the nascent LR and the parent root. It has been documented that vascular parenchyma cells start to divide very early, in StI LRPs in monocots (e.g., *T. aestivum*; Demchenko and Demchenko, 1996a) and StII LRPs in eudicots (e.g., *Glycine Max*; Byrne et al., 1977). During LRP formation in *G. max*, vascular parenchyma derivatives divide periclinally and form files of 4–5 cells that contribute to the formation of vascular tissues connecting the parent and lateral root (Byrne et al., 1977). Similarly, during embryonic LRP morphogenesis in the cucumber (*Cucumis sativus*) radicle, vascular parenchyma cells of the parent root divide 2–3 times periclinally, forming several layers of derivative cells (Dubrovsky, 1986a) (**Figure 4**). The contribution of vascular tissues of the parent root to LRP formation was also documented by the analysis of ploidy chimeras in *Z. mays* roots (Clowes, 1978a). Whether the participation of vascular parenchyma during LRP development is related to transport of nutrients or hormones toward the developing LRP remains to be determined.

THE CELL CYCLE DURING LATERAL ROOT PRIMORDIUM MORPHOGENESIS AND TIMING ASPECTS

In most angiosperms, LR initiation takes place post-germination. However, there are well-documented cases in which LRs are initiated during embryogenesis, such as in Cucurbitaceae

(Clowes, 1982; Dubrovsky, 1986a,b, 1987) and Polygonaceae (buckwheat, *Fagopyrum sagittatum*, O'Dell and Foard, 1969). The extent to which LRP morphogenesis proceeds during embryogenesis ranges from StII, as in *F. sagittatum* (O'Dell and Foard, 1969), to StVII, as in *C. sativum* (Dubrovsky, 1986a). A number of embryonic LRPs are formed within the embryo (O'Dell and Foard, 1969; Dubrovsky, 1987). Interestingly, in some Cucurbitaceae in which embryonic LRP morphogenesis is documented, post-germination LRP initiation takes place in the root apical meristem (Gulyaev, 1964; Dubrovsky, 1987; Demchenko and Demchenko, 2001; Ilina et al., 2018). Some other angiosperms, especially hydrophytes from Pontederiaceae, Araceae and Alismataceae, also begin LRP morphogenesis within the apical meristem of the parent root, as reviewed elsewhere (Dubrovsky and Rost, 2003; Ilina et al., 2018). Whether there is a correlation between the species capability to start LRP morphogenesis during embryogenesis and its capacity to initiate LRPs within the root apical meristem is an open question. In most angiosperm species, however, initiation starts post-germination within the differentiation zone, where LRP morphogenesis takes place. In this review, we consider mostly these cases.

The time from LR initiation to emergence ranges from 2.8 to 3.6 days in pea (*Pisum sativum*), faba bean (*Vicia faba*), *Z. mays*, and common bean (*Phaseolus vulgaris*) (MacLeod and Thompson, 1979), is about 2.5 days in radish (*Raphanus sativus*) (Blakely et al., 1982) and 1.6–2.2 days in *Arabidopsis* (Napsucialy-Mendivil et al., 2014; von Wangenheim et al., 2016). This suggests that the whole new organ can be formed during a relatively short period. Cell cycle studies in developing LRPs using labeled DNA precursors, e.g., tritiated thymidine (^{3}H-thymidine), have restrictions because LRPs at advanced stages do not incorporate ^{3}H-thymidine; for example, in *V. faba* LRPs of 1,500 or fewer cells incorporated ^{3}H-thymidine, whereas LRPs that contained a greater number of cells did not (Davidson and MacLeod, 1968; MacLeod and Davidson, 1968). Similarly, in monocots (*T. aestivum*), LRPs at StIII and later did not incorporate ^{3}H-thymidine (Demchenko and Demchenko, 1996a). Therefore, most earlier studies were based on estimating cell doubling time (*Td*), and contemporary studies use a time-lapse approach (von Wangenheim et al., 2016). *Td* estimations assume an exponential increase in cell number in the LRP (Thompson and MacLeod, 1981) to estimate the maximal duration of the cell cycle. As all LRP cells become polyploid when treated with colchicine (MacLeod and Davidson, 1968; Friedberg and Davidson, 1971), it is accepted that all the LRP cells proliferate, and the proliferation fraction is equal to one.

Cell proliferation dynamics impact the rate of primordium formation and LRP morphogenesis. It has been proposed that the rapid establishment of an LRP after initiation might have a role in lateral inhibition—i.e., preventing the initiation of new LRPs in the vicinity of ones already initiated (Dubrovsky et al., 2001). Therefore, the cell cycle in young LRPs is expected to be shorter than that in LRPs at a later developmental stage. Indeed, a few studies show that the shortest cell cycle is found at the earliest stages of LRP morphogenesis and increases at later stages. In *V. faba*, *P. sativum*, *Z. mays*, *P. vulgaris* (MacLeod and Thompson, 1979), and *Arabidopsis* (Dubrovsky et al., 2001), the *Td* from early to later stages of LRP development increases from 8.2, 2.9, 4.5, 6.9, and 2.7 h to 14.16, 9.96, 17.65, 11.4, and 4.9 h, respectively. For *Arabidopsis,* the average *Td* in LRP cells is 7.1 h (von Wangenheim et al., 2016), about half the average cell cycle duration observed in the primary-root apical meristem (reviewed in Zhukovskaya et al., 2018). Therefore, an overall short cell cycle and a gradual increase in cell cycle duration over time seems to be a general tendency. In species with LRPs already initiated during embryogenesis, the opposite trend is found post-germination. For instance, in *C. sativus, Td* is the longest (8.7 h) when pre-initiated LRP cells first enter the cell cycle soon after seed imbibition and decreases to 2.7 h in the LRP just before LR emergence (Dubrovsky, 1986b), explaining why LRs emerge rapidly after germination in this species.

When *V. faba* LRPs are about to emerge, their cells are less proliferatively active than during previous stages; after emergence, a sharp increase in proliferation is observed (Friedberg and Davidson, 1971; MacLeod, 1972, 1973). The rate of formation of individual LRPs within a parent root is variable, as documented for *V. faba*, *P. sativum*, *Z. mays*, and *P. vulgaris* (MacLeod and Thompson, 1979) and *Arabidopsis* (Dubrovsky et al., 2006; von Wangenheim et al., 2016). This is in agreement with the fact that, contrary to LR initiation, LRP formation along the parent root does not follow an acropetal pattern and is asynchronous. The heterogeneity in the rate of LRP formation explains why younger LRPs are found among the older ones or among emerged LRs, even in the zone where the vascular cambium and secondary tissues are formed (Napsucialy-Mendivil and Dubrovsky, 2018). Whether slow developing or delayed LRPs are capable of later resuming development is not well documented and remains an open question.

The processes of LR initiation and emergence are coordinated (Lucas et al., 2008b). The distance from the apex of the parent root to the site where the LR emerges depends on the site of LR initiation and on the rate of primordium formation. As mentioned above, in *Arabidopsis*, the time between LRP initiation and LR emergence is one of the shortest reported in Angiosperms. Nonetheless, the LR emerges a few centimeters from the apex. When LRs are initiated in the root apical meristem of the parent roots, as in Cucurbitaceae, LRs emerge at a shorter distance, e.g., 12–15 mm from the primary root apex in squash, *Cucurbita pepo* (Demchenko and Demchenko, 2001).

The role of cell cycle duration in LRP morphogenesis has not been extensively studied. The central domains of the LRP seem to develop faster than the flanking domains. **Figure 2** shows the terminology used to describe the LRP domains. The progeny of central founder cells is characterized by an average interphase duration of 6.0 h, whereas the corresponding period in the progeny of peripheral founder cells is 7.2 h (von Wangenheim et al., 2016). This suggests that the difference between cell cycle duration in each cell lineage has a profound impact on morphogenesis. It is not understood how heterogeneity in cell cycle time is related to LRP morphogenesis, whether the differences in cell cycle duration in certain domains have a critical role in defining the dome shape of the developing LRP, or whether

cell cycle time heterogeneity dictates the shape of the LRP or if the shape defines the cell cycle duration in different domains. Future studies should address these questions.

HORMONAL REGULATION OF MORPHOGENESIS

Since early studies, the importance of hormonal regulation in all aspects of LR development was recognized (Wightman et al., 1980). The role of auxin in LR development is well documented (Fukaki and Tasaka, 2009; Lavenus et al., 2013; Du and Scheres, 2017a) and LRP morphogenesis is known to depend on endogenous auxins up to StIV (Laskowski et al., 1995). In *P. sativum* plants treated with auxin transport inhibitors, normal LRP dome organization is lost and the primordium structure is transformed into a globular mass of cells (Hinchee and Rost, 1992), highlighting the significance of auxin in LRP morphogenesis. Accordingly, synthetic auxin-response promoter *DIRECT REPEAT5 (DR5*) (Ulmasov et al., 1997) activity is high during both LR initiation (Dubrovsky et al., 2008) and throughout LRP development (Benková et al., 2003; Dubrovsky et al., 2008). The auxin response maximum is present starting from StI in LRPs. From StIII, it is restricted to the central apical domain (**Figure 2**) of the LRP, corresponding to the prospective location of the QC (Dubrovsky et al., 2008). The auxin maximum apparently has a role in stem cell niche establishment and thus is important for normal LRP morphogenesis (see also the next section).

The localized auxin maximum response is present in different angiosperm orders, from monocots (*Z. mays*, Jansen et al., 2012) to eudicots (*S. lycopersicum* and *Arabidopsis*, Dubrovsky et al., 2008). It has been shown that while LR initiation does not depend on shoot-derived auxin, this source of auxin is essential for post-initiation LRP morphogenesis and LR emergence (Bhalerao et al., 2002; Ditengou et al., 2008; Swarup et al., 2008; Richter et al., 2009). A recent study strongly suggests that formation of an auxin maximum in the LRP also depends on local auxin synthesis in proliferating cells (Brumos et al., 2018). In most angiosperms, LR initiation starts in the young differentiation zone. Interestingly, when the LRP forms within the root apical meristem of the parent root, as in *C. pepo,* the auxin maximum is also established from the very early stages of LRP formation and is subsequently maintained throughout LRP development (Ilina et al., 2018). This suggests that LRP morphogenesis depends on auxin regardless of the differentiation state of the parent root cells giving rise to the LRP.

The auxin gradient with a maximum in the central apical domain (**Figure 2**) of the developing LRP is created by the auxin efflux carriers PIN-FORMED 1 (PIN1), PIN3, PIN4, PIN6, and PIN7 (Benková et al., 2003; Marhavý et al., 2014) and the auxin influx carriers AUX1 and LIKE AUX 3 (LAX3) (Marchant et al., 2002; Péret et al., 2012b). This gradient is formed by auxin flux from the flanking to the central domain and from the basal to the apical domain (**Figure 2**). Mutations that affect auxin transport lead to abnormal LRP formation. In the *pin1* mutant, LRP formation is slow and DR5 promoter activity is extended to more cells (Benková et al., 2003). Similarly, LRP formation takes more time in a *lax3* mutant (Swarup et al., 2008). Additionally, similar phenotypes are found in single and multiple mutants in *LATERAL ORGAN BOUNDARIES-DOMAIN/ASYMMETRIC LEAVES2-LIKE* (*LBD*) genes encoding transcription factors, such as *lbd29* (Porco et al., 2016), *lbd16 lbd18* double and *lbd16 labd18 lbd29* triple mutants (Feng et al., 2012; Lee et al., 2015), which are targets of auxin signaling through AUXIN RESPONSE FACTOR 7 (ARF7) and ARF19 transcription factors (Okushima et al., 2007). These phenotypes are explained by the finding that LBDs directly or indirectly promote expression of auxin influx carriers (Feng et al., 2012; Lee et al., 2015; Porco et al., 2016).

In the p*in1 pin3 pin4* triple mutant, treatment with exogenous auxin results in a massive division of pericycle cells and formation of a multilayered pericycle without a defined LRP structure, a phenotype similar to that of wild-type (Wt) seedlings treated with auxin transport inhibitor (Benková et al., 2003). Similarly, the role of auxin in correct cell division orientation during LRP morphogenesis is shown in *pin2 pin3 pin7* triple mutants that form fused LRs (Laskowski et al., 2008). *S. lycopersicum DIAGEOTROPICA (DGT)* encodes Cyclophilin A, which negatively regulates PIN protein localization and thereby affects both LRP initiation and morphogenesis (Ivanchenko et al., 2015). When pericycle cell proliferation is induced by auxin treatment in a *dgt* mutant, massive cell proliferation without formation of a recognizable primordium is observed (Ivanchenko et al., 2006). Auxin response restriction to the central apical domain of the LRP depends on the APETALA2-class transcription factor *PLETHORA* (PLT) genes (Du and Scheres, 2017b), whose expression in turn depends on AUXIN RESPONSE FACTOR 7 (ARF7) and ARF19 (Hofhuis et al., 2013). In the *plt3 plt5 plt7* triple mutant, DR5 activity is more diffuse and PIN1 and PIN3 expression is low or absent. In addition, due to abolishment of the auxin gradient in the mutant, periclinal cell divisions in LRPs are delayed or absent from StII onwards (Du and Scheres, 2017b). This work underlines the importance of auxin in LRP morphogenesis and cell division orientation. In line with this, it was shown that the correct orientation of pericycle cell divisions leading to LRP formation is abolished when the adjacent endodermal cell is ablated, but it is restored when exogenous auxin is added (Marhavý et al., 2016).

The processes of LRP initiation and LRP morphogenesis are linked, as the first cell division of founder cells triggers a new developmental program that permits *de novo* organ formation (Dubrovsky et al., 2008). This triggering is dependent on ARF7, ARF19, and INDOLE-3 ACETIC ACID 14 (IAA14)/SOLITARY-ROOT, the latter of which represses ARFs (Fukaki et al., 2005). Importantly, in the lateral rootless mutant *solitary root* (*slr*)/*iaa14* (Fukaki et al., 2002) and double mutant *arf7 arf19* (Okushima et al., 2005; Wilmoth et al., 2005), LRP initiation is almost completely abolished, although some StI but no StII LRPs still form. This phenotype cannot be rescued by the application of exogenous auxin (Fukaki et al., 2002; Okushima et al., 2005; Wilmoth et al., 2005).

Overexpression of *CYCLIND3;1* in the *slr* mutant background promotes cell proliferation in pericycle cells but no

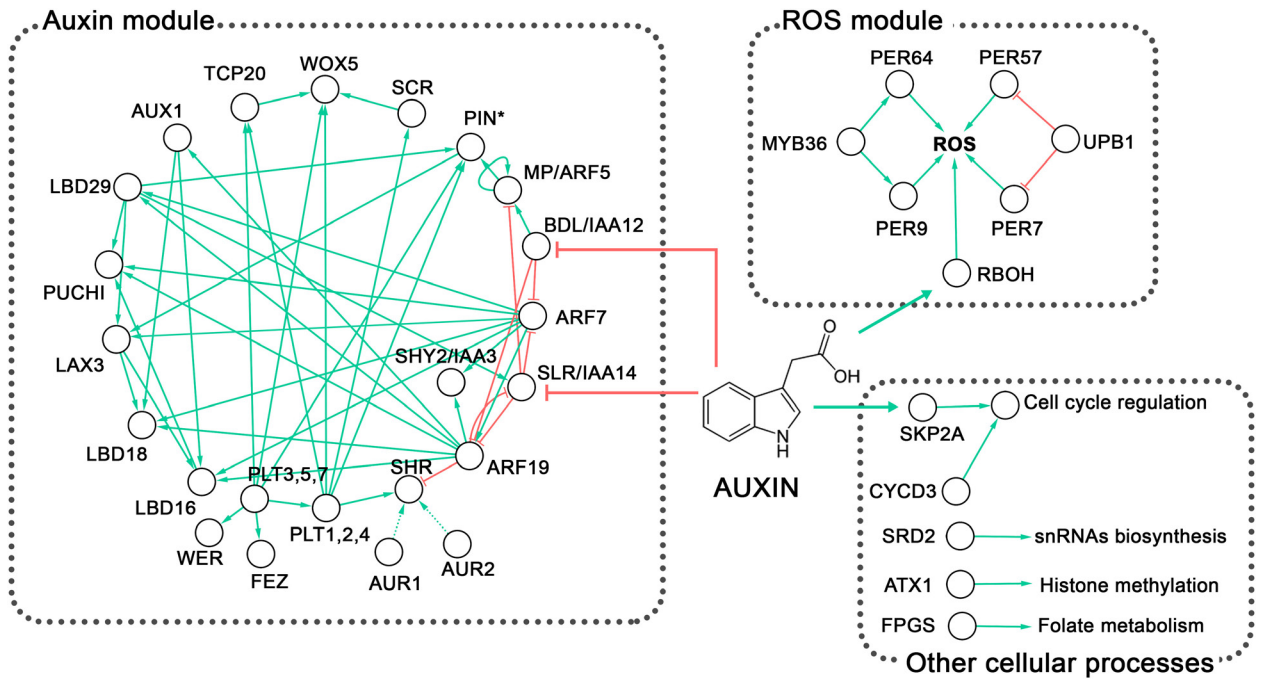

FIGURE 5 | Overview of the genetic control of lateral root primordium (LRP) morphogenesis in *Arabidopsis*. Two well-defined regulatory modules are observed, the auxin regulatory and the reactive oxygen species (ROS) homeostasis modules (discussed in the text). The first module involving ARFs, IAAs, AUX/LAX and PIN proteins (PIN*) also includes the PLT, PUCHI, FEZ, and WER transcription factors; the GRAS transcription cofactors SCR and SHR; and LBD proteins. The Ser/Thr kinases AUR1 and AUR2 are highly redundant and AlphaScreen assays showed that AUR1 interacts with SHR (Takagi et al., 2016); however, this interaction has not been proven *in planta* and hence is depicted with a discontinuous line. The second module includes the transcription factors MYB36 and UPB1, which control the expression of *PER* genes. Peroxidases together with RBOH control ROS homeostasis. Other cellular processes mentioned in the text and involved in LRP formation, such as the cell cycle, snRNA biosynthesis, histone methylation, and folate metabolism, are also depicted. Although particular genes involved in the regulation of these processes have been shown to affect LRP morphogenesis, their interactions with larger gene regulatory modules await to be discovered. Green arrows indicate activation or positive interaction; red lines with blunt ends indicate downregulation. The network was built from literature mining and visualized in Cytoscape v3.2.1 (Shannon et al., 2003). Complete names of the proteins are provided in the text.

organized LRPs are formed beyond StI (Vanneste et al., 2005; De Smet et al., 2010). This LRP arrest is bypassed when the *slr CYCD3;1*^{OE} line is treated with exogenous auxin. The treatment re-establishes normal LRP morphogenesis, which is accompanied by restoration of *ARABIDOPSIS CRINKLY4* (*ACR4*) and *PLT3* expression, which are downregulated in *slr- CYCD3;1*^{OE} (De Smet et al., 2010). Therefore, activation of cell proliferation is necessary but not sufficient to trigger LRP morphogenesis, and both correct auxin signaling and cell proliferation are required for normal LRP morphogenesis (**Figure 5**). It seems that auxin is linked to cell proliferation in this context through an F-box protein S-Phase Kinase-Associated Protein 2A (SKP2A) (Jurado et al., 2010).

Another important auxin-signaling module involved in LRP morphogenesis was revealed based on phenotypic analysis of the *bodenlos (bdl)/iaa12* and *monopteros/arf5* mutants (De Smet et al., 2010). In these mutants, a multilayered pericycle and fused LRPs show clear abnormalities in morphogenesis (**Figure 6**), demonstrating again that auxin signaling is of paramount importance for organized LRP development. Similarly, in the triple mutant affected in proteins involved in auxin perception, TRANSPORT INHIBITOR RESPONSE1 (TIR1), AUXIN SIGNALING F-BOX2 (AFB2), and AFB3 (Dharmasiri et al., 2005; Kepinski and Leyser, 2005), LRP morphogenesis turns out to be abnormal, resulting either in a multilayered pericycle or unusually wide LRPs (**Figure 6**) (Dubrovsky et al., 2011).

Cytokinins (CKs) are likewise important for LRP morphogenesis. CK biosynthesis takes place in the developing LRPs as shown using the PHOSPHATES-ISOPENTENYL TRANSFERASE *pIPT5::GFP* reporter (Takei et al., 2004). CKs are negative regulators of LR development (Li et al., 2006; Laplaze et al., 2007; Marhavý et al., 2011; Bielach et al., 2012). Specifically, CKs inhibit LRP initiation or some of the anticlinal divisions in StI LRPs (Li et al., 2006; Laplaze et al., 2007; Bielach et al., 2012). Later stages of LRP development are also inhibited, but they are less sensitive to CKs and, for this reason, time from initiation to emergence is increased (Li et al., 2006; Laplaze et al., 2007; Bielach et al., 2012). CK-treated plants show abnormal patterns of cell division throughout LRP morphogenesis. During the early stages, a series of periclinal divisions in external and internal layers occurs out of sequence (Laplaze et al., 2007). These irregularities at the cellular level result in a flattened LRP (Laplaze et al., 2007).

Cytokinins affect the auxin response maximum in developing LRPs, diffusing or abolishing it (Laplaze et al., 2007; Marhavý et al., 2011) through downregulation of PIN expression (Laplaze

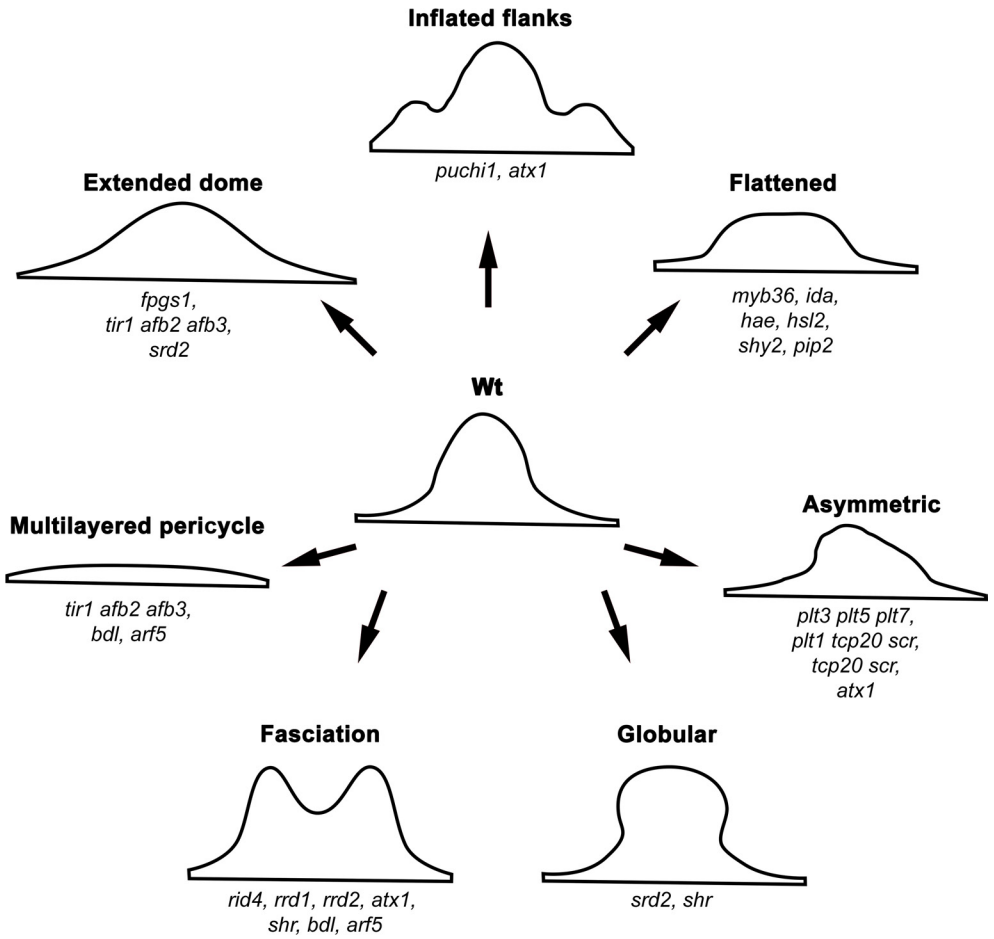

FIGURE 6 | Categories of lateral root primordium phenotype abnormalities in different *Arabidopsis* mutants. See text for details.

et al., 2007). From StIII onwards, low concentrations of exogenous N6-benzyladenine (a synthetic cytokinin) promote depletion of PIN1 in the plasma membrane to a greater extent at anticlinal cell walls than at periclinal ones (Marhavý et al., 2014). In this manner, cytokinin modulates the polarity of PIN1, allowing auxin to flow toward the LRP central apical domain (**Figure 2**) (Marhavý et al., 2014). In support of this notion, in Wt, PIN1 is predominantly found at periclinal cell walls, while in CK receptor mutants, PIN1 becomes localized at anticlinal walls (Marhavý et al., 2014). This CK-dependent redistribution of PIN1 in the mutants does not permit maintenance of the same number of cells in the external layer of the StIV LRP (Marhavý et al., 2014). This analysis clearly demonstrates that both auxins and CKs are involved in maintaining LRP morphogenesis and that crosstalk between these hormones is essential at all LRP developmental stages.

The role of other hormones in LRP morphogenesis is unclear. Ethylene promotes LR emergence through its effect on cell proliferation, at least in the outer LRP layers (Ivanchenko et al., 2008), but the mechanism has not been addressed. Abscisic acid (ABA) inhibits the emergence of LRPs and promotes its dormancy (De Smet et al., 2006b; Fukaki and Tasaka, 2009). In the parent root, a fraction of arrested or slowly developing LRPs is frequently found (Dubrovsky et al., 2006; Napsucialy-Mendivil and Dubrovsky, 2018). The most plausible scenario is that ABA inhibits cell proliferation in the developing LRP, keeping it 'dormant,' but this is yet to be shown.

Knowledge of the role of brassinosteroids and gibberellins (GA) in LRP morphogenesis is fragmentary (Fukaki and Tasaka, 2009). In poplar (*Populus* sp.), GA negatively regulates LRP initiation (Gou et al., 2010), but its role in LRP formation is unknown. The *Gibberellic Acid Stimulated-Like* (*GAST-like*) gene family, regulated by GA, is suggested to be involved in LRP development in rice (*Oryza sativa*) and *Z. mays,* but its exact role has yet to be established (Zimmermann et al., 2010). Nitric oxide was recently considered to be a phytohormone (Santner and Estelle, 2009). It inhibits LRP initiation but does not affect LR emergence (Lira-Ruan et al., 2013); however, its role in LRP morphogenesis is unknown. Many—if not all—of the hormone signaling pathways converge at one point or another. These interactions can potentially influence various aspects of LRP morphogenesis and further investigation is needed to address this complex cross-talk.

MECHANICAL FORCES AND LATERAL ROOT EMERGENCE

Even from early studies, it was known that developing LRPs experience mechanical stress imposed by the overlaying tissues (Pond, 1908). Additionally, the LRP is influenced by external factors such as substrate particles, soil compaction, and parent root curvatures. Roots in soil frequently meet mechanical barriers. The internal and external mechanical forces affect LRP morphogenesis, and we will briefly review what is known in this respect.

When roots were grown in beds of glass spheres, roots curved and LR initiation occurred on the external (convex) root side (Goss, 1977; Goss and Russell, 1980). Moreover, when a root is bent during the gravitropic response, or after permanent or transient manual bending that can be as short as 20 s, the LR is also formed on the convex root side (Ditengou et al., 2008; Laskowski et al., 2008; Lucas et al., 2008a,b; Richter et al., 2009; Kircher and Schopfer, 2016). At the bending site, auxin induces AUX1 expression within the root stele of the young differentiation zone, which together with PIN protein reorientation promotes increased auxin transport toward the convex side of the root, creating a positive feedback loop that results in greater auxin levels and eventually in LR initiation (Ditengou et al., 2008; Laskowski et al., 2008).

The possibility of inducing LR initiation at the desired time and place provides a useful experimental system for studying LRP morphogenesis. With this approach, it has been shown that shootward (basipetal) transport of solutes is important for LR initiation and LRP morphogenesis. After root apical meristem removal and experimental root bending (Ditengou et al., 2008) or only after bending (Lucas et al., 2008b), the LRP develops faster on the convex side compared to intact roots. Interestingly, manual root bending promotes LRP initiation in *slr/iaa14* and *arf7 arf19* mutants and they become capable of proceeding with LRP morphogenesis, though in the latter mutant only LRPs but not LRs are formed (Ditengou et al., 2008). Similarly, the ability of other auxin-related mutants to form LRPs and proceed with morphogenesis increases significantly after root bending (Richter et al., 2009). Specifically, these mutants are those affected in *AUX1*, *AUXIN RESISTANT4 (AXR4)* encoding an accessory protein involved in correct localization of AUX1 (Dharmasiri et al., 2006), and *TRANSPORT INHIBITOR RESPONSE1 (TIR1)* encoding the F-box protein auxin receptor (Tan et al., 2007). Overall, these experiments show a clear link between root bending, LR initiation, auxin accumulation at the convex root side, and the rate of LRP formation. The reasons for accelerated LRP formation in bent roots have not yet been addressed. A potential increase in auxin content during LR initiation could impact posterior development of the LRP. An increase of cytosolic Ca^{2+} in the pericycle on the convex side of bent root (Richter et al., 2009) could also impact LRP morphogenesis. Finally, mechanical forces affect cell wall properties in the root portion from which the LRP is emerging.

Cell wall remodeling and cell separation in tissues overlying the LRP are well documented and required for LRP protrusion. These processes depend on auxin signaling. Cell wall remodeling enzymes encoded by *PECTATE LYASE1* (*PLA1*) and *PLA2* are active during LRP protrusion (Laskowski et al., 2006). During this process, expression of *EXPANSIN14* (*EXPA14*) (Lee et al., 2013) and *EXPA17* (Lee and Kim, 2013), which encode cell wall remodeling proteins, is activated by LBD18 transcription factor in response to auxin. A loss-of-function mutant *lbd18* is significantly affected in the progression of LRP morphogenesis, resulting in delayed LR emergence (Lee and Kim, 2013; Lee et al., 2013). This demonstrates an auxin signaling-dependent crosstalk in the tissues overlying the developing LRP. A similar delayed LR emergence phenotype is found in the loss-of-function auxin influx carrier mutant *lax3* (Swarup et al., 2008). *LAX3* is expressed in the cortex and epidermis overlying the LRP and is involved in regulating the expression of *AUXIN INDUCED IN ROOT3* (*AIR3*), encoding a subtilisin-like protease (Neuteboom et al., 1999). Furthermore, POLYGALACTURONASES (PG) and a XYLOGLUCAN:XYLOGLUCOSYL TRANSFERASE 6 (XTR6) were reported to be regulated by a signaling pathway mediated by ARF7, ARF19-IAA14 and LAX3 and by the peptide INFLORESCENCE DEFICIENT IN ABSCISSION (IDA) through the leucine-rich repeat receptor-like kinases HAESA (HAE) and HAESA-LIKE2 (HSL2) (Swarup et al., 2008; Kumpf et al., 2013). Consequently, mutations in *IDA, HAE,* and *HSL2* result in both delayed LR emergence and flattened LRPs (Kumpf et al., 2013).

A more severe phenotype of no LR emergence and flattened LRPs is found in auxin-treated plants carrying the stabilized variant of *SHY2/IAA3* expressed from the endodermis-specific promoter of *CASPARIAN STRIP DOMAIN PROTEIN* (*CASP1*) (Vermeer et al., 2014). In these transgenic lines, endodermal cells overlying the LRP were unable to decrease their turgor pressure and consequently the cell volume to permit LRP protrusion. The authors also showed that SHY2 activity in the endodermis and not in the cortex and epidermis is important for LR emergence (Vermeer et al., 2014). Furthermore, the aquaporin water channel PLASMA MEMBRANE INTRINSIC PROTEINS (PIPs) have essential roles in the turgor pressure control of both the LRP and the overlying cells (Péret et al., 2012a). As expected, in *pip2* mutants, LRPs are flattened and LRs emerge at a slower rate (Péret et al., 2012a).

These data collectively demonstrate the importance of auxin signaling in the control of cell wall remodeling and turgor pressure in the overlying tissues that impact LRP morphogenesis and LR emergence. However, the mechanism by which the mechanical forces are perceived, the respective signal transduction pathways, the modes of communication between overlying tissues and LRP cells, and the morphogenesis mechanisms dependent on these factors, are still to be discovered.

CELL TYPE IDENTITY ACQUISITION

In vascular plants, three main tissue systems form: dermal, ground, and vascular tissues, originating from the protoderm, periblem, and plerome histogens, respectively (Hanstein, 1870; Esau, 1977; Evert, 2006). The idea that cell types acquire their identity in the very early stages of LRP formation was first

deduced from an anatomical retrospective analysis. Going back from advanced LRP stages, when cell types can be recognized, to earlier stages, Von Guttenberg (1960) proposed that the first periclinal division in StI primordium cells forms two layers, the internal and external layer, with different developmental fates. These layers are marked on **Figure 1** as IL and OL following Malamy and Benfey (1997). The internal layer is already specified at this early stage as plerome, giving rise to the future vascular cylinder or stele. Next, the external layer of StII LRPs (OL) undergoes a second periclinal division that gives rise to two outer layers (the external OL1 and the internal outer OL2), again with different cell fates. The protoderm (prospective epidermis) and the root cap are specified from OL1 layer, and OL2 gives rise to the periblem (prospective ground tissue; Von Guttenberg, 1960). Thus, the main cell types can be recognized already in StIII LRPs. It seems that this holds true in different taxa (Von Guttenberg, 1960; Voronkina, 1978).

Remarkably, although this conclusion was based on anatomical studies, it was later confirmed using cell type-specific marker lines of *Arabidopsis* (Malamy and Benfey, 1997). **Figure 1** illustrates the sequence of the cell type identity acquisitions in the developing LRP based on cell type reporters. It was reported that the enhancer trap markers for different cell types are expressed similarly in the primary and lateral roots. The stele-specific marker *SHORT-ROOT* (*SHR*) is transcribed in the stele of the primary root (Helariutta, 2000), and also in the internal cell layer of the StII LRP (IL), confirming its vascular (stele) identity (Tian et al., 2014; Goh et al., 2016; Du and Scheres, 2017b). The endodermis-specific *SCARECROW* (*SCR*; Di Laurenzio et al., 1996) is expressed in the external layer of the StII LRP (OL), confirming its endodermal identity (Tian et al., 2014; Goh et al., 2016; Du and Scheres, 2017b). After the second periclinal division in OL of StII LRP, both resulting outer layers (OL1 and OL2) maintain endodermal identity, as confirmed by *pSCR::GFP:SCR* expression (Goh et al., 2016). When the third periclinal division occurrs in the StIII LRP, it takes place in the innermost layer (IL). As evidenced by *pSHR::SHR:GFP* expression, both new layers maintain the stele identity (Goh et al., 2016). At this stage (StIV), the endormal cell indentity becomes restricted to the second outer layer (OL2).

When the internal layer of the StIII LRP (IL) divides periclinally, it forms the most internal (IL1) layer, presumably giving rise to pericycle, and the second layer (IL2), giving rise to other provascular tissues of the LRP (Malamy and Benfey, 1997). However, no pericycle-specific markers have been shown to be expressed within the central domains of an LRP. At stages V and VI, the external cells of the central domain of the LRP acquire root cap and epidermis identities, as evidenced by the promoter activity of the NAC domain transcription factor FEZ (Willemsen et al., 2008; Du and Scheres, 2017b) and of the MYB-related transcription factor WEREWOLF (Lee and Schiefelbein, 1999; Du and Scheres, 2017b), respectively. Therefore, the use of cell type-specific marker lines substantially enhanced our understanding of LRP morphogenesis and revealed that practically all meristematic cell type identitites are acquired before LR emergence (Malamy and Benfey, 1997; Du and Scheres, 2017b). These studies clearly demonstrate that differential gene expression involved in cell type identity acquisition starts very early in LRP morphogenesis.

A GFP reporter of the enhancer trap line J0121 is expressed specifically in the protoxylem-adjacent pericycle of the parent root. J0121 GFP expression was detected in all layers of the developing LRP from StI to StIII (Laplaze et al., 2005; Dubrovsky et al., 2006). This suggests that the early LRP cells posess a mixed identity. In the J0121 line, GFP is not expressed in the root apical meristem, but it is expressed throughout the elongation and differentiation zones of the parent root. Importantly, starting from StIV, GFP expression in the J0121 line is excluded from the central domains of the LRP and is maintained in the flanking domains until LR emergence, suggesting that the central and flanking domains have different developmental fates. Furthermore, this pattern suggests that, starting from StIV, the central LRP domain acquires features of a root apical meristem, as it no longer expresses J0121 GFP. This observation is in line with the fact that, from StIV onwards, the LRP becomes less dependent on the parent root (Laskowski et al., 1995), which could be related to the beginning of autonomous auxin synthesis in the LRP. Additionally, a gene regulatory network analysis showed that the formation of the central and flanking domains is controlled by two distinct gene clusters (Lavenus et al., 2015).

As discussed, the first periclinal divisions are developmentally asymmetric (Scheres and Benfey, 1999), i.e., different developmental fates are aquired by the daughter cells. Indeed, each cell type origin is dependent on these asymmetric divisions and we still do not understand how these are regulated. We do not yet know how early pericycle, xylem, phloem, and vascular parenchyma cell type identities are acquired during LRP morphogenesis. Cell type identity acquisition studies with the aid of cell type reporters are limited to *Arabidopsis*. Extension to other angiosperms is needed.

NEW STEM CELL NICHE ESTABLISHMENT

The QC in roots is a population of slowly cycling cells that gives rise to all the cells of the apical meristem and serves as an organizing center with stem cell properties (Clowes, 1954, 1975; Barlow, 1997; Bennett and Scheres, 2010; Dubrovsky and Barlow, 2015). In some species, such as *Malva sylvestris* (Byrne, 1973) and *V. faba* (MacLeod and McLachlan, 1974; MacLeod, 1977), the QC is established after LR emergence. In other species, such as *Eichornia, Pistia* (Clowes, 1958), and *Arabidopsis* (Goh et al., 2016), the QC is established during LRP morphogenesis. In yet other species, e.g., *Z. mays* (Clowes, 1978b), the QC can be established either before or after LR emergence. The establishment of a functional QC requires a critical mass of proliferating cells within a developing LRP. In *Z. mays*, cell proliferation in the CLS of endodermal origin is essential for QC establishment (Clowes, 1978b). This early-established QC vanishes when the CLS cells are sloughed off. Soon after, the new root cap initial cells of pericyclic origin are

produced and simultaneously a new cap and QC are established (Clowes, 1978b).

In *Arabidopsis*, the *WUSCHEL-RELATED HOMEOBOX 5* (*WOX5*) gene is specifically expressed in the QC (Sarkar et al., 2007). The p*WOX5*::*GFP* reporter is expressed already at StI (Ditengou et al., 2008), when LRP initiation is triggered by a primary root bending, or at StII in intact roots (Tian et al., 2014; Du and Scheres, 2017b; Shimotohno et al., 2018). This expression pattern, which resembles the expression of *WOX5* soon after the onset of embryogenesis (Sarkar et al., 2007), suggests that the cell lineage that will lead to QC establishment is specified early in root development. Moreover, the possibility exists that correct *WOX5* expression is required and sufficient to define the central domain of the LRP and could provide a hallmark for the neigboring domains (**Figure 2**). Another QC marker, QC25 (Sabatini et al., 2003; ten Hove et al., 2010), starts to be expressed in the OL2 of StIV LRPs, when the cycle time increases by 70% in that layer compared to that in the most external layer, OL1 (Goh et al., 2016). QC establishment depends on *SCR*, as in the *scr* loss-of-function mutant, the specification of QC identity—as monitored by the *pWOX5::n3GFP* reporter—does not take place in the OL2 LRP layer but in the more internal layers that have stele identity (Goh et al., 2016). QC identity is completely lost in the *plt3 plt5 plt7* mutant, underlying the importance of these transcription factors in QC establishment (Du and Scheres, 2017b). PLT1 or PLT3 and SCR form a protein complex mediated by TCP20/21 (a plant-specific Teosinte-branched-Cycloidea PCNA [Proliferating cell nuclear antigen]) transcription factor that binds to the *WOX5* promoter, and this complex is important for QC specification and LRP morphogenesis (Shimotohno et al., 2018). Triple mutants in genes encoding members of this complex show LRP morphogenesis abnormalities in both the central and flanking domains (Shimotohno et al., 2018). This phenotype reveals a tight link between cell type identity acquisition and morphogenetic processes. The observation that the QC is established before LR emergence suggests that LRP morphogenesis culminates with a new root apical meristem that becomes functional post-emergence. An open question is how the stem cell identiy is acquired during LRP morphogenesis and what other factors are involved in this process. Again, our knowledge of this process for species other than *Arabidopsis* is limited.

GENETIC CONTROL OF LATERAL ROOT PRIMORDIUM MORPHOGENESIS

A morphogenetic process must be considered from a 3D perspective. How gene regulatory networks define an organized structure is a central question for understanding morphogenesis. The 3D structure during embryogenesis was first acquired and fixed in evolution starting from gametophore development in bryophytes. In this basal land plant, rotation in the orientation of the cell division plane in stem cells permitted 3D morphogenesis (Harrison, 2017), an evolutionary novelty involving the *CLAVATA* (*CLV*) signaling pathway (Whitewoods et al., 2018). Time-lapse (4D) analyses of the genetic control of LRP morphogenesis are only beginning to be possible (Lucas et al., 2013; Vermeer et al., 2014; Goh et al., 2016; von Wangenheim et al., 2016) and few detailed studies of mutants affected in LRP morphogenesis have been performed. To examine the genetic control of LRP morphogenesis (**Figure 5**), we consider mutants that exhibit abnormal LRP formation and attempt to discern which morphogenetic processes are affected.

Some of the first mutants reported to be affected in LRP morphogenesis were *shoot rediffferentiation defective (srd2), root initiation defective (rid4)*, and *root rediffferentiation* (*rrd1* and *rrd2*) (Yasutani et al., 1994; Konishi and Sugiyama, 2003; Sugiyama, 2003). These mutants were isolated in a temperature-dependent mutant screen aimed at identifying genes involved in root development that could be essential, and thus conditionally lethal if absent, during early developmental stages. In the *srd2* mutant, time from LRP initiation to LR emergence is significantly increased (Ohtani and Sugiyama, 2005; Ohtani et al., 2010). Furthermore, from StV onwards, LRP morphogenesis becomes abnormal. The altered cell division pattern results in the formation of an LRP with a wider dome than in the Wt (Ohtani et al., 2010) due to increased length and thickness of the flanking domains and a decrease in the apical–basal axis length (see the respective domains in **Figure 2**). This *srd2* phenotype is related to the lack of auxin maximum establishment in the apical domain of the LRP in the mutant, which results from downregulation of the PIN proteins (Ohtani et al., 2010). *SRD2* encodes a nuclear protein that shares sequence similarity with human SOLUBLE NSF ATTACHMENT PROTEIN 50 (SNAP50), a subunit of the SNAPc multiprotein complex required for small nuclear RNA transcription (Ohtani and Sugiyama, 2005; Ohtani et al., 2010). The precise mechanism of *SRD2* action in LRP morphogenesis is unknown.

The phenotype of the *rrd1, rrd2,* and *rid4* mutants during the LRP pre-emergence stages is similar to that described for *srd2*. Surprisingly, the post-emergence LR phenotype in these mutants is different from that of *srd2*. While in *srd2*, the LRs are globular without pronounced growth, those of the *rrd1, rrd2,* and *rid4* mutants do grow, but produce fasciated (fused) roots (Konishi and Sugiyama, 2003; Sugiyama, 2003). During abnormal LRP development, the internal LRP cells form the prospective stele, which appears as a fusion of two adjacent LRPs. This was shown using *pSHR:GFP* and *pPIN1:PIN1-GFP* reporters. At the same time, *pSCR:GFP* expression revealed that the single external layer corresponding to the developing endodermis encloses the fused steles of the developing LRP (Otsuka and Sugiyama, 2012). The molecular function of genes affected in these mutants remains to be identified. The abnormal cell division pattern, which is more evident when seedlings are transferred from permissive to restrictive temperatures during the earlier stages of LRP morphogenesis, is a common feature of the mutants (Otsuka and Sugiyama, 2012). Furthermore, in the non-temperature-dependent *atx1* mutant affected in a H3K4-methyltransferase, similar LRP phenotypes (wider LRP and fasciated primordia) were found (Napsucialy-Mendivil et al., 2014). Abnormalities in cell division pattern and proliferation in the LRP at different developmental stages are also reported in the

shr (Lucas et al., 2011) and *folylpolyglutamate synthetase1* (*fpgs1*) mutants (Reyes-Hernández et al., 2014). LRP morphogenesis in the *srd2*, *rrd1, rrd2, rid4, atx1, shr,* and *fpgs1* mutants shows that correct cell division patterns and proliferation are critical factors in sustaining normal LRP development. In most of these cases, the abnormalities are equally distributed throughout all the LRP domains.

Lateral root primordium morphogenesis could also be affected either at specific stages or in specific LRP domains. Thus, in the *puchi* mutant, anticlinal and periclinal divisions are supernumerary in both the central and flanking domains, resulting in an increased thickness of the flanking domain and an overall flatter LRP at later stages of development (Hirota et al., 2007). *PUCHI* encodes an AP2/EREBP transcription factor that acts downstream of auxin signaling and is most strongly expressed in the flanking and basal domains (Hirota et al., 2007). Thus, *PUCHI* is apparently required to limit the extent of cell proliferation in the flanking domain and to restrict it to the central domain during LRP morphogenesis (Hirota et al., 2007). Similarly, *myb36* mutant LRPs are flatter than those of the Wt and, from StIV onwards, a defect in the transition from the flat to dome-shaped LRP is observed (Fernández-Marcos et al., 2017). More cells along the central basal and flanking domains of the *myb36* LRP are produced, resulting in wider LRPs than in the Wt (Fernández-Marcos et al., 2017). MYB36 is a transcription factor expressed in the LRP from StV onwards and is restricted to the central basal and flanking domains, where it controls the expression of peroxidases PER9 and PER64 (Fernández-Marcos et al., 2017). Thus, MYB36 apparently regulates LRP width through limiting cell proliferation mediated by changes in reactive oxygen species (ROS) balance.

In addition to the genetic control of morphogenesis at specific times and places, another aspect of morphogenesis is the control of cell division patterns and the orientation of the cell division plate. In the *aurora* (*aur*)*1 aur2* double mutant, oblique or irregularly shaped divisions take place during StI, after the first 2–3 anticlinal divisions. Therefore, the typical layered structure of the LRP is not formed (Van Damme et al., 2011). *AUR1* and *AUR2* encode Ser/Thr kinases that phosphorylate Ser 10 of Histone H3 during mitosis (Demidov et al., 2005, 2009; Kawabe et al., 2005). A recent *in vitro* study showed that AUR1 interacts and phosphorylates the SHR transcription factor; however, this interaction has not been confirmed *in planta* (Takagi et al., 2016). Interestingly, despite altered orientation of cell division throughout LRP development, the overall shape of the primordium is not significantly affected (Lucas et al., 2013). Nevertheless, LR emergence is substantially delayed in the *aur1 aur2* mutant (Van Damme et al., 2011; Lucas et al., 2013).

Other genes controlling the cell division orientation are those encoding PLT transcription factors. The triple mutant *plt3 plt5 plt7* is characterized by multiple defects in LRP formation, including irregular cell shapes, aberrant LRP morphology, and a lack of layered LRP structure (Hofhuis et al., 2013; Du and Scheres, 2017b). *PLT1, PLT2*, and *PLT4* are expressed at later stages during LRP development and their expression depends on the expression of *PLT3, PLT5*, and *PLT7*, which are expressed from StI onward. Therefore, the *plt3 plt5 plt7* mutant is affected in these six *PLT* genes, highlighting their importance in LRP morphogenesis. An overview of the genetic control of LRP morphogenesis is presented in **Figure 5**, while categories of the outlined abnormal LRP phenotypes are shown in **Figure 6**.

Together with genetic analysis, transcriptomic approaches (Brady et al., 2007; Moreno-Risueno et al., 2010) have also been used recently to analyze the genetic control of LRP morphogenesis. Together, these two approaches permit construction of gene regulatory networks and thus contribute to the identification of genes involved in LR development (Lavenus et al., 2015; Voß et al., 2015). Recent papers report how the architecture of gene regulatory networks changes during LRP formation. In one such study, the gravistimulation-induced LRP system (Lucas et al., 2008a) was implemented and time-series expression data sets collected starting from LRP initiation. In this way, two mutually exclusive gene clusters regulated by auxin were identified that act in non-overlapping central and flanking domains of the LRP (Lavenus et al., 2015). One cluster involves regulation by ARF7 and ARF19 and first acts in both domains, but soon becomes restricted to the flanking domain, where it is maintained until LR emergence. The second cluster is regulated by MP, ARF6, and ARF8 and acts in the central LRP domain (Lavenus et al., 2015). This analysis confirmed the importance of previously known genes involved in LRP morphogenesis and allowed the identification of new gene regulatory network nodes that potentially participate in LRP morphogenesis (Lavenus et al., 2015). Experimental validation of the identified genes will settle their particular roles in this process.

A transcriptomic approach was also used to identify new genes involved in LRP formation. For this, cell sorting of roots expressing the *pSKP2B:GFP* reporter, which is active at all LRP stages (Manzano et al., 2012), was performed and used to identify SKP2B-coexpressed genes (Manzano et al., 2014). This analysis revealed genes involved in ROS signaling, among others. One of these genes, *UPBEAT1* (*UPB1*), encodes a bHLH transcription factor and is expressed in the flanking LRP domain (Manzano et al., 2014). UPB1 regulates the expression of a subset of *PEROXIDASE* (*PER*) genes involved in maintaining the ROS balance (Tsukagoshi et al., 2010; Manzano et al., 2014). LR emergence is significantly delayed in *per7* and *per57* loss-of-function mutants and is promoted in the *PER7* overexpression line, suggesting the importance of ROS in LRP morphogenesis through UPB1-mediated signaling (Manzano et al., 2014). In line with these studies, RESPIRATORY BURST OXIDASE HOMOLOGS (RBOH) NADPH oxidases that produce extracellular ROS are also involved in LRP development (Manzano et al., 2014; Orman-Ligeza et al., 2016). Interestingly, nitroblue tetrazolium (NBT) staining, employed for the localization of superoxide, was detected in the central domain, but staining was absent or much lower in the flanking LRP domains (Manzano et al., 2014). In double and triple *rboh* mutants, LR emergence was also delayed, while it was accelerated in *RBOHD*-overexpressor lines (Orman-Ligeza et al., 2016). Collectively, these studies demonstrate that ROS promote progression of LRP formation and that redox state is important for LRP morphogenesis, even though it is not known

which specific morphogenetic processes are involved. Overall, transcriptomic approaches permit efficient identification of many new players involved in LRP formation and further studies should clarify their roles.

LATERAL ROOT MORPHOGENESIS AND PLANT HEALTH

A better understanding of LRP morphogenesis is important for both basic and applied science. Correct root primordium morphogenesis is the foundation of a healthy root system and appropriate root architecture. Abnormal primordium morphogenesis is a characteristic of rhizomania disease of sugar beet (*Beta vulgaris*) (D'ambra et al., 1972; Pollini and Giunchedi, 1989). This disease is induced by the beet necrotic yellow vein virus (BNYVV) and causes supernumerary LR formation on the taproot, leading to a dramatic decrease of root mass and yield. The viral P25 virulence factor mimics auxin action by deregulating BvAUX28. As a result, some root-specific LBD transcription factors and EXPANSINS are upregulated, which in turn promote uncontrolled LR formation (Gil et al., 2018) and probably cause abnormal morphogenesis. Early processes of LR development affected by this and other root diseases are underexplored, and studies of these diseases may suggest strategies to control and/or prevent abnormalities in LRP morphogenesis.

CONCLUDING REMARKS AND FUTURE PERSPECTIVES

Here we outlined the main components of LRP morphogenesis in angiosperms. Each facet of LRP morphogenesis reflected in the respective sections of this review outlines specific open questions. Most data on the genetic control of LRP morphogenesis are available for *Arabidopsis* and can be used for comparative studies in angiosperms. Further understanding of LRP morphogenesis in crop species is needed to modulate or adjust root system architecture to specific growth conditions.

The main tendencies, important for further research in this field, are related to the development of new technologies that could be used to address the open questions. These tendencies are as follows:

(1) Addressing the genetic control of morphogenesis in mutants and Wt plants by 3D analysis in time (4D) can significantly advance our understanding of root system formation. New imaging technologies and new microscopy approaches (Ovečka et al., 2018) that could be used for this purpose are already accessible. Deciphering cell division patterns and developmental rules involved in morphogenesis (Yoshida et al., 2014; von Wangenheim et al., 2016) is an important goal.

(2) Gene regulatory networks uncover complex relationships between pathways involved in regulating different processes during LRP morphogenesis (Lavenus et al., 2015; Voß et al., 2015). Further studies of gene regulatory networks at the single cell level and implementation of plant systems biology approaches (Libault et al., 2017) will undoubtedly contribute to answering the questions of how different LRP domains and cell types are specified and maintained, how the overall shape of the developing LRP emerges, and how timing control is operated.

(3) LRPs develop under mechanical constraints imposed by the external parent root tissues. The role of mechanical forces during LRP morphogenesis was recognized in early studies, but only recently did their roles in both LR initiation (Vermeer et al., 2014) and morphogenesis (Stoeckle et al., 2018) begin to be understood. Models of auxin transport coupled to mechanical forces provide explanations for the robust morphogenesis observed in the *Arabidopsis* root (Romero-Arias et al., 2017) and application of these models to LRP morphogenesis should be promising. Developing new biophysical methods to monitor the mechanical properties of live cells (e.g., Elsayad et al., 2016) is challenging, but required to discern the role of the mechanical forces in LRP morphogenesis. LRP formation is closely linked to external and internal mechanical forces and the cytoskeleton (Eng and Sampathkumar, 2018), but it is unclear how the mechanical forces contribute to LRP morphogenesis.

(4) We outlined a possible role of the temporal CLS formed during LRP morphogenesis and attempted to visualize related evolutionary trends of this particular feature of LRP morphogenesis. Understanding the relationships between different facets of LRP morphogenesis (e.g., orientation of cell division, developmental rules, participation of different cell types) and how they change during evolution is challenging but feasible in the post-genomic era. Integration of different approaches from genomics and molecular to cell biology and anatomy could help reveal evo–devo relationships in LRP morphogenesis of angiosperms.

Here we reviewed the main aspects of LRP morphogenesis that have been under investigation for more than a century. Not all available information was discussed; for instance, we did not include the role of environmental factors and mineral nutrition. We hope that the historical perspective combined here with our overview of contemporary studies of LRP morphogenesis highlights key questions that will guide future research aimed at elucidating the morphogenetic processes that take place during LRP development. Such research would yield important insights into root biology and evolution, providing a framework to modulate root system architecture, root production and root adaptation to the environment in crop species.

AUTHOR CONTRIBUTIONS

HT-M and JD conceived the idea and designed the outlines of this review article. SS and JD conceptualized the content. HT-M and JD wrote the article. GR-A performed phylogenetic and gene regulatory network analyses. GR-A, HT-M, and JD

prepared the illustrations. All authors participated in the editorial improvement of the text and approved the final manuscript.

FUNDING

This work was partially supported by Consejo Nacional de Ciencia y Tecnología, Mexico (CONACyT Grants 237430 to JD and 240055 to SS) and DGAPA-PAPIIT-UNAM (Grants IN200818 to JD and IN201318 to SS).

ACKNOWLEDGMENTS

A Ph.D. fellowship to HT-M from CONACyT and DGAPA-PAPIIT-UNAM and postdoctoral fellowship from CONACyT to GR-A are thankfully acknowledged. We thank the members of the Unidad de Cómputo. Instituto de Biotecnologia and S. Ainsworth for logistic help. We also thank K. Farquharson for editing the English text. We apologize to all those authors whose work was not cited due to time and space constraints.

REFERENCES

Atkinson, J. A., Rasmussen, A., Traini, R., Voß, U., Sturrock, C. J., Mooney, S. J., et al. (2014). Branching out in roots: uncovering form, function and regulation. *Plant Physiol.* 166, 538–550. doi: 10.1104/pp.114.245423

Barlow, P. W. (1997). "Stem cells and founder zones in plants, particularly their roots," in *Stem Cells*, ed. C. S. Potten (London: Academic Press), 29–57. doi: 10.1016/B978-012563455-7/50003-9

Beeckman, T., Burssens, S., and Inzé, D. (2001). The peri-cell-cycle in *Arabidopsis*. *J. Exp. Bot.* 52, 403–411.

Beeckman, T., and De Smet, I. (2014). Pericycle. *Curr. Biol.* 24, R378–R379. doi: 10.1016/j.cub.2014.03.031

Bell, J. K., and McCully, M. E. (1970). A histological study of lateral root initiation and development in *Zea mays*. *Protoplasma* 70, 179–205. doi: 10.1007/BF01276979

Benková, E., Michniewicz, M., Sauer, M., Teichmann, T., Seifertová, D., Jürgens, G., et al. (2003). Local, efflux-dependent auxin gradients as a common module for plant organ formation. *Cell* 115, 591–602. doi: 10.1016/S0092-8674(03)00924-3

Bennett, T., and Scheres, B. (2010). "Root development–Two meristems for the price of one?," in *Current Topics in Developmental Biology Plant Development*, ed. C. P. T. Marja (Cambridge, MA: Academic Press), 67–102.

Besson, S., and Dumais, J. (2011). Universal rule for the symmetric division of plant cells. *Proc. Natl. Acad. Sci. U.S.A.* 108, 6294–6299. doi: 10.1073/pnas.1011866108

Bhalerao, R. P., Eklöf, J., Ljung, K., Marchant, A., Bennett, M., and Sandberg, G. (2002). Shoot-derived auxin is essential for early lateral root emergence in *Arabidopsis* seedlings. *Plant J.* 29, 325–332. doi: 10.1046/j.0960-7412.2001.01217.x

Bielach, A., Podlešáková, K., Marhavý, P., Duclercq, J., Cuesta, C., Müller, B., et al. (2012). Spatiotemporal regulation of lateral root organogenesis in *Arabidopsis* by Cytokinin. *Plant Cell Online* 24, 3967–3981. doi: 10.1105/tpc.112.103044

Blakely, L. M., Durham, M., Evans, T. A., and Blakely, R. M. (1982). Experimental studies on lateral root formation in radish seedling roots. I. General methods, developmental stages, and spontaneous formation of laterals. *Bot. Gaz.* 143, 341–352. doi: 10.1086/337308

Bonnett, H. T. (1969). Cortical cell death during lateral root formation. *J. Cell Biol.* 40, 144–159. doi: 10.1083/jcb.40.1.144

Brady, S. M., Orlando, D. A., Lee, J.-Y., Wang, J. Y., Koch, J., Dinneny, J. R., et al. (2007). A high-resolution root spatiotemporal map reveals dominant expression patterns. *Science* 318, 801–806. doi: 10.1126/science.1146265

Brumos, J., Robles, L. M., Yun, J., Vu, T. C., Jackson, S., Alonso, J. M., et al. (2018). Local auxin biosynthesis is a key regulator of plant development. *Dev. Cell* 47, 306–318.e5. doi: 10.1016/j.devcel.2018.09.022

Bunning, E. (1952). Weitere Untersuchungen; uber die Differenzierungsvorgange in Wurzeln. *Z. Bot.* 40, 385–406.

Byrne, J. M. (1973). The root apex of malva sylvestris. III. lateral root development and the quiescent center. *Am. J. Bot.* 60, 657–662. doi: 10.1002/j.1537-2197.1973.tb05970.x

Byrne, J. M., Pesacreta, T. C., and Fox, J. A. (1977). Development and structure of the vascular connection between the primary and secondary root of glycine max (L.) Merr. *Am. J. Bot.* 64, 946–959. doi: 10.1002/j.1537-2197.1977.tb11939.x

Casero, P. J., Casimiro, I., and Lloret, P. G. (1995). Lateral root initiation by asymmetrical transverse divisions of pericycle cells in four plant species: *Raphanus sativus*, *Helianthus annuus*, *Zea mays*, and *Daucus carota*. *Protoplasma* 188, 49–58. doi: 10.1007/BF01276795

Casimiro, I., Beeckman, T., Graham, N., Bhalerao, R., Zhang, H., Casero, P., et al. (2003). Dissecting *Arabidopsis* lateral root development. *Trends Plant Sci.* 8, 165–171. doi: 10.1016/S1360-1385(03)00051-7

Chase, M. W., Christenhusz, M., Fay, M., Byng, J., Judd, W., Soltis, D., et al. (2016). An update of the Angiosperm Phylogeny Group classification for the orders and families of flowering plants: APG IV. *Bot. J. Linn. Soc.* 181, 1–20. doi: 10.1016/j.jep.2015.05.035

Clowes, F. A. L. (1954). The promeristem and the minimal constructional centre in grass root apices. *New Phytol.* 53, 108–116. doi: 10.1111/j.1469-8137.1954.tb05227.x

Clowes, F. A. L. (1958). Development of quiscent centres in root meristems. *New Phytol.* 57, 85–88. doi: 10.1111/j.1469-8137.1958.tb05918.x

Clowes, F. A. L. (1975). "The quiescent centre," in *Development and Function of Roots*, eds J. G. Torrey and D. Clarkson (London: Academic Press), 3–19.

Clowes, F. A. L. (1978a). Chimeras and the origin of lateral root primordia in *Zea mays*. *Ann. Bot.* 42, 801–807. doi: 10.1093/oxfordjournals.aob.a085519

Clowes, F. A. L. (1978b). Origin of the quiescent centre in *Zea mays*. *New Phytol.* 80, 409–419. doi: 10.1111/j.1469-8137.1978.tb01575.x

Clowes, F. A. L. (1982). Changes in cell population kinetics in an open meristem during root growth. *New Phytol.* 91, 741–748. doi: 10.1111/j.1469-8137.1982.tb03353.x

D'ambra, V., Giulini, P., and Orsenigo, M. (1972). Ricerche anatomiche e istologiche sul fittone di bietole rizomani. *Riv. Patol. Veg.* 8, 359–372.

Danilova, M. F., and Serdyuk, E. M. (1982). Formation of the lateral roots in *Hordeum vilgare* (Poaceae) (The data of electron microscopy). *Bot. Z.* 67, 140–145.

Davidson, D., and MacLeod, R. D. (1968). Heterogeneity in cell behaviour in primordia of *Vicia faba*. *Chromosoma* 25, 470–474. doi: 10.1007/BF02327723

De Rybel, B., Vassileva, V., Parizot, B., Demeulenaere, M., Grunewald, W., Audenaert, D., et al. (2010). A novel Aux/IAA28 signaling cascade activates GATA23-dependent specification of lateral root founder cell identity. *Curr. Biol.* 20, 1697–1706. doi: 10.1016/j.cub.2010.09.007

De Smet, I. (2012). Lateral root initiation: one step at a time. *New Phytol.* 193, 867–873. doi: 10.1111/j.1469-8137.2011.03996.x

De Smet, I., and Beeckman, T. (2011). Asymmetric cell division in land plants and algae: the driving force for differentiation. *Nat. Rev. Mol. Cell Biol.* 12, 177–188. doi: 10.1038/nrm3064

De Smet, I., Lau, S., Voá, U., Vanneste, S., Benjamins, R., Rademacher, E. H., et al. (2010). Bimodular auxin response controls organogenesis in *Arabidopsis*. *Proc. Natl. Acad. Sci. U.S.A.* 107, 2705–2710. doi: 10.1073/pnas.0915001107

De Smet, I., Signora, L., Beeckman, T., Inze, D., Foyer, C. H., and Zhang, H. (2003). An abscisic acid-sensitive checkpoint in lateral root development of *Arabidopsis*. *Plant J.* 33, 543–555. doi: 10.1046/j.1365-313X.2003.01652.x

De Smet, I., Tetsumura, T., De Rybel, B., Frei dit Frey, N., Laplaze, L., Casimiro, I., et al. (2007). Auxin-dependent regulation of lateral root positioning in the basal meristem of *Arabidopsis*. *Development* 134, 681–690. doi: 10.1242/dev.02753

De Smet, I., Vanneste, S., Inz, D., and Beeckman, T. (2006a). Lateral root initiation or the birth of a new meristem. *Plant Mol. Biol.* 60, 871–887.

De Smet, I., Zhang, H., Inze, D., and Beeckman, T. (2006b). A novel role for abscisic acid emerges from underground. *Trends Plant Sci.* 11, 434–439.

Demchenko, K. N., and Demchenko, N. P. (1996a). Early stages of lateral root development in *Triticum aestivum* L. *Acta Phytogeogr. Suec.* 81, 71–75.

Demchenko, K. N., and Demchenko, N. P. (1996b). Lateral root initiation in seedlings of *Triticum aestivum* (Poaceae). *Bot. Z.* 81, 47–50.

Demchenko, K. N., and Demchenko, N. P. (2001). "Changes of root structure in connection with the development of lateral root primordia in wheat and pumpkins," in *Recent Advances of Plant Root Structure and Function*, eds M. Čiamporová, I. Mistrík, and F. Baluška (Netherlands: Springer), 39–47.

Demchenko, K. N., Demchenko, N. P., and Danilova, M. F. (2001). Initiation and development of lateral root primordia in *Trticum aestivum* (Poaceae) *Cucurbita pepo* (Cucurbitacea) seedlings. *Bot. Z.* 86, 14–30.

Demidov, D., Hesse, S., Tewes, A., Rutten, T., Fuchs, J., Karimi Ashtiyani, R., et al. (2009). Aurora1 phosphorylation activity on histone H3 and its cross-talk with other post-translational histone modifications in *Arabidopsis. Plant J.* 59, 221–230. doi: 10.1111/j.1365-313X.2009.03861.x

Demidov, D., Van Damme, D., Geelen, D., Blattner, F. R., and Houben, A. (2005). Identification and dynamics of two classes of aurora-like kinases in *Arabidopsis* and other plants. *Plant Cell* 17, 836–848. doi: 10.1105/tpc.104.029710

Dharmasiri, N., Dharmasiri, S., and Estelle, M. (2005). The F-box protein TIR1 is an auxin receptor. *Nature* 435, 441–445. doi: 10.1038/nature03543

Dharmasiri, S., Swarup, R., Mockaitis, K., Dharmasiri, N., Singh, S. K., Kowalchyk, M., et al. (2006). AXR4 is required for localization of the auxin influx facilitator AUX1. *Science* 312, 1218–1220. doi: 10.1126/science.1122847

Di Laurenzio, L., Wysocka-Diller, J., Malamy, J. E., Pysh, L., Helariutta, Y., Freshour, G., et al. (1996). The *SCARECROW* gene regulates an asymmetric cell division that is essential for generating the radial organization of the *Arabidopsis* root. *Cell* 86, 423–433. doi: 10.1016/S0092-8674(00)80115-4

Ditengou, F. A., Teale, W. D., Kochersperger, P., Flittner, K. A., Kneuper, I., van der Graaff, E., et al. (2008). Mechanical induction of lateral root initiation in *Arabidopsis thaliana*. *Proc. Natl. Acad. Sci. U.S.A.* 105, 18818–18823. doi: 10.1073/pnas.0807814105

Dittmer, H. G. (1937). A quantitative study of the roots and root hairs of a winter rye plant (*Secale cereale*). *Am. J. Bot.* 24, 417–420. doi: 10.1002/j.1537-2197.1937.tb09121.x

Du, Y., and Scheres, B. (2017a). Lateral root formation and the multiple roles of auxin. *J. Exp. Bot.* 69, 155–167. doi: 10.1093/jxb/erx223

Du, Y., and Scheres, B. (2017b). PLETHORA transcription factors orchestrate de novo organ patterning during *Arabidopsis* lateral root outgrowth. *Proc. Natl. Acad. Sci. U.S.A.* 114, 11709–11714. doi: 10.1073/pnas.1714410114

Dubrovsky, J. G. (1986a). Origin of tissues of embryonic lateral root in the cucumber, tissue interactions, and positional control in development. *Ontogenez* 17, 176–189 (English translation from Russian appeared in Soviet Journal of Developmental Biology, New York, NY: Consultant Bureau 117, 119–128).

Dubrovsky, J. G. (1986b). Dynamics of cell reproduction and cell complexes (cell packets) in the embryonic lateral root primordium of the cucumber. *Ontogenez* 17, 525–534 (English translation from Russian appeared in Soviet Journal of Developmental Biology, New York, NY: Consultant Bureau, 517, 337–344).

Dubrovsky, J. G. (1987). Latent embryonic root system of the cucumber. *Bot. Z.* 72, 171–176.

Dubrovsky, J. G., and Barlow, P. W. (2015). The origins of the quiescent centre concept. *New Phytol.* 206, 493–496. doi: 10.1111/nph.13307

Dubrovsky, J. G., Doerner, P. W., Colón-Carmona, A., and Rost, T. L. (2000). Pericycle cell proliferation and lateral root initiation in *Arabidopsis*. *Plant Physiol.* 124, 1648–1657. doi: 10.1104/pp.124.4.1648

Dubrovsky, J. G., Gambetta, G. A., Hernández-Barrera, A., Shishkova, S., and González, I. (2006). Lateral root initiation in *Arabidopsis*: developmental window, spatial patterning, density and predictability. *Ann. Bot.* 97, 903–915. doi: 10.1093/aob/mcj604

Dubrovsky, J. G., and Laskowski, M. (2017). "Lateral Root Initiation," in *Encyclopedia of Applied Plant Sciences*, 2nd Edn, eds B. G. Murray and D. J. Murphy (Oxford: Academic Press), 256–264. doi: 10.1016/B978-0-12-394807-6.00126-X

Dubrovsky, J. G., Napsucialy-Mendivil, S., Duclercq, J., Cheng, Y., Shishkova, S., Ivanchenko, M. G., et al. (2011). Auxin minimum defines a developmental window for lateral root initiation. *New Phytol.* 191, 970–983. doi: 10.1111/j.1469-8137.2011.03757.x

Dubrovsky, J. G., and Rost, T. L. (2003). "Lateral root initiation," in *Encyclopedia of Applied Plant Sciences*, eds B. Thomas, D. J. Murphy, and B. J. Murray (Oxford: Elsevier Academic Press), 1101–1107.

Dubrovsky, J. G., and Rost, T. L. (2012). *Pericycle*. Hoboken, NJ: John Wiley & Sons, Ltd. doi: 10.1002/9780470015902.a0002085.pub2

Dubrovsky, J. G., Rost, T. L., Colón-Carmona, A., and Doerner, P. W. (2001). Early primordium morphogenesis during lateral root initiation in *Arabidopsis thaliana*. *Planta* 214, 30–36. doi: 10.1007/s004250100598

Dubrovsky, J. G., Sauer, M., Napsucialy-Mendivil, S., Ivanchenko, M. G., Friml, J., Shishkova, S., et al. (2008). Auxin acts as a local morphogenetic trigger to specify lateral root founder cells. *Proc. Natl. Acad. Sci. U.S.A.* 105, 8790–8794. doi: 10.1073/pnas.0712307105

Elsayad, K., Werner, S., Gallemí, M., Kong, J., Guajardo, E. R. S., Zhang, L., et al. (2016). Mapping the subcellular mechanical properties of live cells in tissues with fluorescence emission–Brillouin imaging. *Sci. Signal.* 9:rs5. doi: 10.1126/scisignal.aaf6326

Eng, R. C., and Sampathkumar, A. (2018). Getting into shape: the mechanics behind plant morphogenesis. *Curr. Opin. Plant Biol.* 46, 25–31. doi: 10.1016/j.pbi.2018.07.002

Esau, K. (1977). *Anatomy of the Seed Plants*, 2nd Edn. New York, NY: John Wiley & Sons Ltd.

Evert, R. F. (2006). *Esau's Plant Anatomy: Meristems, Cells, and Tissues of the Plant Body: their Structure, Function, and Development*. Hoboken, NJ: John Wiley & Sons. doi: 10.1002/0470047380

Feng, Z., Zhu, J., Du, X., and Cui, X. (2012). Effects of three auxin-inducible LBD members on lateral root formation in *Arabidopsis thaliana*. *Planta* 236, 1227–1237. doi: 10.1007/s00425-012-1673-3

Fernández-Marcos, M., Desvoyes, B., Manzano, C., Liberman, L. M., Benfey, P. N., Pozo, J. C., et al. (2017). Control of *Arabidopsis* lateral root primordium boundaries by MYB36. *New Phytol.* 213, 105–112. doi: 10.1111/nph.14304

Friedberg, S., and Davidson, D. (1971). Cell population studies in developing root primordia. *Ann. Bot.* 35, 523–533. doi: 10.1093/oxfordjournals.aob.a084496

Fukaki, H., Nakao, Y., Okushima, Y., Theologis, A., and Tasaka, M. (2005). Tissue-specific expression of stabilized SOLITARY-ROOT/IAA14 alters lateral root development in *Arabidopsis*. *Plant J.* 44, 382–395. doi: 10.1111/j.1365-313X.2005.02537.x

Fukaki, H., Tameda, S., Masuda, H., and Tasaka, M. (2002). Lateral root formation is blocked by a gain-of-function mutation in the *SOLITARY-ROOT/IAA14* gene of *Arabidopsis*. *Plant J.* 29, 153–168. doi: 10.1046/j.0960-7412.2001.01201.x

Fukaki, H., and Tasaka, M. (2009). Hormone interactions during lateral root formation. *Plant Mol. Biol.* 69, 437–449. doi: 10.1007/s11103-008-9417-2

Gil, J. F., Liebe, S., Thiel, H., Lennfors, B. L., Kraft, T., Gilmer, D., et al. (2018). Massive up-regulation of LBD transcription factors and EXPANSIN s highlights the regulatory programs of rhizomania disease. *Mol. Plant Pathol.* 19, 2333–2348. doi: 10.1111/mpp.12702

Goh, T., Toyokura, K., Wells, D. M., Swarup, K., Yamamoto, M., Mimura, T., et al. (2016). Quiescent center initiation in the *Arabidopsis* lateral root primordia is dependent on the *SCARECROW* transcription factor. *Development* 143, 3363–3371. doi: 10.1242/dev.135319

Goss, M. (1977). Effects of mechanical impedance on root growth in barley (*Hordeum vulgare* L.) I. Effects on the elongation and branching of seminal root axes. *J. Exp. Bot.* 28, 96–111. doi: 10.1093/jxb/28.1.96

Goss, M., and Russell, R. S. (1980). Effects of mechanical impedance on root growth in barley (*Hordeum vulgare* L.) III. Observations on the mechanism of response. *J. Exp. Bot.* 31, 577–588. doi: 10.1093/jxb/31.2.577

Gou, J., Strauss, S. H., Tsai, C. J., Fang, K., Chen, Y., Jiang, X., et al. (2010). Gibberellins regulate lateral root formation in populus through interactions with auxin and other hormones. *Plant Cell* 22, 623–639. doi: 10.1105/tpc.109.073239

Gulyaev, V. A. (1964). Initiation and formation of lateral roots in some species of Cucurbitaceae family. *Bot. Z.* 49, 1482–1485.

Hanstein, J. (1870). Die Entwicklung des Keimes der Monocotylen und der Dikotylen. *Bot. Abhandl.* 1:1.

Harrison, C. J. (2017). Development and genetics in the evolution of land plant body plans. *Philos. Trans. R. Soc. Lond. B Biol. Sci.* 372:20150490. doi: 10.1098/rstb.2015.0490

Helariutta, Y. (2000). The *SHORT-ROOT* gene controls radial patterning of the *Arabidopsis* root through radial signaling. *Cell* 101, 555–567. doi: 10.1016/S0092-8674(00)80865-X

Hinchee, M. A. W., and Rost, T. L. (1992). The control of lateral root development in cultured pea seedlings. II. Root fasciation induced by auxin inhibitors. *Bot. Acta* 105, 121–126. doi: 10.1111/j.1438-8677.1992.tb00276.x

Hirota, A., Kato, T., Fukaki, H., Aida, M., and Tasaka, M. (2007). The auxin-regulated AP2/EREBP gene PUCHI is required for morphogenesis in the early lateral root primordium of *Arabidopsis*. *Plant Cell* 19, 2156–2168. doi: 10.1105/tpc.107.050674

Hofhuis, H., Laskowski, M., Du, Y., Prasad, K., Grigg, S., Pinon, V., et al. (2013). Phyllotaxis and rhizotaxis in *Arabidopsis* are modified by three PLETHORA transcription factors. *Curr. Biol.* 23, 956–962. doi: 10.1016/j.cub.2013.04.048

Hou, G., Hill, J., and Blancaflor, E. B. (2004). Developmental anatomy and auxin response of lateral root formation in *Ceratopteris richardii*. *J. Exp. Bot.* 55, 685–693. doi: 10.1093/jxb/erh068

Ilina, E. L., Kiryushkin, A. S., Semenova, V. A., Demchenko, N. P., Pawlowski, K., and Demchenko, K. N. (2018). Lateral root initiation and formation within the parental root meristem of Cucurbita pepo: is auxin a key player? *Ann. Bot.* 122, 873–888. doi: 10.1093/aob/mcy052

Ivanchenko, M. G., Coffeen, W. C., Lomax, T. L., and Dubrovsky, J. G. (2006). Mutations in the Diageotropica (Dgt) gene uncouple patterned cell division during lateral root initiation from proliferative cell division in the pericycle. *Plant J.* 46, 436–447. doi: 10.1111/j.1365-313X.2006.02702.x

Ivanchenko, M. G., Muday, G. K., and Dubrovsky, J. G. (2008). Ethylene-auxin interactions regulate lateral root initiation and emergence in *Arabidopsis thaliana*. *Plant J.* 55, 335–347. doi: 10.1111/j.1365-313X.2008.03528.x

Ivanchenko, M. G., Zhu, J., Wang, B., Medvecká, E., Du, Y., Azzarello, E., et al. (2015). The cyclophilin A *DIAGEOTROPICA* gene affects auxin transport in both root and shoot to control lateral root formation. *Development* 142, 712–721. doi: 10.1242/dev.113225

Janczewski, E. (1874). Recherches sur le Developpement des Radicelles dans les Phanerogames. *Ann. Sci. Nat. Bot.* 20, 208–233.

Jansen, L., Roberts, I., De Rycke, R., and Beeckman, T. (2012). Phloem-associated auxin response maxima determine radial positioning of lateral roots in maize. *Philos. Trans. R. Soc. Lond. B Biol. Sci.* 367, 1525–1533. doi: 10.1098/rstb.2011.0239

Jurado, S., Abraham, Z., Manzano, C. Ý, López-Torrejón, G., Pacios, L. F., and del Pozo, J. C. (2010). The *Arabidopsis* cell cycle F-box protein SKP2A binds to auxin. *Plant Cell* 22, 3891–3904. doi: 10.1105/tpc.110.078972

Karas, I., and McCully, M. E. (1973). Further studies of the histology of lateral root development in *Zea mays*. *Protoplasma* 77, 243–269. doi: 10.1007/BF01276762

Kawabe, A., Matsunaga, S., Nakagawa, K., Kurihara, D., Yoneda, A., Hasezawa, S., et al. (2005). Characterization of plant Aurora kinases during mitosis. *Plant Mol. Biol.* 58, 1–13. doi: 10.1007/s11103-005-3454-x

Kawata, I., and Shibayama, H. (1965). On the lateral root primordia formation in the crown roots of rice plants. *Jpn. J. Crop Sci.* 33, 423–431. doi: 10.1626/jcs.33.423

Kepinski, S., and Leyser, O. (2005). The *Arabidopsis* F-box protein TIR1 is an auxin receptor. *Nature* 435, 446–451. doi: 10.1038/nature03542

Kircher, S., and Schopfer, P. (2016). Priming and positioning of lateral roots in *Arabidopsis*. An approach for an integrating concept. *J. Exp. Bot.* 67, 1411–1420. doi: 10.1093/jxb/erv541

Konishi, M., and Sugiyama, M. (2003). Genetic analysis of adventitious root formation with a novel series of temperature-sensitive mutants of *Arabidopsis thaliana*. *Development* 130, 5637–5647. doi: 10.1242/dev.00794

Kumpf, R. P., Shi, C.-L., Larrieu, A., Stø, I. M., Butenko, M. A., Péret, B., et al. (2013). Floral organ abscission peptide IDA and its HAE/HSL2 receptors control cell separation during lateral root emergence. *Proc. Natl. Acad. Sci. U.S.A.* 110, 5235–5240. doi: 10.1073/pnas.1210835110

Laplaze, L., Benková, E., Casimiro, I., Maes, L., Vanneste, S., Swarup, R., et al. (2007). Cytokinins act directly on lateral root founder cells to inhibit root initiation. *Plant Cell* 19, 3889–3900. doi: 10.1105/tpc.107.055863

Laplaze, L., Parizot, B., Baker, A., Ricaud, L., Martiniere, A., Auguy, F., et al. (2005). GAL4-GFP enhancer trap lines for genetic manipulation of lateral root development in *Arabidopsis thaliana*. *J. Exp. Bot.* 56, 2433–2442. doi: 10.1093/jxb/eri236

Laskowski, M., Biller, S., Stanley, K., Kajstura, T., and Prusty, R. (2006). Expression profiling of auxin-treated *Arabidopsis* roots: toward a molecular analysis of lateral root emergence. *Plant Cell Physiol.* 47, 788–792. doi: 10.1093/pcp/pcj043

Laskowski, M., Grieneisen, V. A., Hofhuis, H., Ten Hove, C. A., and Hogeweg, P. (2008). Root system architecture from coupling cell shape to auxin transport. *PLoS Biol.* 6:e307. doi: 10.1371/journal.pbio.0060307

Laskowski, M. J., Williams, M. E., Nusbaum, H. C., and Sussex, I. M. (1995). Formation of lateral root meristems is a two-stage process. *Development* 121, 3303–3310.

Lavenus, J., Goh, T., Guyomarc'h, S., Hill, K., Lucas, M., Voß, U., et al. (2015). Inference of the *Arabidopsis* lateral root gene regulatory network suggests a bifurcation mechanism that defines primordia flanking and central zones. *Plant Cell* 27, 1368–1388. doi: 10.1105/tpc.114.132993

Lavenus, J., Goh, T., Roberts, I., Guyomarc'h, S., Lucas, M., De Smet, I., et al. (2013). Lateral root development in *Arabidopsis*: fifty shades of auxin. *Trends Plant Sci.* 18, 450–458. doi: 10.1016/j.tplants.2013.04.006

Lee, H. W., Cho, C., and Kim, J. (2015). *Lateral organ boundaries domain16* and *18* act downstream of the AUXIN1 and LIKE-AUXIN$_3$ auxin influx carriers to control lateral root development in *Arabidopsis*. *Plant Physiol.* 168, 1792–1806. doi: 10.1104/pp.15.00578

Lee, H. W., and Kim, J. (2013). EXPANSINA17 up-regulated by LBD18/ASL20 promotes lateral root formation during the auxin response. *Plant Cell Physiol.* 54, 1600–1611. doi: 10.1093/pcp/pct105

Lee, H. W., Kim, M. J., Kim, N. Y., Lee, S. H., and Kim, J. (2013). LBD18 acts as a transcriptional activator that directly binds to the *EXPANSIN14* promoter in promoting lateral root emergence of *Arabidopsis*. *Plant J.* 73, 212–224. doi: 10.1111/tpj.12013

Lee, M. M., and Schiefelbein, J. (1999). WEREWOLF, a MYB-related protein in *Arabidopsis*, is a position-dependent regulator of epidermal cell patterning. *Cell* 99, 473–483. doi: 10.1016/S0092-8674(00)81536-6

Li, X., Mo, X., Shou, H., and Wu, P. (2006). Cytokinin-mediated cell cycling arrest of pericycle founder cells in lateral root initiation of *Arabidopsis*. *Plant Cell Physiol.* 47, 1112–1123. doi: 10.1093/pcp/pcj082

Libault, M., Pingault, L., Zogli, P., and Schiefelbein, J. (2017). Plant systems biology at the single-cell level. *Trends Plant Sci.* 22, 949–960. doi: 10.1016/j.tplants.2017.08.006

Lira-Ruan, V., Mendivil, S. N., and Dubrovsky, J. G. (2013). Heuristic aspect of the lateral root initiation index: a case study of the role of nitric oxide in root branching. *Appl. Plant Sci.* 1:1300029. doi: 10.3732/apps.1300029

Lloret, P. G., and Casero, P. J. (2002). "Lateral root initiation," in *Plant Roots: the Hidden Half*, 3rd Edn, Vol. 2002, eds U. Kafkafi, Y. Waisel, and A. Eshel (Boca Raton, FL: CRC Press), 127–155. doi: 10.1201/9780203909423.ch8

Lucas, M., Godin, C., Jay-Allemand, C., and Laplaze, L. (2008a). Auxin fluxes in the root apex co-regulate gravitropism and lateral root initiation. *J. Exp. Bot.* 59, 55–66.

Lucas, M., Guédon, Y., Jay-Allemand, C., Godin, C., and Laplaze, L. (2008b). An auxin transport-based model of root branching in *Arabidopsis thaliana*. *PLoS One* 3:e3673. doi: 10.1371/journal.pone.0003673

Lucas, M., Kenobi, K., von Wangenheim, D., Voβ, U., Swarup, K., De Smet, I., et al. (2013). Lateral root morphogenesis is dependent on the mechanical properties of the overlaying tissues. *Proc. Natl. Acad. Sci. U.S.A.* 110, 5229–5234. doi: 10.1073/pnas.1210807110

Lucas, M., Swarup, R., Paponov, I. A., Swarup, K., Casimiro, I., Lake, D., et al. (2011). SHORT-ROOT regulates primary, lateral, and adventitious root development in *Arabidopsis*. *Plant Physiol.* 155, 384–398. doi: 10.1104/pp.110.165126

MacLeod, R. (1972). Lateral root formation in *Vicia faba* L. I. The development of large primordia. *Chromosoma* 39, 341–350. doi: 10.1007/BF00290792

MacLeod, R. (1977). Proliferating and quiescent cells in the apical meristem of elongating lateral roots of *Vicia faba* L. *Ann. Bot.* 41, 321–329. doi: 10.1093/oxfordjournals.aob.a085294

MacLeod, R., and Davidson, D. (1968). Delayed incorporation of H 3-thymidine by primordial cells. *Chromosoma* 24, 1–9. doi: 10.1007/BF00329602

MacLeod, R., and McLachlan, S. (1974). The development of a quiescent centre in lateral roots of *Vicia faba* L. *Ann. Bot.* 38, 535–544. doi: 10.1093/oxfordjournals.aob.a084839

MacLeod, R. D. (1973). The response of root meristems to colchicine and Indol-3yl-acetic acid in *Vicia faba* L. *Ann. Bot.* 37, 687–697. doi: 10.1093/oxfordjournals.aob.a084736

MacLeod, R. D., and Thompson, A. (1979). Development of lateral root primordia in *Vicia faba, Pisum sativum, Zea mays* and *Phaseolus vulgaris*: Rates of

primordium formation and cell doubling times. *Ann. Bot.* 44, 435–449. doi: 10.1007/BF00384887

Malamy, J. E. (2010). "Lateral root formation," in *Root Development. Annual Plant Reviews*, Vol. 37, ed. T. Beeckman (Hoboken, NJ: Blackwell Publishing), 83–126.

Malamy, J. E., and Benfey, P. N. (1997). Organization and cell differentiation in lateral roots of *Arabidopsis thaliana*. *Development* 124, 33–44.

Mallory, T. E., Chiang, S., Cutter, E. G., and Gifford, E. M. Jr. (1970). Sequence and pattern of lateral root formation in five selected species. *Am. J. Bot.* 57, 800–809. doi: 10.1093/jxb/erv346

Manzano, C., Pallero-Baena, M., Casimiro, I., De Rybel, B., Orman-Ligeza, B., Van Isterdael, G., et al. (2014). The emerging role of reactive oxygen species signaling during lateral root development. *Plant Physiol.* 165, 1105–1119. doi: 10.1104/pp.114.238873

Manzano, C., Ramirez-Parra, E., Casimiro, I., Otero, S., Desvoyes, B., De Rybel, B., et al. (2012). Auxin and epigenetic regulation of *SKP2B*, an F-Box that represses lateral root formation. *Plant Physiol.* 160, 749–762. doi: 10.1104/pp.112.198341

Marchant, A., Bhalerao, R., Casimiro, I., Eklöf, J., Casero, P. J., Bennett, M., et al. (2002). AUX1 promotes lateral root formation by facilitating Indole-3-Acetic acid distribution between sink and source tissues in the *Arabidopsis* seedling. *Plant Cell* 14, 589–597. doi: 10.1105/tpc.010354

Marhavý, P., Bielach, A., Abas, L., Abuzeineh, A., Duclercq, J., Tanaka, H., et al. (2011). Cytokinin modulates endocytic trafficking of PIN1 auxin efflux carrier to control plant organogenesis. *Dev. Cell* 21, 796–804. doi: 10.1016/j.devcel.2011.08.014

Marhavý, P., Duclercq, J., Weller, B., Feraru, E., Bielach, A., Offringa, R., et al. (2014). Cytokinin controls polarity of PIN1-dependent auxin transport during lateral root organogenesis. *Curr. Biol.* 24, 1031–1037. doi: 10.1016/j.cub.2014.04.002

Marhavý, P., Montesinos, J. C., Abuzeineh, A., Van Damme, D., Vermeer, J. E., Duclercq, J., et al. (2016). Targeted cell elimination reveals an auxin-guided biphasic mode of lateral root initiation. *Genes Dev.* 30, 471–483. doi: 10.1101/gad.276964.115

McCully, M. E. (1975). "The development of lateral roots," in *The Development and Function of Roots*, eds J. G. Torrey and D. T. Clarkson (Cambridge, MA: Academic Press).

Moreno-Risueno, M. A., Van Norman, J. M., Moreno, A., Zhang, J., Ahnert, S. E., and Benfey, P. N. (2010). Oscillating gene expression determines competence for periodic *Arabidopsis* root branching. *Science* 329, 1306–1311. doi: 10.1126/science.1191937

Nakajima, K., Sean, G., Nawy, T., and Benfey, P. N. (2001). Intercellular movement of the putative transcriprion factor SHR in root patterning. *Nature* 413, 307–311. doi: 10.1038/35095061

Napsucialy-Mendivil, S., Alvarez-Venegas, R., Shishkova, S., and Dubrovsky, J. G. (2014). *ARABIDOPSIS HOMOLOG of TRITHORAX1* (*ATX1*) is required for cell production, patterning, and morphogenesis in root development. *J. Exp. Bot.* 65, 6373–6384. doi: 10.1093/jxb/eru355

Napsucialy-Mendivil, S., and Dubrovsky, J. G. (2018). Genetic and phenotypic analysis of lateral root development in *Arabidopsis thaliana*. *Methods Mol. Biol.* 1761, 47–75. doi: 10.1007/978-1-4939-7747-5_4

Neuteboom, L. W., Ng, J. M., Kuyper, M., Clijdesdale, O. R., Hooykaas, P. J., and Van Der Zaal, B. J. (1999). Isolation and characterization of cDNA clones corresponding with mRNAs that accumulate during auxin-induced lateral root formation. *Plant Mol. Biol.* 39, 273–287. doi: 10.1023/A:1006104205959

O'Dell, D. H., and Foard, D. E. (1969). Presence of lateral root primordia in the radicle of buckwheat embryos. *Bull. Torrey Bot. Club* 96, 1–3. doi: 10.2307/2484002

Ohtani, M., Demura, T., and Sugiyama, M. (2010). Particular significance of SRD2-dependent snRNA accumulation in polarized pattern generation during lateral root development of *Arabidopsis*. *Plant Cell Physiol.* 51, 2002–2012. doi: 10.1093/pcp/pcq159

Ohtani, M., and Sugiyama, M. (2005). Involvement of SRD2-mediated activation of snRNA transcription in the control of cell proliferation competence in *Arabidopsis*. *Plant J.* 43, 479–490. doi: 10.1111/j.1365-313X.2005.02469.x

Okushima, Y., Fukaki, H., Onoda, M., Theologis, A., and Tasaka, M. (2007). ARF7 and ARF19 regulate lateral root formation via direct activation of *LBD/ASL* Genes in *Arabidopsis*. *Plant Cell* 19, 118–130. doi: 10.1105/tpc.106.047761

Okushima, Y., Overvoorde, P. J., Arima, K., Alonso, J. M., Chan, A., Chang, C., et al. (2005). Functional genomic analysis of the *AUXIN RESPONSE FACTOR* gene family members in *Arabidopsis thaliana*: unique and overlapping functions of *ARF7* and *ARF19*. *Plant Cell* 17, 444–463. doi: 10.1105/tpc.104.028316

Orman-Ligeza, B., Parizot, B., De Rycke, R., Fernandez, A., Himschoot, E., Van Breusegem, F., et al. (2016). RBOH-mediated ROS production facilitates lateral root emergence in *Arabidopsis*. *Development* 143, 3328–3339. doi: 10.1242/dev.136465

Otsuka, K., and Sugiyama, M. (2012). Tissue organization of fasciated lateral roots of *Arabidopsis* mutants suggestive of the robust nature of outer layer patterning. *J. Plant Res.* 125, 547–554. doi: 10.1007/s10265-011-0471-5

Ötvös, K., and Benková, E. (2017). Spatiotemporal mechanisms of root branching. *Curr. Opin. Genet. Dev.* 45, 82–89. doi: 10.1016/j.gde.2017.03.010

Ovečka, M., von Wangenheim, D., Tomančák, P., Šamajová, O., Komis, G., and Šamaj, J. (2018). Multiscale imaging of plant development by light-sheet fluorescence microscopy. *Nat. Plants* 4, 639–650. doi: 10.1038/s41477-018-0238-2

Péret, B., De Rybel, B., Casimiro, I., Benková, E., Swarup, R., Laplaze, L., et al. (2009). *Arabidopsis* lateral root development: an emerging story. *Trends Plant Sci.* 14, 399–408. doi: 10.1016/j.tplants.2009.05.002

Péret, B., Li, G., Zhao, J., Band, L. R., Voß, U., Postaire, O., et al. (2012a). Auxin regulates aquaporin function to facilitate lateral root emergence. *Nat. Cell Biol.* 14, 991. doi: 10.1038/ncb2573

Péret, B., Swarup, K., Ferguson, A., Seth, M., Yang, Y., Dhondt, S., et al. (2012b). *AUX/LAX* genes encode a family of auxin influx transporters that perform distinct functions during *Arabidopsis* development. *Plant Cell Online* 24, 2874–2885. doi: 10.1105/tpc.112.097766

Pollini, C. P., and Giunchedi, L. (1989). Comparative histopathology of sugar beets that are susceptible and partially resistant to rhizomania. *Phytopathol. Mediterr.* 28, 16–21.

Pond, R. H. (1908). Emergence of lateral roots. *Bot. Gazette* 46, 410–421. doi: 10.1086/329783

Popham, R. A. (1955). Zonation of primary and lateral root apices af *Pisum sativum*. *Am. J. Bot.* 42, 267–273. doi: 10.1002/j.1537-2197.1955.tb11118.x

Porco, S., Larrieu, A., Du, Y., Gaudinier, A., Goh, T., Swarup, K., et al. (2016). Lateral root emergence in *Arabidopsis* is dependent on transcription factor LBD29 regulating auxin influx carrier LAX3. *Development* 143, 3340–3349. doi: 10.1242/dev.136283

Reyes-Hernández, B. J., Srivastava, A. C., Ugartechea-Chirino, Y., Shishkova, S., Ramos-Parra, P. A., Lira-Ruan, V., et al. (2014). The root indeterminacy-to-determinacy developmental switch is operated through a folate-dependent pathway in *Arabidopsis thaliana*. *New Phytol.* 202, 1223–1236. doi: 10.1111/nph.12757

Richter, G. L., Monshausen, G. B., Krol, A., and Gilroy, S. (2009). Mechanical stimuli modulate lateral root organogenesis. *Plant Physiol.* 151, 1855–1866. doi: 10.1104/pp.109.142448

Romero-Arias, J. R., Hernández-Hernández, V., Benítez, M., Alvarez-Buylla, E. R., and Barrio, R. A. (2017). Model of polar auxin transport coupled to mechanical forces retrieves robust morphogenesis along the *Arabidopsis* root. *Phys. Rev. E* 95:032410. doi: 10.1103/PhysRevE.95.032410

Rywosch, S. (1909). Untersuchungen uber die Entwicklungsgeschichte der Seitenwurzeln der Monocotylen. *Z. Bot.* 1, 253–283.

Sabatini, S., Heidstra, R., Wildwater, M., and Scheres, B. (2003). SCARECROW is involved in positioning the stem cell niche in the *Arabidopsis* root meristem. *Genes Dev.* 17, 354–358. doi: 10.1101/gad.252503

Santner, A., and Estelle, M. (2009). Recent advances and emerging trends in plant hormone signalling. *Nature* 459, 1071–1078. doi: 10.1038/nature08122

Sarkar, A. K., Luijten, M., Miyashima, S., Lenhard, M., Hashimoto, T., Nakajima, K., et al. (2007). Conserved factors regulate signalling in *Arabidopsis thaliana* shoot and root stem cell organizers. *Nature* 446, 811–814. doi: 10.1038/nature05703

Scheres, B., and Benfey, P. N. (1999). Asymmetric cell division in plants. *Annu. Rev. Plant Physiol. Plant Mol. Biol.* 50, 505–537. doi: 10.1146/annurev.arplant.50.1.505

Seago, J. L. (1973). Developmental anatomy in roots of *Ipomoea purpurea*. II. initiation and development of secundary roots. *Am. J. Bot.* 60, 607–618. doi: 10.1002/j.1537-2197.1973.tb05965.x

Shannon, P., Markiel, A., Ozier, O., Baliga, N. S., Wang, J. T., Ramage, D., et al. (2003). Cytoscape: a software environment for integrated models of biomolecular interaction networks. *Genome Res.* 13, 2498–2504. doi: 10.1101/gr.1239303

Shimotohno, A., Heidstra, R., Blilou, I., and Scheres, B. (2018). Root stem cell niche organizer specification by molecular convergence of PLETHORA and SCARECROW transcription factor modules. *Genes Dev.* 32, 1085–1100. doi: 10.1101/gad.314096.118

Stoeckle, D., Thellmann, M., and Vermeer, J. E. (2018). Breakout—lateral root emergence in *Arabidopsis thaliana*. *Curr. Opin. Plant Biol.* 41, 67–72. doi: 10.1016/j.pbi.2017.09.005

Sugiyama, M. (2003). Isolation and initial characterization of temperature-sensitive mutants of *Arabidopsis thaliana* that are impaired in root redifferentiation. *Plant Cell Physiol.* 44, 588–596. doi: 10.1093/pcp/pcg077

Swarup, K., Benkova, E., Swarup, R., Casimiro, I., Peret, B., Yang, Y., et al. (2008). The auxin influx carrier LAX3 promotes lateral root emergence. *Nat. Cell Biol.* 10, 946–954. doi: 10.1038/ncb1754

Takagi, M., Sakamoto, T., Suzuki, R., Nemoto, K., Obayashi, T., Hirakawa, T., et al. (2016). Plant Aurora kinases interact with and phosphorylate transcription factors. *J. Plant Res.* 129, 1165–1178. doi: 10.1007/s10265-016-0860-x

Takei, K., Ueda, N., Aoki, K., Kuromori, T., Hirayama, T., Shinozaki, K., et al. (2004). *AtIPT3* is a key determinant of nitrate-dependent cytokinin biosynthesis in *Arabidopsis*. *Plant Cell Physiol.* 45, 1053–1062. doi: 10.1093/pcp/pch119

Tan, X., Calderon-Villalobos, L. A., Sharon, M., Zheng, C., Robinson, C. V., Estelle, M., et al. (2007). Mechanism of auxin perception by the TIR1 ubiquitin ligase. *Nature* 446, 640–645. doi: 10.1038/nature05731

ten Hove, C. A., Willemsen, V., de Vries, W. J., van Dijken, A., Scheres, B., and Heidstra, R. (2010). *SCHIZORIZA* encodes a nuclear factor regulating asymmetry of stem cell divisions in the *Arabidopsis* root. *Curr. Biol.* 20, 452–457. doi: 10.1016/j.cub.2010.01.018

Thompson, A., and MacLeod, R. D. (1981). Increase in size and cell number of lateral root primordia in the primary of intact plants and in excised roots of *Pisum sativum* and *Vicia faba*. *Am. J. Bot.* 68, 955–964. doi: 10.1002/j.1537-2197.1981.tb07812.x

Tian, H., Jia, Y., Niu, T., Yu, Q., and Ding, Z. (2014). The key players of the primary root growth and development also function in lateral roots in *Arabidopsis*. *Plant Cell Rep.* 33, 745–753. doi: 10.1007/s00299-014-1575-x

Tschermak-Woess, E., and Doležal, R. (1953). Durch Seitenwurzelbildung induzierte und spontane Mitosen in den Dauergeweben der Wurzel. *Österreichische Bot. Z.* 100, 358–402. doi: 10.1007/BF01805779

Tsukagoshi, H., Busch, W., and Benfey, P. N. (2010). Transcriptional Regulation of ROS controls transition from proliferation to differentiation in the root. *Cell* 143, 606–616. doi: 10.1016/j.cell.2010.10.020

Ulmasov, T., Murfett, J., Hagen, G., and Guilfoyle, T. J. (1997). Aux/IAA proteins repress expression of reporter genes containing natural and highly active synthetic auxin response elements. *Plant Cell* 9, 1963–1971. doi: 10.1105/tpc.9.11.1963

Van Damme, D., De Rybel, B., Gudesblat, G., Demidov, D., Grunewald, W., De Smet, I., et al. (2011). *Arabidopsis* α Aurora kinases function in formative cell division plane orientation. *Plant Cell* 23, 4013–4024. doi: 10.1105/tpc.111.089565

Van Norman, J. M., Xuan, W., Beeckman, T., and Benfey, P. N. (2013). To branch or not to branch: the role of pre-patterning in lateral root formation. *Development* 140, 4301–4310. doi: 10.1242/dev.090548

Van Tieghem, P., and Douliot, H. (1886). Origine des Radicelles et des Racines Laterales Chez les Legumineuses et les Cucurbitacees. *Bull. Soc. Bot. France* 8, 494–501. doi: 10.1080/00378941.1886.10828482

Van Tieghem, P., and Douliot, H. (1888). Recherches comparatives sur l'origine des membres endogénes dans les plantes vasculaires. *Ann. Sci. Natur. Bot. Ser.* 8:660.

Vanneste, S., De Rybel, B., Beemster, G. T. S., Ljung, K., De Smet, I., Van Isterdael, G., et al. (2005). Cell cycle progression in the pericycle is not sufficient for SOLITARY ROOT/IAA14-mediated lateral root initiation in *Arabidopsis thaliana*. *Plant Cell* 17, 3035–3050. doi: 10.1105/tpc.105.035493

Vermeer, J. E., von Wangenheim, D., Barberon, M., Lee, Y., Stelzer, E. H., Maizel, A., et al. (2014). A spatial accommodation by neighboring cells is required for organ initiation in *Arabidopsis*. *Science* 343, 178–183. doi: 10.1126/science.1245871

Von Guttenberg, H. (1960). *Grundzüge der Histogenese höherer Pflanzen. I Die Angiospermen*. Berlin: Gebruder Bomtraeger.

Von Guttenberg, H. (1968). *Der Primare Bau der Angiospermenwurzel VIII/5*. Berlin: Gebruder Bomtraeger.

von Wangenheim, D., Fangerau, J., Schmitz, A., Smith, R. S., Leitte, H., Stelzer, E. H., et al. (2016). Rules and self-organizing properties of post-embryonic plant organ cell division patterns. *Curr. Biol.* 26, 439–449. doi: 10.1016/j.cub.2015.12.047

Voronin, N. S. (1957). On evolution of plant roots. 2, Evolution of the root's origin. *Bull. Moscow Soc. Nat. Biol. Ser. Russ.* 62, 35–49.

Voronin, N. S. (1964). Evolution of the primary structures in plant roots. *Uchenye Zapiski Kaluzhskogo Gosudarstvennogo Pedagogicheskogo Instituta* 13, 3–179.

Voronkina, N. (1978). Early ontogenetic stages of lateral root development and their significance for understanding of the evolution of root hystogenesis. *Bot. Z.* 63, 205–214.

Voß, U., Wilson, M. H., Kenobi, K., Gould, P. D., Robertson, F. C., Peer, W. A., et al. (2015). The circadian clock rephases during lateral root organ initiation in *Arabidopsis thaliana*. *Nat. Commun.* 6:7641. doi: 10.1038/ncomms8641

Whitewoods, C. D., Cammarata, J., Venza, Z. N., Sang, S., Crook, A. D., Aoyama, T., et al. (2018). CLAVATA was a genetic novelty for the morphological innovation of 3D growth in land plants. *Curr. Biol.* 28, 2365–2376.e5. doi: 10.1016/j.cub.2018.05.068

Wightman, F., Schneider, E. A., and Thimann, K. V. (1980). Hormonal factors controlling the initiation and development of lateral roots II. effects of exogenous growth factors on lateral root formation in pea roots. *Physiol. Plant.* 49, 304–314. doi: 10.1111/j.1399-3054.1980.tb02669.x

Willemsen, V., Bauch, M., Bennett, T., Campilho, A., Wolkenfelt, H., Xu, J., et al. (2008). The NAC domain transcription factors FEZ and SOMBRERO control the orientation of cell division plane in *Arabidopsis* root stem cells. *Dev. Cell* 15, 913–922. doi: 10.1016/j.devcel.2008.09.019

Wilmoth, J. C., Wang, S., Tiwari, S. B., Joshi, A. D., Hagen, G., Guilfoyle, T. J., et al. (2005). NPH4/ARF7 and ARF19 promote leaf expansion and auxin-induced lateral root formation. *Plant J.* 43, 118–130. doi: 10.1111/j.1365-313X.2005.02432.x

Yasutani, I., Ozawa, S., Nishida, T., Sugiyama, M., and Komamine, A. (1994). Isolation of temperature-sensitive mutant of *Arabidopsis thaliana* that are in the redifferentiation of shoots. *Plant Physiol.* 105, 815–822. doi: 10.1104/pp.105.3.815

Yoshida, S., de Reuille, P. B., Lane, B., Bassel, G. W., Prusinkiewicz, P., Smith, R. S., et al. (2014). Genetic control of plant development by overriding a geometric division rule. *Dev. Cell* 29, 75–87. doi: 10.1016/j.devcel.2014.02.002

Yu, P., Gutjahr, C., Li, C., and Hochholdinger, F. (2016). Genetic control of lateral root formation in cereals. *Trends Plant Sci.* 21, 951–961. doi: 10.1016/j.tplants.2016.07.011

Zhukovskaya, N. V., Bystrova, E. I., Dubrovsky, J. G., and Ivanov, V. B. (2018). Global analysis of an exponential model of cell proliferation for estimation of cell cycle duration in the root apical meristem of angiosperms. *Ann. Bot.* 122, 811–822. doi: 10.1093/aob/mcx216

Zimmermann, R., Sakai, H., and Hochholdinger, F. (2010). The gibberellic acid stimulated-like gene family in maize and its role in lateral root development. *Plant Physiol.* 152, 356–365. doi: 10.1104/pp.109.149054

Conflict of Interest Statement: The authors declare that the research was conducted in the absence of any commercial or financial relationships that could be construed as a potential conflict of interest.

frontiers in Plant Science

MINI REVIEW
published: 29 March 2019
doi: 10.3389/fpls.2019.00363

Plasticity of Lateral Root Branching in Maize

Peng Yu[1], Frank Hochholdinger[1] and Chunjian Li[2]**

[1]*Crop Functional Genomics, Institute of Crop Science and Resource Conservation (INRES), University of Bonn, Bonn, Germany,* [2]*Department of Plant Nutrition, College of Resources and Environmental Science, China Agricultural University, Beijing, China*

Extensively branched root systems can efficiently capture soil resources by increasing their absorbing surface in soil. Lateral roots are the roots formed from pericycle cells of other roots that can be of any type. As a consequence, lateral roots provide a higher surface to volume ratio and are important for water and nutrients acquisition. Discoveries from recent studies have started to shed light on how plant root systems respond to environmental changes in order to improve capture of soil resources. In this Mini Review, we will mainly focus on the spatial distribution of lateral roots of maize and their developmental plasticity in response to the availability of water and nutrients.

Keywords: maize, lateral root, plasticity, nitrate, water

OPEN ACCESS

Edited by:
Joseph G. Dubrovsky, National Autonomous University of Mexico, Mexico

Reviewed by:
Jonathan Lynch, Pennsylvania State University, United States
Ricardo Fabiano Hettwer Giehl, Leibniz-Institut für Pflanzengenetik und Kulturpflanzenforschung (IPK), Germany

****Correspondence:***
Peng Yu
yupeng@uni-bonn.de
Chunjian Li
lichj@cau.edu.cn

Specialty section:
This article was submitted to Plant Development and EvoDevo, a section of the journal Frontiers in Plant Science

Received: *28 November 2018*
Accepted: *08 March 2019*
Published: *29 March 2019*

Citation:
Yu P, Hochholdinger F and Li C (2019) Plasticity of Lateral Root Branching in Maize. Front. Plant Sci. 10:363. doi: 10.3389/fpls.2019.00363

INTRODUCTION

Maize forms a structurally and functionally complex root system composed of different root types (Hochholdinger et al., 2017) to efficiently acquire water and nutrients (Lynch, 2013) and to tolerate biotic and abiotic stresses (Lynch et al., 2014). Lateral roots of different orders are the most eminent root type for nutrient and water uptake from soil because of their high surface to volume ratio (Rogers and Benfey, 2015). Compared to other root types, lateral roots display the highest developmental plasticity when exposed to unfavorable environmental conditions (Yu et al., 2014a, 2016a). The formation and spatial distribution of lateral roots, e.g., lateral root branching is the most important factor governing root system architecture and soil exploration in plants (Atkinson et al., 2014). Thus, genotypes with lateral root defects display a strong inhibition of nutrient uptake and biomass production in crops (Yu et al., 2016a). The molecular mechanisms and hormonal crosstalk involved in lateral root formation and positioning has been extensively studied in the model plant *Arabidopsis thaliana* (Möller et al., 2017; Ötvös and Benková, 2017). Genetic and molecular control of lateral root initiation and formation in maize has been summarized in the recent review (Yu et al., 2016a). In this Mini Review, we provide an update on the molecular mechanisms involved in the lateral root branching response to environmental cues such as nutrients and water in maize.

ARCHITECTURAL RESPONSES OF LATERAL ROOTS TO THE AVAILABILITY OF SOIL RESOURCES

The significantly higher surface area of the lateral roots compared to their parental roots is a major determinant that is instrumental for water uptake in maize (Ahmed et al., 2016). Lateral roots are efficient in the short-distance exploitation and transport of water from soil to the vasculature in young and adult maize plants (Ahmed et al., 2016, 2018).

Genotypic differences in lateral root branching and their vertical distribution along the root system are a measure for drought tolerance in soil (Hund et al., 2009). Maize genotypes with reduced lateral root branching have been shown to be highly tolerant against drought under both greenhouse and field conditions (Zhan et al., 2015). A possible explanation for this observation is the negative correlation between lateral root branching and axial root elongation (Lynch, 2015). In maize, distinct orders of lateral roots make up the majority of total length of the root system (Lynch, 2013). Different plant species display distinct responses to nitrogen and phosphorus starvation with respect to their lateral root branching patterns, although dicot and monocot plants show similar patterns of lateral root spacing along the primary root under optimal conditions (Chen et al., 2018). The optimal branching density of lateral roots in maize has been predicted by the functional-structural model *SimRoot* based on the observation that nutrient acquisition is proportional to the spatial availability and mobility of resources in the soil profile (Postma et al., 2014). Genotypes with sparsely distributed and long lateral roots are optimal for nitrate acquisition, whereas genotypes with densely spaced and short lateral roots are optimal for phosphorus acquisition in maize (Postma et al., 2014). Recent results in maize have indicated that genotypes with higher lateral root branching density display significantly increased phosphorus acquisition under phosphorus-deficient conditions (Liu et al., 2013; Jia et al., 2018). By contrast, maize genotypes with few and long lateral roots are more competent for nitrogen uptake than genotypes with many and short lateral roots under suboptimal nitrogen concentrations in soil (Zhan and Lynch, 2015). Thus, availability of soil nutrients and water determines compensatory growth and patterning of lateral roots along the parental root axes.

LATERAL ROOT BRANCHING IN RESPONSE TO PATCHY SOIL RESOURCES

Lateral root branching patterns reflect the uneven distribution of water and nutrients in soil (Robinson, 1994). Plants adapt to heterogeneous water conditions by altering their lateral root branching in contact with water by using "hydropatterning" response (Bao et al., 2014; Robbins and Dinneny, 2018). High-resolution non-invasive microcomputed tomography imaging has revealed that the formation and patterning of lateral roots is highly responsive to local water availability in *A. thaliana* and crop species (Bao et al., 2014; Robbins and Dinneny, 2015; Orman-Ligeza et al., 2018). Xerobranching, describing the repression of lateral root branching when root tips are not in contact with wet soil, suggests that abscisic acid is involved as key signal regulating branches of lateral roots in their local microenvironment (Orman-Ligeza et al., 2018). For hydropatterning, high availability of water results in the induction of auxin biosynthesis and transport, independent of endogenous abscisic acid signals (Bao et al., 2014; **Figure 1A**). A recent study with *A. thaliana* demonstrated that hydropatterning is dependent on SUMO-mediated posttranslational regulation of auxin signaling pathway (ARF7/IAA3) controlling lateral root branching pattern in response to water availability (Orosa-Puente et al., 2018; **Figure 1A**). ARF7 transcription factor induces asymmetric expression of its target gene LATERAL ORGAN BOUNDARIES (LOB) domain 16 (LBD16) in lateral root founder cells (Orosa-Puente et al., 2018; **Figure 1A**). Future work will be necessary to understand how the water and nutrient signals are integrated to regulate lateral root branching in response to local water/nutrients availability (Giehl and von Wirén, 2018). Through a combination of empirical and mathematical-modeling approaches in maize, it has been shown a central role of tissue growth and developmental competence, which is necessary to sustain the normal hydropatterning, although the molecular mechanism is unknown in crop plants (Robbins and Dinneny, 2018). This result implies that the water requirement for fast developing tissue is an important contribution process on water perception and developmental reprogramming during the postembryonic root development.

Lateral root formation in response to systemic and local nitrate signaling has been recently summarized in *A. thaliana* (Sun et al., 2017). A series of experiments have demonstrated that local nitrate supply can considerably stimulate lateral root production also in crops, such as maize (Wang et al., 2004; Guo et al., 2005; Liu et al., 2008, 2010), rice (Huang et al., 2015), barley (Drew et al., 1973), and wheat (Hackett, 1972). Hydroponics allows local nutrient application under well-controlled conditions, which can also avoid influences of other factors such as physical properties of soil and microbes. Local application of nutrients in hydroponics includes two strategies: one is the vertical split system that the middle part of the root was supplied with high nutrients along the longitudinal axis (Drew et al., 1973); another strategy is horizontal split system that the axial roots are separated into different compartments or rhizoslides with diverse nutrient levels (Yu et al., 2014b; Dina in't Zandt et al., 2015). The complex nature of the root system of maize plants makes split-root experiments challenging. Most common ways to carry out such experiments is by placing the primary root into one compartment and the other root types are placed into the other one (Yu et al., 2014b, 2015, 2016b) or the crown roots are equally separated and cultured in different compartments after removing the primary and seminal roots (Wang et al., 2004; Guo et al., 2005; Liu et al., 2008, 2010). Vertical hydroponics experiments by Drew and his colleagues demonstrated that lateral root formation in barley depends on the dose and type of nutrient application (reviewed in Yu et al., 2014a). Both length and density of lateral roots are significantly induced by local high nitrate (control: 0.01 mM; high nitrate 1 mM) in barley seedlings (Drew et al., 1973). By contrast, only elongation of the lateral roots on primary root is induced in maize seedlings split supplied by local high nitrate (control: 0.5 mM; high nitrate 4 mM) in 7-day-old maize seedlings grown in the left-right hydroponic system (Yu et al., 2014b). This is consistent with the lateral root formation from the crown roots of maize,

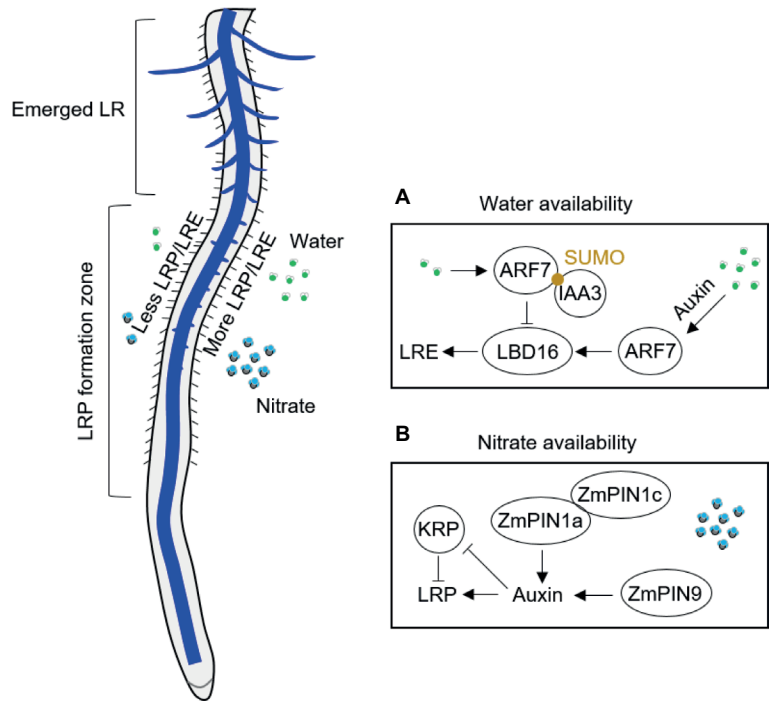

FIGURE 1 | Schematic illustration of lateral root branching response to availability of water in *A. thaliana* **(A)** and of nitrate in maize **(B)**. ARF, auxin response factor; IAA3, Aux/IAA3 (Aux/indole-3-acetic acid protein 3); KRP, Kip-related protein; LBD, LATERAL ORGAN BOUNDARIES (LOB) domain; LR, lateral root; LRE, lateral root emergence; LRP, lateral root primordia; PIN, PIN-Formed; SUMO, small ubiquitin-like modifier.

that localized nitrate mainly induced lateral root formation but little effects on the density of lateral roots in both hydroponics (Liu et al., 2010) and rhizoslides (Dina in't Zandt et al., 2015). This is further validated by a microarray analysis of pericycle cells indicating common mechanisms for lateral root initiation in maize primary and crown roots (Jansen et al., 2013). Different responses on lateral root branching between barley and maize can be explained by species-specific responses to nitrate but also by different developmental stages of root types surveyed in these plant species. Thus, lateral root specific responses to local nitrate depend on the developmental stage when certain root type is formed. For instance, shoot-borne roots specifically initiated during silking form more lateral roots in response to localized nitrate supply than other root types including the shoot-borne roots formed before silking (Yu et al., 2015, 2016b). This divergent finding can be explained by the higher shoot demand for nutrients during and after silking (Yu et al., 2014b) but also the possibility of specific hormone signaling from the reproductive process (Yu et al., 2016b). For example, basipetal auxin transport is facilitated by ZmPIN1a and ZmPIN1c in response to local nitrate supply (Yu et al., 2016b; **Figure 1B**). Moreover, monocot-specific *PIN9* gene in phloem pole cells of shoot-borne roots at silking modulates auxin efflux to pericycle cells and subsequent cell cycle activation by alleviating the inhibition of Kip-related proteins (KRP) coding genes in maize (Yu et al., 2016b; **Figure 1B**). Moreover, CPP-like (cysteine-rich polycomb-like) transcription factors have been found specifically enriched in brace roots of maize, which may play an important role in development of reproductive organs and control of cell division in plants (Yu et al., 2016b). It would be interesting to compare the responses of different root types to local nitrogen supply at the flowering stage in order to answer whether in maize this divergent response is root type specific and/or developmental stage dependent.

A study with *A. thaliana* mutants with reduced number of lateral roots indicate that complex architecture and branching pattern of lateral roots are mainly required for the acquisition of immobile resources, such as phosphate, whereas mobile ions like nitrate can be effectively taken up even by restricted root systems (Fitter et al., 2002). This raises the hypothesis that root proliferation in nutrient-rich patches could be more important for the enhanced capture of immobile than mobile ions. In fact, field studies have suggested that enhanced root proliferation in nutrient-rich patches of ammonium and phosphate during seedling stage and adult development is essential for improving phosphate uptake and ultimately grain yield (Jing et al., 2010; Li et al., 2012, 2016; Ma et al., 2013). One possible explanation for this observation could be indirect effects of solubilization of mineral phosphate by rhizosphere acidification using ammonium fertilization. Alternatively, fine lateral root proliferation substantially increases exudate secretion to the rhizosphere, which can be used as the carbon source for beneficial interactions of the microbiome at the root-soil interface.

ROOT TYPE-SPECIFIC BRANCHING PATTERNS

Recent experiments highlight root type-specific transcriptomic, anatomical, and physiological differences in maize (Tai et al., 2015; Ahmed et al., 2018). Distinct root types of maize show diverse branching responses to nitrate and also host different fungal taxa in their axial and lateral roots (Yu et al., 2016b, 2018). A novel phenotyping approach demonstrates distinct growth rates of three types of lateral roots contribution to the random patterning of lateral root formation in pearl millet and maize (Passot et al., 2018). This phenomenon raises the question whether lateral root types with divergent lengths show distinct competences of their corresponding pericycle cells for dividing. To further study this question, diverse inbred lines with natural variation for lateral root patterning and spacing could be studied in maize.

CONCLUSIONS AND PERSPECTIVES

Lateral root branching of maize plants grown in soil is root type specific and depends on hormonal crosstalk and signal transduction based on local sensing of water and nutrients. Nevertheless, these molecular processes have not been understood in full detail at the cellular level. Therefore, systemic cell-type-specific analyses in different root types will be instrumental to clarify the identity of pericycle and endodermis cells in maize in response to local water and nutrient supply (Kortz et al., 2019). In particular, root type has to be considered when studying the mechanism of lateral root formation as maize has a unique architectural pattern in comparison to the other crop species (Burton et al., 2013; Tai et al., 2015; Yu et al., 2016a). Signal transduction induced by water and nutrients at the root-soil interface needs to be explored in large genetic populations on the molecular level and by advanced *in situ* imaging (van Dusschoten et al., 2016; Tardieu et al., 2017). To this end, understanding the reprogramming of lateral root formation and architectural plasticity in response to water and nutrient availability in the context of yield acquisition and resource use efficiency can be relevant for rational breeding approaches.

AUTHOR CONTRIBUTIONS

PY, FH and CL contributed to the writing of this minireview.

FUNDING

Root research in CL's laboratory is supported by the National Natural Science Foundation of China (no. 31272232). FH is funded by the Deutsche Forschungsgemeinschaft (DFG) grant no. HO2249/12-1 and the Bundesministerium für Bildung und Forschung (BMBF) grant no. 031-B0195C. PY's work on lateral roots in maize is funded by DFG grant no. YU 272/1-1.

REFERENCES

Ahmed, M. A., Zarebanadkouki, M., Kaestner, A., and Carminati, A. (2016). Measurements of water uptake of maize roots: the key function of lateral roots. *Plant Soil* 398, 59–77. doi: 10.1007/s11104-015-2639-6

Ahmed, M. A., Zarebanadkouki, M., Meunier, F., Javaux, M., Kaestner, A., and Carminati, A. (2018). Root type matters: measurement of water uptake by seminal, crown, and lateral roots in maize. *J. Exp. Bot.* 69, 1199–1206. doi: 10.1093/jxb/erx439

Atkinson, J. A., Rasmussen, A., Traini, R., Voß, U., Sturrock, C. J., Mooney, S. J., et al. (2014). Branching out in roots: uncovering form, function and regulation. *Plant Physiol.* 178, 538–550. doi: 10.1104/pp.114.245423

Bao, Y., Aggarwal, P., Robbins, N. E., Sturrock, C. J., Thompson, M. C., Tan, H. Q., et al. (2014). Plant roots use a patterning mechanism to position lateral root branches toward available water. *Proc. Natl. Acad. Sci. USA* 111, 9319–9324. doi: 10.1073/pnas.1400966111

Burton, A. L., Brown, K. M., and Lynch, J. P. (2013). Phenotypic diversity of root anatomical and architectural traits in *Zea* species. *Crop Sci.* 53, 1042–1055. doi: 10.2135/cropsci2012.07.0440

Chen, Y., Xie, Y., Song, C., Zheng, L., Rong, X., Jia, L., et al. (2018). A comparison of lateral root patterning among dicot and monocot plants. *Plant Sci.* 274, 201–211. doi: 10.1016/j.plantsci.2018.05.018

Dina in't Zandt, D., Le Marie, C., Kirchgessner, N., Visser, E. J., and Hund, A. (2015). High-resolution quantification of root dynamics in split-nutrient rhizoslides reveals rapid and strong proliferation of maize roots in response to local high nitrogen. *J. Exp. Bot.* 66, 5507–5517. doi: 10.1093/jxb/erv307

Drew, M. C., Saker, L. R., and Ashley, T. W. (1973). Nutrient supply and the growth of the seminal root system in barley: I. The effect of nitrate concentration on the growth of axes and laterals. *J. Exp. Bot.* 24, 1189–1202. doi: 10.1093/jxb/24.6.1189

Fitter, A., Williamson, L., Linkohr, B., and Leyser, O. (2002). Root system architecture determines fitness in an Arabidopsis mutant in competition for immobile phosphate ions but not for nitrate ions. *Proc. R. Soc. Lond. B Biol. Sci.* 269, 2017–2022. doi: 10.1098/rspb.2002.2120

Giehl, R. F., and von Wirén, N. (2018). Hydropatterning-how roots test the waters. *Science* 362, 1358–1359. doi: 10.1126/science.aav9375

Guo, Y., Chen, F., Zhang, F., and Mi, G. (2005). Auxin transport from shoot to root is involved in the response of lateral root growth to localized supply of nitrate in maize. *Plant Sci.* 169, 894–900. doi: 10.1016/j.plantsci.2005.06.007

Hackett, C. (1972). A method of applying nutrients locally to roots under controlled conditions, and some morphological effects of locally applied nitrate on the branching of wheat roots. *Aust. J. Biol. Sci.* 25, 1169–1180. doi: 10.1071/BI9721169

Hochholdinger, F., Yu, P., and Marcon, C. (2017). Genetic control of root system development in maize. *Trends Plant Sci.* 23, 79–88. doi: 10.1016/j.tplants.2017.10.004

Huang, S., Chen, S., Liang, Z., Zhang, C., Yan, M., Chen, J., et al. (2015). Knockdown of the partner protein OsNAR2.1 for high-affinity nitrate transport represses lateral root formation in a nitrate-dependent manner. *Sci. Rep.* 5:18192. doi: 10.1038/srep18192

Hund, A., Ruta, N., and Liedgens, M. (2009). Rooting depth and water use efficiency of tropical maize inbred lines, differing in drought tolerance. *Plant Soil* 318, 311–325. doi: 10.1007/s11104-008-9843-6

Jansen, L., Hollunder, J., Roberts, I., Forestan, C., Fonteyne, P., Van Quickenborne, C., et al. (2013). Comparative transcriptomics as a tool for the identification of root branching genes in maize. *Plant Biotechnol. J.* 11, 1092–1102. doi: 10.1111/pbi.12104

Jia, X., Liu, P., and Lynch, J. P. (2018). Greater lateral root branching density in maize improves phosphorus acquisition from low phosphorus soil. *J. Exp. Bot.* 69, 4961–4970. doi: 10.1093/jxb/ery252

Jing, J., Rui, Y., Zhang, F., Rengel, Z., and Shen, J. (2010). Localized application of phosphorus and ammonium improves growth of maize seedlings by stimulating root proliferation and rhizosphere acidification. *Field Crops Res.* 119, 355–364. doi: 10.1016/j.fcr.2012.04.009

Kortz, A., Hochholdinger, F., and Yu, P. (2019). Cell type-specific transcriptomics of lateral root formation and plasticity. *Front. Plant Sci.* 10:21. doi: 10.3389/fpls.2019.00021

Li, H., Wang, X., Rengel, Z., Ma, Q., Zhang, F., and Shen, J. (2016). Root over-production in heterogeneous nutrient environment has no negative effects on *Zea mays* shoot growth in the field. *Plant Soil* 409, 405–417. doi: 10.1007/s11104

Li, H., Zhang, F., and Shen, J. (2012). Contribution of root proliferation in nutrient-rich soil patches to nutrient uptake and growth of maize. *Pedosphere* 22, 776–784. doi: 10.1016/S1002-0160(12)60063-0

Liu, J., An, X., Cheng, L., Chen, F., Bao, J., Yuan, L., et al. (2010). Auxin transport in maize roots in response to localized nitrate supply. *Ann. Bot.* 106, 1019–1026. doi: 10.1093/aob/mcq202

Liu, J., Han, L., Chen, F., Bao, J., Zhang, F., and Mi, G. (2008). Microarray analysis reveals early responsive genes possibly involved in localized nitrate stimulation of lateral root development in maize (*Zea mays* L.). *Plant Sci.* 175, 272–282. doi: 10.1016/j.plantsci.2008.04.009

Liu, Y., Donner, E., Lombi, E., Li, R. Y., Wu, Z. C., Zhao, F. J., et al. (2013). Assessing the contributions of lateral roots to element uptake in rice using an auxin-related lateral root mutant. *Plant Soil* 372, 125–136. doi: 10.1007/s11104-012-1582-z

Lynch, J. P. (2013). Steep, cheap and deep: an ideotype to optimize water and N acquisition by maize root systems. *Ann. Bot.* 112, 347–357. doi: 10.1093/aob/mcs293

Lynch, J. P. (2015). Root phenes that reduce the metabolic costs of soil exploration: opportunities for 21st century agriculture. *Plant Cell Environ.* 38, 1775–1784. doi: 10.1111/pce.12451

Lynch, J. P., Chimungu, J. G., and Brown, K. M. (2014). Root anatomical phenes associated with water acquisition from drying soil: targets for crop improvement. *J. Exp. Bot.* 65, 6155–6166. doi: 10.1093/jxb/eru162

Ma, Q., Zhang, F., Rengel, Z., and Shen, J. (2013). Localized application of NH_4^+-N plus P at the seedling and later growth stages enhances nutrient uptake and maize yield by inducing lateral root proliferation. *Plant Soil* 372, 65–80. doi: 10.1007/s11104-013-1735-8

Möller, B. K., Xuan, W., and Beeckman, T. (2017). Dynamic control of lateral root positioning. *Curr. Opin. Plant Biol.* 35, 1–7. doi: 10.1016/j.pbi.2016.09.001

Orman-Ligeza, B., Morris, E. C., Parizot, B., Lavigne, T., Babé, A., Ligeza, A., et al. (2018). The xerobranching response represses lateral root formation when roots are not in contact with water. *Curr. Biol.* 28, 3165–3173. doi: 10.1016/j.cub.2018.07.074

Orosa-Puente, B., Leftley, N., von Wangenheim, D., Banda, J., Srivastava, A. K., Hill, K., et al. (2018). Root branching toward water involves posttranslational modification of transcription factor ARF7. *Science* 362, 1407–1410. doi: 10.1126/science.aau3956

Ötvös, K., and Benková, E. (2017). Spatiotemporal mechanisms of root branching. *Curr. Opin. Genet. Dev.* 45, 82–89. doi: 10.1016/j.gde.2017.03.010

Passot, S., Moreno-Ortega, B., Moukouanga, D., Balsera, C., Guyomarc'h, S., Lucas, M., et al. (2018). A new phenotyping pipeline reveals three types of lateral roots and a random branching pattern in two cereals. *Plant Physiol.* 177, 896–910. doi: 10.1104/pp.17.01648

Postma, J. A., Dathe, A., and Lynch, J. P. (2014). The optimal lateral root branching density for maize depends on nitrogen and phosphorus availability. *Plant Physiol.* 166, 590–602. doi: 10.1104/pp.113.233916

Robbins, N. E., and Dinneny, J. R. (2015). The divining root: moisture-driven responses of roots at the micro-and macro-scale. *J. Exp. Bot.* 66, 2145–2154. doi: 10.1093/jxb/eru496

Robbins, N. E., and Dinneny, J. R. (2018). Growth is required for perception of water availability to pattern root branches in plants. *Proc. Natl. Acad. Sci. USA* 115, 822–831. doi: 10.1073/pnas.1710709115

Robinson, D. (1994). The responses of plants to non-uniform supplies of nutrients. *New Phytol.* 127, 635–674. doi: 10.1111/j.1469-8137.1994.tb02969.x

Rogers, E. D., and Benfey, P. N. (2015). Regulation of plant root system architecture: implications for crop advancement. *Curr. Opin. Biotechnol.* 32, 93–98. doi: 10.1016/j.copbio.2014.11.015

Sun, C. H., Yu, J. Q., and Hu, D. G. (2017). Nitrate: a crucial signal during lateral roots development. *Front. Plant Sci.* 8:485. doi: 10.3389/fpls.2017.00485

Tai, H., Lu, X., Opitz, N., Marcon, C., Paschold, A., Lithio, A., et al. (2015). Transcriptomic and anatomical complexity of primary, seminal, and crown roots highlight root type-specific functional diversity in maize (*Zea mays* L.). *J. Exp. Bot.* 67, 1123–1135. doi: 10.1093/jxb/erv513

Tardieu, F., Cabrera-Bosquet, L., Pridmore, T., and Bennett, M. (2017). Plant phenomics, from sensors to knowledge. *Curr. Biol.* 27, 770–783. doi: 10.1016/j.cub.2017.05.055

van Dusschoten, D., Metzner, R., Kochs, J., Postma, J. A., Pflugfelder, D., Buehler, J., et al. (2016). Quantitative 3D analysis of plant roots growing in soil using magnetic resonance imaging. *Plant Physiol.* 170, 1176–1188. doi: 10.1104/pp.15.01388

Wang, Y., Mi, G., Chen, F., Zhang, J., and Zhang, F. (2004). Response of root morphology to nitrate supply and its contribution to nitrogen accumulation in maize. *J. Plant Nutr.* 27, 2189–2202. doi: 10.1081/PLN-200034683

Yu, P., Baldauf, J., Lithio, A., Marcon, C., Nettleton, D., Li, C., et al. (2016b). Root type specific reprogramming of maize pericycle transcriptomes by local high nitrate results in disparate lateral root branching patterns. *Plant Physiol.* 170, 1783–1798. doi: 10.1104/pp.15.01885

Yu, P., Eggert, K., von Wirén, N., Li, C., and Hochholdinger, F. (2015). Cell-type specific gene expression analyses by RNA-Seq reveal local high nitrate triggered lateral root initiation in shoot-borne roots of maize by modulating auxin-related cell cycle-regulation. *Plant Physiol.* 169, 690–704. doi: 10.1104/pp.15.00888

Yu, P., Gutjahr, C., Li, C., and Hochholdinger, F. (2016a). Genetic control of lateral root formation in cereals. *Trends Plant Sci.* 21, 951–961. doi: 10.1016/j.tplants.2016.07.011

Yu, P., Li, X., Yuan, L., and Li, C. (2014b). A novel morphological response of maize (*Zea mays*) adult roots to heterogeneous nitrate supply revealed by a split-root experiment. *Physiol. Plant.* 150, 133–144. doi: 10.1111/ppl.12075

Yu, P., Wang, C., Baldauf, J. A., Tai, H., Gutjahr, C., Hochholdinger, F., et al. (2018). Root type and soil phosphate determine the taxonomic landscape of colonizing fungi and the transcriptome of field-grown maize roots. *New Phytol.* 217, 1240–1253. doi: 10.1111/nph.14893

Yu, P., White, P., Hochholdinger, F., and Li, C. (2014a). Phenotypic plasticity of the maize root system in response to heterogeneous nitrogen availability. *Planta* 240, 667–678. doi: 10.1007/s00425-014-2150-y

Zhan, A., and Lynch, J. P. (2015). Reduced frequency of lateral root branching improves N capture from low-N soils in maize. *J. Exp. Bot.* 66, 2055–2065. doi: 10.1093/jxb/erv007

Zhan, A., Schneider, H., and Lynch, J. (2015). Reduced lateral root branching density improves drought tolerance in maize. *Plant Physiol.* 168, 1603–1615. doi: 10.1104/pp.15.00187

Conflict of Interest Statement: The authors declare that the research was conducted in the absence of any commercial or financial relationships that could be construed as a potential conflict of interest.

frontiers in Plant Science

ORIGINAL RESEARCH
published: 10 April 2019
doi: 10.3389/fpls.2019.00365

Lateral Root Initiation in the Parental Root Meristem of Cucurbits: Old Players in a New Position

Alexey S. Kiryushkin[1], Elena L. Ilina[1], Vera A. Puchkova[1], Elizaveta D. Guseva[1], Katharina Pawlowski[2] and Kirill N. Demchenko[1,3]**

[1] Laboratory of Cellular and Molecular Mechanisms of Plant Development, Komarov Botanical Institute, Russian Academy of Sciences, Saint Petersburg, Russia, [2] Department of Ecology, Environment and Plant Sciences, Stockholm University, Stockholm, Sweden, [3] Laboratory of Molecular and Cellular Biology, All-Russia Research Institute for Agricultural Microbiology, Saint Petersburg, Russia

While in most higher plants, including the model system *Arabidopsis thaliana*, the formation of lateral root primordia is induced in the elongation zone of the parental root, in seven plant families, including Cucurbitaceae, an alternative root branching mechanism is established such that lateral roots are initiated directly in the apical meristem of the parental root. In Arabidopsis, the transcription factor GATA23 and MEMBRANE-ASSOCIATED KINASE REGULATOR4 (MAKR4) are involved in the gene regulatory network of lateral root initiation. Among all marker genes examined, these are the earliest known marker genes up-regulated by auxin during lateral root initiation. In this study, putative functional orthologs of Arabidopsis *GATA23* and *MAKR4* were identified in cucumber (*Cucumis sativus*) and squash (*Cucurbita pepo*). Both cucurbits contained 26 genes encoding GATA family transcription factors and only one *MAKR4* gene. Phylogenetic and transcriptional analysis of up-regulation by auxin led to the identification of *GATA23* putative functional orthologs in Cucurbitaceae – *CpGATA24* and *CsGATA24*. In squash, *CpMAKR4* was up-regulated by naphthylacetic acid (NAA) and, similar to *MAKR4* in Arabidopsis, indole-3-butyric acid (IBA). A detailed analysis of the expression pattern of *CpGATA24* and *CpMAKR4* in squash roots from founder cell specification until emergence of lateral root primordia was carried out using promoter-fluorescent reporter gene fusions and confocal microscopy. Their expression was induced in the protoxylem, and then expanded to founder cells in the pericycle. Thus, while the overall expression pattern of these genes was significantly different from that in Arabidopsis, in founder cells their expression was induced in the same order as in Arabidopsis. Altogether, these findings suggest that in Cucurbitaceae the putative functional orthologs of *GATA23* and *MAKR4* might play a role in founder cell specification and primordium positioning during lateral root initiation. The role of the protoxylem in auxin transport as a trigger of founder cells specification and lateral root initiation is discussed.

Keywords: cucumber, squash, GATA23, lateral root initiation, MAKR4, pericycle, root meristem, xylem

OPEN ACCESS

Edited by:
Marta Joan Laskowski, Oberlin College, United States

Reviewed by:
Guy Wachsmann, Duke University, United States
Hans Motte, VIB-UGent Center for Plant Systems Biology, Belgium

****Correspondence:***
Kirill N. Demchenko
demchenko@binran.ru
Katharina Pawlowski
katharina.pawlowski@su.se

Specialty section:
This article was submitted to Plant Development and EvoDevo, a section of the journal Frontiers in Plant Science

Received: *06 December 2018*
Accepted: *08 March 2019*
Published: *10 April 2019*

Citation:
Kiryushkin AS, Ilina EL, Puchkova VA, Guseva ED, Pawlowski K and Demchenko KN (2019) Lateral Root Initiation in the Parental Root Meristem of Cucurbits: Old Players in a New Position. Front. Plant Sci. 10:365. doi: 10.3389/fpls.2019.00365

INTRODUCTION

During a plant's lifetime, the development of the root system is associated with the initiation and development of lateral root primordia. In seed plants lateral roots are initiated in the pericycle, but in ferns, in the endodermis [reviewed by Charlton (1991)]. However, the radial location of the initiation site, as well as the position along the longitudinal axis of the parental root, can vary considerably (Mallory et al., 1970; Charlton, 1991; Demchenko and Demchenko, 2001; Hou et al., 2004; Ilina et al., 2018). The ancestral form of root branching is dichotomous, as shown by fossils of the ancestors of current ferns and Lycopodiophyta (Hetherington and Dolan, 2017, 2018, 2019; Liu and Xu, 2018), while in extant angiosperms, root branching is monopodial [reviewed by Motte and Beeckman (2018)]. Here, lateral roots emerge from a main axis formed by the parental roots. Thus, one of the basic questions in root evolution is how dichotomous and monopodial branching evolved.

Over the past several decades, most developmental biological studies have focused on model plant species, in the case of dicotyledonous herbs on *Arabidopsis thaliana* (hereafter Arabidopsis). Yet, model species do not encompass all types of morphogenetic mechanisms. In most higher plants, the formation of lateral root primordia is induced in the elongation zone of the parental root by a well-studied mechanism [reviewed by Du and Scheres (2018)]. However, in seven families of Angiosperms, including Cucurbitaceae, an alternative root branching mechanism is established in that lateral roots are initiated directly in the apical meristem of the parental root (Ilina et al., 2018). The study of alternative mechanisms can help us understand the evolution of root branching.

The gene regulatory network involved in lateral root initiation is well known for Arabidopsis. Key genes encoding the transcription factor GATA23, MEMBRANE-ASSOCIATED KINASE REGULATOR4 (MAKR4), and RAPID ALKALINIZATION FACTOR-like34 (RALFL34) are the earliest known markers, the transcription of which is induced during lateral root initiation in Arabidopsis (De Rybel et al., 2010; Xuan et al., 2015; Murphy et al., 2016). During founder cell specification, auxin acts through auxin regulatory components and their target genes *GATA23* and *MAKR4* (De Rybel et al., 2010; Xuan et al., 2015).

GATA transcription factors are a group of regulators that contain the highly conserved type IV zinc finger motif in the form $CX_2CX_{17-20}CX_2$. These factors were named by their ability to bind the consensus DNA sequence (A/T)GATA(A/G). They were originally identified and characterized in animals and fungi, and are typically encoded by multi-gene families (Reyes et al., 2004). The transcription factor GATA23, which belongs to the B-class of GATA-family proteins and is specific for Brassicaceae (Behringer et al., 2014; Behringer and Schwechheimer, 2015), was found using meta-analysis of transcriptomic databases related to lateral root initiation events (De Rybel et al., 2010). In Arabidopsis, *GATA23* is specifically expressed in the primed pericycle cells prior to the first asymmetric divisions (De Rybel et al., 2010).

Priming of founder cells is a rhythmically repetitive event. Founder cell specification depends on ARF6–ARF8-mediated signaling with *GATA23* as a target (Lavenus et al., 2013). Expression levels of *GATA23* are upregulated by naphthylacetic acid (NAA) in an IAA28- and SLR/IAA14-dependent manner, indicating that auxin is directly involved in the regulation of *GATA23* expression. At the cellular level, the transcription factor GATA23 acts cell-autonomously: its activity commences in the two sister xylem pole pericycle cells before the first asymmetric division (De Rybel et al., 2010). The stages of lateral root development were defined by Malamy and Benfey (1997). Using a *pGATA23::NLS-GFP* and a *pGATA23::GATA23-GFP* fusion construct, *GATA23* expression could be detected in the pericycle up to stage II (De Rybel et al., 2010). Arabidopsis RNAi lines with 70% reduction in the expression levels of *GATA23* displayed strongly reduced numbers of lateral root primordia in stages I and II, while overexpression of *GATA23* led to an increase in the number of non-emerged primordia (De Rybel et al., 2010).

A search for proteins showing amino acid sequence similarity with the C-terminal end of the BRASSINOSTEROID KINASE INSENSITIVE 1 (BKI1) protein resulted in the identification of a new family of Arabidopsis proteins, which was named MEMBRANE-ASSOCIATED KINASE REGULATOR (MAKR) (Jaillais et al., 2011). Studies on auxin metabolism showed that one member of this family is involved in root branching. Auxin derived from the root cap due to the conversion of indole-3-butyric acid (IBA) to indole-3-acetic acid (IAA) plays an important role in the regulation of root branching (De Rybel et al., 2012). Comparisons of the transcriptome of an Arabidopsis *ibr1ibr3ibr10* triple mutant, which lacks the enzymes of the IBA-to-IAA conversion pathway, with that of the wild type after IBA treatment led to the identification of a novel IBA-regulated component of root patterning, MEMBRANE-ASSOCIATED KINASE REGULATOR 4 (MAKR4) (Xuan et al., 2015).

MAKR4 promoter activity was found to be initially induced in the protoxylem cells within the root apical meristem, and transcription was upregulated after IAA- or IBA treatment (Xuan et al., 2015). In the Arabidopsis *ibr1ibr3ibr10* triple mutant, *MAKR4* expression levels were strongly reduced compared to the wild type even after treatment with IBA. At the cellular level, MAKR4 located to the plasma membrane and nuclei (Xuan et al., 2015; Simon et al., 2016). Roots carrying estradiol-inducible artificial microRNA constructs targeting *MAKR4* had significantly lower numbers of lateral root primordia and emerged lateral roots than wild type roots, while numbers of prebranch sites resembled those of wild type roots. Therefore, MAKR4 has been suggested to be involved in converting prebranch sites in the pericycle into a regular spacing of lateral roots (Xuan et al., 2015).

Little is known about the other members of the MAKR protein family. MAKR1, like BKI1, may interact with the BRASSINOSTEROID INSENSITIVE 1 (BRI1) receptor (Jaillais et al., 2011; Jiang et al., 2015). Unlike BKI1, a negative regulator of brassinosteroid signaling, MAKR5 is a positive effector of CLAVATA3/EMBRYO SURROUNDING REGION 45 (CLE45) signaling through the BARELY ANY MERISTEM 3 (BAM3)

receptor (Kang and Hardtke, 2016). Arabidopsis *MAKR6* is one of 72 targets of the KANADI1 transcription factor, which regulates the adaxial-abaxial polarity of leaves (Xie et al., 2015). Expression of the *MAKR6* gene was upregulated in roots after 6 h of treatment with 1 μM exogenous IAA (Omelyanchuk et al., 2017).

Previously, we have shown in detail the sequence of events involved in the initiation and development of lateral root primordia in squash (*Cucurbita pepo*, Cucurbitaceae) (Ilina et al., 2018). In squash, the first symmetric anticlinal division was preceded by the formation of cellular auxin response maxima in two adjacent cells in files of the pericycle in the parental root apical meristem at a distance of 250–350 μm from the initial cells, among proliferating cells of the parental root meristem. Cellular auxin response maxima appeared at the xylem pole in pairs of sister cells (founder cells) of the three inner pericycle files, two files of the outer pericycle, and endodermis files. These observations are similar to those for Arabidopsis, where the simultaneous activation of pairs of cells took place in three files of pericycle cells at the xylem pole (Casimiro et al., 2003). Thus, the first divisions initiating lateral root formation, regardless of the place of the initiation, were anticlinal divisions in a pair of sister cells. Further development of squash lateral root primordia was associated with the involvement of three to four layers of the inner cortex. Cortex cells formed an auxin response maximum and contributed to primordium development after periclinal divisions in the pericycle and endodermis.

While in squash, exogenous application of auxin transport inhibitors led to a reduction of the number of lateral roots, exogenous auxins neither led to an increase in the total number of lateral roots nor did they affect the Dubrovsky LRI index (Ilina et al., 2018). Nevertheless, DR5 promoter mediated visualization of auxin response maxima at the earliest stages of primordium formation demonstrated a key role for endogenous auxin in lateral root initiation in squash (Ilina et al., 2018).

As already noted by Xuan et al. (2015) for Arabidopsis, so far the exact role of auxin during lateral root pre-patterning and founder cell specification remains elusive. Similarly, the genetic mechanisms leading to lateral root initiation, including founder cell specification, in Cucurbitaceae are poorly understood. In this study, we focused on two genes expressed during the initiation of lateral root primordia. In Arabidopsis, *GATA23* and *MAKR4* play a key role in specifying pericycle cells to become founder cells prior to the first formative divisions during lateral root initiation. We report the identification and expression patterns of the putative functional orthologs of *GATA23* and *MAKR4* in Cucurbitaceae.

MATERIALS AND METHODS

Plant Material and Bacterial Strains

Squash (*Cucurbita pepo* L. var. *giromontina*) cv. Beloplodniy and cucumber (*Cucumis sativus* L.) cv. Kustovoy (Sortsemovosch, Saint Petersburg, Russia) were used in this study. *Agrobacterium rhizogenes* strain R1000-mediated transformation of squash seedlings was performed as described previously (Ilina et al., 2012). *Escherichia coli* strain XL-1 Blue was used for molecular cloning.

Molecular Cloning

A set of genetic constructs harboring promoter–reporter fusions was developed via multisite Gateway technology using Gateway LR Clonase II Plus (Thermo Fisher Scientific, Waltham, MA, United States). To create the 242_pKGW-RR-MGW-pCpGATA24::mNeonGreen-H2B construct (*pCpGATA24::mNeonGreen-H2B*), containing the human histone *H2B* ORF (Nam and Benezra, 2009) and the 242_pKGW-RR-MGW-pCpMAKR4::eGFP-H2B construct (*pCpMAKR4::eGFP-H2B*), a series of entry vectors was generated. A list of plasmids and vectors used for entry vector construction is given in **Supplementary Table S1**. Constructions of binary vectors are given in **Supplementary Table S2**.

A set of promoter-containing entry vectors was developed containing 3036 bp of the promoter region of the *C. pepo GATA24* gene identified in this study (from −3062 to −27 before the predicted translational start site) and 2683 bp of the promoter region of the *C. pepo MAKR4* gene identified in this study (from −2688 to −6 before the predicted translational start site). Promoters were PCR-amplified using squash genomic DNA as a template, and cloned in the 369_pENTRattL4attR1_BSAI vector (Thermo Fisher Scientific) using *Sma*I restriction sites. Sequences of mNeonGreen-H2B-C6 (Shaner et al., 2013) and eGFP-H2B fusions were PCR amplified from commercial plasmid templates (**Supplementary Table S1**) and cloned in the pUC18-entry8 vector (Hornung et al., 2005) using *Kpn*I and *Not*I restriction sites. The *A. thaliana Actin2* gene terminator (TermAct) (Engler et al., 2014) was PCR amplified from a commercial plasmid and cloned in the 373_pENTRattR2attL3 vector (Thermo Fisher Scientific) via a Gateway BP Clonase reaction (Thermo Fisher Scientific). The resulting 373_pENTRattR2attL3-TermAct vector was used as a donor of TermAct in all further constructions.

All fusions in all constructs were verified by PCR amplification of fragments and sequencing of the products. All primers sequences are given in **Supplementary Table S3**. All binary vectors were introduced into *A. rhizogenes* R1000 cells by electroporation (Ilina et al., 2012).

Plant Transformation

Agrobacterium rhizogenes-mediated plant transformation was carried out as described previously (Ilina et al., 2012) with several modifications. Surface sterilized seeds of squash were germinated in sterile vermiculite moistened with d H_2O in Magenta^{TM} GA-7 vessels (Merck, Kenilworth, NJ, United States). Plants were grown in an MLR-352H incubator (Panasonic, Osaka, Japan) under controlled conditions: 16/8 h light/darkness, light intensity 600 μM/(m^2·sec), humidity 96%, at 25/22°C (day/night) for seed germination and growth of transformants and at 21°C for co-cultivation of plants and agrobacteria. The first putative transformed roots were harvested approximately 2 weeks after the inoculation of squash seedlings. Further on, transformed roots 5–10 cm in length were harvested three to five times with 5-day intervals from a single transformation.

Treatments With Exogenous Auxins

Indole-3-acetic acid (IAA, 0.3, 1, or 5 μM), naphthylacetic acid (NAA, 10 μM), and indole-3-butyric acid (IBA, 5 μM) were used as exogenous auxins. Four-day-old wild type seedlings with 5–7 cm long roots were incubated in aerated 1/4 strength Hoagland's medium supplemented with the respective phytohormones for 6 h at 25°C during the light period. The auxins concentrations and period of exposition used in this study were selected based on data reported previously (Paponov et al., 2008; De Rybel et al., 2010; Xuan et al., 2015). The seedlings were located on a floating opaque raft, and vessels were protected by aluminum foil from light. After the treatment, root tips (1 cm from the root cap) were flash-frozen in liquid nitrogen. Frozen plant material was stored at −80°C. Each experiment included at least 25–30 seedlings and was repeated at least five times independently.

Quantitative Real-Time PCR Assays

Total RNA was extracted from frozen plant material using the RNeasy Plant Mini Kit (QIAGEN, Hilden, Germany). To assess the integrity of the total RNA, an aliquot of each RNA sample was run on an 1% agarose gel following by staining with ethidium bromide. The quantity of each RNA sample was measured using a Qubit 2.0 fluorometer (Thermo Fisher Scientific) using the Qubit RNA BR Assay Kit.

Total RNA (1 μg) was used for reverse transcription with the Maxima First Strand cDNA synthesis kit for RT-qPCR with dsDNase (Thermo Fisher Scientific). Reverse transcription conditions were as follows: dsDNase treatment at 37°C for 10 min; addition of reverse transcription components to the same tube; incubation for 10 min at 25°C followed by 15 min at 50°C; the reaction was terminated by incubation at 85°C for 5 min. 0.4 μl of cDNA from a non-diluted sample (total volume 20 μl) was used for each qPCR reaction.

The RT-qPCR analysis was performed using an Eco Real-Time PCR system (Illumina, San Diego, CA, United States). Each qPCR reaction was carried out in a total volume of 10 μl. For *GATA* genes, detection based on SYBR Green I dye chemistry was used (Maxima SYBR Green/ROX qPCR master mix (2X), Thermo Fisher Scientific). PCR conditions were as follows: 1 cycle of 95°C for 10 min; 40 cycles of 95°C for 15 s, 52°C (for cucumber) or 60°C (for squash) for 30 s, and 72°C for 30 s; followed by reheating of PCR products at 95°C and then by starting a gradual temperature decrease from 95 to 55°C with a step of −0.3°C per s. For the squash *MAKR4* gene, detection based on TaqMan chemistry was used (Maxima Probe/ROX qPCR master mix (2X), Thermo Fisher Scientific). PCR conditions were as follows: 1 cycle of 95°C for 10 min; 40 cycles of 95°C for 15 s, 60°C for 30 s, and 72°C for 30 s. A TaqMan probe carrying carboxyfluorescein (FAM) as a fluorophore and Black Hole Quencher1 (BHQ1) as a quencher was used. All primers and probes used for qPCR are listed in **Supplementary Table S4**. Primers and probes were designed using the Vector NTI Advance v11.0 software (Thermo Fisher Scientific). Purified PCR primers were purchased from Evrogen (Moscow, Russia). TaqMan probes were synthetized by BioBeagle (Saint Petersburg, Russia). Each experiment was carried out with at least five biological replicates and three technical replicates. The specificity of the amplified qPCR products was verified by sequencing.

Quantification cycles (Cq) were determined using the Eco Real-Time PCR System software v4.1.11.2 (Illumina). Relative transcript levels were calculated using the $2^{-\Delta\Delta CT}$ method (Livak and Schmittgen, 2001). PCR efficiency for all primer pairs was between 93 and 98%. Elongation factor *EF1a* was chosen as reference gene according to literature data about the stability of reference gene expression in cucumber (Wan et al., 2010) and squash (Obrero et al., 2011).

Plots for qPCR data were prepared using the R software default code for the boxplot function (R Core Team, 2017). Statistical analysis of the data was performed with Wilcoxon's test from the base R package. Differences with P-values <0.05 were considered statistically significant. RT-qPCR analysis of the relative expression levels of *GATA* genes was performed with five biological replicates. For *MAKR4*, this analysis was performed using four to eight biological replicates.

Phylogeny and Bioinformatics

Arabidopsis GATA and MAKR proteins from TAIR[1] (Berardini et al., 2015) were used as query to find amino acid sequences of *C. sativus* (cucumber, Chinese long v. 2 and Gy14) (Li et al., 2011; Yang et al., 2012), *Cucumis melo* (melon) (Garcia-Mas et al., 2012), *Citrullus lanatus* (watermelon, 97103) (Guo et al., 2013), *Cucurbita moshata*, and *Cucurbita maxima* (pumpkin) (Sun et al., 2017), *Lagenaria siceraria* (bottle gourd) (Wu et al., 2017), and *C. pepo* (squash) (Montero-Pau et al., 2018) in the Cucurbit Genomics Database[2]. For the cucumber GATA and MAKR proteins, searches in other databases were also used: Phytozome[3] (Goodstein et al., 2012), NCBI[4] and PlantTFDB v 4.0[5] (Jin et al., 2017). The search for the *GATA1* gene of *Momordica charantia* (bitter gourd) was conducted in the bitter gourd transcriptome available from NCBI (Urasaki et al., 2017). All alignments were performed using Clustal Omega at default settings[6]. Phylogenetic trees were constructed in MEGA7.0 (Kumar et al., 2016). The neighbor-joining method (Saitou and Nei, 1987) of phylogenetic reconstruction was used with the Poisson model (Zuckerkandl and Pauling, 1965) with rate uniformity among sites. The maximum likelihood method of phylogenetic reconstruction was used with the Whelan and Goldman + Freq. model (Whelan and Goldman, 2001) with the rate of variation across sites (+G parameter = 3.7181) (Yang, 1994) and with the proportion of invariable sites (+I) (Shoemaker and Fitch, 1989). This model was chosen from the list of models with the lowest Bayesian Information Criterion (BIC) scores. Models with the lowest BIC scores are considered to best describe the substitution pattern. The maximum likelihood tree inference options were used at default settings. Bootstrap tests with 1000 replicates were used.

[1] www.arabidopsis.org
[2] cucurbitgenomics.org
[3] phytozome.jgi.doe.gov
[4] www.ncbi.nlm.nih.gov
[5] planttfdb.cbi.pku.edu.cn
[6] www.ebi.ac.uk/Tools/msa/clustalo

Fluorescence Protein Reporter Assay

For the localization of eGFP-H2B and mNeonGreen-H2B reporters, 7–10 mm long tips of transgenic hairy roots of squash were vacuum infiltrated with a fixative (McLean and Nakane, 1974) modified by Brian Lin (Tufts University, Boston, MA, United States): 1% paraformaldehyde, 5% DMSO, 0.1 M L-lysine, 0.01 M sodium-m-periodate in 0.02 M phosphate buffer (PB) pH 7.2 for eGFP and pH 8.0 for mNeonGreen, fixed for 1 h at RT and rinsed with 0.02 M PB pH 8.0. The root tips were sectioned with a vibrating-blade microtome as described previously (Ilina et al., 2018). Nuclei were counterstained for 30–50 min with 0.3 μg/ml DAPI. Longitudinal or cross sections (65 μm) of root tips were mounted in consecutive order onto microscope slides in a non-hardening antifade mountant CFMR2 (Citifluor, London, United Kingdom) for eGFP or in PB pH 8.0 supplemented with 0.1 M L-lysine for mNeonGreen under coverslips.

Microscopy

All microscopy procedures, three-dimensional reconstructions, animations, and maximum intensity projections were performed as described previously (Kitaeva et al., 2016; Ilina et al., 2018). Examination and imaging of fluorescent protein patterns were performed under a LSM 780 upright confocal laser scanning microscope (ZEISS, Germany) equipped with a Plan-Apochromat 20×/0.8 numerical aperture DICII objective and a Plan-Apochromat 40×/1.3 numerical aperture DICIII oil immersion objective. Samples were imaged with a 488 nm excitation laser line and an emission spectrum of 490–525 nm for both eGFP or mNeonGreen. For DAPI-stained nuclei, the 405 nm excitation laser line and an emission spectrum of 412–464 nm were used. A multitrack (line by line) scan mode was applied. The ZEN 2.3pro software (ZEISS) was used for image processing. At least 14 roots were used for each reporter assay. The distance from the initial cell to the first cell in file labeled with eGFP or NeonGreen in nuclei was measured in the ZEN software (ZEISS) after acquisition. Statistical analysis and graphical visualization were performed in SigmaPlot 12.5 (Systat Software, United States) using one-way analysis of variance (ANOVA) on ranks (Kruskal–Wallis).

RESULTS

Identification of the Putative Ortholog of Arabidopsis GATA23 in *Cucumis sativus* and *Cucurbita pepo* by Phylogenetic Analysis

Using BlastP searches in Phytozome, NCBI, Cucurbit Genomics Database, and PlantTFDB, 26 members of the GATA family of transcription factors were found both in cucumber (*C. sativus*) and squash (*C. pepo*). The 26 cucumber GATA transcription factors were named CsGATA1 to CsGATA26, according to their chromosomal positions, as was done for the *GATA* gene family of apple and soybean (Zhang et al., 2015; Chen et al., 2017), while squash GATAs were named according to their sequence similarity with cucumber GATA proteins (**Supplementary Table S5**). Phylogenetic analysis of GATA protein DNA-binding domains from cucumber and squash showed that, like in Arabidopsis (Reyes et al., 2004), cucurbit GATA transcription factors can be divided into four classes (**Figure 1**). The majority of *GATA* genes from cucumber and squash belong to classes A (11 genes per species) and B (eight genes). From 29 *GATA* genes in Arabidopsis, 14 and ten belong to the classes A and B, respectively. Two genes from cucumber and squash, respectively, belong to class C, compared to three genes in Arabidopsis. The number of genes from class D is equal both for Arabidopsis and cucurbits (four genes per species).

Like their homologs in Arabidopsis (Reyes et al., 2004), all squash and cucumber GATA proteins have only one DNA-binding domain (zinc-finger domain) with the core structure $CX_{2/4}CX_{18/20}CX_2C$ (**Supplementary Figures S1**, **S2**). Members of class A, B, and C have the structure $CX_2CX_{18}CX_2C$ (**Supplementary Figure S1**) with one exception: in cucurbits GATA16 protein (Class B), like in Arabidopsis GATA29 (Class B), the sequence of the zinc-finger domain is $CX_4CX_{18}CX_2C$ (**Supplementary Figure S2**). GATA proteins from class D show the domain structure $CX_2CX_{20}CX_2C$ (**Supplementary Figure S1**).

Since GATA23 belongs to class B (Behringer and Schwechheimer, 2015), the amino acid sequences of cucurbit GATAs of this class were analyzed in detail. B-GATAs with a HAN-domain and an LLM-domain have been described previously for Arabidopsis (Behringer et al., 2014; Behringer and Schwechheimer, 2015). Class B of cucurbit GATAs was divided into proteins with a HAN-domain and proteins with an LLM-domain (**Supplementary Figures S2**, **S3**). It was previously reported that cucumber contains two GATA genes encoding proteins with a complete HAN-domain, named HAN1 and HAN2 (Ding et al., 2015). Squash HAN-domain GATAs were given the same names according to their level of identity to cucumber GATA proteins. Cucurbit GATA16 proteins, like Arabidopsis GATA29, have a degenerate HAN-domain (**Supplementary Figure S2**).

Cucumber and squash have five GATA proteins with a complete LLM-domain: four of them have short amino acid sequences (GATA9, GATA17, GATA19, and GATA24), while one is a long protein (GATA2) (**Supplementary Figure S3**). For GATA1, which also belongs to the short proteins, the structure of the LLM-domain differs between cucurbit genera (**Supplementary Figure S3**). In the genus *Cucurbita*, it has the complete domain with the leucine-leucine-methionine sequence, as was also described for short Arabidopsis GATAs with a complete LLM-domain (Behringer and Schwechheimer, 2015). However, in *C. melo*, *C. lanatus*, *L. siceraria*, and *M. charantia*, the first leucine of the LLM-domain is substituted by serine. Interestingly, GATA1 from cucumber shows two substitutions in the LLM-domain: the first leucine is substituted by serine, like in melon, watermelon, calabash and bitter gourd, and methionine by isoleucine. Amino acid substitutions in cucumber GATA1 are similar to the substitutions in Arabidopsis GATA23 with regard to their positions. The degenerate LLM-domain from Arabidopsis GATA23 also contains substitutions of the first leucine and the methionine. However, the amino acid residues

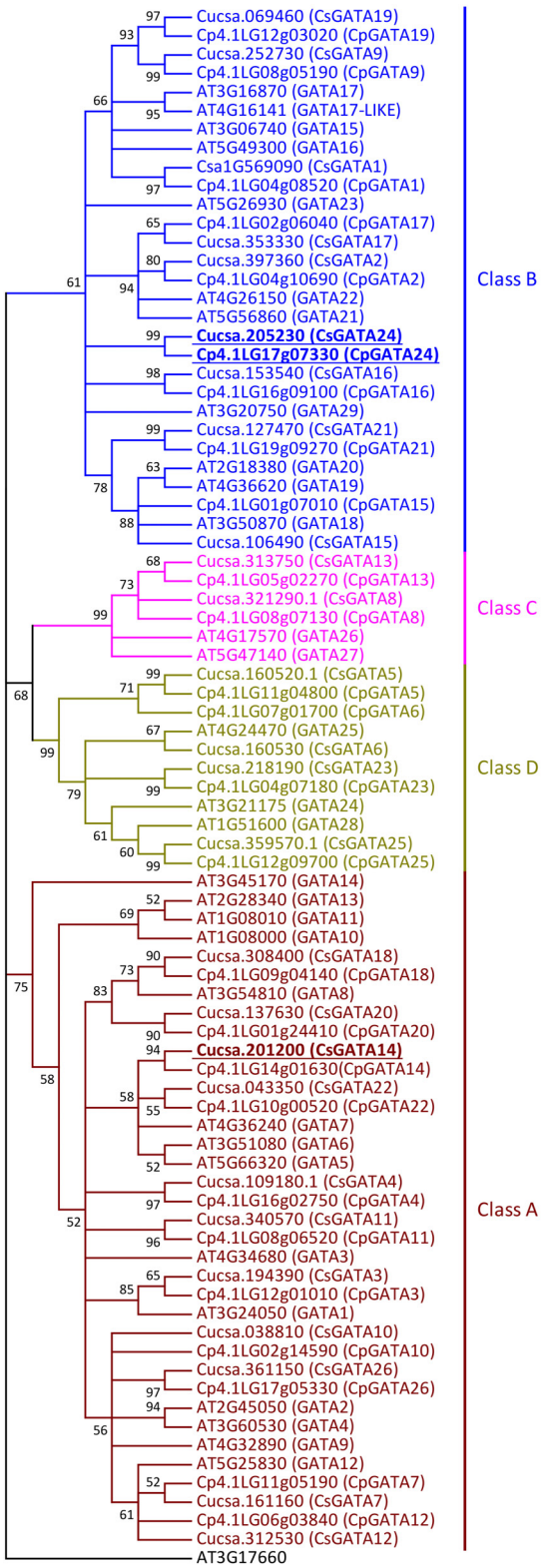

FIGURE 1 | Neighbor-joining phylogenetic tree of the DNA-binding regions of GATA proteins from *Arabidopsis thaliana*, *Cucumis sativus*, and *Cucurbita pepo*. The phylogenetic tree was constructed based on a Clustal

(Continued)

FIGURE 1 | Continued

Omega alignment. Evolutionary analyses were carried out in MEGA7 software by the Neighbor-Joining method with 1000 bootstrap replicates using the Poisson model with rate uniformity among sites. All ambiguous positions were removed for each sequence pair. Bootstrap values are indicated by each node (≥50%). The amino acid sequence of the zinc finger domain from AT3G17660 protein was used as outgroup. The four different classes of GATA proteins are represented in different colors. Putative orthologs of *At*GATA23 in *C. sativus* and *C. pepo* are indicated (underlined bold). Gene ID prefixes: AT, *A. thaliana*; Cucsa, *C. sativus* Gy14 gene IDs on Phytozome; Csa, *C. sativus* Chinese Long v.2 gene IDs on Cucurbit Genomics Database; Cp, *C. pepo*.

in these positions are different from those in cucumber GATA1: in Arabidopsis GATA23, the first leucine in the LLM-domain is substituted by cysteine and the methionine by leucine. Altogether, based on the phylogenetic analysis (**Figure 1**) and on the alignment of the GATA-domain and LLM-domain sequences in class B GATA proteins (**Supplementary Figure S3**), GATA1, GATA9, GATA17, GATA19, and GATA24 could represent putative orthologs of Arabidopsis GATA23.

Cucurbit *GATA* Expression Levels Change in Response to Exogenous Auxin

The expression of Arabidopsis *GATA23* is upregulated by the auxin analog NAA at a concentration of 10 μM, leading to a maximal level of expression after 6 h (De Rybel et al., 2010). To identify orthologs of Arabidopsis *GATA23*, roots of cucumber and squash seedlings were treated with exogenous NAA, which can pass the plant plasma membrane by diffusion, while IAA requires uptake transporters (Marchant et al., 1999; Michniewicz et al., 2007). Expression levels of all members of the GATA family were compared in mock- and NAA-treated roots using reverse transcription – quantitative polymerase chain reaction (RT-qPCR).

In cucumber and squash, the genes *GATA2*, *GATA16*, and *GATA17* were not expressed in roots, either with or without NAA treatment (**Figures 2**, **3**). Most of the 26 *GATA* genes of both cucurbits were expressed in roots, but did not show significant changes in their expression levels in roots in response to exogenous NAA. This group included 15 cucumber *GATA* genes (*CsGATA3*, *CsGATA5*, *CsGATA6*, *CsGATA8*, *CsGATA11*, *CsGATA12*, *CsGATA13*, *CsGATA14*, *CsGATA15*, *CsGATA18*, *CsGATA19*, *CsGATA21*, *CsGATA22*, *CsGATA23*, and *CsGATA25*; **Figure 2**) and 16 squash genes (*CpGATA1*, *CpGATA3*, *CpGATA4*, *CpGATA5*, *CpGATA6*, *CpGATA8*, *CpGATA10*, *CpGATA11*, *CpGATA12*, *CpGATA13*, *CpGATA14*, *CpGATA15*, *CpGATA19*, *CpGATA21*, *CpGATA23*, and *CpGATA25*; **Figure 3**). For seven cucumber *GATA* genes (*CsGATA1*, *CsGATA4*, *CsGATA7*, *CsGATA9*, *CsGATA10*, *CsGATA20*, and *CsGATA26*; **Figure 2**) and six genes from squash (*CpGATA7*, *CpGATA9*, *CpGATA18*, *CpGATA20*, *CpGATA22*, and *CpGATA26*; **Figure 3**), NAA treatment led to a significant reduction of expression levels in roots. Only three *GATA* genes could be identified for which the expression levels increased in response to treatment with NAA: two from cucumber (*CsGATA14* and *CsGATA24*; **Figure 2**) and one from squash (*CpGATA24*; **Figure 3**). Expression levels of *CsGATA14* increased 2–3 fold. Transcript levels of *CsGATA24*

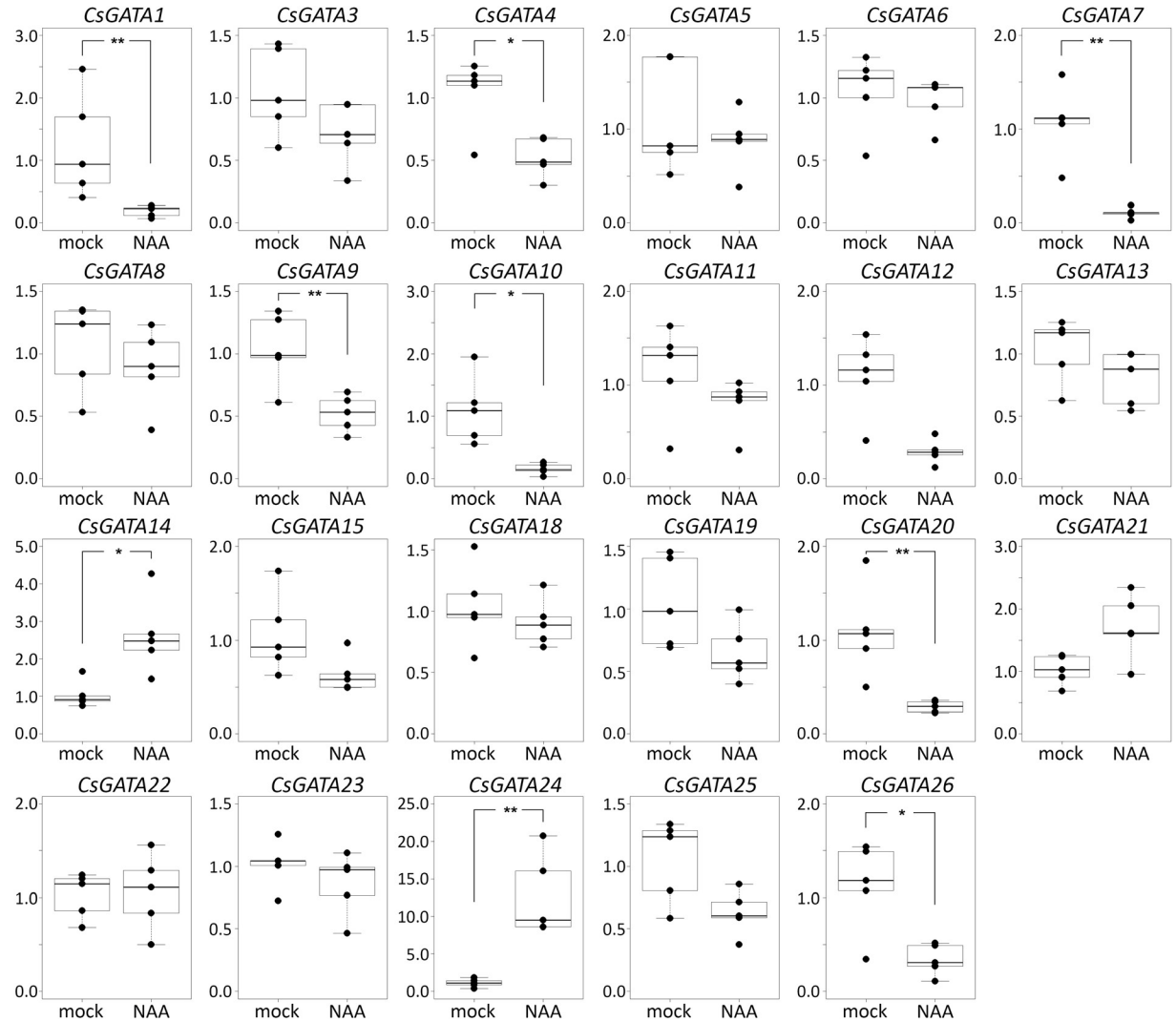

FIGURE 2 | Relative transcript levels of *Cucumis sativus GATA* genes in response to NAA treatment. Four-day-old *C. sativus* seedlings were incubated with 10 μM NAA for 6 h. Reverse transcription-qPCR analysis was performed using RNA isolated from the first centimeter of the primary roots. Graphs were drawn using R software default code for boxplot function (Wilcoxon test, $*p < 0.05$, $**p < 0.01$). The *y* axis indicates the relative transcript level ($2^{-\Delta\Delta CT}$ method).

were 6–20 fold higher in NAA-treated roots than in mock-treated roots, while relative expression levels of *CpGATA24* increased 2–6 fold.

Class B of cucurbit *GATA* genes consists of nine members (*GATA1*, *GATA2*, *GATA9*, *GATA15*, *GATA16*, *GATA17*, *GATA19*, *GATA21*, and *GATA24*; **Figure 1**). The expression of only one of these, *GATA24*, was upregulated in response to NAA in both cucumber and squash. The cucumber *GATA14* gene, the expression of which, like that of *GATA24,* was upregulated in response to NAA, belongs to class A. As mentioned above, cucurbits contain one class B *GATA* gene encoding a protein with a degenerate LLM domain, *GATA1*; the expression of this one was downregulated in response to NAA in cucumber, and not regulated in response to NAA in squash.

In summary, Arabidopsis *GATA23* belongs to class B, and the corresponding gene is upregulated by auxin. Only one cucurbit GATA shares these features, namely *GATA24* (gene ID in Phytozome Cucsa.205230 and in the Cucurbit Genomics Database Cp4.1LG17g07330; **Supplementary Table S5**). Phylogenetic (**Figure 1**) as well as expression analysis (**Figures 2**, **3**) indicate that the *GATA24* genes of cucumber and squash represent putative functional orthologs of Arabidopsis *GATA23*.

Identification of the Putative Ortholog of Arabidopsis MAKR4 in *Cucumis sativus* and *Cucurbita pepo* by Phylogenetic Analysis

The cucumber proteome contains 13 amino acid sequences of MEMBRANE-ASSOCIATED KINASE REGULATOR-like (MAKR) proteins (**Figure 4**). Six of these 13 proteins were

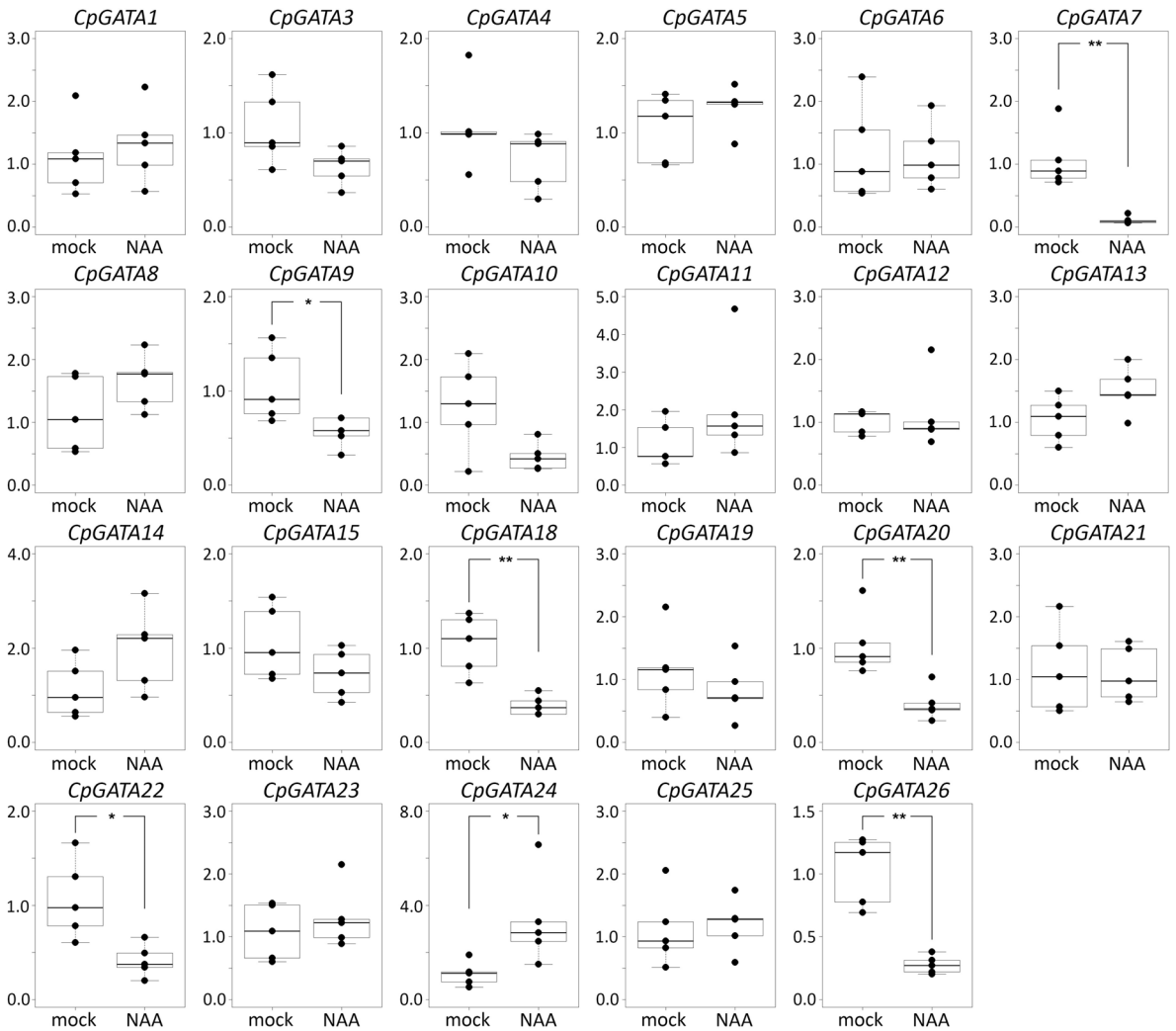

FIGURE 3 | Relative transcript levels of *Cucurbita pepo GATA* genes in response to NAA treatment. Four-day-old *C. pepo* seedlings were incubated with 10 μM NAA for 6 h. RT-qPCR was performed using RNA isolated from the first centimeter of the primary roots. Graphs were drawn using R software default code for the boxplot function (Wilcoxon test, $*p < 0.05$, $**p < 0.01$). The y axis indicates the relative transcript level ($2^{-\Delta\Delta CT}$ method).

annotated in Phytozome as members of MAKR family (gene IDs Cucsa.012770, Cucsa.165730, Cucsa.185600, Cucsa.201740, Cucsa.201790, and Cucsa.254170), while two of them were annotated as BKI1, a member of the MAKR protein family (gene IDs Cucsa.123690 and Cucsa.232770). Three truncated MAKR amino acid sequences, including two annotated as MAKRs, were found in Phytozome (gene IDs Cucsa.012770, Cucsa.108280, and Cucsa.254170); therefore, in this study they were replaced by the full-size protein sequences available from the Cucurbit Genomics Database (gene IDs Csa3G363150, Csa3G184590, and Csa3G149330). The watermelon (*C. lanatus*) genome encodes ten MAKR-like proteins (**Figure 4**). Two of these proteins were annotated in the Cucurbit Genomics Database as BKI1 (gene IDs Cla020683 and Cla022558), while eight of them were not annotated at all as MAKR-like proteins.

Phylogenetic analysis based on the MAKR protein family from Arabidopsis suggests that there is only one MAKR4 protein in cucurbits. The putative MAKR4 protein from squash (gene ID from the Cucurbit Genomics Database Cp4.1LG01g04380) showed 57% amino acid similarity and 45.3% identity with AtMAKR4 and therefore was assumed to be a putative ortholog (**Figure 4**). The *CpMAKR4* cDNA was cloned, sequenced, and deposited in NCBI GenBank under the accession number KY352352.

CpMAKR4 Expression Levels Differ in Their Response to Different Types of Auxin

To confirm that *CpMAKR4* represents a putative functional ortholog of Arabidopsis *MAKR4,* expression levels of *CpMAKR4* were analyzed in squash roots after treatment with different auxins (**Figure 5**). Arabidopsis *MAKR4* expression has been reported to be upregulated in response to IAA and IBA (Xuan

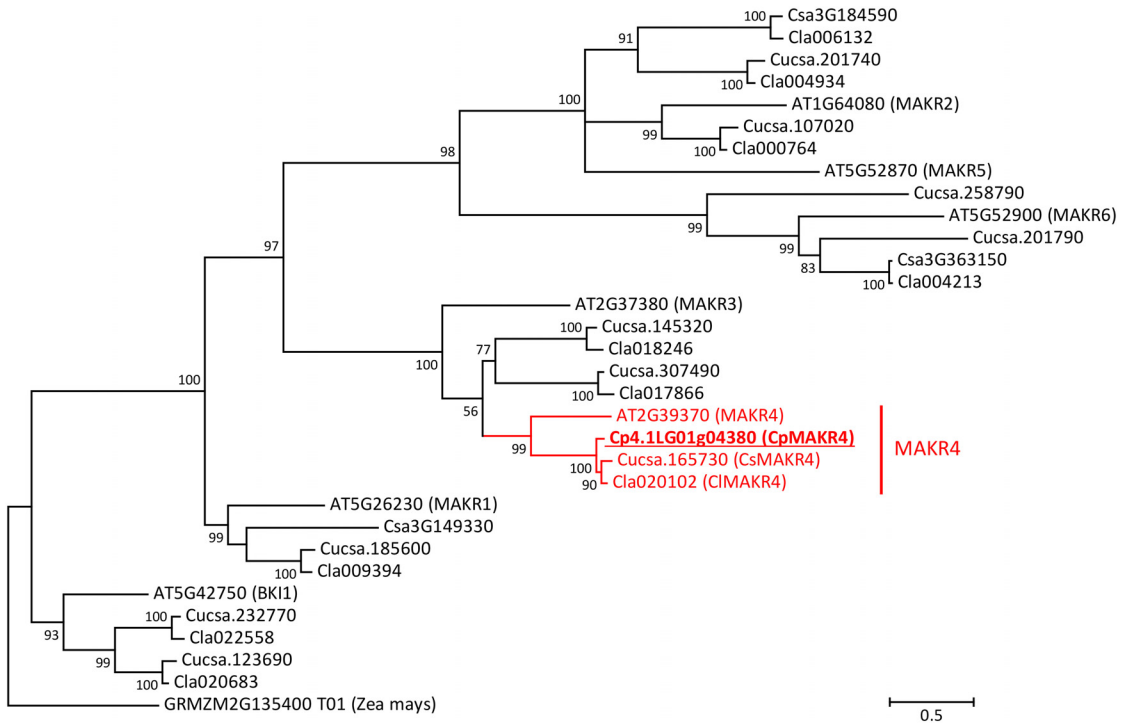

FIGURE 4 | Phylogenetic tree of MAKR proteins from *A. thaliana*, *C. sativus*, *Citrullus lanatus*, and *C. pepo*. Amino acid sequence of putative ortholog of MAKR4 in *C. pepo* was used together with all known sequences of MAKR proteins from *A. thaliana*, *C. sativus*, and *C. lanatus*. The phylogenetic tree was constructed based on a Clustal Omega alignment. Evolutionary analyses were carried out in MEGA7 software using the Maximum Likelihood method with 1000 bootstrap replicates based on the gamma distributed (+G) Whelan and Goldman + Freq. model with invariant sites (+I). The amino acid sequence of the BKI1 protein (GRMZM2G135400_T01) from *Zea mays* was used as outgroup. The putative ortholog of *At*MAKR4 in *C. pepo* is indicated (underlined bold). Scale bar denotes 0.5 amino acid substitutions per site. Gene ID prefixes: AT, *A. thaliana*; Cucsa, *C. sativus* Gy14 on Phytozome; Csa, *C. sativus* Chinese Long v.2 on Cucurbit Genomics Database; Cla, *C. lanatus*; Cp, *C. pepo*.

et al., 2015). RT-qPCR analysis showed that transcript levels of *CpMAKR4* did not change in response to treatment with 0.3, 1, or 5 μM IAA for 6 h. However, expression levels increased 3–4 fold in response to treatment with 5 μM IBA, and 3–5 fold in response to 10 μM NAA.

CpGATA24 and *CpMAKR4* Expression Patterns in *Cucurbita pepo* Root

Transgenic squash hairy roots harboring promoter fusion constructs *CpGATA24::mNeonGreen-H2B* or *CpMAKR4::eGFP-H2B* were used to investigate the expression patterns and involvement in lateral root primordium initiation of the corresponding genes. To visualize gene expression patterns, a series of longitudinal (**Figures 6**, **8**, **9**) and cross (**Figures 7**, **10**) root sections were analyzed.

Expression of *CpGATA24* Is Induced in the Protoxylem Before Founder Cell Specification in the Pericycle

Expression of *CpGATA24* began in the protoxylem at an average distance of 265 μm from the initial cell (**Figures 6A,B**, **7A** and **Supplementary Figure S4**). This event occurred 50–60 μm before the periclinal T-division in a file of protoxylem cells (**Figures 6B**, **7A**). Such a division leads to the formation of two xylem files. The outer file is usually designated as protoxylem, and the inner one as peripheral metaxylem (**Figures 6B**, **7A**). Throughout a file, *CpGATA24* expression was maintained in all cells of the protoxylem and peripheral metaxylem (**Figures 6**, **7**, **8**) until a point at about a distance of 1500 μm from the initial cells where terminal differentiation of the protoxylem cells commenced. In the pericycle, expression of *CpGATA24* began at a distance of approx. 300 μm from the initial cells, before the first anticlinal divisions (**Figures 6B–D**). This occurred in the cells of the inner pericycle layer approximately opposite to the T-division in the protoxylem. Expression of *CpGATA24* in the cells of the inner pericycle layer was triggered simultaneously in several (6–8) cells (**Figures 6C,D**). In the outer layer of the pericycle, expression was induced a bit later and only in the putative founder cells (**Figures 6C,D**, **7C**). Upon completion of the first anticlinal formative divisions in the pericycle, expression of *CpGATA24* was extended to the endodermal cells involved in the formation of the lateral root primordium (**Figures 6C,D**, **7B,C**). When the first periclinal divisions took place in a primordium (**Figures 6F,G**), *CpGATA24* expression was extended also to the files of stelar parenchyma surrounding the peripheral metaxylem (**Figures 7B–D**). The pattern of *CpGATA24* expression in the cells of the inner

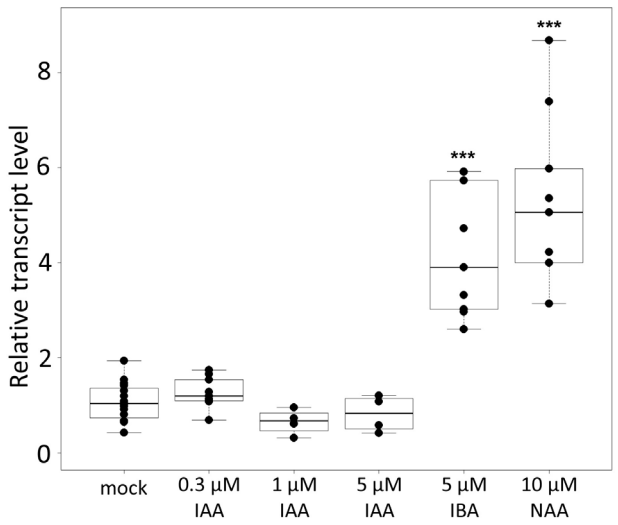

FIGURE 5 | Relative transcript levels of *Cucurbita pepo MAKR4* in response to treatment with exogenous phytohormones. Four-day-old *C. pepo* seedlings were incubated for 6 h with 0.3, 1, 5 µM IAA, 5 µM IBA, or 10 µM NAA, respectively. RT-qPCR analysis was performed using RNA isolated from the first centimeter of the primary roots. Graphs were drawn using R software default code for the boxplot function (Wilcoxon test, $***p < 0.001$). The *y* axis indicates the relative transcript level ($2^{-\Delta\Delta CT}$ method).

pericycle layer was also maintained between the developing primordia until a distance of approx. 600 µm from the initial (**Figures 6E–G**). Cells of 2–3 inner cortical layers opposite the primordium also expressed *CpGATA24* (**Figures 7D**, **8A**). At a distance of approx. 1 mm from the initial cells, expression of *CpGATA24* was maintained in all primordium cells (**Figure 8A**). *CpGATA24* expression was maintained in all stelar parenchyma cells adjacent to the protoxylem until a distance of 1.5–2 mm from the initial. Then, the number of cells expressing *CpGATA24* in primordia decreased gradually (**Figure 8B**). The last *CpGATA24* expressing cells were found in the zone of initial cells of lateral root primordia at a distance of approx. 2–2.5 mm from the root tip (**Figure 8C**).

Thus, the expression of *CpGATA24* is directly correlated to the determination of the site of lateral root initiation at a xylem pole. Protoxylem cells appear to play a crucial role in the positioning of the primordium. *CpGATA24* expression extends from the protoxylem file to the founder cells in the pericycle, immediately after the completion of the last periclinal formative division in the protoxylem.

Expression of *CpMAKR4* Is Induced in the Protoxylem Before the First Formative Division in Pericycle

CpMAKR4 expression began in the protoxylem at an average distance of 330 µm from the initial cell (**Figures 9A–D**, **10A** and **Supplementary Figure S4**). This occurred just before the periclinal T-division in the protoxylem, which leads to a split of this cell file to the protoxylem and peripheral metaxylem files (**Figures 9B,D**, **10A,B**). *CpMAKR4* expression was maintained in the protoxylem and peripheral metaxylem until a distance of approx. 2–2.5 mm (**Figure 9F**). In the inner layer of the pericycle, the expression of this gene was triggered a bit later than in protoxylem (**Figures 9B–D**). In **Figure 9D**, the site of lateral root primordium initiation is shown with an asterisk: one of the two sister cells of the inner pericycle layer has already divided, and the second (basal) is in the metaphase. All three cells show activity of the *CpMAKR4* promoter. The cells of the outer layer of the pericycle, already involved in the initiation of the lateral root primordium, have begun to express *CpMAKR4* in pairs of cells immediately before the first formative anticlinal divisions (**Figures 9B,C**). As the primordium developed, proceeding to involve the endodermis and several layers of the inner cortex, *CpMAKR4* expression extended to all cells of the primordium (**Figures 9E,F**, **10C,D**). The decrease in its expression level in primordium cells was complete at a distance of 3 mm from the root tip.

Thus, *CpMAKR4* expression begins in the protoxylem, shortly before the first formative divisions in the pericycle, and is likely to be connected with the determination of the site of lateral root initiation at a xylem pole. *CpMAKR4* expression is triggered directly before the anticlinal divisions of the pericycle cells, which initiate the formation of a lateral root primordium. The expression of this gene is maintained for the entire subsequent development of the primordium, before it emerges from the parental root.

DISCUSSION

The first problem we sought to address in this study was the identification of orthologs of Arabidopsis GATA23 and MAKR4 in cucurbits. The number of *GATA* genes identified in cucumber and squash genomes was 26 for each species, which is less than in the Arabidopsis genome (Reyes et al., 2004). Therefore, it could be assumed that some gene family members in Arabidopsis did not have an ortholog in cucumber and/or squash. Using phylogenetic analysis, cucurbit GATA transcription factors were divided into four classes according to their DNA-binding domain structure like in Arabidopsis and rice (Reyes et al., 2004). All squash and cucumber GATA proteins have the $CX_{2/4}CX_{18/20}CX_2C$ structure of the zinc-finger domain, which is typical for GATA proteins from the entire plant kingdom (Reyes et al., 2004). Phylogenetic analysis did not allow the unambiguous identification of the ortholog of Arabidopsis GATA23 in cucurbits. Another criterion had to be added, namely that the expression of a putative functional ortholog of Arabidopsis *GATA23* had to be upregulated in roots by exogenous application of auxin (De Rybel et al., 2010). Only one gene from cucurbits, *GATA24*, fulfilled the phylogenetic and transcriptional criteria and was therefore proposed as the putative functional ortholog of Arabidopsis *GATA23*.

Phylogenetic search for a putative ortholog of Arabidopsis *MAKR4* in the squash genome was easy in that there is only one *MAKR4* gene in squash despite the whole genome duplication event postulated for the genus *Cucurbita*

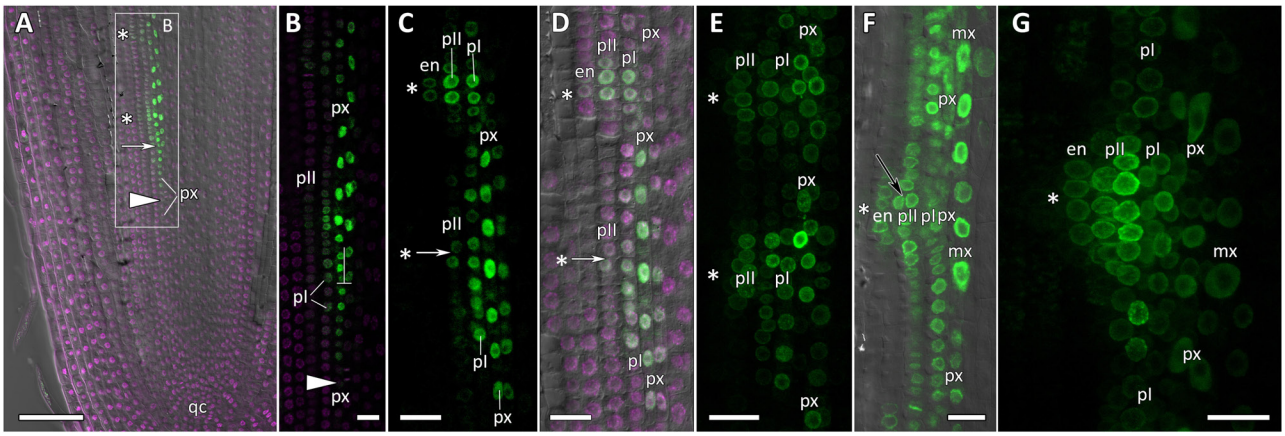

FIGURE 6 | Localization of *CpGATA24* expression along the longitudinal axis of *Cucurbita pepo* root tips. Confocal laser scanning microscopy of longitudinal vibratome sections. Green channel – fluorescence of mNeonGreen-H2B, magenta channel – DNA in nuclei stained with DAPI, gray channel – differential interference contrast. **(A)** An overview and **(B)** close-up of the parental root meristem shows the acropetal sequence of *GATA24* promoter activity in protoxylem and pericycle. *GATA24* expression arises first in the protoxylem at a distance of 275 μm from the initial cells (arrowhead), before the formative T-division (arrow). **(C,D)** The establishment of *GATA24* activity in xylem, pericycle layers and endodermis. Founder cell specification in the outer pericycle (white arrows). Two endodermal cells with local *GATA24* activity can be seen in the upper developing primordium. **(E,F)** Asterisks indicate the position of young lateral root primordia after the first anticlinal and periclinal (black arrow) divisions in the pericycle. *GATA24* transcription can be seen in the protoxylem between primordia. **(G)** Lateral root primordium within the parental root meristem at a distance of 500–600 μm from the QC. **(A–D,F)** Single optical sections. Maximum intensity projection of *z*-series: **(E)** of 26 optical sections, 27 μm in depth; **(G)** of 47 optical sections, 50 μm in depth. Asterisks indicate developing lateral root primordia; en, endodermis; mx, metaxylem; pI, inner pericycle layer; pII, outer pericycle layer; px, protoxylem; qc, quiescent centre. Scale bars denote 100 μm in **(A)**, and 20 μm in **(B–G)**.

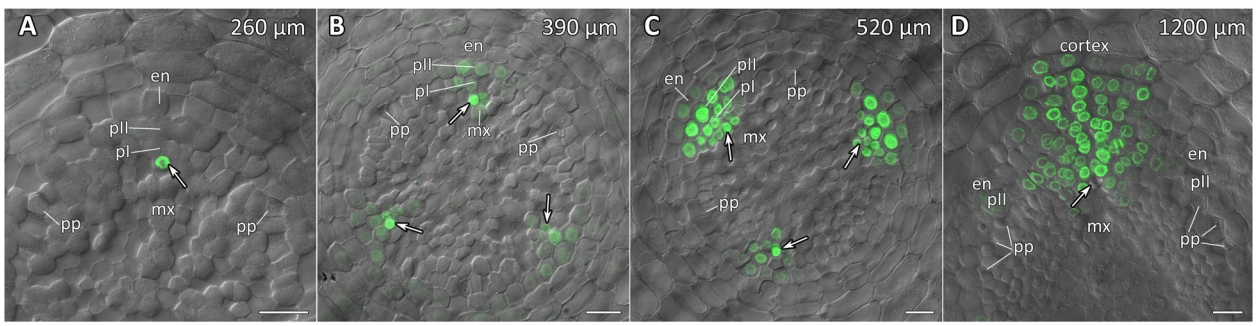

FIGURE 7 | Radial pattern of *CpGATA24* expression along the longitudinal axis of *Cucurbita pepo* root tip. Confocal laser scanning microscopy of vibratome cross-sections. Overlays of single optical sections with differential interference contrast and maximum intensity projections of a *z*-series of mNeonGreen-H2B fluorescence in the green channel (32 optical sections, 36 μm in depth). Distances from initial cells are shown in the upper right corner of each panel. **(A)** Expression of *GATA24* in the protoxylem (arrow). **(B)** In both pericycle layers, expression of *GATA24* begins in the founder cells (arrows point at protoxylem cells expressing *GATA24*). **(C)** Before periclinal divisions in the pericycle (stage I of lateral root primordium formation), expression of *GATA24* is induced in 2–3 files of the endodermis, too. **(D)** Lateral root primordium at a distance of 1200 μm from the initial cells. Protoxylem undergoes terminal differentiation (arrow). Arrows indicate protoxylem; en, endodermis; mx, metaxylem; pI, inner pericycle layer; pII, outer pericycle layer; pp, protophloem. Scale bars denote 20 μm.

(Montero-Pau et al., 2018). Here, cucumber was not included in the search. Transcriptional analyses on the effects of auxin were performed with 10 μM of the synthetic auxin NAA for GATA genes. For MAKR, however, three effects of different auxins – the synthetic NAA and the natural IAA and IBA – were compared, with the result that only NAA and IBA had an effect. Thus, in cucurbits IBA must be converted to IAA in the root cap, as was previously reported for Arabidopsis (De Rybel et al., 2012; Xuan et al., 2015). The lack of induction of *CpMAKR4* by the natural auxin IAA in spite of the effect of the synthetic auxin NAA could be explained by the fact that, as was shown for Arabidopsis, while NAA can pass the plasma membrane by diffusion, IAA requires active uptake systems (Marchant et al., 1999; Michniewicz et al., 2007).

Arabidopsis *GATA23* and *MAKR4* function in a cell-autonomous manner (De Rybel et al., 2010; Xuan et al., 2015); thus, it is very likely that their homologs in Cucurbitaceae also act cell-autonomously. Therefore, the analysis of their promoter activities should indicate the distribution of the corresponding proteins.

The expression pattern of *GATA23* in Arabidopsis has been analyzed in a few studies (De Rybel et al., 2010; Xuan et al., 2015;

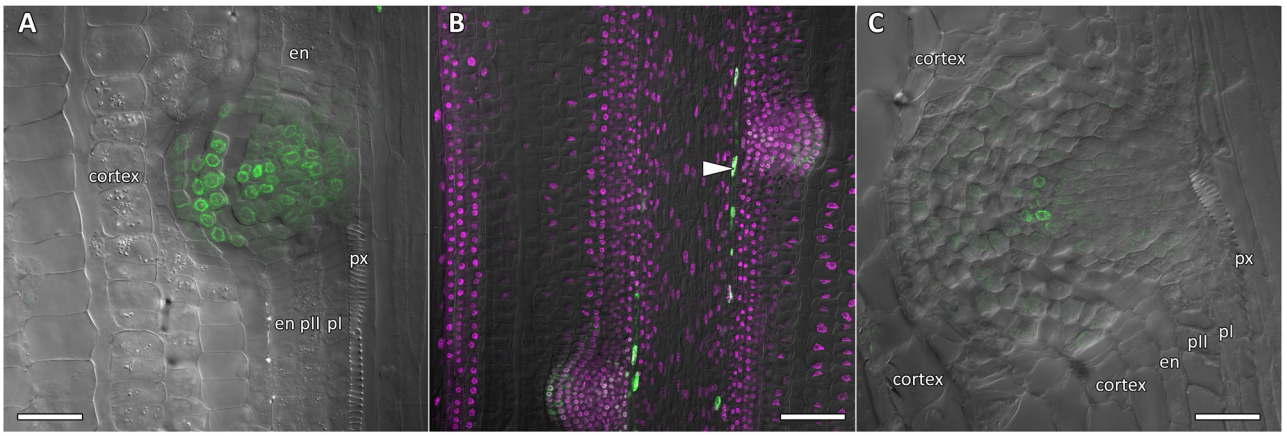

FIGURE 8 | Localization of *CpGATA24* expression in lateral root primordia of *Cucurbita pepo* root. Confocal laser scanning microscopy of longitudinal vibratome sections. Green channel – fluorescence of mNeonGreen-H2B, magenta channel – DNA in nuclei stained with DAPI, gray channel – differential interference contrast. **(A)** Lateral root primordium at a distance of 1000 μm from the QC. **(B)** *CpGATA24* expression is remained in metaxylem cells (arrowhead) and lateral root primordia at a distance of 1500 μm from the QC. **(C)** *CpGATA24* expression has disappeared in lateral root primordia at a distance of 2000 μm from the QC. en, endodermis; pI, inner pericycle layer; pII, outer pericycle layer; px, protoxylem. Scale bars denote 50 μm in **(A,C)**, and 100 μm in **(B)**.

Murphy et al., 2016). The authors concluded that *GATA23* expression is induced before the first asymmetric division and synchronous nuclear migration in two pericycle cells, and that this expression is only maintained up to and including stage II. That is, *GATA23* expression finishes with the first periclinal divisions (De Rybel et al., 2010). According to Murphy et al. (2016), *GATA23* expression is triggered in the pericycle at xylem poles within the elongation zone. Xuan et al. (2015) also convincingly showed the induction of *GATA23* expression in two pericycle cells before the asymmetric formative division. In addition, the cellular auxin response maxima (as evidenced by *DR5* promoter activity) also appear in two pericycle cells just before the nuclear migration (De Rybel et al., 2010). *GATA23* expression is controlled by the activity of the Aux/IAA28-dependent signaling module in the basal part of the apical root meristem (De Rybel et al., 2010), where the priming of founder cells occurs. Altogether, based on the expression pattern of *GATA23*, it was concluded that specification of founder cells takes place in the pericycle above the elongation zone (De Rybel et al., 2010; Lavenus et al., 2013), and that GATA23 and a small signaling peptide, GLV6, may be involved in the nuclear migration mechanism in polarized founder cells (De Rybel et al., 2010; Fernandez et al., 2015).

During the initiation of lateral root primordia within the elongation zone, nuclear migration is typically observed in two adjacent pericycle cells prior to the asymmetric division (Casero et al., 1993; Demchenko and Demchenko, 1996; Casimiro et al., 2003; De Rybel et al., 2010). The coordinated, synchronous nuclear migration of two neighboring pericycle nuclei in Arabidopsis roots depends on Aux/IAA28 and ARF-dependent signaling and is an absolute prerequisite for primordium initiation (De Rybel et al., 2010). In contrast, in *C. pepo* roots, where the initiation of lateral root primordia takes place in the parental root meristem, the cells of different pericycle files are short (meristematic) and their nuclei are already positioned near the center of future primordia. In this case, nuclear migration is unnecessary (Ilina et al., 2017, 2018). Most likely, *CpGATA24*, the putative functional ortholog of *GATA23*, does not target genes required for coordinated nuclear migration in the pericycle (Bone and Starr, 2016).

In the current study, we show that the pattern of expression of *CpGATA24* is much broader than that of *GATA23*. The onset of *CpGATA24* expression is associated with the protoxylem, and only expands to individual pericycle cells (the founder cells) before the anticlinal formative divisions that lead to lateral root initiation (**Figures 6**, **7**). In addition, *CpGATA24* expression is maintained in all primordial cells up to and including stage V, gradually decreasing in the later stages (**Figure 8**). Comparative analysis of cellular auxin response maxima (Ilina et al., 2018) and *CpGATA24* expression shows that in *C. pepo,* unlike in Arabidopsis, they do not coincide. At a distance of approx. 390 μm from the initials, an auxin response maximum is present in all metaxylem files, but *CpGATA24* is only expressed in the protoxylem and the peripheral metaxylem. At larger distances from the root tip, the *CpGATA24* expression pattern is wider than the cellular auxin response maximum. It is important to note that in the protoxylem as well as in adjacent cell files of the stelar parenchyma, *CpGATA24* expression is constant in all cells of a given file up to a distance of approx. 1500 μm from the initials, in contrast with the expression of *GATA23* in Arabidopsis which is only induced in pre-branch sites and maintained during lateral root primordia formation (De Rybel et al., 2010). This might indicate the presence of an additional transcriptional activator of *CpGATA24* beyond auxin signal transduction. Based on the expression pattern of *CpGATA24* in the central cylinder, this putative trigger would likely move through the protoxylem file from the basal parts of the root down to the apical meristem.

In Arabidopsis, MAKR4 converts the prebranch sites into a regular spacing of lateral roots (Xuan et al., 2015). In the

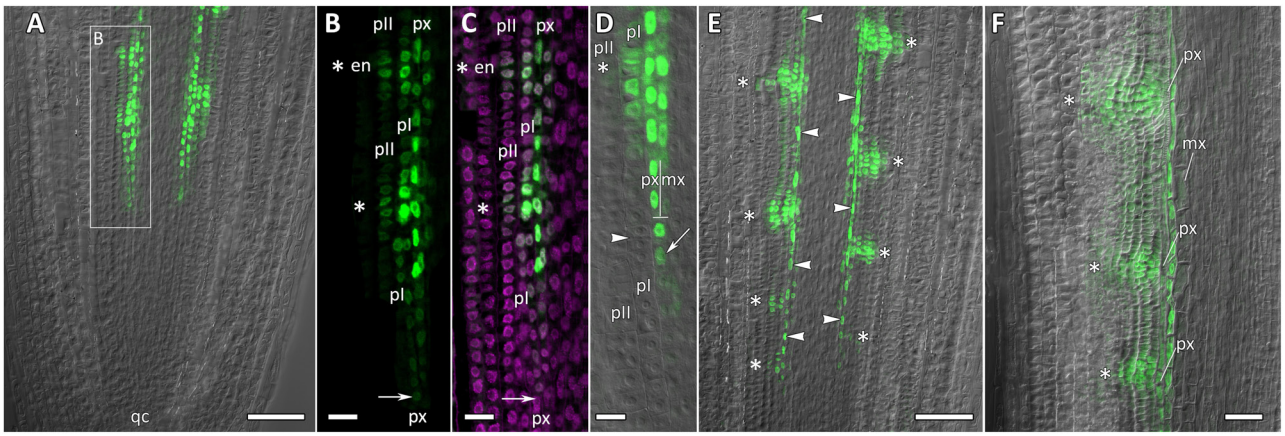

FIGURE 9 | Localization of *CpMAKR4* expression along the longitudinal axis of *Cucurbita pepo* root tips. Confocal laser scanning microscopy of longitudinal vibratome sections. Green channel – fluorescence of eGFP-H2B, magenta channel – DNA in cell nuclei stained with DAPI, gray channel – differential interference contrast. **(A)** An overview and **(B,C)** close-up of the parental root meristem shows the acropetal sequence of *CpMAKR4* promoter activity in protoxylem and pericycle. *CpMAKR4* expression arises first in the protoxylem at a distance of 330 μm from the initial cells (arrows). **(D)** *CpMAKR4* expression takes place just before the last formative T-division in the protoxylem. An arrow points at the first cell expressing *CpMARK4* in the protoxylem cell file. Two putative founder cells in the inner pericycle layer are labeled with an arrowhead. The first anticlinal division (metaphase) in an inner pericycle cell expressing *CpMAKR4* is visible (asterisk). **(E)** Young lateral root primordia (asterisks) and protoxylem cells between primordia (arrowheads) expressing *CpMAKR4*. **(F)** *CpMAKR4* expression is remained in protoxylem cells and lateral root primordia at a distance of 1500 μm from the initials. Asterisks indicate developing lateral root primordia; en, endodermis; mx, metaxylem; pI, inner pericycle layer; pII, outer pericycle layer; px, protoxylem; qc, quiescent centre. Scale bars denote 100 μm in **(A,E)**, 20 μm in **(B,C)**, 10 μm in **(D)**, 50 μm in **(F)**.

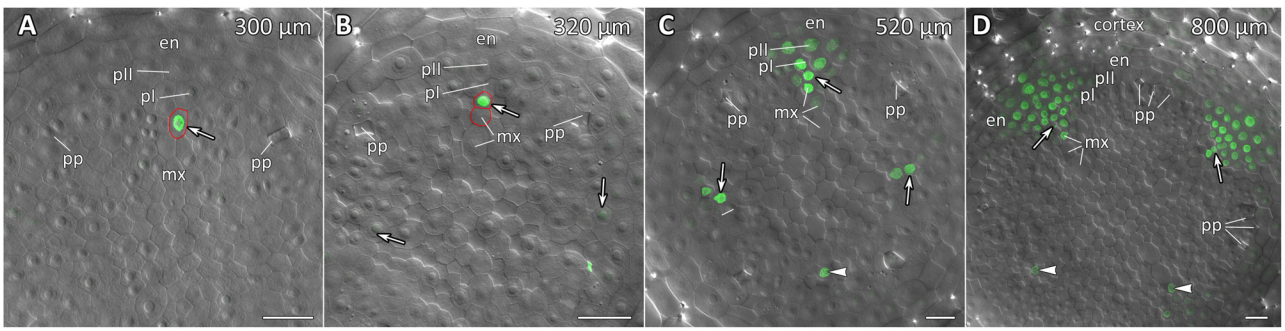

FIGURE 10 | Radial pattern of *CpMAKR4* expression along the longitudinal axis of *Cucurbita pepo* root tip. Confocal laser scanning microscopy of vibratome cross-sections. Overlays of single optical sections with differential interference contrast and maximum intensity projections of a *z*-series of eGFP-H2B fluorescence in the green channel (16 optical sections, 15 μm in depth). Distances from initial cells are given in the right upper corner of each panel. **(A)** Expression of *CpMAKR4* in the protoxylem (arrow, cell outlined in red) before the T-division. **(B)** Two cell files (outlined in red) are formed at a xylem pole. Expression of *CpMAKR4* in the protoxylem is visible. **(C)** Expression of *CpMAKR4* is induced in the founder cells of the inner and outer pericycle layer, also in metaxylem cells opposite young lateral root primordia. **(D)** Lateral root primordia at a distance of 800 μm from the initial cells. Expression of *CpMAKR4* takes place in 3–4 files of the endodermis as well. Protoxylem and metaxylem (arrowheads) cells between primordia show *CpMAKR4* transcription. Arrows indicate protoxylem; en, endodermis; mx, metaxylem; pI, inner pericycle layer; pII, outer pericycle layer; pp, protophloem. Scale bars denote 20 μm.

sequence of events leading to founder cell specification, induction of *MAKR4* expression usually takes place after induction of *GATA23* expression. The expression of the squash *CpMAKR4* gene, the putative functional ortholog of *MAKR4*, is activated in the protoxylem a little bit later than that of *CpGATA24* (**Supplementary Figure S4**). Interestingly, both of these events occur before the last periclinal T-division, which leads to the formation of the cell files of proto- and metaxylem (**Figures 6A**, **9D**, **10A,B**). In squash, *CpMAKR4* and *CpGATA24* expression is maintained in all protoxylem cells, while in Arabidopsis roots, *MAKR4* is only expressed in the protoxylem of the parental root in the basal part of the lateral root meristem (Xuan et al., 2015).

Above the elongation zone in Arabidopsis, MAKR4 is located at the plasma membrane on the border of two adjacent founder cells in the pericycle prior to the synchronous nuclear migration (Xuan et al., 2015). After completion of the first anticlinal division, it is localized throughout the plasma membrane of sister cells. During further primordium development, *AtMAKR4* is expressed in overlaying cell layers of early-stage lateral root primordia. Also, in the pericycle of squash roots, *CpMAKR4* expression is induced directly before the first anticlinal division

(**Figures 9B–D**), and this always happens in two adjacent founder cells. Subsequently, *CpMAKR4* expression is maintained in primordia up to stage V (**Figures 9E,F**). This is consistent with a direct involvement of *CpMAKR4* in the development of lateral root primordia before the formation of their own initial cells in the quiescent center of the emergent lateral root meristem, and is also consistent with the defect in lateral root emergence observed in a *MAKR4* knock-down line (Xuan et al., 2015).

In Arabidopsis, it was proposed that periodic fluctuations in auxin distribution or responsiveness determine the longitudinal spacing of lateral root initiations (De Smet et al., 2007). Because of the failure of exogenously applied IAA to affect the frequency of pulses in the oscillation zone, it was concluded that the pace of oscillation is set by an endogenously regulated clock with a stable, auxin-independent periodicity (Moreno-Risueno et al., 2010; Van Norman et al., 2013), suggesting that the pathway determining prebranch site formation is largely independent of the pathway leading to lateral root formation. In Arabidopsis, the specific induction of expression of *GATA23* and *MAKR4* in founder cells in the pericycle cell files can only be explained by the oscillation of a trigger. Yet, in squash, lateral root initiation takes place at a distance of 250–300 μm from the initial cells, indicating that prebranch site formation takes place even closer to the root tip. Thus, it is unlikely that in cucurbit roots there is enough space for the formation of such auxin oscillations as were described for Arabidopsis basal meristem. However, the expression of *CpGATA24* and *CpMAKR4* in cell files of the stelar parenchyma argues for the involvement of a second regulator that on the one hand is independent of auxin, and on the other hand likely moves from the basal part of the root toward the meristem. Since the trigger of *CpGATA24* and *CpMAKR4* expression always extends centrifugally from the protoxylem, speculation about the movement of auxin as a trigger from dying root cap cells in Arabidopsis (Möller et al., 2017) cannot apply to Cucurbitaceae.

Further identification of the target genes of the transcription factor GATA23 and of its orthologs in other plants, as well as the elucidation of the actual role of MAKR4 in the signaling cascade that leads to prebranch sites formation, will shed light on the mechanisms of formation of local competence for lateral root initiation in pericycle cells. Expansion of our knowledge in this area will also lead to the identification of mechanisms of systemic regulation of branching, which is necessary for the development of targeted breeding strategies in agriculture.

AUTHOR CONTRIBUTIONS

KND and KP planned and designed the research. ASK, ELI, KND, EDG, and VAP performed most experiments and analyzed data. ASK performed phylogeny and bioinformatics. KND and ELI carried out the design of all vectors. KND performed the microscopy. KND, KP, ASK, and ELI wrote the manuscript. All authors contributed to the final version.

FUNDING

This research was financially supported by the Russian Science Foundation (Grant No. 16-16-00089).

ACKNOWLEDGMENTS

We are grateful to Erik Limpens (Wageningen University, Wageningen, Netherlands), and Michael Davidson (Florida State University, United States) for providing plasmids. We thank the Charlesworth Author Services Team (www.cwauthors.com) for editing drafts of this manuscript. This study was performed using equipment of the Core Facility of Cell and Molecular Technologies in Plant Science at the Komarov Botanical Institute (Saint Petersburg, Russia) and the Core Facility of Genomic Technologies, Proteomics and Cell Biology at the Research Institute for Agricultural Microbiology (Saint Petersburg, Pushkin, Russia). We are also grateful to ZEISS and the Optec Group (Olga Seredkina, Moscow, Russia) for providing the full license to the ZEN 2.3 software.

SUPPLEMENTARY MATERIAL

The Supplementary Material for this article can be found online at: https://www.frontiersin.org/articles/10.3389/fpls.2019.00365/full#supplementary-material

REFERENCES

Behringer, C., Bastakis, E., Ranftl, Q. L., Mayer, K. F. X., and Schwechheimer, C. (2014). Functional diversification within the family of B-GATA transcription factors through the leucine-leucine-methionine domain. *Plant Physiol.* 166, 293–305. doi: 10.1104/pp.114.246660

Behringer, C., and Schwechheimer, C. (2015). B-GATA transcription factors – insights into their structure, regulation, and role in plant development. *Front. Plant Sci.* 6:90. doi: 10.3389/fpls.2015.00090

Berardini, T. Z., Reiser, L., Li, D., Mezheritsky, Y., Muller, R., Strait, E., et al. (2015). The arabidopsis information resource: making and mining the "gold standard" annotated reference plant genome. *Genesis* 53, 474–485. doi: 10.1002/dvg.22877

Bone, C. R., and Starr, D. A. (2016). Nuclear migration events throughout development. *J. Cell Sci.* 129, 1951–1961. doi: 10.1242/jcs.179788

Casero, P. J., Casimiro, I., Rodriguez-Gallardo, L., Martin-Partigo, G., and Lloret, P. G. (1993). Lateral root initiation by asymmetrical transverse divisions of pericycle cells in adventitious roots of *Allium cepa*. *Protoplasma* 176, 138–144. doi: 10.1007/BF01378950

Casimiro, I., Beeckman, T., Graham, N., Bhalerao, R., Zhang, H., Casero, P., et al. (2003). Dissecting *Arabidopsis* lateral root development. *Trends Plant Sci.* 8, 165–171. doi: 10.1016/S1360-1385(03)00051-7

Charlton, W. A. (1991). "Lateral root initiation," in *Plant Roots: The Hidden Half*, eds Y. Waisel, A. Eshel, and U. Kafkafi (New York, NY: Marcel Dekker Inc), 103–128.

Chen, H., Shao, H., Li, K., Zhang, D., Fan, S., Li, Y., et al. (2017). Genome-wide identification, evolution, and expression analysis of GATA transcription factors in apple (*Malus* × *domestica* Borkh.). *Gene* 627, 460–472. doi: 10.1016/j.gene.2017.06.049

De Rybel, B., Audenaert, D., Xuan, W., Overvoorde, P., Strader, L. C., Kepinski, S., et al. (2012). A role for the root cap in root branching revealed by the non-auxin probe naxillin. *Nat. Chem. Biol.* 8, 798–805. doi: 10.1038/nchembio.1044

De Rybel, B., Vassileva, V., Parizot, B., Demeulenaere, M., Grunewald, W., Audenaert, D., et al. (2010). A novel Aux/IAA28 signaling cascade activates GATA23-dependent specification of lateral root founder cell identity. *Curr. Biol.* 20, 1697–1706. doi: 10.1016/j.cub.2010.09.007

De Smet, I., Tetsumura, T., De Rybel, B., Frey, N. F. D., Laplaze, L., Casimiro, I., et al. (2007). Auxin-dependent regulation of lateral root positioning in the basal meristem of *Arabidopsis*. *Development* 134, 681–690. doi: 10.1242/dev.02753

Demchenko, K. N., and Demchenko, N. P. (1996). "Early stages of lateral root development in *Triticum aestivum* L.," in *Acta Phytogeographica Suecica: Plant Root Systems and Natural Vegetation*, eds H. Persson and I. O. Baitulin (Uppsala: Opulus Press AB), 71–75.

Demchenko, K. N., and Demchenko, N. P. (2001). "Changes of root structure in connection with the development of lateral root primordia in wheat and pumpkins," in *Recent Advances of Plant Root Structure and Function. Developments in Plant and Soil Sciences*, Vol. 90, eds O. Gašparíková, M. Čiamporová, I. Mistrík, and F. Baluška (Dordrecht: Springer), 39–47. doi: 10.1007/978-94-017-2858-4_5

Ding, L., Yan, S., Jiang, L., Liu, M., Zhang, J., Zhao, J., et al. (2015). HANABA TARANU regulates the shoot apical meristem and leaf development in cucumber (*Cucumis sativus* L.). *J. Exp. Bot.* 66, 7075–7087. doi: 10.1093/jxb/erv409

Du, Y., and Scheres, B. (2018). Lateral root formation and the multiple roles of auxin. *J. Exp. Bot.* 69, 155–167. doi: 10.1093/jxb/erx223

Engler, C., Youles, M., Gruetzner, R., Ehnert, T.-M., Werner, S., Jones, J. D. G., et al. (2014). A Golden Gate modular cloning toolbox for plants. *ACS Synth. Biol.* 3, 839–843. doi: 10.1021/sb4001504

Fernandez, A., Drozdzecki, A., Hoogewijs, K., Vassileva, V., Madder, A., Beeckman, T., et al. (2015). The GLV6/RGF8/CLEL2 peptide regulates early pericycle divisions during lateral root initiation. *J. Exp. Bot.* 66, 5245–5256. doi: 10.1093/jxb/erv329

Garcia-Mas, J., Benjak, A., Sanseverino, W., Bourgeois, M., Mir, G., González, V. M., et al. (2012). The genome of melon (*Cucumis melo* L.). *Proc. Natl. Acad. Sci. U.S.A.* 109:11872. doi: 10.1073/pnas.1205415109

Goodstein, D. M., Shu, S., Howson, R., Neupane, R., Hayes, R. D., Fazo, J., et al. (2012). Phytozome: a comparative platform for green plant genomics. *Nucleic Acids Res.* 40, D1178–D1186. doi: 10.1093/nar/gkr944

Guo, S., Zhang, J., Sun, H., Salse, J., Lucas, W. J., Zhang, H., et al. (2013). The draft genome of watermelon *(Citrullus lanatus)* and resequencing of 20 diverse accessions. *Nat. Genet.* 45, 51–58. doi: 10.1038/ng.2470

Hetherington, A. J., and Dolan, L. (2017). The evolution of lycopsid rooting structures: conservatism and disparity. *New Phytol.* 215, 538–544. doi: 10.1111/nph.14324

Hetherington, A. J., and Dolan, L. (2018). Stepwise and independent origins of roots among land plants. *Nature* 561, 235–238. doi: 10.1038/s41586-018-0445-z

Hetherington, A. J., and Dolan, L. (2019). Rhynie chert fossils demonstrate the independent origin and gradual evolution of lycophyte roots. *Curr. Opin. Plant Biol.* 47, 119–126. doi: 10.1016/j.pbi.2018.12.001

Hornung, E., Krueger, C., Pernstich, C., Gipmans, M., Porzel, A., and Feussner, I. (2005). Production of (10E,12Z)-conjugated linoleic acid in yeast and tobacco seeds. *Biochim. Biophys. Acta* 1738, 105–114. doi: 10.1016/j.bbalip.2005.11.004

Hou, G., Hill, J. P., and Blancaflor, E. B. (2004). Developmental anatomy and auxin response of lateral root formation in *Ceratopteris richardii*. *J. Exp. Bot.* 55, 685–693. doi: 10.1093/jxb/erh068

Ilina, E. L., Kiryushkin, A. S., Semenova, V. A., Demchenko, N. P., Pawlowski, K., and Demchenko, K. N. (2018). Lateral root initiation and formation within the parental root meristem of *Cucurbita pepo*: is auxin a key player? *Ann. Bot.* 122, 873–888. doi: 10.1093/aob/mcy052

Ilina, E. L., Kiryushkin, A. S., Tsyganov, V. E., Pawlowski, K., and Demchenko, K. N. (2017). Molecular, genetic and hormonal outlook in root branching. *Agric. Biol.* 52, 856–868. doi: 10.15389/agrobiology.2017.5.856eng

Ilina, E. L., Logachov, A. A., Laplaze, L., Demchenko, N. P., Pawlowski, K., and Demchenko, K. N. (2012). Composite *Cucurbita pepo* plants with transgenic roots as a tool to study root development. *Ann. Bot.* 110, 479–489. doi: 10.1093/aob/mcs086

Jaillais, Y., Hothorn, M., Belkhadir, Y., Dabi, T., Nimchuk, Z. L., Meyerowitz, E. M., et al. (2011). Tyrosine phosphorylation controls brassinosteroid receptor activation by triggering membrane release of its kinase inhibitor. *Genes Dev.* 25, 232–237. doi: 10.1101/gad.2001911

Jiang, J., Wang, T., Wu, Z., Wang, J., Zhang, C., Wang, H., et al. (2015). The intrinsically disordered protein BKI1 is essential for inhibiting BRI1 signaling in plants. *Mol. Plant* 8, 1675–1678. doi: 10.1016/j.molp.2015.07.012

Jin, J., Tian, F., Yang, D.-C., Meng, Y.-Q., Kong, L., Luo, J., et al. (2017). PlantTFDB 4.0: toward a central hub for transcription factors and regulatory interactions in plants. *Nucleic Acids Res.* 45, D1040–D1045. doi: 10.1093/nar/gkw982

Kang, Y. H., and Hardtke, C. S. (2016). Arabidopsis MAKR5 is a positive effector of BAM3-dependent CLE45 signaling. *EMBO Rep.* 17, 1145–1154. doi: 10.15252/embr.201642450

Kitaeva, A. B., Demchenko, K. N., Tikhonovich, I. A., Timmers, A. C. J., and Tsyganov, V. E. (2016). Comparative analysis of the tubulin cytoskeleton organization in nodules of *Medicago truncatula* and *Pisum sativum*: bacterial release and bacteroid positioning correlate with characteristic microtubule rearrangements. *New Phytol.* 210, 168–183. doi: 10.1111/nph.13792

Kumar, S., Stecher, G., and Tamura, K. (2016). MEGA7: molecular evolutionary genetics analysis version 7.0 for bigger datasets. *Mol. Biol. Evol.* 33, 1870–1874. doi: 10.1093/molbev/msw054

Lavenus, J., Goh, T., Roberts, I., Guyomarc'h, S., Lucas, M., De Smet, I., et al. (2013). Lateral root development in *Arabidopsis*: fifty shades of auxin. *Trends Plant Sci.* 18, 450–458. doi: 10.1016/j.tplants.2013.04.006

Li, Z., Zhang, Z., Yan, P., Huang, S., Fei, Z., and Lin, K. (2011). RNA-Seq improves annotation of protein-coding genes in the cucumber genome. *BMC Genomics* 12:540. doi: 10.1186/1471-2164-12-540

Liu, W., and Xu, L. (2018). Recruitment of IC-*WOX* genes in root evolution. *Trends Plant Sci.* 23, 490–496. doi: 10.1016/j.tplants.2018.03.011

Livak, K. J., and Schmittgen, T. D. (2001). Analysis of relative gene expression data using real-time quantitative PCR and the $2^{-\Delta\Delta C_T}$ method. *Methods* 25, 402–408. doi: 10.1006/meth.2001.1262

Malamy, J. E., and Benfey, P. N. (1997). Organization and cell differentiation in lateral roots of *Arabidopsis thaliana*. *Development* 124, 33–44.

Mallory, T. E., Chiang, S.-H., Cutter, E. G., and Gifford, E. M. (1970). Sequence and pattern of root formation in five selected species. *Am. J. Bot.* 57, 800–809. doi: 10.1093/jxb/erv346

Marchant, A., Kargul, J., May, S. T., Muller, P., Delbarre, A., Perrot-Rechenmann, C., et al. (1999). AUX1 regulates root gravitropism in *Arabidopsis* by facilitating auxin uptake within root apical tissues. *EMBO J.* 18, 2066–2073. doi: 10.1093/emboj/18.8.2066

McLean, I. W., and Nakane, P. K. (1974). Periodate-lysine-paraformaldehyde fixative. A new fixation for immunoelectron microscopy. *J. Histochem. Cytochem.* 22, 1077–1083. doi: 10.1177/22.12.1077

Michniewicz, M., Brewer, P. B., and Friml, J. (2007). Polar auxin transport and asymmetric auxin distribution. *Arabidopsis Book* 5:e0108. doi: 10.1199/tab.0108

Möller, B. K., Xuan, W., and Beeckman, T. (2017). Dynamic control of lateral root positioning. *Curr. Opin. Plant Biol.* 35, 1–7. doi: 10.1016/j.pbi.2016.09.001

Montero-Pau, J., Blanca, J., Bombarely, A., Ziarsolo, P., Esteras, C., Martí-Gómez, C., et al. (2018). *De novo* assembly of the zucchini genome reveals a whole-genome duplication associated with the origin of the *Cucurbita* genus. *Plant Biotechnol. J.* 16, 1161–1171. doi: 10.1111/pbi.12860

Moreno-Risueno, M. A., Van Norman, J. M., Moreno, A., Zhang, J., Ahnert, S. E., and Benfey, P. N. (2010). Oscillating gene expression determines competence for periodic *Arabidopsis* root branching. *Science* 329, 1306–1311. doi: 10.1126/science.1191937

Motte, H., and Beeckman, T. (2018). The evolution of root branching: increasing the level of plasticity. *J. Exp. Bot.* 70, 785–793. doi: 10.1093/jxb/ery409

Murphy, E., Vu, L. D., Van den Broeck, L., Lin, Z., Ramakrishna, P., van de Cotte, B., et al. (2016). RALFL34 regulates formative cell divisions in *Arabidopsis* pericycle during lateral root initiation. *J. Exp. Bot.* 67, 4863–4875. doi: 10.1093/jxb/erw281

Nam, H.-S., and Benezra, R. (2009). High levels of Id1 expression define B1 type adult neural stem cells. *Cell Stem Cell* 5, 515–526. doi: 10.1016/j.stem.2009.08.017

Obrero, Á, Die, J. V., Román, B., Gómez, P., Nadal, S., and González-Verdejo, C. I. (2011). Selection of reference genes for gene expression studies in zucchini

(*Cucurbita pepo*) using qPCR. *J. Agric. Food Chem.* 59, 5402–5411. doi: 10.1021/jf200689r

Omelyanchuk, N. A., Wiebe, D. S., Novikova, D. D., Levitsky, V. G., Klimova, N., Gorelova, V., et al. (2017). Auxin regulates functional gene groups in a fold-change-specific manner in *Arabidopsis thaliana* roots. *Sci. Rep.* 7:2489. doi: 10.1038/s41598-017-02476-8

Paponov, I. A., Paponov, M., Teale, W., Menges, M., Chakrabortee, S., Murray, J. A. H., et al. (2008). Comprehensive transcriptome analysis of auxin responses in *Arabidopsis*. *Mol. Plant* 1, 321–337. doi: 10.1093/mp/ssm021

R Core Team (2017). *R: A Language and Environment for Statistical Computing [Online]. Vienna, Austria: R Foundation for Statistical Computing*. Available at: https://www.R-project.org

Reyes, J. C., Muro-Pastor, M. I., and Florencio, F. J. (2004). The GATA family of transcription factors in arabidopsis and rice. *Plant Physiol.* 134, 1718–1732. doi: 10.1104/pp.103.037788

Saitou, N., and Nei, M. (1987). The neighbor-joining method: a new method for reconstructing phylogenetic trees. *Mol. Biol. Evol.* 4, 406–425.

Shaner, N. C., Lambert, G. G., Chammas, A., Ni, Y., Cranfill, P. J., Baird, M. A., et al. (2013). A bright monomeric green fluorescent protein derived from *Branchiostoma lanceolatum*. *Nat. Methods* 10, 407–409. doi: 10.1038/nmeth.2413

Shoemaker, J. S., and Fitch, W. M. (1989). Evidence from nuclear sequences that invariable sites should be considered when sequence divergence is calculated. *Mol. Biol. Evol.* 6, 270–289. doi: 10.1093/oxfordjournals.molbev.a040550

Simon, M. L. A., Platre, M. P., Marquès-Bueno, M. M., Armengot, L., Stanislas, T., Bayle, V., et al. (2016). A PI4P-driven electrostatic field controls cell membrane identity and signaling in plants. *Nat. Plants* 2: 16089. doi: 10.1038/nplants.2016.89

Sun, H., Wu, S., Zhang, G., Jiao, C., Guo, S., Ren, Y., et al. (2017). Karyotype stability and unbiased fractionation in the paleo-allotetraploid *Cucurbita* genomes. *Mol. Plant* 10, 1293–1306. doi: 10.1016/j.molp.2017.09.003

Urasaki, N., Takagi, H., Natsume, S., Uemura, A., Taniai, N., Miyagi, N., et al. (2017). Draft genome sequence of bitter gourd (*Momordica charantia*), a vegetable and medicinal plant in tropical and subtropical regions. *DNA Res.* 24, 51–58. doi: 10.1093/dnares/dsw047

Van Norman, J. M., Xuan, W., Beeckman, T., and Benfey, P. N. (2013). To branch or not to branch: the role of pre-patterning in lateral root formation. *Development* 140, 4301–4310. doi: 10.1242/dev.090548

Wan, H., Zhao, Z., Qian, C., Sui, Y., Malik, A. A., and Chen, J. (2010). Selection of appropriate reference genes for gene expression studies by quantitative real-time polymerase chain reaction in cucumber. *Anal. Biochem.* 399, 257–261. doi: 10.1016/j.ab.2009.12.008

Whelan, S., and Goldman, N. (2001). A general empirical model of protein evolution derived from multiple protein families using a maximum-likelihood approach. *Mol. Biol. Evol.* 18, 691–699. doi: 10.1093/oxfordjournals.molbev.a003851

Wu, S., Shamimuzzaman, M., Sun, H., Salse, J., Sui, X., Wilder, A., et al. (2017). The bottle gourd genome provides insights into Cucurbitaceae evolution and facilitates mapping of a Papaya ring-spot virus resistance locus. *Plant J.* 92, 963–975. doi: 10.1111/tpj.13722

Xie, Y., Straub, D., Eguen, T., Brandt, R., Stahl, M., Martinez-Garcia, J. F., et al. (2015). Meta-analysis of Arabidopsis KANADI1 direct target genes identifies a basic growth-promoting module acting upstream of hormonal signaling pathways. *Plant Physiol.* 169, 1240–1253. doi: 10.1104/pp.15.00764

Xuan, W., Audenaert, D., Parizot, B., Möller, B. K., Njo, M. F., De Rybel, B., et al. (2015). Root cap-derived auxin pre-patterns the longitudinal axis of the *Arabidopsis* root. *Curr. Biol.* 25, 1381–1388. doi: 10.1016/j.cub.2015.03.046

Yang, L., Koo, D.-H., Li, Y., Zhang, X., Luan, F., Havey, M. J., et al. (2012). Chromosome rearrangements during domestication of cucumber as revealed by high-density genetic mapping and draft genome assembly. *Plant J.* 71, 895–906. doi: 10.1111/j.1365-313X.2012.05017.x

Yang, Z. (1994). Maximum likelihood phylogenetic estimation from DNA sequences with variable rates over sites: approximate methods. *J. Mol. Evol.* 39, 306–314. doi: 10.1007/bf00160154

Zhang, C., Hou, Y., Hao, Q., Chen, H., Chen, L., Yuan, S., et al. (2015). Genome-wide survey of the soybean GATA transcription factor gene family and expression analysis under low nitrogen stress. *PLoS One* 10:e0125174. doi: 10.1371/journal.pone.0125174

Zuckerkandl, E., and Pauling, L. (1965). "Evolutionary divergence and convergence in proteins," in *Evolving Genes and Proteins*, eds V. Bryson and H. J. Vogel (London: Academic Press), 97–166. doi: 10.1016/B978-1-4832-2734-4.50017-6

Conflict of Interest Statement: The authors declare that the research was conducted in the absence of any commercial or financial relationships that could be construed as a potential conflict of interest.

frontiers in Plant Science

ORIGINAL RESEARCH
published: 08 August 2019
doi: 10.3389/fpls.2019.01020

Analysis and Modeling of the Variations of Root Branching Density Within Individual Plants and Among Species

*Loïc Pagès**

INRA, Centre PACA, UR 1115 PSH, Avignon, France

OPEN ACCESS

Edited by:
Laurent Laplaze, Institut de recherche pour le développement (IRD), France

Reviewed by:
Peng Yu, University of Bonn, Germany
Joseph G. Dubrovsky, National Autonomous University of Mexico, Mexico
Larry Matthew York, Noble Research Institute, LLC, United States

***Correspondence:**
Loïc Pagès
Loic.Pages@inra.fr

Specialty section:
This article was submitted to Plant Development and EvoDevo, a section of the journal Frontiers in Plant Science

Received: *04 April 2019*
Accepted: *22 July 2019*
Published: *08 August 2019*

Citation:
Pagès L (2019) Analysis and Modeling of the Variations of Root Branching Density Within Individual Plants and Among Species. Front. Plant Sci. 10:1020. doi: 10.3389/fpls.2019.01020

Branching density (or the reciprocal: inter-branch distance) is an important trait which contributes to defining the number of roots in individual plants. The environmental and local variations in inter-branch distance have often been stressed, and simulations models have been put forward to take them into account within the dynamics of root system architecture (RSA). However, little is known about the interspecific and intra-plant variations of inter-branch distance. In this paper, we present an analysis which draws on 40 samples of plants belonging to 36 species collected in homogeneous soils, to address how the variations in inter-branch distance are structured within individual plants, and how this structure varies from one species to another. Using measurements of inter-branch distance on various roots of the same species and our knowledge of the branching process, we defined a simple and generic model dedicated to the simulation of the observed variations. This model distinguishes between two sub-processes: i) the longitudinal location of potential branching sites and ii) the effective emergence of lateral roots at these sites. Thus, it represents the variations in distance between the potential sites (with two parameters), and the probability of emergence of a lateral root at each site (one parameter). We show the ability of this model to account for the main variations in inter-branch distances with a limited number of parameters, and we estimated them for the different species. These parameters can be considered as promising traits to characterize—in a comprehensive and simple way—the genetic and environmental variations in the whole branching process at plant level. Based on the results, we make recommendations for carrying out comparable measurements of the branching density in developed plants. Moreover, we suggest the integration of this new model as a module in future RSA simulators, to improve their capacity to account for this important and highly variable characteristic of plant species.

Keywords: root branching, branching density, inter-branch distance, model, root system architecture, interspecific diversity, phenotype

INTRODUCTION

The linear branching density for a given root can be defined as the number of lateral branches per length unit along this root. It can be characterized by the reciprocal variable, the inter-branch distance (IBD), and is often measured on the branching parts of roots, i.e., excluding the distal end where laterals have not emerged yet (Dubrovsky and Forde, 2012).

It is a very important trait at the root system level, because it largely contributes to defining the total number of roots in the whole plant. Since the root system is usually ramified up to several branching orders, typically between 3 and 5, the effect of inter-branch distance on the total number of roots is potentially raised to the power of the number of branching orders. However, note that some species, among the Amaryllidaceae, for example, have roots which are not branched, but they seem to constitute exceptions.

Several authors have quantified IBD (or branching density) in certain species (e.g., banana: Riopel, 1966; Charlton, 1982; Lecompte and Pagès, 2006; maize: Varney et al., 1991; Pagès and Pellerin, 1994; Wu et al., 2016; pea: Hinchee and Rost, 1992; tomato: Barlow and Adam, 1988) and stressed the importance of this morphological trait to characterize the root system architecture of the studied species. Others have compared several species and shown that IBD varies among species and genotypes within species (Mallory et al., 1970; Kong et al., 2014; Bui et al., 2015; Pagès, 2016; Pagès and Kervella, 2018). For example, in a recent paper based on a large range of species, Pagès (2016) observed considerable variations of IBD, with a 10-fold factor between the extreme average values. Within a given species, the variations among genotypes are usually lower, but they were significant for several Solanaceae species (e.g., Bui et al., 2015). Intra-plant variations have received much less attention. Physiologists usually characterize branching density based on the young radicle (Dubrovsky et al., 2006; Lavenus et al., 2013), whereas ecologists propose global average evaluations on mature plants (Kong et al., 2014). Wu et al. (2016) observed intra-plant structured variations, with a dependence of branching density on the diameter of the parent root in field-grown maize plants.

Beyond all these interspecific and intraspecific constitutive variations, the environmental and local plasticity of inter-branch distance have often been stressed, as a key process to cope with heterogeneous soil and locate numerous roots at favorable sites and fewer at unfavorable sites (Drew, 1975; Robinson, 1994; Malamy, 2005; Hodge, 2009; Orman-Ligeza et al., 2018). Several environmental factors were shown to be able to trigger these root responses, such as nutrient (Drew, 1975; Drew and Saker, 1975) or water availability (Orman-Ligeza et al., 2018). The inter-species variations of these plastic responses have not been studied.

Inter-branch distance is a common input parameter in models that simulate the dynamics of the root system architecture, especially in former models (Diggle, 1988; Pagès and Aries, 1988) in which a fixed average value of inter-branch distance was given to each branching order. In other and more recent models (Dunbabin et al., 2013; Henke et al., 2014), inter-branch distance was assumed to be a function which depends on environmental conditions in the vicinity of the root tip. However, the processes included in these latter models were not precisely evaluated against data, because data are lacking concerning both plant response and diversity of root responses. Additional investigations are required to be able to simulate both the variations in IBD within the root system and the plasticity to local conditions.

To inspire this new generation of simulation models, it is interesting to use the outcome of recent physiological works. The processes leading to the construction of branching density have been thoroughly investigated in recent years, usually along the seminal roots of plantlets, mainly in the *Arabidopsis* model (e.g., Dubrovsky et al., 2006; Moreno-Risueno et al., 2010; Dubrovsky et al., 2011; Lavenus et al., 2013). From these studies, it appears that the process of lateral root branching can be valuably divided into several sub processes which occur successively: priming and specification of founder cells in the proximal vicinity of the parent root meristem; initiation of a primordium from these founder cells; development of the primordium, leading to the formation of the apical meristem of the lateral root; emergence of the lateral root from the parent root. Defining these steps allows for a better understanding of the clue signals that operate successively throughout the whole process. For example, a given initial step may define the potential location for branching, whereas a further step may confirm (or not) the branching in that particular place.

Another complementary approach to the topic is to take a macroscopic view of the emergent result of these sequences leading to patterns of inter-branch distances, and to quantify expression variations within the whole root system, taking into account several roots from the same plants and looking at variations among species. In this paper, we present such an analysis based on 40 different samples (36 species) observed in homogeneous soils to investigate how inter-branch distance varies within individual plants and from one species to another. Using this analysis and knowledge of mechanisms, we put forward a new generic and quantitative model to depict and simulate the observed variations.

MATERIALS AND METHODS

Sampling Species

The data used in this paper come from a large data set of plants sampled since spring 2013 either *In Natura* or in pot cultures (**Table 1**). The growing environments were described in several preceding papers (Pagès, 2014; Pagès and Picon-Cochard, 2014; Pagès, 2016; Pagès and Kervella, 2018). Plants observed *In Natura* were obtained in two different French regions that have homogeneous, light, and deep soils. For obtaining these samples, cylindrical soil monoliths (diameter, 25 cm; depth, 30 cm) were extracted around the sampled plants, inserted into a mesh bag, immersed in a large bucket of water, and gently cleaned. Pot-grown plants were cultivated in greenhouses using long PVC tubes (between 50 and 150 cm long, 10 to 15 cm in

TABLE 1 | List of considered samples, with the name of the species, the family, the site of observation (Thouzon and Nozeyrolles represent two different French regions) and the abbreviation used in **Figures 1**, **4**, and **5**.

Species	Family	Site	Abbreviation
Acanthus mollis	Acanthaceae	Thouzon	AcMoT
Agrostis capillaris	Poaceae	Nozeyrolles	AgCaN
Agrostis vinealis	Poaceae	Nozeyrolles	AgViN
Ajuga reptans	Lamiaceae	Nozeyrolles	AjReN
Alliaria petiolata	Brassicaceae	Nozeyrolles	AlPeN
Amaranthus retroflexus	Amaranthaceae	Thouzon	AmReT
Anthoxanthum odoratum	Poaceae	Pot Clermont-Ferrand	AnOdPC
Anthoxanthum odoratum	Poaceae	Nozeyrolles	AnOdN
Antirrhinum majus	Plantaginaceae	Thouzon	AnMaT
Arabidopsis thaliana	Brassicaceae	Nozeyrolles	ArThN
Arrhenatherum elatius	Poaceae	Pot Clermont-Ferrand	ArElPC
Cirsium vulgare	Asteraceae	Thouzon	CiVuT
Dactylis glomerata	Poaceae	Nozeyrolles	DaGlN
Geranium molle	Geraniaceae	Nozeyrolles	GeMoN
Lactuca sativa	Asteraceae	Thouzon	LaSaT
Lolium perenne	Poaceae	Thouzon	LoPeT
Mentha suaveolens	Lamiaceae	Thouzon	MeSuT
Mercurialis annua	Euphorbiaceae	Thouzon	MeAnT
Misopates orontium	Plantaginaceae	Nozeyrolles	MiOrN
Panicum capillare	Poaceae	Thouzon	PaCaT
Panicum miliaceum	Poaceae	Thouzon	PaMiT
Papaver rhoeas	Papaveraceae	Nozeyrolles	PaRhN
Plantago lanceolata	Plantaginaceae	Nozeyrolles	PlLaN
Poa pratensis	Poaceae	Pot Clermont-Ferrand	PoPrPC
Poa trivialis	Poaceae	Pot Clermont-Ferrand	PoTrPC
Poa trivialis	Poaceae	Thouzon	PoTrT
Prunus domestica	Rosaceae	Thouzon	PrDoT
Pseudotsuga menziesii	Pinaceae	Nozeyrolles	PsMeN
Rubus ulmifolius	Rosaceae	Nozeyrolles	RuUlN
Rubus ulmifolius	Rosaceae	Thouzon	RuUlT
Silene vulgaris	Caryophyllaceae	Thouzon	SiVuT
Solanum laciniatum	Solanaceae	Thouzon	SoLaT
Sorghum halepense	Poaceae	Thouzon	SoHaT
Urtica dioica	Urticaceae	Thouzon	UrDiT
Verbascum nigrum	Scrophulariaceae	Nozeyrolles	VeNiN
Vinca minor	Apocynaceae	Nozeyrolles	ViMiN
Vinca minor	Apocynaceae	Thouzon	ViMiT
Viola odorata	Violaceae	Nozeyrolles	ViOdN
Vulpia myuros	Poaceae	Thouzon	VuMyT
Zea Mays	Poaceae	Pot Avignon	ZeMaPC

diameter) filled with either sieved soil or a mixture of sandy soil and sieved compost. Each species was sampled from two to five well-developed plants, usually before flowering. Sampled trees were young, between 2 and 4 years old.

From our initial data set, containing more than 200 samples (i.e., a species observed at a given site), we selected only those which had at least 150 branch roots that were measured on parent roots with a sufficient range of diameters to study the effect of this factor. Thus, we kept 40 samples belonging to 36 different species (listed in **Table 1**) that met these conditions for the present study.

Imaging the Roots

Once the soil had been carefully cleaned, the sampled parts of root systems were spread out in a layer of water contained in a transparent plastic tray. During this operation, lateral roots were carefully spread out on either side of their parent root to facilitate the subsequent measurements. The densest root systems were cut into several pieces to avoid root overlap in the tray. They were then scanned using flatbed scanners equipped with light in the cover (EPSON perfection V700 and V850) at a resolution of 2,400 to 3,200 dots per inch, using the transparent mode. The resolution was adjusted for each species so as to get at least 10 pixels transversally for the finest roots to measure them with sufficient accuracy. Images were stored in jpeg format.

Measuring the Inter-Branch Distance and Diameter of the Parent Root

Measurements were made on the computer screen by mouse clicking on the displayed images using the measuring tools (i.e., length of straight line and segmented line) provided by the ImageJ software (http://rsbweb.nih.gov/ij/). We measured the diameter of the parent root and the distance along the parent root from each lateral to its proximal closest neighbor (from axis to axis). We quantified branching density based on the inter-branch distance (the reciprocal value), because this variable could be

measured for each lateral root. Measurements were done in the young branching zone, where laterals had reached at least 2 mm, to discard the very distal zone where emergence was taking place and where lateral roots might be not visible. Let us note that some lateral roots were broken during washing and imaging, but their trace was clearly visible because of the relative transparency of the parent root cortex.

Analyzing Data and Modeling

All calculations, plots, and modeling were done using the R software (R Core team, 2013). We made Student *t* tests and analyses of variance using linear models (using the "lm" and "anova" functions), as well as analyses of distributions using several functions of the "moments" package of R (functions: skewness, agostino.test, shapiro.test). We represented the distributions of inter-branch distances graphically using boxplots (**Figure 1**) or using the "density" function that calculates a probability density from the observed or simulated frequencies of inter-branch distances (**Figures 2** and **6**).

Then, we wrote a specific R function (given in **Supplementary Material**) to simulate a model that considers branching as a two-step process. First, potential branching sites are defined along the root, each potential branching site being separated from the previous one (its proximal neighbor) from a distance whose distribution is assumed to be normal. The mean of the distances between potential branching sites is noted *ISD* (inter-site distance), and its coefficient of variation is CV_D. This is the first step that gives a distribution of potential branching sites along the virtual parent root. Second, it is assumed that each potential branching site may actually give rise to an emerged lateral root (i.e., branching success) with a given probability P_{em}, or it may remain unbranched (branching failure), because one of the following steps could not be accomplished, with a probability of $(1\text{-}P_{em})$. This is the second step that simulates the positions of the emerged lateral roots along the parent root and allows calculating the distribution of inter-branch distances that can be compared with the observed ones. This simple model does not distinguish between reasons of failure. It could occur during the inception or later development of the primordium or during the emergence as a lateral root. We did not specify the radial angle that defines the orientation of the laterals around the parent root. The proposed model has three parameters: average distance between the potential sites (ISD), coefficient of variation of this distance (CV_D), and probability (P_{em}) of success of the whole branching process. These parameters, which quantify the two sub-processes, had to be estimated on the whole, using the observed IBD distributions. The calibrations and tests were done on the whole root population for each species first, and then the model was used to analyze the effects of the diameter of the parent root.

RESULTS

Distribution of Inter-Branch Distances

Figure 1 presents box-plots for the empirical distributions of inter-branch distances (IBD) of all species. Large variations are observed,

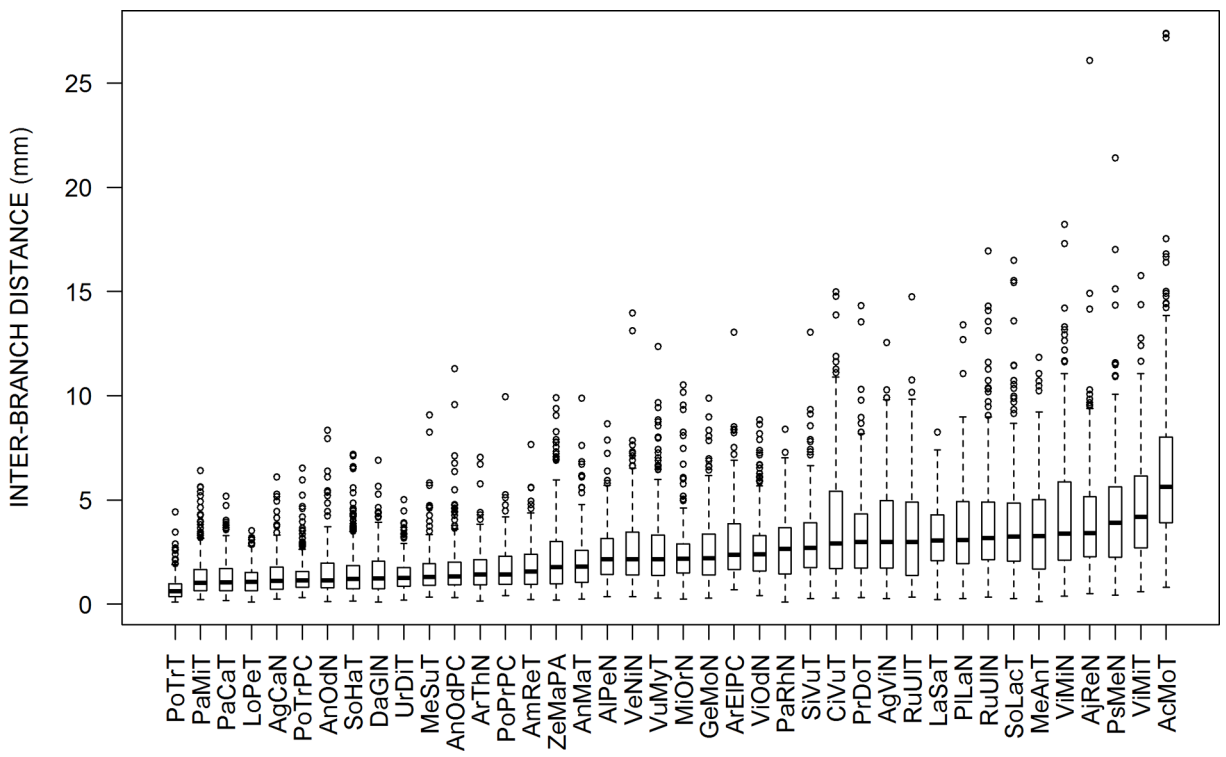

FIGURE 1 | Box plots presenting the distributions of inter-branch distances for each sample. They are sorted from left to right according to the increasing values of the medians. The abbreviations are given in **Table 1**.

both within and among species. Within species, the coefficients of variation in IBD varied between 0.5 and 0.8. The median values among species also varied in a large range (9-fold factor) between 0.62 mm (*Poa trivialis* at Thouzon) and 5.63 mm (*Acanthus mollis* at Thouzon). When several samples exist for the same species (*Anthoxanthum odoratum, Poa trivialis, Rubus ulmifolius, Vinca minor*), these samples are rather close to each other.

The IBD distributions were neither normal nor symmetrical. The Shapiro–Wilk normality test rejected the normality hypothesis for all species. The values of skewness and the Agostino test also showed a clear asymmetry for almost all species, with a systematic right-hand tail of the distributions, i.e., an excess of high values above the last quartile, as we can see in **Figure 1** with outliers for high values of IBD. This skewness is reinforced by the fact that we cannot measure negative values of IBD.

When faced with such distributions, it is common to make a logarithmic transformation (e.g., Pagès, 2014; Landl et al., 2018) to obtain a quasi-normal distribution of the response variable [log(IBD)] and to carry out ANOVA on this transformed variable. Using this transformation, we effectively corrected the initial skewness but we obtained an opposite skewness (left tail) for a number of cases (15 of 40 cases according to the Agostino test; normality is accepted in 23 cases according to the Shapiro–Wilk test). As expected, the ANOVA made on this new response variable confirmed a clear species effect ($P < 0.001$).

We also explored the effect of the diameter of the parent root on IBD using correlation tests. Among the 40 samples, the correlation between the diameter of the parent root and IBD was not significant in 12 cases, significant and positive in 5 cases, and significant and negative in 23 cases. Thus, for a majority of species, the laterals tend to be more spaced out on the fine parent roots, but the inverse phenomenon also occurs, although less frequently.

Fitting and Evaluation of the Branching Model on All Roots

Since the proposed branching model is a numerical and stochastic simulation model, the fitting is not straightforward. To adjust it to the empirical (measured) distributions of IBD, we used a set of intermediate indicators that we constructed first based on simulated distributions and that met three conditions: i) simplicity to estimate these indicators based on the empirical distributions; ii) tight correlations between these indicators and input parameters (ISD, CV_D, P_{em}); iii) low correlations between these indicators. For the construction, we made 8,000 simulations of distributions with 60,000 laterals for each of them, combining parameter values distributed within the plausible ranges for each parameter (20 regularly spaced values for each of the three parameters), and we calculated a number of common characteristics for each simulated distribution of IBD: mean, standard deviation, mode, quantiles at probability levels of 0.10, 0.20, 0.30, …, 0.90, 1.0. Based on this preliminary work (not shown), we retained three indicators that fulfilled the three conditions relatively well. They are: the mode of the IBD distribution, which was tightly correlated to the parameter ISD; the ratio: quantile 0.10/mode, tightly correlated to CV_D; the ratio quantile 0.80/mode, tightly correlated to P_{em}. Then, we estimated the three model parameters independently using these three indicators *via* the linear interpolation of the relationships between average parameter values and indicator values that we obtained from preliminary simulations.

We calculated chi square values for each sample to evaluate the quality of the fitting. These values were significant and rejected the hypothesis of identical simulated and empirical distributions in only 3 of the 40 cases (for *Lolium perenne*, *Rubus ulmifolius,* and *Sorghum Halepense* at Thouzon). **Figure 2** shows the three best (**Figures 2A–C**) and three worst (**Figures 2D–F**) fittings obtained. The model distributions are very close to the empirical ones, and the general shape and skewness are very well rendered. A majority of them, but not all, slightly overestimated the probability density of the modal value.

The distributions of parameters are presented in **Figure 3**. In our population, we obtained very large variations in *ISD,* between 0.40 and 4.6 mm (12-fold factor), confirming the importance of the species effect on this trait. Other parameters were less variable: CV_D varied between 0.28 and 0.69 (2.5-fold factor), and P_{em} varied between 0.37 and 0.98 (2.6-fold factor). We also obtained positive and significant correlations between estimates of the three parameters, but the R^2 values were below 0.3.

Analysis of the Effect of Parent Root Diameter

For each sample, we divided the population of lateral roots into two sub-populations: those roots originating from parent roots that are finer than the central value of the diameter [0.5*(minimal diameter + maximal diameter)] and those on parent roots with a diameter above this central value. We calibrated the model separately for each sub-population.

Figure 4 shows the relationship between the *ISD* parameter values as estimated for the two populations. We observed a highly significant correlation between both sets, and we tested that the regression line was not significantly different from the bisecting line (shown in **Figure 4**). A Student *t* test confirmed that there was no global difference between the two sub-populations regarding the *ISD* parameter. For the two other parameters (CV_D and P_{em}) on the contrary, we did not observe correlations between the two estimates. Again, the Student *t* test did not reveal differences between the two sub-populations. However, the values of P_{em} tended to be slightly higher for thick roots in a number of species, confirming a tendency for these species to have a heavier right tail in their IBD distribution for the finer roots.

We also observed that the relative differences of estimated *ISD* were correlated to the relative differences of P_{em}, as shown in **Figure 5**. This highly significant correlation means that when the potential branching sites are more spaced out in one of the two sub-populations, this is compensated by a higher probability of emergence of laterals on these potential branching sites, and vice-versa. Most species are close to the center of this graph, which shows that they have similar branching parameters for thick and fine roots, but several species exhibited the compensation between the spacing of branching sites and the probability of emergence. This was the case for *Merculialis annua* observed in Thouzon and *Pseudotsuga menziesii* observed in Nozeyrolles, whose IBD

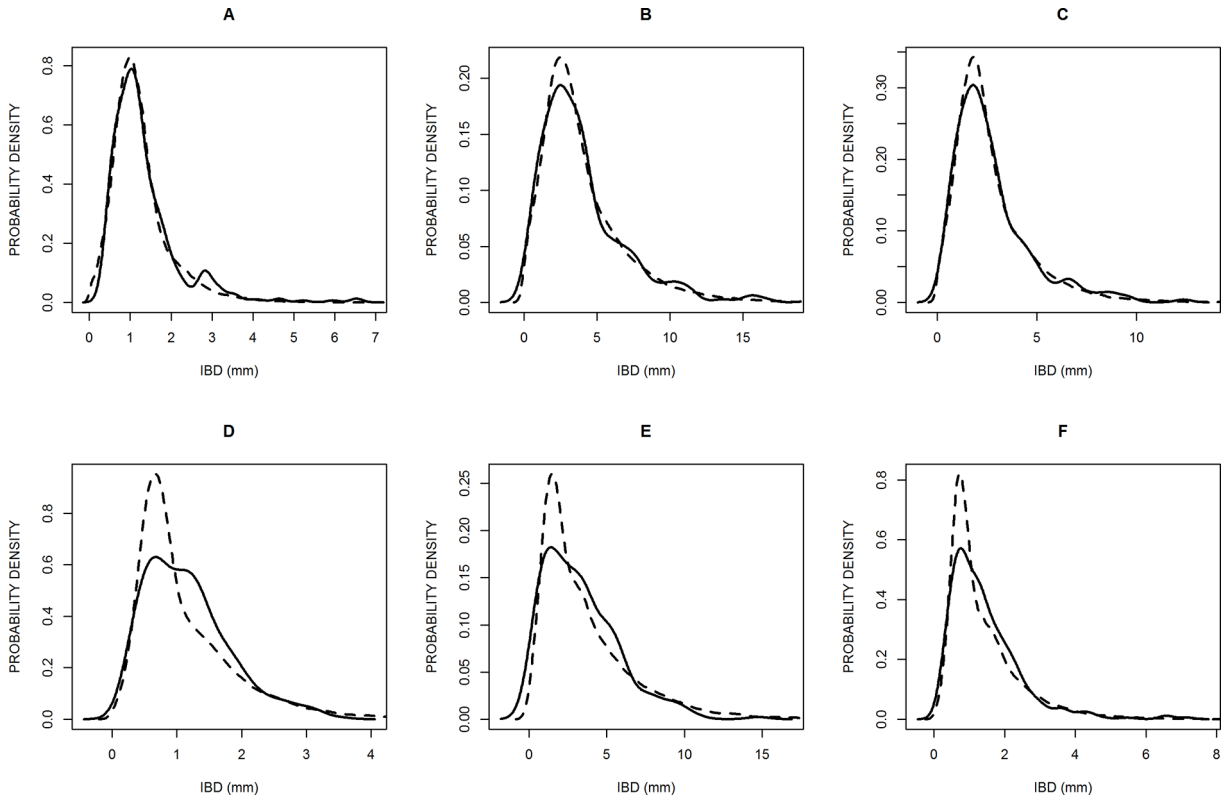

FIGURE 2 | Probability density distributions of six samples to illustrate the best model fittings **(A, B, C)** and the worst **(D, E, F)**, according to the chi square criterion. The solid lines are the observed distributions and the dashed lines are the simulated distributions. The samples are: *Poa trivialis* in Clermont **(A)**, *Solanum laciniatum* in Thouzon **(B)**, *Vulpia myuros* in Thouzon **(C)**, *Lolium perenne* in Thouzon **(D)**, *Rubus ulmifolius* in Thouzon **(E)**, and *Sorghum halepense* in Thouzon **(F)**.

distributions are represented in **Figure 6**. These species showed extreme behaviors regarding distributions: for *Mercurialis annua*, the lateral roots on fine roots were more spaced out, whereas *Pseudotsuga menziesii* showed higher densities on its fine roots.

DISCUSSION

Main Characteristics of the Distributions of IBD

In this study, we confirm that IBD exhibits large variations in each of the 40 species samples, both within the species and between species, as reported for example by Mallory et al., (1970); Kong et al., (2014); Bui et al., (2015); Landl et al., (2018), or Pagès and Kervella (2018). In most works, however, intra-species variations were not studied and were dismissed as noise. These variations are often smoothed over using other measure variables, such as branching density, evaluated by various counting protocols relying on root segments, whole roots, or even whole root systems. The problem is that such estimates of branching density are hardly comparable from one study to another because the obtained values are more or less buffered, and they depend on the developmental stage of the root or root system. The point was thoroughly discussed by Dubrovsky and Forde (2012). Following their main recommendations, we measured this IBD trait in young, although fully branched, parts of individual roots, because such measurements are more suitable to reflect the underlying developmental process of acropetal branching, even though highly variable measurements are obtained when following this method. The point is even more important when the objective of the study is to link the branching process to local environmental variables, such as water and nutrient availability. In our study, we did not consider the radial pattern of emergence that is usually influenced by the internal vascular structure. It would have been difficult because the number of vascular poles varies from one root to the other, and it may even vary along the roots (personal observations).

Despite the large intra-plant variations of IBD, the inter-species variability was so high (nine-fold factor in our study) that the species effect was significant. Because of the large intra-plant and intra-root variations, testing a species or genotype effect requires a sufficient number of measurements for each one of them as well as measurements made in very comparable situations for all. In this study, we had at least 150 measurements per sample combined with 40 different samples. The species effect was not specifically the subject of the present study, but it was demonstrated earlier by Pagès and Kervella (2018) using a dedicated sampling design for the purpose. Our large sampling numbers were also justified because in addition, we intended to evaluate the intra-sample variations associated to the diameter of the parent roots.

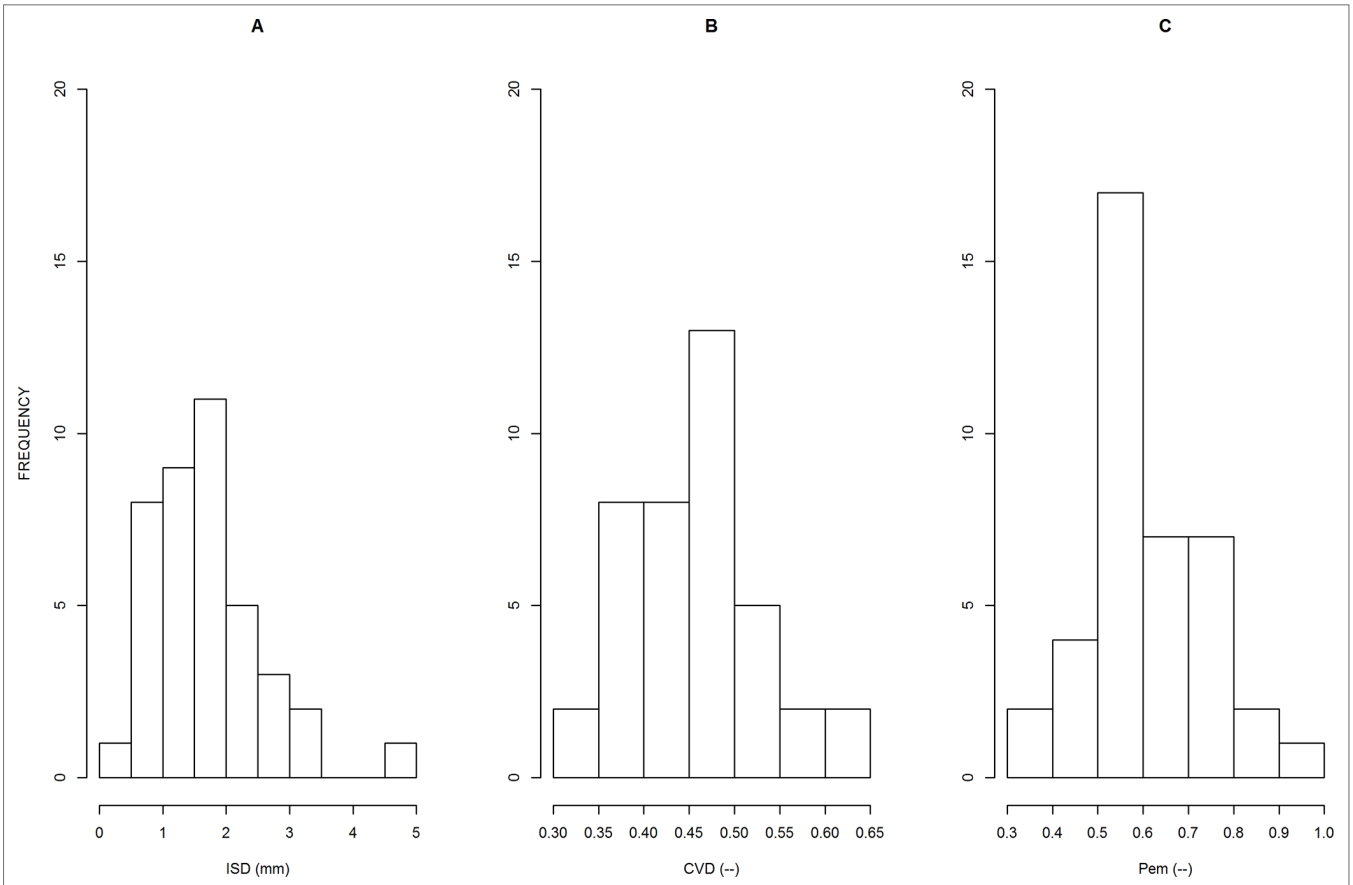

FIGURE 3 | Distributions of the 40 parameter values, as estimated for each sample, for parameter ISD **(A)**, CV_D **(B)** and P_{em} **(C)**. The meanings of these parameters are explained in the text.

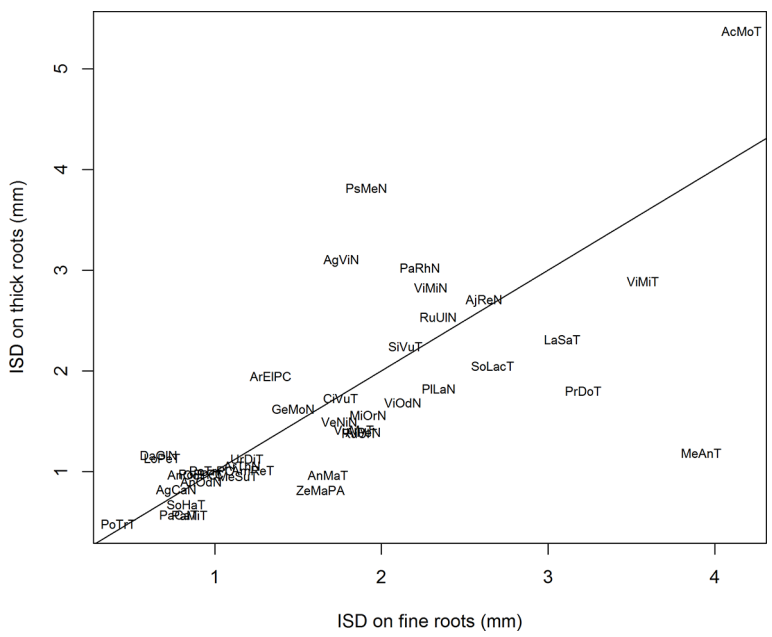

FIGURE 4 | Relationship between the values of *ISD* estimated on thick parent roots versus the values of *ISD* estimated on fine parent roots. The line is the bisecting line. The abbreviations are given in **Table 1**.

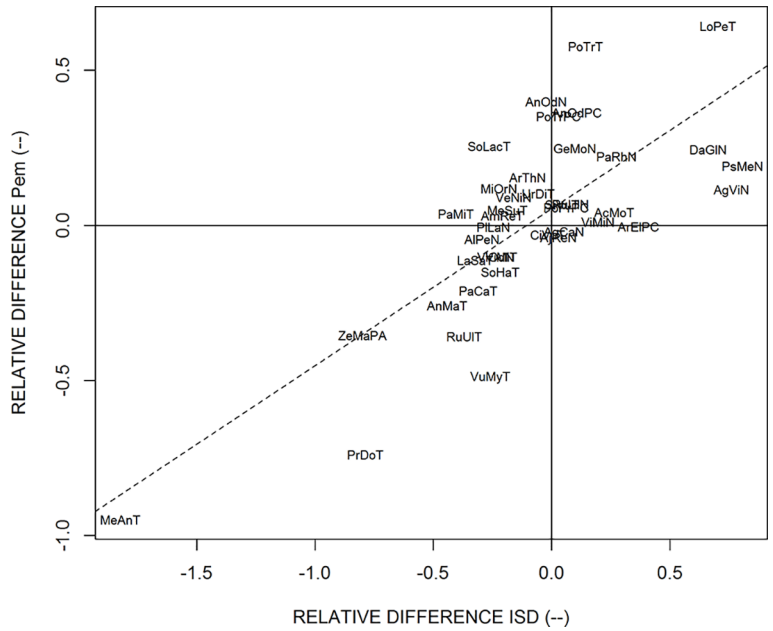

FIGURE 5 | Relationship for the relative difference between the estimates of *ISD* and P_{em}, when estimated on thick parent roots and fine parent roots separately. The dotted line is the regression line. The abbreviations are given in **Table 1**.

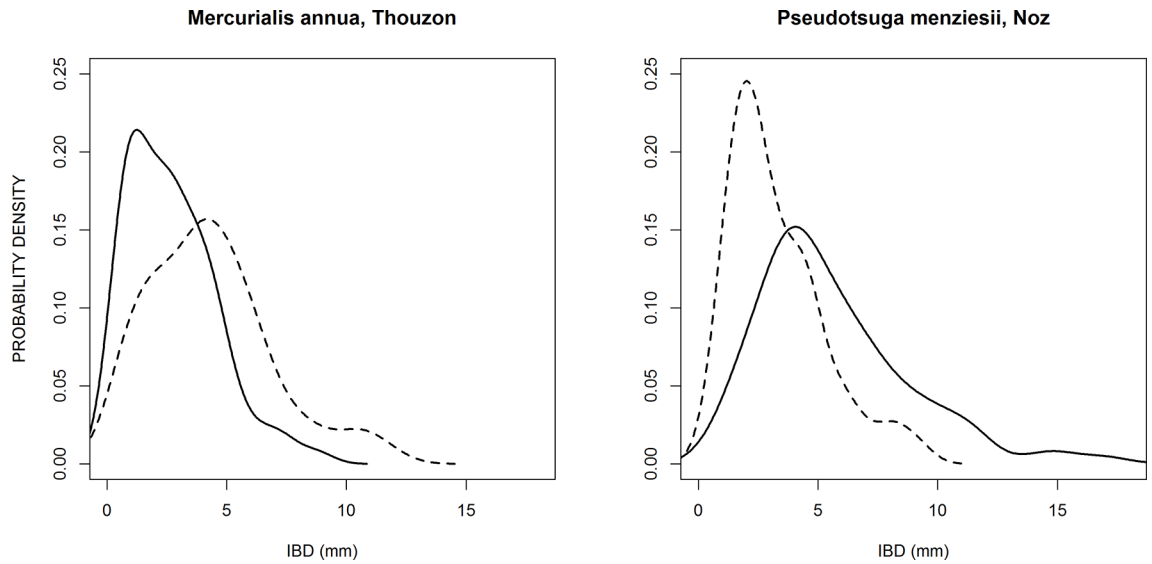

FIGURE 6 | Probability density distributions of two species that exhibited large and opposite differences between the branching patterns of thick parent roots (solid line) and fine parent roots (dashed line).

Interest of Modeling

This model is the first attempt to simultaneously represent several aspects of the longitudinal branch distribution that have been observed by a number of authors, but on a very limited number of species, using either detailed morphological descriptions (e.g., Riopel, 1966; Riopel, 1969; Charlton, 1975; Charlton, 1982; Charlton, 1983; Varney et al., 1991; Hinchee and Rost, 1992; Newson et al., 1993; Charlton, 1996; Draye, 2002; Landl et al., 2018) or physiologically oriented studies (Dubrovsky et al., 2006; Moreno-Risueno et al., 2010; De Smet, 2012). The main aspects that were reported by several of these authors are that regular longitudinal spacing between laterals tends to be maintained along the parent roots, and that the distributions of IBD are usually skewed with a tail toward the large values (Pagès, 2014; Landl et al., 2018). Using our simple model with three input parameters, these aspects, as well as the general shape of the IBD distributions, can be rendered and quantified in a comprehensive and parsimonious way. This study, which relies on a large number of species, is a

way of validating the model and asserting its robustness. Thus, the modeling approach opens the possibility of linking highly focused studies that investigate underlying mechanisms with global and macroscopic observations that aim at simply characterizing the emergent branching pattern, because of its important functional significance. This link helps quantify simply and separately several sub-processes: the creation of the archetypal distance (model parameter *ISD*), its variations (model parameter CV_D), and the probability of accomplishing the whole branching process until lateral emergence takes place on each branching site (summarized by the P_{em} parameter). These different sub-processes are worth separating because they occur successively, involve various molecular mechanisms, and respond to different environmental stimuli (Dubrovsky et al., 2006; De Smet, 2012).

This model can be integrated as a component (or module) in larger models of the root system architecture (Dunbabin et al., 2013). Branching density is a central process in such models, having the prime role in defining the number of roots and eventually the total root length of the whole root system. Several models of the root system architecture use an average IBD input parameter calibrated for each category of roots, defined by their branching order or other typology. Our results suggest that there are differences between roots regarding their branching distribution, but they are not independent, since the *ISD* parameter estimates were significantly correlated for fine and thick roots. Therefore, we suggest using a common *ISD* parameter for all roots and adapting the other important parameter (P_{em}) to the parent root diameter and possibly to the root position in the surrounding soil. This method would lead to a reduced number of parameters with a more clear and biological meaning.

Use in a Phenotyping Perspective

The parameters of the present model may also be used as interesting traits for root phenotyping approaches. Among the three parameters, we can guess that *ISD* is rather genetically controlled, whereas P_{em} may be more sensitive to local conditions and would reflect plasticity. These speculations based on the present results are worth verifying using suitable experimental designs that cross genotypes and environmental conditions. We have seen that *ISD* can easily be estimated based on the mode of the empirical distribution of IBD, which represents the most frequent inter-branch distance. This value seems relatively easy to obtain, and could be estimated on a reduced number of lateral roots, several tens for instance. The probability parameter P_{em} has a very different impact on distribution. Its value modifies the right tail of the distribution, so that it can be conveniently estimated *via* the high-probability quantiles of the distribution. We used the 0.8 level in the present study. According to our model, a Gaussian distribution is obtained as the limit distribution when $P_{em} = 1$, i.e., when all branching sites give rise to an emerged lateral root. The importance of the right tail increases with decreasing values of P_{em}. Therefore, *ISD* would summarize a genetic potential for the plant regarding branching density, and P_{em} would summarize the accomplishment of this branching density in the given environmental conditions. The impact of the third parameter (CV_D) on the global distribution is lower, and its estimation is more difficult. Thus, its interest from a phenotyping perspective is much lower.

Exploration of Intra-Plant Variations

Thanks to our original data set which relies on many different species and well-developed and highly branched root systems, we could study the inter-branch distance on main roots as well as lateral roots, and chose to study the effects of the diameter of the parent root. We showed that in most species, the *ISD* values were not impacted by the parent root diameter. Thus, for all these species, the fineness of roots did not modify this archetypal distance. On the other hand, the diameter of the parent root had a higher -although unpredictable- impact on the probability of accomplishing the branching process (P_{em} parameter). For a majority of species, this probability decreases with decreasing diameters, but it is not a generally observed phenomenon. We also observed opposite cases, where it seems that failure is more probable for thick roots than fine roots.

Since the differences observed for the values of ISD and Pem in the sub-populations of parent roots (thick versus fine) were not independent, we can suspect that it might reflect different plant strategies regarding the positioning of their laterals. Some species had higher densities on their main thick roots, whereas others favored higher densities on their fine roots. Both strategies can make sense and participate in the development of a diversity of branching patterns, in coordination with other developmental processes, as described by Pagès (2014) and Pagès (2016).

It would be very interesting to use this diversity to further explore the molecular mechanisms explaining that laterals have a higher chance to emerge on thick or fine roots within the same genotype.

CONCLUSION

Therefore, studying simultaneously intra-plant and inter-species variations and using well-developed root systems is an interesting means of raising new questions regarding both the diversity in the foraging strategies of plants and regarding the physiological mechanisms underlying this diversity. The construction and use of such a simple and generic model is a prime way of allowing the quantitative exploration of this diversity.

DATA AVAILABILITY

The datasets generated for this study are available on request to the corresponding author.

AUTHOR CONTRIBUTIONS

LP made the conception, data acquisition and analysis, and wrote the paper.

SUPPLEMENTARY MATERIAL

The Supplementary Material for this article can be found online at: https://www.frontiersin.org/articles/10.3389/fpls.2019.01020/full#supplementary-material

REFERENCES

Barlow, P. W., and Adam, J. S. (1988). The position and growth of lateral roots on cultured root axes of tomato, *Lycopersicon esculentum* (Solanaceae). *Plant Syst. Evol.* 158, 141–154. doi: 10.1007/BF00936340

Bui, H. H., Serra, V., and Pagès, L. (2015). Root system development and architecture in various genotypes of the Solanaceae family. *Botany* 93, 465–474. doi: 10.1139/cjb-2015-0008

Charlton, W. A. (1975). Distribution of lateral roots and pattern of lateral initiation in *Pontederia cordata* L. *Bot. Gaz.* 36, 225–235. doi: 10.1086/336808

Charlton, W. A. (1982). Distribution of lateral root primordia in root tips of *Musa acuminata* Colla. *Ann. Bot.* 49, 509–520. doi: 10.1093/oxfordjournals.aob.a086276

Charlton, W. A. (1983). Patterns of distribution of lateral root primordia. *Ann. Bot.* 51, 417–427. doi: 10.1093/oxfordjournals.aob.a086486

Charlton, W. A. (1996). "Lateral root initiation," in *Plant roots: hidden half*. Eds. Y. Waisel, A. Eshel, and U. Kafkaf (New York: Marcel Dekker), 149–173.

De Smet, I. (2012). Lateral root initiation: one step at a time. *New Phytol.* 193, 867–873. doi: 10.1111/j.1469-8137.2011.03996.x

Diggle, A. J. (1988). Rootmap—a model in 3-dimensional coordinates of the growth and structure of fibrous root systems. *Plant Soil* 105, 169–178. doi: 10.1007/BF02376780

Draye, X. (2002). Consequences of root growth kinetics and vascular structure on the distribution of lateral roots. *Plant Cell Environ.* 25, 1463–1474. doi: 10.1046/j.0016-8025.2002.00924.x

Drew, M. C. (1975). Comparison of effects of localized supply of nitrate, phosphate, ammonium and potassium on growth of seminal root system of Barley. *New Phytol.* 75, 479–490. doi: 10.1111/j.1469-8137.1975.tb01409.x

Drew, M. C., and Saker, L. R. (1975). Nutrient supply and growth of seminal root system in Barley. 2. Localized, compensatory increases in lateral root growth and rates of nitrate uptake when nitrate supply is restricted to only part of root system. *J. Exp. Bot.* 26, 79–90. doi: 10.1093/jxb/26.1.79

Dubrovsky, J. G., and Forde, B. G. (2012). Quantitative analysis of lateral root development: pitfalls and how to avoid them. *Plant Cell* 24, 4–14. doi: 10.1105/tpc.111.089698

Dubrovsky, J. G., Gambetta, G. A., Hernandez-Barrera, A., Shishkova, S., and Gonzalez, I. (2006). Lateral root initiation in Arabidopsis: developmental window, spatial patterning, density and predictability. *Ann. Bot.* 97, 903–915. doi: 10.1093/aob/mcj604

Dubrovsky, J. G., Napsucialy-Mendivil, S., Duclercq, J., Cheng, Y., Shishkova, S., Ivanchenko, M. G., et al. (2011). Auxin minimum defines a developmental window for lateral root initiation. *New Phytol.* 191, 970–983. doi: 10.1111/j.1469-8137.2011.03757.x

Dunbabin, V. M., Postma, J., Schnepf, A., Pagès, L., Javaux, M., Wu, L., et al. (2013). Modelling root–soil interactions using three-dimensional models of root growth, architecture and function. *Plant Soil* 372, 93–124. doi: 10.1007/s11104-013-1769-y

Henke, M., Sarlikioti, V., Buck-Sorlin, G., Kurth, W., and Pagès, L. (2014). Exploring root developmental plasticity to nitrogen with a three-dimensional architectural model. *Plant Soil* 385, 49–62. doi: 10.1007/s11104-014-2221-7

Hinchee, M. A. W., and Rost, T. L. (1992). The control of lateral root development in cultured pea seedlings. III. Spacing intervals. *Bot. Acta* 105, 127–131. doi: 10.1111/j.1438-8677.1992.tb00277.x

Hodge, A. (2009). Root decisions. *Plant Cell Environ.* 32, 628–640. doi: 10.1111/j.1365-3040.2008.01891.x

Kong, D., Ma, C., Zhang, Q., Li, L., Chen, X., Zeng, H., et al. (2014). Leading dimensions in absorptive root trait variation across 96 subtropical forest species. *New Phytol.* 203, 863–872. doi: 10.1111/nph.12842

Landl, M., Schnepf, A., Vanderborght, J., Bengough, A. G., Bauke, S. L., Lobet, G., et al. (2018). Measuring root system traits of wheat in 2D images to parameterize 3D root architecture models. *Plant Soil* 425, 457–477. doi: 10.1007/s11104-018-3595-8

Lavenus, J., Goh, T., Roberts, I., Guyomarc'h, S., Lucas, M., De Smet, I., et al. (2013). Lateral root development in Arabidopsis: fifty shades of auxin. *Trends in Plant Sci.* 18, 450–458. doi: 10.1016/j.tplants.2013.04.006

Lecompte, F., and Pagès, L. (2006). Apical diameter and branching density affect lateral root growth in banana. *Environ. Exp. Bot.* 59, 243–251. doi: 10.1016/j.envexpbot.2006.01.002

Malamy, J. E. (2005). Intrinsic and environmental response pathways that regulate root system architecture. *Plant Cell Environ.* 28, 67–77. doi: 10.1111/j.1365-3040.2005.01306.x

Mallory, T. E., Chiang, S., Cutter, E. G., and Gifford, E. M. (1970). Sequence and pattern of lateral root formation in five selected species. *Am. J. Bot.* 57, 800–809. doi: 10.1002/j.1537-2197.1970.tb09875.x

Moreno-Risueno, M. A., Van Norman, J. M., Moreno, A., Zhang, J., Ahnert, S. E., and Benfey, P. N. (2010). Oscillating gene expression determines competence for periodic Arabidopsis root branching. *Science* 329, 1306–1311. doi: 10.1126/science.1191937

Newson, R. B., Parker, J. S., and Barlow, P. W. (1993). Are lateral roots of tomato spaced by multiples of a fundamental distance. *Ann. Bot.* 71, 549–557. doi: 10.1006/anbo.1993.1071

Orman-Ligeza, B., Morris, E. C., Parizot, B., Bennet, M. J., Beeckman, T., and Draye, X. (2018). The xerobranching response represses lateral root formation when roots are not in contact with water. *Curr. Biol.* 28, 3165–3173. doi: 10.1016/j.cub.2018.07.074

Pagès, L. (2014). Branching patterns of root systems: quantitative analysis of the diversity among dicotyledonous species. *Ann. Bot.* 114, 591–598. doi: 10.1093/aob/mcu145

Pagès, L. (2016). Branching patterns of root systems: comparison of monocotyledonous and dicotyledonous species. *Ann. Bot.* 118, 1337–1346. doi: 10.1093/aob/mcw185

Pagès, L., and Aries, F. (1988). SARAH: modèle de simulation de la croissance, du développement, et de l'architecture des systèmes racinaires. *Agronomie* 8, 889–896. doi: 10.1051/agro:19881008

Pagès, L., and Kervella, J. (2018). Seeking stable traits to characterize the root system architecture. Study on 60 species located at 2 sites in natura. *Ann. Bot.* 122, 107–115. doi: 10.1093/aob/mcy061

Pagès, L., and Pellerin, S. (1994). Evaluation of parameters describing the root system architecture of field grown maize plants (*Zea mays* L.). II. Density, length, and branching of first-order lateral roots. *Plant Soil* 164, 169–176. doi: 10.1007/BF00010068

Pagès, L., and Picon-Cochard, C. (2014). Modelling the root system architecture of Poaceae. Can we simulate integrated traits from morphological parameters of growth and branching? *New Phytol.* 204, 149–158. doi: 10.1111/nph.12904

R Core Team. (2013). *R: A language and environment for statistical computing*. Vienna, Austria: R Foundation for Statistical Computing. URL http://www.R-project.org/

Riopel, J. L. (1966). The distribution of lateral roots in *Musa acuminata* 'Gros Michel'. *Am. J. Bot.* 53, 403–406. doi: 10.1002/j.1537-2197.1966.tb07352.x

Riopel, J. L. (1969). Regulation of lateral root positions. *Bot. Gaz.* 130, 80–83. doi: 10.1086/336472

Robinson, D. (1994). The responses of plants to nonuniform supplies of nutrients. *New Phytol.* 127, 635–674. doi: 10.1111/j.1469-8137.1994.tb02969.x

Varney, G. T., Canny, M. J., Wang, X. L., and McCully, M. E. (1991). The branch roots of Zea. 1. 1st order branches, their number, sizes and division into classes. *Ann. Bot.* 67, 357–364. doi: 10.1093/oxfordjournals.aob.a088203

Wu, Q., Pagès, L., and Wu, J. (2016). Relationships between root diameter, root length and root branching along lateral roots in adult, field-grown maize. *Ann. Bot.* 117, 379–390. doi: 10.1093/aob/mcv185

Conflict of Interest Statement: The author declares that the research was conducted in the absence of any commercial or financial relationships that could be construed as a potential conflict of interest.

Advantages of publishing in Frontiers

OPEN ACCESS
Articles are free to read for greatest visibility and readership

FAST PUBLICATION
Around 90 days from submission to decision

HIGH QUALITY PEER-REVIEW
Rigorous, collaborative, and constructive peer-review

TRANSPARENT PEER-REVIEW
Editors and reviewers acknowledged by name on published articles

Frontiers
Avenue du Tribunal-Fédéral 34
1005 Lausanne | Switzerland

Visit us: www.frontiersin.org
Contact us: info@frontiersin.org | +41 21 510 17 00

REPRODUCIBILITY OF RESEARCH
Support open data and methods to enhance research reproducibility

DIGITAL PUBLISHING
Articles designed for optimal readership across devices

FOLLOW US
@frontiersin

IMPACT METRICS
Advanced article metrics track visibility across digital media

EXTENSIVE PROMOTION
Marketing and promotion of impactful research

LOOP RESEARCH NETWORK
Our network increases your article's readership